City Research Online

City St George's, University of London

Citation: Koller, Anton W. (2014). The friction coefficient of soft contact lens surfaces in relation to comfort and performance. (Unpublished Doctoral thesis, City University London)

This is the accepted version of the paper.

This version of the publication may differ from the final published version. To cite this item please consult the publisher's version.

Permanent repository link: https://openaccess.city.ac.uk/id/eprint/13791/

Copyright and Reuse: Copyright and Moral Rights remain with the author(s) and/or copyright holders. Copies of full items can be used for personal research or study, educational, or not-for-profit purposes without prior permission or charge, unless otherwise indicated, provided that the authors, title and full bibliographic details are credited, a hyperlink and/or URL is given for the original metadata page and the content is not changed in any way. For full details of reuse please refer to City Research Online policy.

City Research Online: http://openaccess.city.ac.uk/ publications@citystgeorges.ac.uk

The friction coefficient of soft contact lens surfaces in relation to comfort and performance.

A thesis submitted for the degree of

Doctor of Philosophy

to City University London

Division of Optometry and Visual Sciences

by

Anton W. Koller

March 2014

Index

List of Tables **6**

List of Figures **11**

ACKNOWLEDGEMENTS **14**

Declaration: **14**

Abstract **15**

Chapter 1 - Introduction **16**

1.1 Aims of this research 18

Chapter 2 - Anatomy and physiology of the eye **19**

2.1 The Visual Organ: 19

Cornea and Sclera 20

Crystalline Lens 22

The Retina 23

The Uveal Tract 23

2.1 The eyelids 24

2.2 Tears 25

2.3 Structure of the tear film 25

2.4 Properties of the tear film 26

Chapter 3 - Contact lenses **27**

3.1 Historical development 27

3.2 Hydrophilic Contact Lens Materials 29

3.3 Silicone Contact Lenses 32

3.4 Silicone Hydrogel Contact Lenses 32

3.5 Contact lens manufacturing techniques 33

3.6 Soft contact lens fitting 34

3.7 Contact lens movement on the eye 37

What keeps the lens in position on the eye? 37
3.8 Contact lens comfort 38
Chapter 4 - Friction **40**
4.1 Introduction 40
4.2 Friction and Contact Lenses 41
4.3 Fluid friction between solids 42
4.4 Polymer friction 43
4.5 Viscosity 44
4.6 Rheology 44
Plastic fluids (Bingham- substances) 45
Dilatant fluids 45
Thixotropic fluids 45
4.7 Tribology 45
Stick-slip phenomenon 46
Surface quality 47
4.8 Contact lens friction and lubricity 47
4.9 Review of soft contact lens tribometry 56
Chapter 5 - Rationale for in vitro experiments **61**
5.1 Introduction 61
5.2 Experiment 1 - The construction and testing of a Contact Lens Tribometer 64
5.3 Physical principles 65
5.4 The force to be applied to the substrate 66
5.5 Apparatus 66
Tribometer Schema 66
Mechanical Scale 68
High resolution stepper motor 69
Slider FX Stepper motor driver 70

NC-Pilot stepper motor controller 71

Kistler high resolution force sensor 9215-1 72

Charge Amplifier Kistler ICAM 5073 73

Kistler Manuware Software 73

Substrate used for testing 74

Hydrogel samples 75

5.6 Experiment 1A - Verification of linear and radial swell rates 76

5.7 Experiment 1B – Calibration of the sensor 78

5.8 Experiment 2 –Friction coefficients of the reference materials 79

5.9 Experiment 3 – Evaluation of soft lens materials 87

Chapter 6 - Rationale for the in vivo experiments 97

6.1 Introduction 97

6.2 Corneal shape, bulbar shape and contact lens design 98

6.3 Predicting contact lens geometry by a mathematical approach 100

6.4 Design of the experimental soft lenses 108

6.5 Experiment 4 – Use of a Scheimpflug image 110

Discussion 111

6.6 Experiment 5 - Evaluation of the PMMA semi-scleral lenses on one eye. 112

Introduction 112

Materials 112

Method 113

Discussion 116

6.7 Experiment 6 - Measurement of soft lens parameters at elevated temperature 118

Introduction 118

Aim: 120

Materials 120

Method 120

Results 121

Discussion 121

Chapter 7 - In vivo experiments 123

7.1 Ethical approval, inclusion and exclusion criteria 123

Ethical approval 123

Inclusion criteria 123

Exclusion criteria 123

Subjects 124

7.2 Equipment and materials 125

7.3 The clinical record forms. 128

Clinical Record Form 1 (CRF1) 128

Clinical Record Form 2 (CRF2) 129

Clinical Record Form 3 (CRF 3) 129

7.4 Experiment 7 – In vivo experiments 130

Introduction 130

Materials 130

Methods 131

Results 139

7.5 Discussion of the in-vivo results 161

Chapter 8 - General discussion and conclusions 170

Chapter 9 - CONCLUSIONS 184

Chapter 10 - Appendices 186

10.1 Results of CRF 1 tests 186

10.2 Results of CRF 2 tests 189

Performance 189

Chapter 11 - Annexes 202

11.1 Annex A- The influence of scleral shape in relation to the Back Optic Zone Radius of a monocurve contact lens 202

11.2 Annex B- Patient information and consent form 204

11.3 Annex C- Clinical record forms 1-3 207

Chapter 12 - References **211**

Chapter 13 - Abbreviations **223**

List of Tables

Table 2.1 Surface parameters of Liu's eye model 20

Table 2.2 Refractive indices of Liu's eye model 20

Table 3.1 ISO 18369-1 Classification of soft contact lens materials. 30

Table 3.2 ISO 18369-1 Classification of soft contact lens materials 31

Table 3.3 An example of how the ISO nomenclature is used 31

Table 4.1 Average circumference of sphere segments. 54

Table 4.2 Sample calculations related to mass causing force 55

Table 4.3 Reported friction coefficients 60

Table 5.1 Stepper motor settings for a 24mm diameter disc. 72

Table 5.2 Specification of tested materials. 75

Table 5.3 Linear swell rates of the five chosen materials. 77

Table 5.4 Radial swell rates of the five chosen materials 78

Table 5.5 Friction coefficients of rigid materials tested against each other. 83

Table 5.6 Coefficient of friction. 85

Table 5.7 Resulting (frictional) force for all tests normalised to a 10 g load. 86

Table 5.8 Coefficient of friction for materials 86

Table 5.9 Dry friction mesurements of 5 simulated blinks, ... 92

Table 5.10 Borderline friction measurement of 5 simulated blinks, ... 92

Table 5.11 Mixed friction measurement of 5 simulated blinks, ... 93

Table 5.12 Friction measurement of 5 simulated blinks, using the lubricating agent Celluvisc. 93

Table 6.1 Calculation of the scleral diameter and radius 103

Table 6.2 Calculated monocurve BOZRs for a 14.0mm diameter TD lens. 105

Table 6.3 Calculated monocurve lens 105

Table 6.4 Chord length "s" for contact lens diameter 14.5mm 107

Table 6.5 The production data and the measured values for the set of semi scleral PMMA lenses. 117

Table 6.6 Comparison of radii, diameters and sags between ambient room temperature and 34°C for the five different soft lens materials. 121

Table 7.1 Sequence of lenses tested in subjects eyes 132

Table 7.2 Contrast sensitivity values. Rows 1-8 define contrast,..... 135

Table 7.3 Contrast sensitivity for participating subjects with spectacle prescription. 139

Table 7.4 CRF1 results: Ocular tissue grades and corneal diameters for all 16 subjects. 140

Table 7.5 CRF1 results: Tear meniscus height at lower lid and keratometer readings. 141

Table 7.6 Best spectacle correction. 142

Table 7.7 Excluded subjects and reason for exclusion. 143

Table 7.8 The retinoscopy spot findings and tear break-up times. 144

Table 7.9 Best aligned PMMA trial lenses as described in 6.6 145

Table 7.10 Comfort values as recorded using the VAS. 146

Table 7.11 VAS results in Table 7.9 minus the VAS results using PMMA trial lenses 147

Table 7.12 Average VAS results in cm for each material and each subject. 148

Table 7.13 Comfort difference in VAS between PMMA semi scleral test lenses and the tested materials for the five subjects. 149

Table 7.14 Results of a two way analysis of variance in comfort between materials and subjects tested. 150

Table 7.15 Average, SD, median and absolute median (MAD) of lens movement for VSO 38, LM55 and GM3 materials. 151

Table 7.16 Average, SD, median and absolute median (MAD) of lens movement for VSO75 and Definitive materials. 152

Table 7.17 Average and standard deviation of vertical lens movement.....153

Table 7.18 Mean and average lens movements after a blink. 153

Table 7.19 Results of PUT test.....156

Table 7.20 Frequency of lens movements for lenses judged as normal using the PUT 156

Table 7.21 The number of lenses judged as loose using the PUT.....157

Table 7.22 Visual acuitiy with soft lenses and best overcorrection 158

Table 7.23 Difference in VA between spectacle correction and VA obtained with contact lens plus over-correction.....158

Table 7.24 Summarised difference between contrast sensitivity with spectacle correction and CS with contact lenses and overcorrection.....159

Table 7.25 Average contrast sensitivity results for all subjects using best correction 159

Table 7.26 Average difference between CS results with contact lenses using best overcorrection and best spectacle correction.....159

Table 7.27 Summarised retinoscopic spot occurrences for all five materials. 160

Table 7.28 CRF 3 results.....161

Table 7.29 Comfort results from research literature. pm = afternoon.....162

Table 7.30 Comfort difference on the VAS between PMMA semi scleral trial lenses and the 5 soft lens materials. 163

Table 8.1 Published coefficients of friction for a range of contact lenses. 175

Table 8.2 Coefficients of friction measured under unlubricated conditions and different lubricated states with the experimental contact lens tribometer. 176

Table 8.3 Average VAS differences in comfort between the tested material and PMMA test lens. Positive values indicate better comfort. 179

Table 8.4 Average visual acuity with best spectacle correction and with contact lenses 180

Table 8.5 Average contrast sensitivity of all eyes tested.....180

Table 8.6 Overall retinoscopic spot appearances with the best overcorrection. 181

Table 8.7 Average lens movement with video analysis compared with CoF at borderline and mixed lubrication with saline and mixed lubrication with a lubricating agent. 182

Table 8.8 Spearmans rho rank correlation for CL movement after a blink and CoF 182

Table 8.9 Push-up test results compared with borderline and mixed friction CoF's 183

Table 10.1 Contrast sensitivity with best correction CRF 1 for selected individuals 186

Table 10.2 Results of CRF 1: Fundamental data, K-readings, spectacle correction and if CL wearer. 187

Table 10.3 Results of CRF1: Exterior part of the eye, Tear meniscus Retinoscopic spot, NIBUT, lid tension, exclusion reasons 188

Table 10.4 Visual acuity with soft CL and best overcorrection 189

Table 10.5 Visual acuity with soft CL and best overcorrection minus best visual acuity with spectacle correction. 190

Table 10.6 Retinoscopic spot occurrences VSO 38 material 191

Table 10.7 Retinoscopic spot occurrences LM 55 material 192

Table 10.8 Retinoscopic spot occurrences GM3 material 193

Table 10.9 Retinoscopic spot occurrences VSO 75 material 194

Table 10.10 Retinoscopic spot occurrences Definitive material 195

Table 10.11 Contrast sensitivity 30 min. after lens insertion 196

Table 10.12 Comparison of contrast sensitivity with CL + overcorrection and spectacle contrast sensitivity 197

Table 10.13 Soft lens friction by measuring lens movement between blinks 198

Table 10.14 Average, SD, median and MAD for VSO 38, LM55 and GM3 materials. 199

Table 10.15 Average, SD, median and median absolute deviation for VSO75 and Definitive materials. 199

Table 10.16 Ratio between lid force and lens movement after blink 199

Table 10.17 Prevalence of vertical travel in 0.1mm increments after blink 200

Table 10.18 Results of push up tests where n = normal and l = loose. 201

Table 11.1Clinical Record Form 1 (CRF 1) 207

Table 11.2 Clinical record Form 2 page 1 (CRF2) 208

Table 11.3Clinical record form Page 2 209

Table 11.4 Clinical record Form 3 (CRF3) 210

List of Figures

Figure 2.1 A cross-section of the human eye 19

Figure 2.2 A cross section of the human cornea 21

Figure 2.3 A longitudinal section of the anterior part of the eye 23

Figure 2.4 The lacrimal apparatus right side 24

Figure 4.1 Dynamic friction of Polytetrafluoroethylene (PTFE) 44

Figure 4.2 A schematic Stribeck curve showing the three different friction phases. 45

Figure 4.3 Stick-slip phenomenon seen while adding force five times for 3 seconds 47

Figure 4.4 Contact lens rotation in situ. Due to the structure and movement of the lid, the lens of the right eye rotates in the opposite direction to that of the left eye. 48

Figure 4.5 Explanation of flat, parallel (aligned) and steep contact lens fit. 48

Figure 4.6 (A) minus lens with peripheral shoulder, (B) back surface parallel to front surface (C) positive lens with anterior second curve. 48

Figure 4.7 The relationship between force, mass and gravity. 50

Figure 4.8 Spherical cap (Wikipedia 2015) 50

Figure 4.9 Force upon a projected area 51

Figure 4.10 a projected area. 51

Figure 4.11 Explanation of average circumference of a sphere or sphere segment .. 52

Figure 4.12 Explanation for the calculation of the slice diameter of a sphere 53

Figure 5.1 Tribometer Schema 66

Figure 5.2 Tribometer set up. 67

Figure 5.3 Tribometer base showing the substrate attached to the stepper motor and the disc holder 68

Figure 5.4 Tribometer balance attached to base. 68

Figure 5.5 Torque graphs for stepper motor 70

Figure 5.6 Mechapro motor control window 71

Figure 5.7 Kistler low force sensor 9215-1 72
Figure 5.8 Kistler Charge Amplifier 73
Figure 5.9 Sensor readings as shown on the computer screen. 74
Figure 5.10 Calibration of the low force sensor. 78
Figure 5.11 Oscilloscope display during sensor calibration 79
Figure 5.12 10g total force on top of the substrate 81
Figure 5.13 Example reading of static friction. 82
Figure 5.14 Oscilloscope reading for HEMA 90
Figure 5.15 Oscilloscope reading for the LM material 90
Figure 5.16 Oscilloscope reading for GM material 91
Figure 5.17 Oscilloscope reading of Definitive material at mixed friction 91
Figure 6.1 Explanation of the scleral model 101
Figure 6.2 Separation of corneal and scleral sagittal heights 102
Figure 6.3 Composition of sagittal heights 104
Figure 6.4 Section of a monocurve contact lens with effective inner lens diameter 106
Figure 6.5 “Aligned” fit of a soft contact lens 106
Figure 6.6 Approximation of contact area (not to scale). Central angle α defined . 107
Figure 6.7 Scheimpflug image of the author’s left eye. 110
Figure 6.8 Explanatory drawing showing the resulting radius 110
Figure 6.9 Semi-scleral PMMA lens 8.6/14.5mm. 114
Figure 6.10 Semi-scleral PMMA lens 8.7/14.5mm. 114
Figure 6.11 Semi-scleral PMMA Lens 8.80/14.5mm. 114
Figure 6.12 Semi-scleral PMMA lens 8.9/14.5mm 115
Figure 6.13 Semi-scleral PMMA lens 9.0/14.5mm 115
Figure 6.14 Semi-scleral PMMA lens 9.1/14.5mm. 115

Figure 6.15 Semi-scleral PMMA lens 9.2/14.5mm. 116

Figure 7.1 Reticule photograph for calibration 137

Figure 7.2 Overlay demonstration with 3 visible out of 4 overlaid frames. 138

Figure 7.3 Comfort separated by material types in ascending order. 148

Figure 7.4 Comfort difference between the PMMA semi scleral lenses and the tested soft lenses. 149

Figure 7.5 Median lens movement in mm. 152

Figure 7.6 The association between lens movement and friction coefficient. 154

Figure 7.7 Contact lens movement versus lid force for the five subjects 155

Figure 7.8 Scattergram of lens movement, measured in 0.1mmsteps, after a blink 155

Figure 7.9 Lens movement for lenses judged as normal using the PUT 156

Figure 7.10 Lens movement for the lenses judged as loose (using the PUT) 157

Figure 7.11 Ultrahigh resolution OCT of the limbal area of an eye and a conjunctival impression caused by a soft lens 167

Figure 8.1 Average coefficients of friction in ascending order 177

Figure 11.1 The influence of scleral shape in relation to the BOZR 202

ACKNOWLEDGEMENTS

First of all I thank my supervisor Dr. Mike Port for suggesting the idea for this thesis, for his patience, for his support, the elegant way of keeping me on track and leading me, the non-native English speaking student, over possible obstacles. Further I thank my second supervisor Prof. David Edgar for his support in preparing my thesis resolving formal tasks. As a foreign student I am further grateful for the support from City University which was excellent. I also thank my dear friend Univ. Prof. Dr. Steinkogler for his help to resolve legal requirements with the Vienna Ethics committee. I am also grateful to my daughter Victoria who managed to recruit my subjects for the in vivo tests and helped me to manufacture the huge number of test lenses. She was an excellent assistant who was cheerful, helpful and supportive. I am also grateful to the Vienna "Akademie für Augenoptik, Optometrie und Hörakustik" for using their equipment which was not available in my own premises. Last but not least I am grateful to my wife Eva, who encouraged me to stay seated in front of my personal computer to write this thesis and being so very patient for this last nearly two years as well as keeping me out of other enterprises which might have been time-consuming.

Finally I thank Contamac Ltd. and Vista Optics Ltd. for providing contact lens blanks for the tests.

Declaration:

City University's librarian is empowered to allow this thesis to be copied in whole or in part without further reference to the author. This permission covers only single copies made for study purposes, subject to normal conditions of acknowledgement.

Abstract

The soft contact lenses of today are made from a variety of hydrogel materials. These materials have different properties in terms of water content, monomers, hardness and other tensile characteristics. It is likely that the frictional properties also vary between materials. It is known that constituents of the tear film interact with contact lens materials to form a biofilm on the lens surface. The hypothesis of this research is that although the frictional properties of lens materials may vary these properties do not affect the comfort and performance of the lenses in vivo.

A tribometer is a device to measure the coefficient of friction of materials. There was no commercially available tribometer designed specifically for use with contact lens materials, so one was constructed and validated against standard solid materials. The same equipment was used to determine the friction coefficients of five contemporary soft lens materials under different conditions of lubrication but, unlike other tribometers, this unique design simulated human blinking as far as possible. The experimental friction coefficients varied widely from 0.27 to 5.89 under different conditions of lubrication. The largest variation between materials was seen using the most viscous lubricant.

For the in vivo studies the author coordinated the manufacture of 250 contact lenses, which were lathe cut and polished to a standard design, achieving exceptionally tight tolerances, using the same five materials. This rigourous process was carried out to minimise variations in the geometry of each contact lens. Subjects were screened to minimise ocular heterogeneities between subjects. Clinical performance of each lens was assessed using comfort, contrast sensitivity, visual acuity, entoptic phenomena, non-invasive tear break-up time and lens movement on the eye. In a clinical environment none of these parameters showed any associations with the coefficients of friction found in vitro, apart from a moderate correlation (rho = 0.5) between lens movement and the coefficient of friction under borderline friction conditions. In conclusion, the findings of this research support the hypothesis that frictional properties of soft lenses do not affect comfort and performance in vivo.

Chapter 1 - Introduction

Since the first hydrophilic contact lenses manufactured by Wichterle, movement of soft contact lenses, *in situ*, has been judged as an indicator for comfort and physiological tolerance. Because of the soft structure of the material, it was believed that fitting techniques similar to those used for hard contact lenses were not required. Wichterle mentioned (Gasson, 2008) in a letter that contained basic instruction for a practitioner, that *"if the patient has observed the formation of Sattler's veil during wear, the lens should be decentred for a certain period to re-establish physiological conditions"*. Research and experience in the following decades confirmed that movement of soft lenses on the eye is of high importance in order to maintain physiological and morphological conditions while a soft contact lens is worn (Gasson and Morris, 1992, Bürki, 1991, Hom and Bruce, 2006).

Contact lens fitters have to consider contact lens geometry in relation to the ocular topography while, at the same time, attending to the physiological requirements of the eye. Despite the fitters efforts to ensure the best fitting lens, complications frequently occur following lens wear. An internet search produced more than two million hits regarding complications of contact lenses wear, while a search in PubMed found more than 2500 citations relating to this topic. Most of the educational literature mentions complications in soft contact lens wear. For example, the "Manual of Contact Lens Prescribing" (Hom and Bruce, 2006) cites 200 publications on soft lens wear complications. With the use of "disposable" and planned replacement contact lenses, these problems have been partially solved. An example is the problem of non-soluble deposits on the anterior surface of hydrophilic lenses caused by daily or extended wear for several months or longer (Galifa, 2006). The problem is solved by disposing of a used lens after a defined, but shorter, period of time. Manufacturers have learnt to produce lenses with geometries that better fit the eye. As a result, most contact lens wearers who do not tolerate soft lenses for long periods wear them only occasionally. Although many of the causes of contact lens complications and intolerance have been addressed, some remain to be fully investigated, including the role played by friction in contact lens wear. Friction and lubricity play important roles in contact lens wear and tolerance. Contact lenses need to move adequately to assure nutrition, oxygen supply and tear

exchange with blinking, and friction is an important determinant of lens movement. Although the topic of friction in contact lens wear has been investigated using different lubricants and/or tear substitutes, these investigations have been carried out in an undifferentiated manner (Yao et al., 2008, Sivamani et al., 2003, Rennie et al., 2005, Kim, 2001, Niarn and Jiang, 1995) i.e. these investigations have only considered specific conditions with specifically chosen materials and methods. To understand and appreciate the requirements for the surface structure of a contact lens and the resultant lens movement on the eye, the dynamics of contact lenses on the eye, lid dynamics and the surface characteristics of lenses and tissues all have to be evaluated.

The general anatomy and physiology of the eye is discussed in Chapter 2 of this thesis, with emphasis on the cornea, tears, tear film, and eyelids, all of which have particular relevance to the contact lens research which follows. Chapter 3 focuses on developments in contact lens materials, including PMMA, hydrophilic materials, silicone elastomers, silicone hydrogels, together with their different manufacturing processes, and soft contact lens fitting technique. This chapter concludes with consideration of contact lens movement on the eye and comfort when wearing contact lenses. In Chapter 4, the physics of friction is discussed, with particular emphasis on friction as it affects contact lens materials and contact lens wear. The topic of tribology, the investigation of friction, is introduced, and tribometry, the measurement of friction, is discussed in relation to contact lenses. Chapter 5 introduces and describes the in vitro experiments which were the precursor to the in vivo experiments which follow later in the thesis. A major element of Chapter 5 is the construction and testing of the author's own design of tribometer, specifically constructed for use with contact lens materials and contact lenses themselves. This leads on to the preparation of lenses for the in vivo experiments described in Chapter 6. This required the design and construction to exceptionally rigourous tolerances of 250 soft contact lenses under the author's supervision. These lenses were manufactured with such rigour in order to minimise the variation between lenses when worn in the eye during the in vivo experiments. These experiments make up Chapter 7, in which the clinical effects of the variations in coefficient of friction of 5 different soft contact lens materials were measured when the lenses were worn by 5

subjects. The final chapter (Chapter 8) contains a general discussion and conclusions of this research.

1.1 *Aims of this research*

Our knowledge of the frictional behaviour of contact lens materials themselves requires expansion to increase our understanding of whether differences between materials might influence the success of contact lens wear and, if so, why some materials may perform better than others. The work presented in this thesis addresses these issues and aims to investigate the behaviour of identical soft contact lenses, made of different types of soft contact lens materials, with regard to their frictional properties under laboratory conditions as well as *in situ* on healthy eyes.

Chapter 2 - Anatomy and physiology of the eye

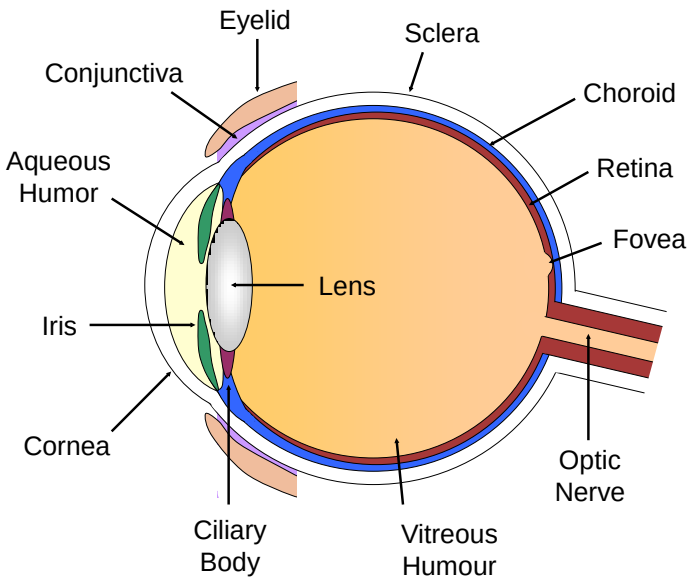

Figure 2.1 A cross-section of the human eye
(Reproduced with permission of Brent Cornell)

2.1 *The Visual Organ:*

The visual organ consists of the two eyes, their protecting and supporting organs, the visual pathway and the visual cortex (Grehn, 2012). The light sensitive retina represents the most important part of the eye. The retina is judged as an advanced extension of the brain consisting of several sequential switched neurons. Electromagnetic wavelengths between 380 and 760 nanometres are able to stimulate the photo-receptors. Each location of the visible space corresponds to a related retinal area. The differentiation of the stimulating light sensations to the retina is called visual perception.

Similar to a video camera, the eye has imaging elements (rods and cones). Refracting elements are the cornea and the crystalline lens while the retina represents the overall imaging element. The physical, i.e. electromagnetic stimuli striking the retinal surface cause photochemical reactions which translate the light sensations to nervous reactions which are routed via the optic nerve through the chiasma, the optic tracts, the inter-cerebral pathway and the optic radiations to the visual cortex. The eye is embedded in an adipose tissue which is located in the

orbital cavity. The orbit contains multiple ocular muscles which control eye movement and various connective tissues.

Gullstrand (Helmholtz, 1909) *"developed the most authorative model of the eye"*. While this model and others, such as Emsley's reduced eye, Listing's reduced eye, or Schwiegerling's eye are good for paraxial domains, modern models relate to the modulation transfer function (Sturzu and Luca-Motoc, 2011). The Arizona eye model (Greivenkamp et al., 1995) developed a method to calculate the changes of the optical properties of an eye and the resulting visual performance. Liu et al. (2005) proposed an eye model, containing a shell-structured lens. The parameters are given in Table 2.1 and Table 2.2.

Surface	Radius (mm)	Conic constant	Thickness (mm)
Anterior surface of cornea	7.77	0.18	0.50
Posterior surface of cornea	6.4	-0.60	3.16
Anterior surface of lens	12.4	-0.94	4.02
Posterior surface of lens	−8.10	0.96	

Table 2.1 Surface parameters of Liu's eye model

Surface	Media	Index (543 nm)
Anterior surface of cornea	Cornea	1.3777
Posterior surface of cornea	Aqueous	1.3371
Anterior surface of lens	Lens	Shell
Posterior surface of lens	Vitreous	1.3377

Table 2.2 Refractive indices of Liu's eye model

Cornea and Sclera

The outermost layer of the eye is a connective tissue, which consists of the transparent cornea and the white sclera. The junction between cornea and sclera is termed the limbus. The radius of the transparent cornea is 7.2 – 8.5 mm. It has a diameter of 10 – 13mm. The length of the eye is approximately 24mm.

From the viewpoint of contact lenses the cornea itself is the area of greatest interest.

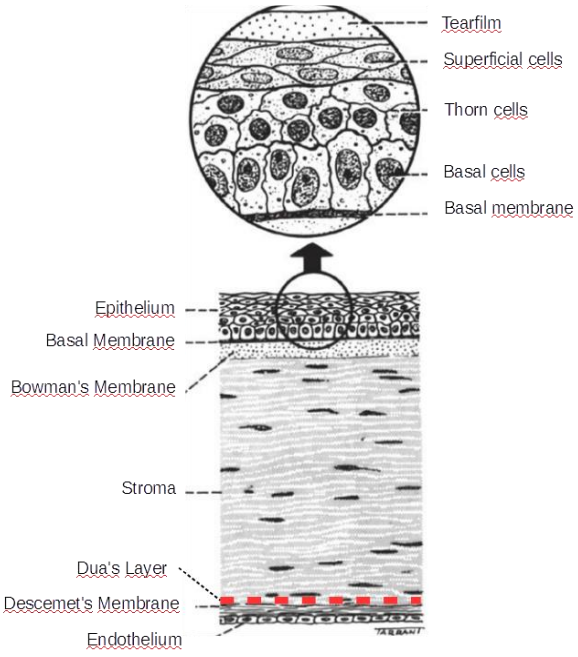

Figure 2.2 A cross section of the human cornea

(reproduced with the permission of Elsevier, Dua's layer marked by the author

The anatomy of the cornea is as follows (Figure 2.2). The three layered epithelium consists, from outside to inside, of flat and cubic cells, two to three rows of thorn cells and cylindrical epithelial cells adhered to the basal membrane which resides on the transparent, glassy Bowman's membrane, also named anterior elastic lamina, followed by the main structure, the substantia propria or stroma. Dua et al. (2013) described a 15µm thick layer between corneal stroma and endothelium withstanding up to 2 bars of pressure. The understanding and the function of this layer might influence the understanding of corneal diseases such as hydrops and pre- Descemet dystrophies (Kanski and Bowling, 2012).

Descemet's membrane covers the stroma at the posterior side of the cornea. The non- regenerating one layered corneal endothelium represents the inner corneal limit towards the anterior chamber of the eye.

The margins of the anterior chamber are the surface of the cornea, the chamber angle, the front surface of the iris and within the area of the pupil, the front surface of the crystalline lens. The junction between cornea and iris is called the chamber angle. Its adjacent structures are the trabecular meshwork and the canal of Schlemm. These structures are responsible for the drainage of the intraocular fluid (aqueous humour) produced by the ciliary body which is located in the posterior chamber. The 20-30 drainage channels connected to Schlemm's canal end within the deep venous patch and partially in the conjunctival surface veins.

Comfort and success of contact lens wear depends on the sensory responses of the cornea and conjunctiva. About seventy non myelinated nerve fibres, coming from the sensory nerve branches of the ophthalmic nerve, enter the cornea radially developing a dense structure by binary branching. Most of these ciliary nerves are

located beneath the basal membrane while some nerves reach the epithelium and end near the epithelial surface (Augustin, 2007). Sensory events on the corneal surface trigger the blink reflex, a protective mechanism of the eye. Temperature drop because of tear evaporation is one of the reasons to blink in order to keep the eye wet and lubricated. For this reason, contact lens wearers mostly blink habitually as their blink reflex is not directly triggered because the tears between the contact lens and the eye do not evaporate and, therefore, corneal temperature does not drop (Wolkoff et al., 2005). Honegger et al. (1980) compared the duration of stay of ophthalmic preparations in the conjunctival sac. Watery and a viscous formulations were compared. While 17.5% ± 6.3% of the watery preparation remained in the conjunctival sac, 69.5% ± 17.4% of the viscous formulation containing 2% methylcellulose remained after one minute of installation. Forty minutes after instillation approximately 10% of the watery drops remained in the eye compared with approximately 20% of the drops containing methylcellulose. An initial tear turnover of 52%/minute was reported by Nelson (1995) from adults between 20 and 45 years of age and of 38%/minute from persons between 50 and 89 years of age. The physiological tear turnover rate of the younger group was reported to be 16%/minute compared with 18%/minute for the older group using a fluorophotometric method. Another study (Tomlinson and Khanal, 2005) reported tear turnover rates between 7%/minute and 22.2 %/minute in normal subjects measured by different authors. They observed a significant decrease of fluorescein concentration within the first five minutes after instillation and suggested that this was caused by reflex tearing. As mentioned, tear exchange not only plays an important role in keeping the cornea transparent and to assure metabolic exchange but also requires attention in conjunction with the efficacy, the use and the dilution of tear substitutes and lubricants in vivo.

Crystalline Lens

The posterior chamber is located behind the anterior chamber (Figure 2.3). The boundaries consist of the back surface of the iris, the ciliary body, the front surface of the crystalline lens and the posterior area of the iris. The crystalline lens is located behind the pupil in a dish-like pit of the vitreous body. The zonules of the ciliary body run from the ciliary muscle, located at the pars plana, the peripheral retinal area, to the crystalline lens, and maintain the position of the lens. Contractive forces

of the circular ciliary muscle alter the curvature of the lens and enable the eye to have proper focus at distance and near. This phenomenon is called accommodation. The space behind the crystalline lens is filled with the vitreous body and consists of a gel embedded in a fine structural substance. The refractive indices of the refractive portions of the eye are as follows:

- Cornea: 1.376
- Aqueous humour: 1.336
- Vitreous body: 1.336

The Retina

The retina or neural tunic of the eye should be considered as a brain extension responsible for perception of visual events and translating them to nervous signals. Light entering the eye and absorbed by the photoreceptors, the rods and cones, is transposed to electric signals via a chemical reaction using rhodopsin. These signals reach the visual cortex via the retinal ganglia and the optic nerve. They are separated at the optic chiasma as left and right hemisphere signals passing through the optic tract, the lateral geniculate body and the optic radiation of each side (Damms and Guzek, 2014).

The Uveal Tract

The iris, the ciliary body and the choroid form the uvea. The iris separates the anterior chamber from the posterior chamber and has the pupil in its centre. It slides on the front surface of the crystalline lens and is the variable diaphragm (aperture) of the eye. The iris root joins the ciliary body which controls accommodation. The ciliary body also produces the aqueous humour which flows from the posterior chamber to the anterior chamber and leaves the

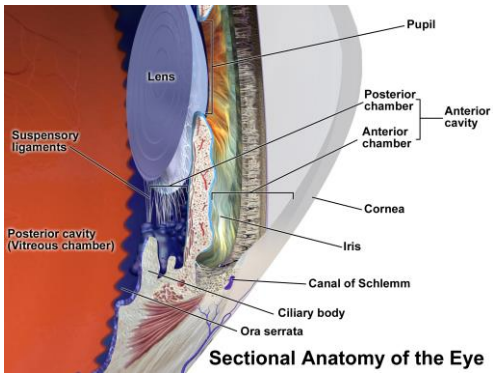

Figure 2.3 A longitudinal section of the anterior part of the eye
(Blausen.com, 2014)

intraocular structure through the canal of Schlemm and the trabecular meshwork. The choroid is separated from the retina by the lamina vitrea which sits on the retinal pigment epithelium of the retina. The next layer is the chorio-capillaris which provides nutrition to the outer layers of the retina.

2.1 *The eyelids*

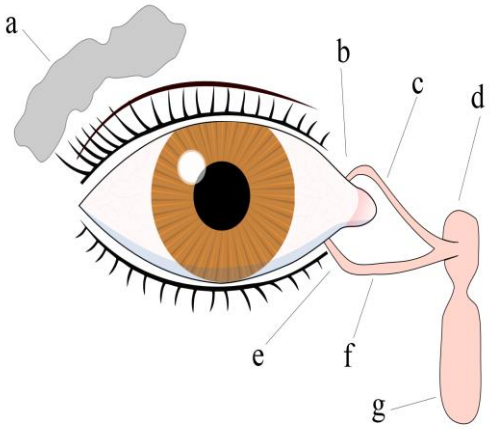

Figure 2.4 The lacrimal apparatus right side

a. tear gland / lacrimal gland, b. superior lacrimal punctum, c. superior lacrimal canal, d. tear sac / lacrimal sac, e. inferior acrimal punctum, f. inferior lacrimal canal, g. nasolacrimal canal (Wikimedia commons 2014)

The eyelids consist of outer skin, and contain the circular orbicularis muscle innervated by the nervus facialis, which closes the upper lid and the tarsal plate containing the Meibomian glands. The inner layer of the eyelid is the tarsal conjunctiva which everts at the fornix and connects to the eye at the limbus. It contains mucin producing goblet cells, Krause's and Wolfrings glands which are accessory tear glands. The eyelashes are located at the outer edge of the lids. The glands of Zeiss and Moll are located in the neighbourhood of the lashes. The upper lid is opened by the levator palpebrae, innervated by the nervus oculomotorius and the smooth Muller's muscle innervated by the sympathetic nerve. The tension of the upper eyelid plays an important role in contact lens movement. It is well known (Ehrmann et al., 2001) that lid tension is different from one person to another and it is reported that 10.7 mN/mm to 35.5mN/mm is the range of pulling motion. A figure of 10.3mm Hg which equals 1.4mN/mm^2 has been reported in previous literature (Miller, 1967). More recent literature (Shaw et al., 2009) described new piezoelectric techniques for assessment but only provided raw data. The eyelids have a protective task and help to keep the eye wet by blinking. The sensory innervation of the upper eyelid arises from the infratrochlear the supratrochlear, the supraorbital and the lacrimal nerves of the ophthalmic branch of the trigeminal nerve. The infratrochlear nerve also supplies the skin of the lower lid. Stapleton et al. (2013) write that the eyelid margins are supplied by branches of the

supratrochleal, supraorbital, infratrochlear and lacrimal nerves and mention the importance of the eyelid and the cornea as a *"key contact zone between the contact lens and the ocular surface"* and mention that the relationship between contact lens wearing and ocular comfort has been known for many years. The eyelids provide protection for the eye, and distribute the tears over the eye, keeping it wet, clear and clean (Kaufmann and de Decker, 2003). The 'lid wiper' is the 0.4 to 0.6mm wide inner conjunctiva of the upper lid near the canthus that wipes the ocular surface during blinking.

2.2 *Tears*

The interactions between tear secretion, lid function (blinking) and contact lenses have a major influence on the success of contact lens wear. Mann and Tighe (2013) have described the interactions between a contact lens and the tear film. Young et al. (2011) reported that neither lens material, lens care system nor gender had any significant influence on the contact lens related dry eye status. Mc Monnies (2007) described the consequences of incomplete blinking resulting in deficient mucin and lipid distribution, longer interblink intervals for the inferior cornea and contact lens deposition. He suggested that "*the cornea-central nervous system-lacrimal gland loop for basal and reflex tear secretion may not function normally with soft CL induced depression of corneal innervation."* Lemp and Bielory (2008) described strategies to identify patients with ocular allergy and dry eye management with contact lens wearers. A telephone survey carried out by Lemp and Nichols (2009) reported that blepharitis is seen in 37% to 47% of optometrists' and ophthalmologists' patients.

2.3 *Structure of the tear film*

The pre-corneal tear film is composed of three layers (Wolff, 1954). The outermost, lipid layer is about 100nm thick and prevents evaporation of the middle layered watery phase and is the boundary against the outside world. The lipid layer consists of cholesterol, cholesterol esters, triglycerides and phospholipids. The lipids are produced by the Meibomian glands in the area of the lid canthus. Holly (1986) described the structure of the tear film of the open eye as two fluid layers consisting of the aqueous layer and the overlying lipid layer. 99% of the tear film consists of the aqueous layer. Holly postulated that the semi-solid mucous layer, a hydrated

mucous glycoprotein, which covers the epithelial surface, should physio-chemically "*be considered as part of the epithelium"* (Holly, 1986). While the innermost semi-solid mucous layer by smoothing the relatively rough corneal epithelium assures, in conjunction with the aqueous layer and the lipid layer, the optical transparency and the refractive properties that the corneal surface is known for, it cannot be understood to be an overall homogenous film. Mucus forms drop -like shaped formations which develop an uneven landscape-like surface which is covered by the aqueous tears.

As soon as a contact lens is placed on the corneal surface, the pre-corneal tear film is divided into the pre-lens and the post-lens tear film. Indirect measurements with Optical Coherence Tomography (Wang et al., 2003) reported an average pre-corneal tear film thickness of 3.3µm, and a pre-lens tear film thickness for two different soft contact lens products of 3.9µm and 3.6µm. The post-lens tear film thickness was 4.7µm and 4.5µm. The border between the outside world and the tears is still represented by the lipid layer.

2.4 *Properties of the tear film*

All tear components are blood derivatives and do have, to some extent, similar properties. Tears are non-Newtonian fluids (Millar, 2006) with shear-thinning properties (Gouveia and Tiffany, 2005). With Newtonian fluids, linearity between pushing force and shear applies. This property is known as viscosity. An example of a Newtonian fluid is water. Non-Newtonian fluids change their viscosity properties under changing conditions and their viscosity values do not remain constant. The watery tears have a pH value of about 7.2 and a molality of about 300milliosmol. The average range of surface tension for the tears as a whole was measured as 42.6mN (Nagyová, 1999).

Chapter 3 - Contact lenses

3.1 *Historical development*

As a compensation for ametropia the use of contact lenses was first mentioned by Mueller (1889) and Fick (1888). Improvements of these scleral lenses led to better physiological tolerance and to the use of other materials. Resin lenses in PMMA material and celluloid were introduced by Obrig (1942), Györffy (1990). Tuohy (1948) first used a small PMMA contact lens floating on the corneal tear film. 1970 Norman Gaylord developed a siloxane-methacrylate polymer (Gasson, 2008, Pearce, 2001) which was patented in 1974 (Gaylord, 1977). In comparison to PMMA the advantage of the new material was that it had enhanced gas permeability. Gas permeability enhances oxygen supply to the corneal epithelium and reduces the risk of epithelial oedema and/or oedemative stippling. Rigid Gas Permeable (RGP) contact lens materials developed independently from soft lenses. The RX 56 contact lens material, a Cellulose Acetate Butyrate (CAB) was suggested by Dr. Irving Fatt in 1973 (Bowden, 2009). Polymer Technology Corporation, owned by Bausch & Lomb, developed the first Boston material in 1975 (Gasson, 2008). In 1986 Polymer Technology launched a fluorosilicone polymer, the Boston Equalens material with a Dk of 50. Oxygen permeability and transmissibility is described by Snyder (2004) as *"numbers to compare generic lens materials and proprietary/brand lenses to determine gaseous interchange through the lens to and from the cornea. Permeability is a laboratory measurement of the bulk polymer involving the material's diffusion coefficient (D) multiplied by the solubility constant (k). Dk is a function of the oxygen permeable components in the plastic"*. The Japanese Menicon Company launched the very successful O2 Material in 1979 and other manufacturers of contact lens materials and contact lenses subsequently launched gas permeable materials. Currently, materials with an oxygen permeability (Dk) of up to 163 are available. The invention of poly-hydroxymethylmethacrylate called poly-HEMA (Walcott, 1998), a transparent hydrogel absorbing approximately 40% water, was the basis for the invention of soft contact lenses (Wichterle and Lim, 1960). The Czechoslovakian ophthalmologist Dreifus raised the idea of producing soft contact lenses from the material (Wichterle et al., 1961). Contact lenses made from this new material were produced by a self-assembled prototype machine. The equipment had

been constructed from a Meccano-like (Märklin Metallbaukasten) set at Christmas 1961(Wichterle, 1990, Wichterle and Lim, 1956). Wichterle used an upright mounted electrically driven spindle holding a concave mould. Monomer in the mould was polymerised while the device rotated and a contact lens in the xerogel state was produced. The first commercial production was carried out by the Czech pharmaceutical firm "Spofa". They packed the contact lenses in physiological saline and shipped them in tubes closed with a cork and sealed with sealing wax. The patents were later sold to a US firm (National Patent and Development Corporation) which further sold on the patent to Bausch and Lomb, a major supplier of optical and ophthalmological appliances. Bausch and Lomb improved production technology and obtained FDA approval for their Soflens made of HEMA. The spun-cast B&L Soflens marketed in 1971was available in two different shapes: F, for flat and N for normal. They produced many different lens series based on the spin casting technology. Other contact lens manufacturers produced soft contact lenses by lathe cutting utilizing HEMA and newly developed polymers and polymer combinations. For example, the 55% water Bionite lens was made using HEMA, Ethylene Glycoldimethacrylate (EGDMA) and Polyvinylpyrrolidone (PVP). Various material compositions containing MMA, methacrylic acid, PVA and PVP have been used to produce water contents ranging from 30% to 85%. Glycerol methacrylate materials with water binding properties were produced with water contents of 40% to 65%. Snyder (2004) mentioned common components used in contact lens materials together with their main properties. These were as follows: "

a. *Methylmethacrylate (MMA), which contributes hardness and strength*
b. *Silicone which increases flexibility and gas permeability through the material's silicon-oxygen bonds but has the disadvantage of poor wettability*
c. *Fluorine which also adds a smaller degree of gas permeability and improves wettability and deposit resistance in silicone-containing lenses*
d. *Hydroxyethyl-methacrylate (HEMA), the basic water-absorbing monomer of most soft lenses*
e. *Methacrylic acid (MAA) and n vinyl pyrolidone (NVP) monomers, both of which absorb high amounts of water and are usually adjuncts to HEMA to increase lens water content*

f. *Ethylene glycol dimethacrylate (EGDMA), a cross-linking agent that adds dimensional stability and stiffness but reduces water content"*

The silicone rubber lens (being a non-hydrogel) had the big advantage of high gas permeability but, being essentially hydrophobic, did not succeed because of poor comfort and fitting abilities. Today's contact lens materials are of a hydrophilic nature, containing siloxane components to achieve high gas transmissibility and maintain good wearing comfort. Many silicone hydrogels are based on TRIS polymers. Most of these lenses are planned replacement lenses to be used between one day and one month on a daily wear basis or an extended wear basis for up to 30 days (Bowden, 2009). Silicone Hydrogel contact lenses were first marketed by CibaVision and Bausch & Lomb (Bowden, 2009). These lenses are normally produced by a moulding process but Contamac, a UK-based contact lens company, launched the first commercially available silicone hydrogel material which could be lathe cut in 2007 (Young and Tapper, 2008).

3.2 *Hydrophilic Contact Lens Materials*

Hydrophilic contact lens materials are produced by the use of different monomers. These monomers play an important role concerning water content, mechanical stability, oxygen permeability, biocompatibility, wetting characteristics, stiffness and flexibility (Snyder, 2004). In a process called polymerisation the monomers are bonded together using catalytic and/or thermal processing. Careful temperature control during polymerisation is necessary to avoid material stress. Contact lens materials containing inner stress result in deformed contact lenses as soon as the lenses are hydrated. The main requirements for a suitable soft contact lens material are:

a. Good comfort
b. Good optical properties
c. Good physiological tolerance (biocompatibility)
d. Good flexibility and strength
e. Good wettability

Most standard contact lens materials are categorised by water content. Oxygen permeability (Dk) of hydrophilic contact lens materials which do not contain silicone is a function of water content of the specific material. A theoretical contact

lens material with a water content of 100% would have a Dk of 80 units. Most conventional hydrogels have a Dk range between 10 and 35 units. ISO 18369-1:2006 classifies soft contact lens materials as shown inTable 3.1 to Table 3.3 An example of how the ISO nomenclature is used

Classification with regard to water content and ionic load		
Group suffix	Hydrogel material	Description
I	Low water content, non-ionic	Materials which contain less than 50 % water and which contain 1 % or less (expressed as mole fraction) of monomers that are ionic at pH 7.2
II	Low water content, non-ionic	Materials which contain less than 50 % water and which contain 1 % or less (expressed as mole fraction) of monomers that are ionic at pH 7.2
III	Low water content, ionic	Materials which contain less than 50 % water and which contain greater than 1 % (expressed as a mole fraction) of monomers which are ionic at pH 7.2
IV	Mid and high water content, ionic	Materials which contain 50 % water or more, and which contain greater than 1 % (expressed as a mole fraction) of monomers which are ionic at pH 7.2
V	Enhanced oxygen permeable materials* (e.g. silicone hydrogel)	Materials having an oxygen permeability (Dk) greater than 30 Dk units as defined in 4.4 of ISO 18369-4:2006 (using hPa−1) and that have a Dk greater than that expected on the basis of the materials' water content alone
Low water content is defined as less than 50 % water (< 50 %); mid water content is from 50 % to 65 % water, inclusive (50 % to 65 % water); and high water content is greater than 65 % water (> 65 %). Hence, group suffixes II and IV include all materials having water content of 50 % or greater.		
* It is expected that this classification will be further subdivided as more information is gained about the materials in this category.		

Table 3.1 ISO 18369-1 Classification of soft contact lens materials.

Classification with regard to oxygen permeability using standard ISO methods		
Category	DK units using hPA	Dk units using mmHG
0	< 0.75 Dk unit	<1 Dk unit
1	0.75 Dk to 11.75 Dk units	1 Dk unit to 15 Dk units
2	12.0 Dk to 22.5 Dk units	16 Dk units to 30 Dk units
3	22.75 Dk to 45 Dk units	31 Dk units to 60 Dk units
4	45.25 Dk to 75 Dk units	61 Dk units to 100 Dk units
5	75.25 Dk to 112.5 Dk units	101 Dk units to 150 Dk units
6	112.75 Dk to 150 Dk units	151 Dk units to 200 Dk units
7, etc	increasing in increments of 37.5 Dk units	increasing in increments of 50 Dk units
Note:	The prefix description is omitted	
	The series description is omitted	
	The stem for hydrophilic lens materials is "**filcon**"	

Table 3.2 ISO 18369-1 Classification of soft contact lens materials regarding oxygen permeability

Sample:	Austrofilcon II 2
Prefix	Austro
Stem for hydrophilic lens materials	filcon
Mid water content non ionic	II
16-30 Dk units	2

Table 3.3 An example of how the ISO nomenclature is used to name a contact lens material.

Bürki (2008) mentions the ACLM Contact Lens Classification for hydrophilic contact lens materials. This includes average Dk values for low, mid and high water content material.

3.3 *Silicone Contact Lenses*

Since the oxygen permeability of hydrophilic lenses was limited, attempts were made by the Toyo Company in Japan, Bausch and Lomb in 1979, and Dow Chemical in 1981(Gasson, 2008) to use silicone elastomers, often named silicon rubber, as a material for contact lenses. The remarkable advantage of silicone elastomers was the high oxygen permeability while its hydrophobicity was a severe disadvantage. Silicone elastomer lenses are only commercially available in a limited range from Bausch and Lomb today (Bausch and Lomb, 2015). Heunen (2012) described the method attempted by the manufacturers' mentioned to overcome this property to make the material usable for contact lenses. The methods to hydrophilize the surfaces were: Plasma discharge, grafting of polyvinyl-pyrrolidone and/or esters and sugars, which decreased the gas permeability of the silicone elastomers.

3.4 *Silicone Hydrogel Contact Lenses*

The combination of a hydrogel and a silicone elastomer component was first introduced in 1999. In his book *"Contact lenses The Story"* Bowden (2009) describes the development and the unfulfilled expectation, that this new material will fulfil the criteria for overnight contact lens wear, decreased risk of infection, decreased appearance of epithelial micro cysts, reduced contact lens binding and, last but not least, prolonged comfort. Cast moulding was the initial method of manufacture of silicone hydrogel contact lenses. The first silicone hydrogel latheable contact lens blanks were commercially available in 2008 and manufactured by Contamac (2008). The essential advantage of the Definitive silicone hydrogel was that after lathe turning and eventually lens polishing a surface treatment was not required. The cast moulded lenses required treatment to achieve wettability. Several techniques to enhance surface properties of contact lens materials were discussed by Keir and Jones (2013).

These were:

- Plasma coatings with high refractive index
- Plasma oxidation processes creating hyodrophilic silicate compounds on the surface

- Patented nanoglass technologies
- Nonsurface treatment technologies migrating to the surfaces and a long chain, high molecular-weight internal wetting agent based on polyvinylpyrrolidone
- A patented MeniSilk technology to achieve the hydrophilic property of the lenses which is believed to be essential for contact lens comfort.
- Delefilcon A daily disposable silicone hydrogel contact lenses contain 33% water and containing an outer surface layer with 80% water. This technique assured high oxygen permeability in combination with good wettability and lubricaton (Pruitt et al., 2012).

3.5 *Contact lens manufacturing techniques*

The main techniques are as follows:

- Lathe cut and polished.
- Lathe cut with modern computer controlled lathes consisting of air bearing main spindles that produce surfaces which do not need polishing.
- Spin casting produces one surface which does not have contact to a mould and probably has the most homogenous surface possible. This concave surface is formed in air by the centrifugal force of the spinning mould. The convex surface will reproduce asperities found in the mould surface and when the xerogel is hydrated the asperities will be larger due to the inherent expansion that occurs.
- Cast moulding copies the milling and lathing marks of the casting tool on the surface of the produced lens. Atomic force microscopy showed the difference in surface quality of some commercially available contact lenses produced by the different techniques in both new and used condition (Guryca et al., 2007, González-Méijome et al., 2009).

3.6 *Soft contact lens fitting*

In addition to the tests required for a routine examination of the eye, certain basic procedures need to be carried out for proper fitting of soft contact lenses.

These are:

Patient history

Inspection of the visible part of the eye without instruments or magnification

For first time wearers, the lid sensitivity can be tested by touching the lower lid and pulling it down a little to assess reaction

Retinoscopy

Subjective refraction

Ophthalmometry (measuring the central corneal curvatures and radii, peripheral corneal radii at an agle of 30°)

Calculation of corneal eccentricity as described by Wilms and Rabbetts (1977) using the formula for the numerical excentricity for 30°:

$$\varepsilon = 2\sqrt{1 - \frac{r_c^2}{r_s^2}} \qquad \text{Equation 1}$$

Where ε= numeric excentricity, r_c= mean apical corneal radius and r_s= mean peripheral sagittal radius at 30° and measurements taken at 90° relative to the corneal meridian. Due to their physical limitations, two position ophthalmometers such as Javal or Littmann type Ophthalmometers can only measure sagittal radii. The parameter of interest, of course, is the tangential radius. Corneal astigmatism is expressed by the difference in corneal radius between the two meridians, measured at the apex. Wilms suggested adding this difference to the sagittal radii taken in the horizontal meridians and deducting this from the vertical meridians. By doing so, the sagittal radii were transposed to their tangential equivalents. There are several variations believed to be more accurate than using this technique. One of them uses the mean values of the horizontal meridians and those of the vertical meridians. Another is to calculate the tangential radii for each of the four measurements.

With these “quasi” tangential radii, the formula in Equation 1 is used to calculate the numerical excentricity for each meridian or for each of the four peripheral measurements taken.

This method is commonly named the sagittal measurement technique.

A slit-lamp inspection of :

Lids, lid margins and eyelashes
Bulbar conjunctiva
Careful inspection of the cornea and its layers
Conjunctiva of upper and lower lid
Tear meniscus
Tear film and its stability

Fitting instructions issued by the early manufacturers related mainly to movement of the lenses in situ, avoidance of perilimbal impression marks and avoidance of corneal oedema. Wichterle (Gasson, 2008) gave basic fitting instructions with relevant advice. Currently, soft contact lenses are fitted according to recommendations by the manufacturers. Depending on the total diameter, the BOZR of the lenses need to be between 0.3mm and 1.3 mm flatter than the average ophthalmometer (keratometer) reading. Although the geometry of contact lenses has seen a major improvement within the last 20 years it is still an underestimated topic (Guillon, 2009).

With the contact lens on the eye, the following should be achieved (Gasson and Morris, 1992):

“good centration of the lens,
complete corneal coverage by the lens,
good visual acuity,
retinoscopy reflex should be crisp and sharp before and after blinking,
vision remains stable on blinking,
over-refraction gives a precise end-point,
refraction correlates with spectacle back vertex power,
keratometer mires stable and undistorted,
no irritation of limbal vessels,
no compression of bulbar cornea.”

In addition, contrast sensitivity (CS) chart testing (Ginsburg, 1984) showed a decrease of CS at high spatial frequencies for soft contact lenses (Thai et al., 2002). Thai et al. believed that the tear break up time could not be the reason for the intermittent blurred vision but did not consider whether the test lenses were steep fitted. Other publications, assuming properly fitted contact lenses, (Guillon et al., 1988) reported better CS with soft contact lenses in comparison with spectacles. Steep, flat, thin and thick soft lenses all produced a decrease in CS (Cox, 1995). Other literature regarding CS with contact lenses (Boxer Wachler et al., 1999) compared different products of soft contact lenses probably assuming a correct fit and found a significant difference between spectacles and CibaSoft lenses at 12 cycles per degree. There is a decrease in CS with standard soft lenses used on a daily wear basis after about 12 months' use. CS charts were used by the author as a tool to explain why lenses judged "good" by the users required replacement. The results with properly fitted soft lenses presented in Section 7.5 of this thesis are in accord with the author's experience. The author's lifetime experience in contact lens fitting confirms a decrease in CS with non disposable contact lenses over a period of 12 months' daily use. The author further confirms a connection between steep fitted contact lenses and a decrease in CS at high frequencies.

The shape and the power of soft hydrophilic lenses, as labelled in the original packing, are values at ambient room temperature when the lenses are immersed in isotonic saline solution. This ideal contact lens environment is not available for the soft lens when it is placed on the eye.

The ocular environment involves:

higher temperature,

slightly changing pH values,

different osmotic conditions,

air drying of the tear layer on the anterior lens surface

All these effects will change the parameters of the lens itself and these changes can affect the fit of the lens on the eye (Tranoudis and Efron, 2004).

3.7 *Contact lens movement on the eye*

The difference in cap volume between the contact lens itself and the cap volume of the eye covered with the contact lens played an important role with regard to contact lens movement (Leicht et al., 2005). In this model, Leicht dealt with a horizontal corneal diameter of 11.5mm, a vertical diameter of 10.7mm and a numerical eccentricity of 0.55 with corneal radii from 7.20 to 8.40mm. Leicht calculated an average corneal cap volume of 200mm^3 with a standard deviation of 15mm^3. They found the average cap volume of a disposable contact lens was 277mm^3. Leicht et al. further commented that with the slightest movement of the lens in situ, the difference in volume dramatically changes and the desired uniform lens dynamic on the eye cannot be expected. It is obvious that the difference in cap volume between lens and the bulbar area covered by the contact lens represents the tear lens. Leicht's work discussed the volume difference and its change due to lens movement only. An accurate contact lens fit was described as follows (Gasson and Morris, 1992): "*1 mm of vertical lens movement on blinking in primary position, a lens lag of up to 1.5mm on upwards gaze or lateral eye movements."* The movement of today's thin lenses on blinking and lag are significantly smaller (Leicht et al., 2005).

What keeps the lens in position on the eye?

Forst developed corneal models (Forst, 1981) and postulated, by utilising a simple equation, that deformation of contact lenses developed elastic forces when centring the contact lens again. He compared the cap volumes of the eye covered by a soft contact lens with the cap volume of the soft contact lens. He subtracted the two volumes and calculated the remaining volume between posterior lens surface and anterior surface of the eye covered by the contact lens. Forst found on a "*calculated model eye a volume of 0.7mm³"* representing the tear layer between contact lens and eye in primary gaze. The volume size influenced lens movement because a *"certain negative pressure"* built up due to contact lens movement caused by blinking. Forst suggested that the *"volume at least temporarily was closed while the tear liquid builds a tear meniscus around the lens edge."* For HEMA material he reported a negative pressure of *"a few tenths of a Torr"* while Forst estimated a negative pressure *"up to some Torr"* for silicone rubber lenses. Forst also calculated the negative pressure for rigid contact lenses with a model eye. The increase of cap

volume due to decentration was 0.4 mm^3 and resulted in a negative pressure of about 4 Torr.

A major part of lens movement is initiated by the motion of the upper lid. When lid closure starts, the upper lid starts to touch the lower lid from the temporal side towards the nasal side in a “zipper” fashion. The lacrimal gland, due to the squeezing force of the activated upper lid, releases a small quantity of fresh nutrition-rich and oxygen-rich tears which flush over and under the contact lens. Gas and nutrition are transported via the tears to the corneal epithelium. The old tears are washed away towards the punctum lacrimale. While rigid PMMA and soft HEMA contact lenses are oxygen barriers, modern contact lens materials have better gas permeability and provide more oxygen to the corneal surface. Tear mixing between the posterior lens surface and the front surface of the cornea is of essential importance (Lin et al., 1999, Guillon and Maissa, 1999). As soon the lids open again, the contact lens is pulled with the opening motion of the upper lid upwards and rotates from nasal to temporal and centres again after the lens reached the highest point.

3.8 *Contact lens comfort*

Contact lens comfort increased with the use of hydrophilic contact lenses but it remains an issue that causes drop outs of contact lens wearers as discussed by Epstein and Stone (2010). Prolonged research ended in a new silicone hydrogel material, with increased oxygen permeability, which was believed to resolve the problem of microbial keratitis which occurred more frequently in overnight contact lens wearing than with daily warers, which could not be proved. In his editorial article Jones (2013) summarized literature which reported whether the use of silicone hydrogel materials tended to improve the use of contact lenses by decreasing both the drop out rate of people using contact lenses and complication rates. Tucker et al. (2012) and Kern et al. (2013) measured the COF of different lens materials using an inclined plane measuring method. Tucker et al claimed that the measuring method presented measures kinetic friction applying a force of 0.8g to the test sample placed on glass plate in a saline bath which was inclined to get the sample moving. Both groups reported a correlation between the COF's they measured with the different materials and comfort. Neither the 0.8g force applied

nor the saline bath reflect the ‘in eye’ situation nor is there information on how the COF of the saline in which the experimental setup was soaked was considered. The outcomes of the friction measurements reflect the results of a combination of surface tension, van der Waals forces and an unknown type of friction, which could have been borderline, mixed or fluid friction. Furthermore, the method used to assess comfort was not described. Fonn et al. (1999) reported a reduced pre contact lens tear break up time (NIBUT) and increased dryness with Etafilcon A and Omafilcon A lenses with lens wearers who suffered dryness symptoms after 0.1, 3.5 and 7 hours wearing time. A correlation between subjective dryness and dehydration was not found. Decreased wearing time went together with measurable decreased comfort, increased dryness ratings and a reduced NIBUT. A negative correlation between water content and lens comfort was found by Efron et al. (1986) with soft lenses having a water content of 38%, 55% and 70%.

Chapter 4 - Friction

4.1 *Introduction*

There are two laws of friction. Firstly, that the frictional resistance is proportional to the load and secondly, that it is independent of the area of the sliding surfaces (Bowden and Tabor, 1950).

The three basic types of friction are:

a. Static friction
b. Dynamic friction
c. Fluid friction

These three types are dealt with in more detail below.

Static friction is defined as the force required to start a solid object moving on a solid surface. Where there is more force required to get the object moving, while maintaining movement, this is termed dynamic friction and this requires less force. It is known that even polished surfaces have microscopic small imperfections which block or hinder movement. Lubricants provide a layer between two surfaces. Any fluid acting as lubricant between two objects will reduce the resistance and will allow easier movement. If two objects separated by a lubricant layer move against each other the frictional properties of the lubricant have a frictional effect against the object only.

The first notes on the topic of friction were found in Leonardo Da Vinci's Codex-Madrid I dated 1495. Amonton (1699) rediscovered Da Vinci's two laws of friction:

"The areas in contact have no effect on friction.
If the load on an object is doubled, its friction will also be doubled."

Charles August Coulomb added in 1785 (Popov, 2009, Bowden and Tabor, 1950):

"Strength due to friction is proportional to compressive force"

Amonton's laws of friction are described as follows (Zeng, 2013):

The friction force is directly proportional to the applied load

The friction force is independent of the apparent contact area"

The equation expressing the coefficient of friction is:

$$\mu = \frac{F_r}{F_n}$$ Equation 2

where F_r is the resulting force and F_n is the normal force applied to the surfaces. The coefficient of friction, μ is a dimensionless number, which can be expressed as a percentage of the applied force. For example, if a coefficient of friction was 0.22 then the resulting force F_r was 22% of the normal force F_n applied. A difference between μ = 0.2 and μ=0.3 would be 10% of the normal force applied.

Static friction corresponds to the maximum adhering force. Static frictional force is the force required to get a stationary body moving. Human life would not function without static friction. Walking on concrete represents higher friction than walking on ice. Static friction is induced by adhesive forces and 'toothing' between surfaces. Related to the contact lens environment, static friction is represented by a contact lens placed on the eye and not moving. To measure static friction the contact lens needs to be moved. The measured initial force required to get an object, i.e. the contact lens, just moving is known as static friction. Dynamic friction is present at the contact surfaces between bodies moving linearly to each other. Coulomb stated that kinetic friction is independent of sliding velocity. Between some material pairings friction increases with speed which is called creep. Sliding or dynamic frictional forces are always smaller than static frictional forces as long the "normal force" F_n remains constant. In other words, more force is required to get a body moving than to keep it moving. Exceptions to Amonton's law of friction have been found in many cases (Zeng, 2013).

4.2 *Friction and Contact Lenses*

Contact lenses need to move with each blink and the space between lens and cornea must contain tear fluid. The movement of the contact lens with the blink exchanges the watery tears between the back surface of the contact lens and the front surface of the eye. Fresh tears produced by the lacrimal gland circulate under the lens. To maintain the tear environment when a contact lens is worn, tear exchange between contact lens and corneal epithelium must be maintained. Lipid secreted by the Meibomian glands, located on the lid edge, is present as a thin protective cover over the aqueous tears to minimise evaporation.

Analysis of in vivo contact lens motion is necessary to understand the frictional characteristics of contact lens materials and tear fluid. The investigations of Forst (1981) showed that modulus, lens thickness and thickness of tear layer between lens and eye influence lens movement. In human physiology, friction and lubrication play an important role with regard to joints and the flow characteristics of blood vessels. Hip joints and knee joints are surrounded by articular capsules and lubricated with synovial fluid. Hip and knee joints carry the weight of the body and still need to have low to zero friction. This is achieved by synovial fluid lubrication. Artificial joints suffer from wear and tear but do last some 15 to 20 years (Jin, 2002). Contact lenses float between the tears and the eyelids during blinking. Due to the different lubricating fluids, the differences in force, motion, friction and lubricating properties of natural and artificial joints cannot be compared with contact lenses in situ. The properties of soft contact lens materials play an important role regarding friction, as discussed in Section 4.4 Polymer friction. Soft contact lenses placed on the eye are surrounded by the tear fluid, acting as a lubricant and the implications of this are considered in Sections 4.3 Fluid friction between solids, 4.5, and 4.7 Tribology.

4.3 *Fluid friction between solids*

If two solid surfaces, which are separated by a liquid layer, are moved in a parallel motion with the speed "v" against each other, a decrease of speed develops within the separating layer. This is termed the 'declining shear' (v/h, where v is the speed and h the thickness of the fluid layer).

To move the surfaces with the speed v against each other, the force (F) is required and results in the pushing tension "$\boldsymbol{\tau}$". Fluid friction is a function of fluid viscosity only (Cimbala, 2012).

$$\boldsymbol{\tau} = F / A \qquad \text{Equation 3}$$

where F is the force and A is the surface area.

4.4 *Polymer friction*

Unlike friction between solids, polymer friction is dependent on speed between substrate and specimen and influenced by intermolecular and surface forces. Zeng (2013) mentions that various forces influence tribological properties. Zeng mentioned:

- van der Waals forces,
- forces between two molecules,
- electrostatic charged forces between charged molecules and/or surfaces in liquid, which might be attractive or repulsive.
- hydrophobic interactions,
- solvation,
- temperature dependent forces
- hydrogen bonding

Gong et al. (2001) described the dependence between COF and area of contact. She further described the relevance of van der Waals forces and speed. Gong *et al's* work on gel friction was based on a surface repulsion and absorption model that described the difference in contact between two solids and a solid and a water-swollen gel. The smaller elastic modulus of the gel causes the gel to deform even at a low pressure. Additionally, surface tension of a gel helps to make contact with the solid surface. Gel friction depends on the relation between load, elastic modulus and velocity (Gong and Osada, 1998). Gong et al. (2000) described the friction on gels and its dependence caused by pressure, repulsive and attractive forces surface properties of the opposing substrates as an interfacial interaction. They showed that increased attraction causes more friction and is also more dependent on load, with increasing attraction between gel and substrate when the load increases.

A simple comparison made by an anonymous author on the internet explains the issue: "*Imagine, something like chewing gum is sticking on the road. It is very lightweight but you already need a quite huge force to remove it (adhesion is dominating hence the friction coefficient is bigger than 1.0). Now imagine you have a complete tyre standing on the road. The adhesion force is still the same as on the chewing gum but your tyre and the car are bigger. Adhesion force is no longer dominating any more so your coefficient drops to under 1.0."* (mep, 2010)

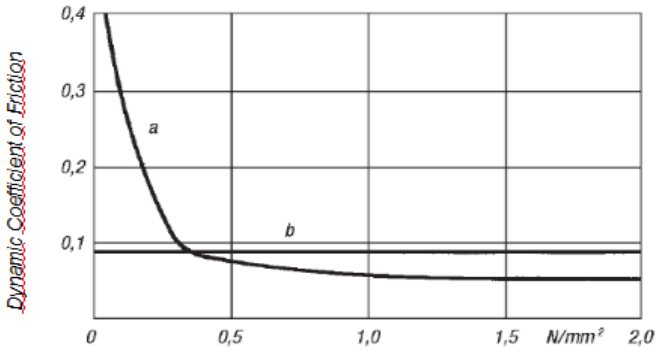

Figure 4.1 Dynamic friction of Polytetrafluoroethylene (PTFE) „Virginal Rundstäbe“ manufactured by Polytetra Moenchengladbach/Germany. Line a: Standard PTFE, line b: Fibreglass enhanced PTFE (Domininghaus, 2007)

In other words: As soon as the normal force applied to an elastomer is bigger than the adhesive forces between elastomer and substrate, the coefficient of friction decreases. The phenomenon was described in the dissertation of Deladi (2006), by Stoll and Strangfeld (2012), and in a literature survey by van der Steen (2007) and by Domininghaus (2007). Manufacturers of Polytetrafluoroethylene (PTFE) material made similar statements (Polytetra, 2013, Du Pont, 2013). DuPont (1996) described the frictional properties of PTFE in detail regarding the dependence of normal force and coefficient of friction. The friction coefficient at room temperature was reported to be 0.3 to 0.4 at 0.0134 kPa, 0.21 at 0.345 to 3.45 kPa, 0.08 at 1.52 to 15.17 kPa at a speed of < 0.00507m/sec (<2ft/min). The friction measurement results with the PTFE used in this work are comparable with these found by Polytetra and DuPont.

4.5 *Viscosity*

Viscosity defines the thickness of a fluid. A thick fluid has high viscosity and flows slowly while a thin fluid has low viscosity and flow fast. Fluids have a resistance to flow caused by the retarding force of adjacent molecules in the fluid.

4.6 *Rheology*

Rheology is a field of science related to flow. Flow appears with substances such as liquids, or soft solids, for example muds, suspensions or polymers. Fluids which do not change their viscosity when mechanical properties change, i.e. they are independent of declining shear, are called Newtonian fluids. Non-Newtonian fluids change their viscosity with the change of mechanical properties, i.e. speed or force. Non-Newtonian fluids are divided into the following groups:

Plastic fluids (Bingham- substances)

As soon as a defined shear tension is exceeded the substance starts to flow e.g. grease.

Dilatant fluids

These are fluids where viscosity increases with shear speed. Dynamic viscosity is not constant.

Thixotropic fluids

These are fluids where the viscosity is dependent on mechanical force and time of exposure. A thixotropic fluid displays a decrease in viscosity over time at a constant shear rate. In other words, viscosity increases as shear rate decreases. Tears, blood and synovial liquid are non-Newtonian thixotropic fluids.

4.7 *Tribology*

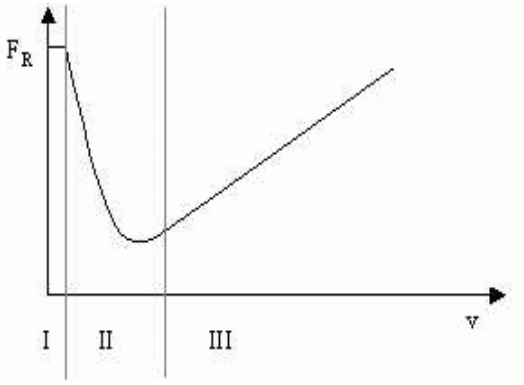

Figure 4.2 A schematic Stribeck curve showing the three different friction phases.
F_R= Frictional force. v=velocity, I - solid/boundary friction, II - mixed friction and III - fluid friction (with an increase in friction as the velocity [v] increases) (Wikipedia,2011)

Tribology is the scientific investigation of friction, lubrication and wear (Bartz, 1988). In tribology, the interaction of surfaces involving relative movement is studied. With regard to contact lenses, the following aspects of friction are relevant:

Solid/boundary friction, mixed friction and fluid friction. Stribeck (Jacobson, 2003) postulated that prior to relative movement static friction appears. As soon as surfaces begin to move against each other, boundary friction takes place. With increasing speed a lubricant layer builds up and mixed friction takes place. The period of change from mixed friction to fluid friction is called the transition point.

With increasing speed more (molecular) surfaces of the lubricant slide between each other and the resulting increase of inner friction of the lubricant increases the friction of lubricated substances.

Fluid friction is a function of fluid viscosity and as long as fluid is provided, the friction measured is the friction of the fluid and not of the lens. The graph in Figure 4.2 shows a Stribeck curve at all three stages. The curve describes the development of the frictional force which depends on the frictional speed under hydrodynamic conditions. In section I boundary lubrication took place. It shows a high coefficient of friction because there was contact between the surfaces. Section II shows the intermediate or transition phase where mixed friction appeared. The frictional forces decreased with increasing velocity. Section III shows a steady increase of friction which was the result of increasing speed. The thickness of the lubricating layer plays a role regarding the type of friction and is proportional to velocity, proportional to viscosity and inversely proportional to load. Zeng (2013) named ~1nm film thickness for boundary lubrication, 2-5nm for intermediate or mixed friction and ~10nm for fluid friction with an undefined lubricant. The tears, acting as a lubricant on the eye, are thixotropic which might lead to different layer thickness and different frictional behaviour, not only between the lubricants but among different subjects. In lubricated systems friction depends on a the viscosity of the lubricant, the sliding speed and the normal force. However, with boundary or dry friction the lubricant layer is either non- existent or ~ 1nm thick. Layer thickness at mixed or intermediate friction is 2-5nm, and the lubricant thickness is between ~10nm and 10µm with thick film or fluid friction (Zeng, 2013).

Stick-slip phenomenon

In an unlubricated environment, the change from static to dynamic friction, in many cases, does not result in a Stribeck curve. It is common knowledge that unlubricated door hinges start to squeak and that chair legs make a noise when moved on the floor. This undesired noise is caused by a type of stop-and-go motion called the ‘stick-slip’ phenomenon. A graph of a friction measurement showing the stick-slip phenomenon is shown in Figure 4.3.

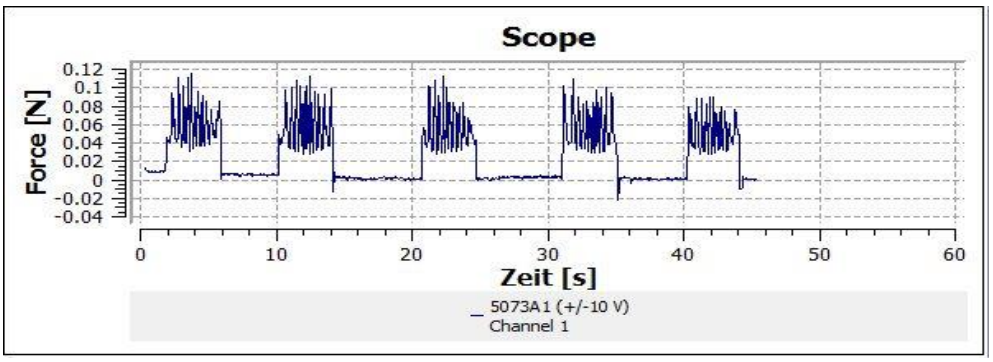

Figure 4.3 Stick-slip phenomenon seen while adding force five times for 3 seconds

Note:Zeit = Time

Surface quality

It is known that an absolutely even homogenous surface cannot exist (Bowden and Tabor, 1950, Besdo et al., 2010, Axel, 2009). Even polished or cast surfaces do have microscopic small asperities that cause friction. The size and nature of these asperities in conjunction with the type of material friction can vary (Bowden and Tabor, 1950). This applies, of course, to contact lens surfaces. Today, a number of different methods of smoothing contact lens surfaces are used.

4.8 *Contact lens friction and lubricity*

Movement of contact lenses on the cornea is essential for nutrition and gas exchange. The tear film between the posterior lens surface and the anterior surface of the cornea causes capillary attraction which prevents the contact lens from falling out of the eye. It is a cushion and a lubricating layer between the posterior lens surface and the cornea and a lubricating layer between anterior lens surface and the eyelids. The reason for friction between flat surfaces are the microscopic small asperities (Bowden and Tabor, 1950). Lubricants such as grease or oil on metals, or tears between a contact lens and the eye, produce a thin layer covering the asperities and reduce friction.

When the upper lid opens, the contact lens is pulled upwards until the lens edge stops as the upper lens edge touches the superior limbal area (Veys et al., 2003, Golding et al., 1995a). The lens then starts to drop slightly and centres again due to

the elastic forces of the lens material (Forst, 1981). Rotationally symmetrical contact lenses rotate with each blink from nasal to temporal (Figure 4.4).

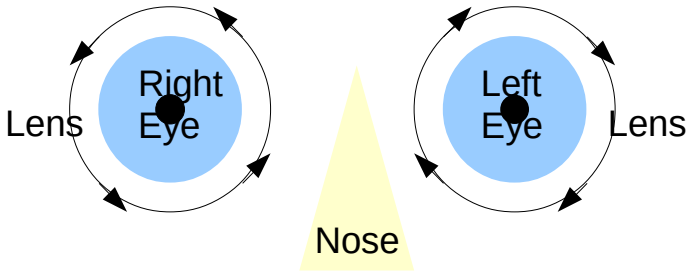

Figure 4.4 Contact lens rotation in situ. Due to the structure and movement of the lid, the lens of the right eye rotates in the opposite direction to that of the left eye.

It is suggested that the rotational movement is caused by the specific dynamic of the lid referred to above (Abel and Thiele, 1968, Hanks and Weisbarth, 1983). In contact lens fitting, the relationship between the anterior shape of the eye and the posterior shape of a contact lens is conventionally described as flat, parallel (or aligned) and steep. A flat fit will generally produce a loose fitting lens, a steep fit will produce a tight fitting lens and an aligned fit should give the optimal fit.

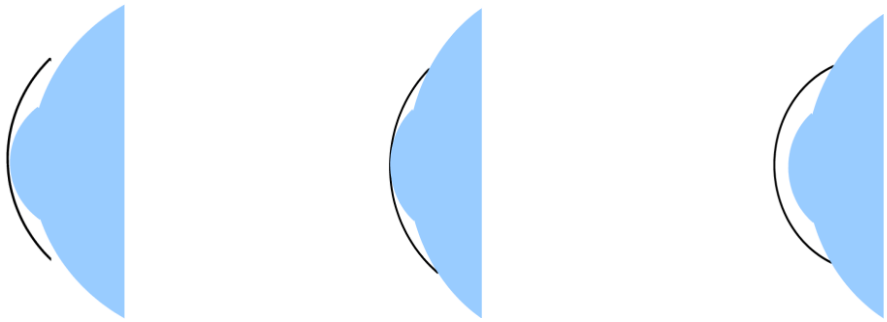

Figure 4.5 Explanation of flat, parallel (aligned) and steep contact lens fit.
In reality, a soft contact lens will bend around the eye surface and not leave air gaps as seen in this diagram.

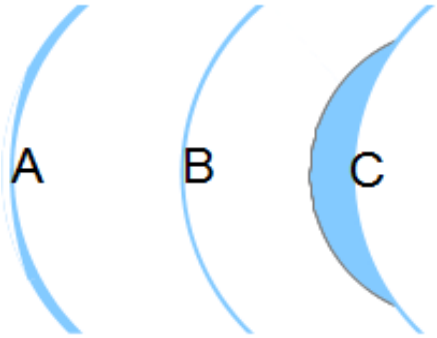

Figure 4.6 (A) minus lens with peripheral shoulder, (B) back surface parallel to front surface (C) positive lens with anterior second curve.

Besides the necessity to fit to the cornea, the required optical correction influences the shape of the lens. While a concave shaped lens (minus lens) correcting a myopic (short sighted) subject consists of a thick edge and a thin centre, a convex shaped lens (plus lens) has a thick centre and will be thin at the edge. To reduce centre or edge thickness the optical useable areas are

smaller than the lens itself. The optical usable area is the optic zone which is surrounded by a shoulder, called lenticular zone. In nearly all cases these design elements are present on the anterior surface of the lens while elements related to the shape of the eye are located on the posterior surface.

Depending on the fit of the contact lens on the eye, the elastic forces of the lens material will influence the lens movement dynamics (see page 37). An aligned lens fit is required in order to exclude undesired lens movements.

A liquid layer is always present at the posterior surface of the contact lens so that fluid friction under comparable conditions (i.e. at body temperature) can be assumed. It is known that a sufficient tear layer between the posterior lens surface and the cornea has to be maintained to provide proper metabolic conditions for the corneal epithelium.

Friction during the blinking process

The movement of soft contact lenses on the eye is necessary to achieve nutrition and gas exchange by exchange of the tear layer between the inner contact lens surface and the outer corneal surface. The literature regarding the importance and behaviour of lens movement in conjunction with a lid blink is to some extent controversial. Some authors (Veys et al., 2003, Walker et al., 2003, Wolffsohn et al., 2009), claim that lens movement is not important and static lenses give better fitting results than mobile contact lenses – a view not held by others (Leicht et al., 2005, Gasson and Morris, 1992, Cox, 1995). The impact of a hydrogel lens settling on the eye with time was investigated (Nichols and King-Smith, 2003) and showed an average thinning of the post lens tear film from an initial 4.5 micrometres to 2.5 micrometres after 30 minutes of soft lens wear. The posterior lens surface is separated by the tear film from the mucous layer which covers the corneal epithelium. Fluid friction takes place at this interface as explained in Section 4.3. It can be postulated that the pressure of the eyelid squeezes out the tear layer between the conjunctiva of the lid and the front surface of the lens and fluid friction momentarily does not exist. Thus, during lid opening, there is very little fluid between the lens' front surface and the lid, resulting in the lens being dragged upwards. A more constant level of fluid between the cornea and the lens implies a smaller degree of friction. The lid closes and opens again and forces the contact lens to rotate and to move relative to the eye.

During the blink downwards, fluid friction probably takes place again which applies for both soft and rigid lenses.

Calculating friction for a segment of a spherical shell

Projected area and force

Vertical force acting against a horizontal surface is the normal force F_n and is calculated as:

$$F_n = m * g \qquad \text{Equation 4}$$

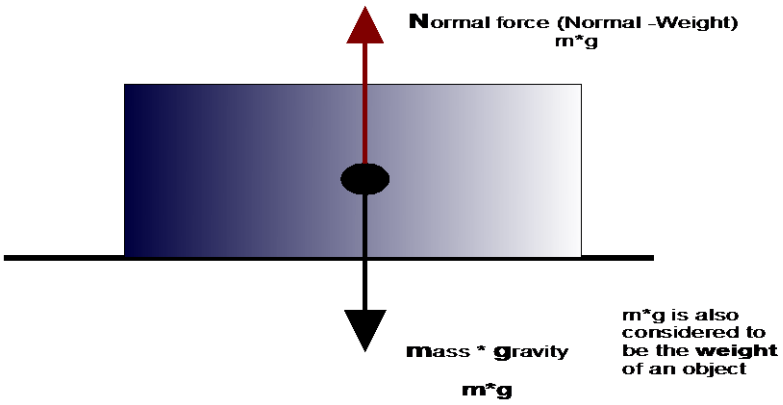

Figure 4.7 The relationship between force, mass and gravity.

where m stands for mass and g stands for gravity, and is expressed as weight.

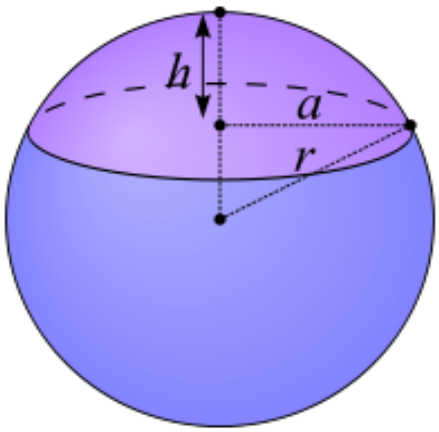

Figure 4.8 Spherical cap (Wikipedia 2015)

Viewing a spherical cap, the area seen from the top is the 'projected' area of the segment. This projected flat area is smaller than the 3-dimensional surface area of the shell segment (Figure 4.8)

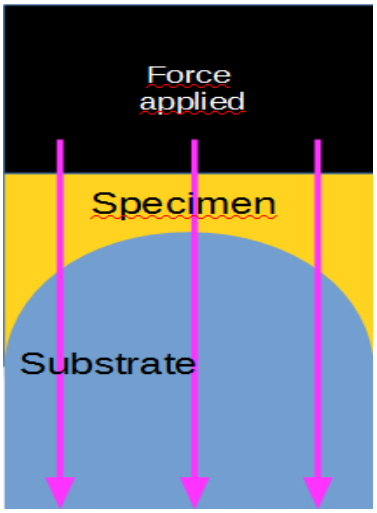

Figure 4.9 Force upon a projected area

The normal force is evenly distributed upon the projected area see Figure 4.9 and **Error! Reference source not found.**. As illustrated, the pressure distribution on the projected area is uniform while it is not over the ball shaped area of the spherical cap. Logically, and according to Brinckmann et al. (2000), it is the projected area of the cap of a ball which is relevant for the force distribution. The maximum partial force on a hemisphere is to be found at the apical area whereas the partial force at the edge of the hemisphere is zero. The force acting against the sphere is split into the normal force, acting radially to the spherical surface, and the resulting tangential force. The tangential force compensates itself for symmetry reasons (**Error! Reference source not found.**).

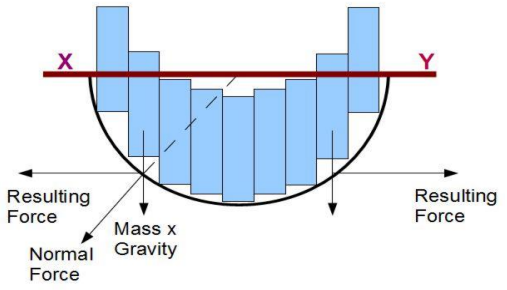

The line X-Y indicates the edge of the semi circular shell

Figure 4.10 a projected area.

The average pressure acting against the surface of a sphere is calculated by calculating the force acting against the projected area of a shell (Brinckmann et al., 2000). The projected area A is calculated by the conventional formula

$$A = r^2 * \pi \qquad \text{Equation 5}$$

Where r stands for the radius of the projected area.

The Average force (F_m) is calculated as follows:

$$Fm = \frac{Fn}{A} \qquad \text{Equation 6}$$

where F_n is the normal force and A the area.

Average circumference of a sphere segment

The following calculations were necessary to be able to simulate the blink speed of an eye. Attention had to be drawn to the difference between friction produced between plain shaped contact areas between substrate and specimen and the apparatus described in Section 5.5. The apparatus used a ball shaped substrate to produce friction. Friction between two plain surfaces is produced by the same speed over the complete area of contact. With the use of a rotating sphere, a speed difference beteween the apex and off the apex naturally exists. Outside the apex the speed in terms of distance (i.e. mm) per revolution, called circumference speed, is lower. The ball shape drawn in Figure 4.11 gives an explanation.

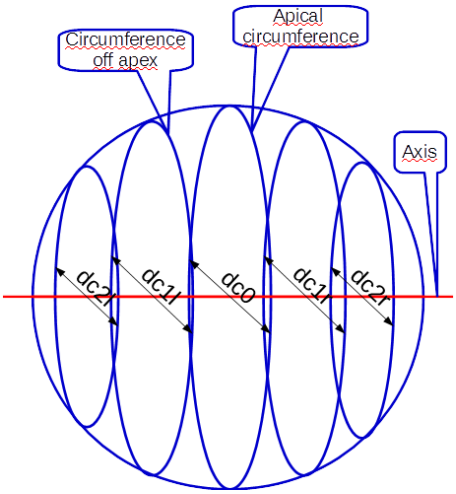

Figure 4.11 Explanation of average circumference of a sphere or sphere segment

The apical diameter is marked dc0. Off apex diameters dc1l and dc2l are located left of the apex. Off apex diameters dc1r and dc2r are located right of the apex.

When the sphere rotates around the axis the surface velocity varies from a maximum at the apex to a minimum at the axis. The circumference at the apex of the sphere mounted on a spindle equals the normal circumference of the sphere. Spatial diameters off the apex, for example diameters marked dc1 and dc2 in Figure 4.11 result in a smaller spatial circumference than the apical diameter. By dividing the shell into small annular slices it is possible to use the spatial diameters to calculate an average circumference and the average circumference velocity of a sphere or a sphere segment. In the test planned, the ball will turn to simulate eye movement. If the suggested ball with a diameter of 24mm rotates once per second the speed at the apex is 75.4mm per second. On top of the sphere a semi finished soft, hydrated contact lens with a BOZR of 12mm and a diameter of 10mm, representing the

specimen was placed. The average circumference and the average circumference speed for the area was calculated by dividing these areas into small steps.

Sphere radius (r): 12mm. Resolution 0.1mm for half the chord length. There are 51 steps for a chord length of 5mm. For symmetry reasons the calculations were necessary for half of the sphere only. The slice diameter was calculated by deducting the sagittal height from the radius. Equation 7 was used and Figure 4.12 gives an explanation:

$$2\sqrt{(r^2-(\frac{chord}{2})^2)}\pi \qquad \text{Equation 7}$$

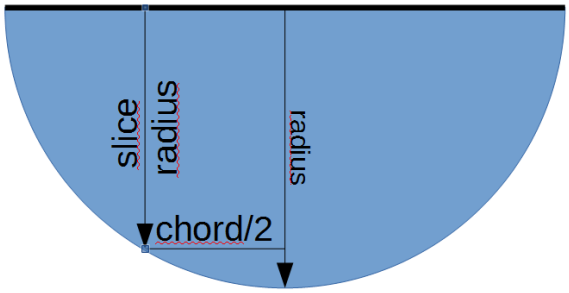

Figure 4.12 Explanation for the calculation of the slice diameter of a sphere (spatial diameter) Note: the diameter is 2 times the radius.

The diameter at the apex then is 24mm and at h equal to r=12mm the slice diameter is 0mm. At h=5mm the slice diameter is 73.13 mm. Note: The edge of the 10mm diameter specimen placed at the apex of the sphere (the substrate) is located at 5mm displaced left and right from the apex.

Disk diameter 24mm, width 10mm,				
No.of slices for 10mm chord length	Average diameter= Sum of slice diameters/number of Slices	Average circumference for 10mm chord length	Circumference of 24mm sphere	Projected Area of 10mm cap
51	23.28	73.13 mm	75.40 mm	78.54 mm

Table 4.1 Average circumference of sphere segments.

To measure dynamic friction the sample or the substrate needs to be moved at a constant speed. A given sphere segment having a diameter of 24 mm has a circumference of $24*\pi = 75.398$ mm at the apex. The diameter at the infinitely small axle is zero. The infinitely small circumference is zero. So the spatial speed at the axle is zero. At the apex the circumference is largest and therefore the circumference speed is highest. It was believed to be necessary to evaluate the difference in speed between the apex and the outermost area of contact between the test sample and substrate. The above technique was used to calculate the slice diameters for the contact area in 0.1mm increments. There were 121 circumference slices for a hemisphere and 51 for a width of 5mm. The results start at 75.398mm and end at 68.451 mm at a chord length of 10mm or 5mm left and right off the apex. The sum of all the circumferences divided by the number of calculations gives the average diameter of the ball. For a projected area of a shell having a radius of 12mm and a segment diameter of 10mm the average circumference was 73.132mm.

The relationships between force, normal force, weight, and eventually pressure can be explained as follows:

Weight and mass on earth are about the same in most circumstances. Weight however depends on gravity which is a given constant on earth. If a defined mass having a specified weight on earth is moved to the moon, which has less gravity, the mass in question is less. Free falling objects affected by gravity accelerate at $9.80665\frac{m}{sec^2}$.

One newton (N) is the force required to accelerate 1 kilogram of mass at the rate of 1metre per second squared. To achieve a force of 1N a mass of 1/9.80665 is required. This equals 101.97gram. Pressure is defined in Pascals which can be

expressed in N/m². Both the Newton and Pascal (Pa) units are derived SI[1] base units. 1Pa equals 1N per m². In medicine pressure often is expressed in millimetres of mercury, i.e. blood pressure or intraocular pressure. For instance the standard atmospheric pressure at mean sea level is 1013.2 hectopascal equalling 760mm Hg (millimetres of mercury).

Gram	Milli newton	Newton	mm²	m²	Pascal	N/mm²	mN/mm²
101.97	1,000.00	1.000	1,000,000.00	1.0000	1.00	0.00000	0.001
10.20	100.00	0.100	1,000.00	0.0010	100.00	0.00010	0.100
1.02	10.00	0.010	100.00	0.0001	100.00	0.00010	0.100
100.00	980.67	0.981	1,000,000.00	1.0000	0.98	0.00000	0.001
10.00	98.07	0.098	1,000.00	0.0010	98.07	0.00010	0.098
10.00	98.07	0.098	100.00	0.0001	980.67	0.00098	0.981
10.00	**98.07**	**0.098**	**78.54**	0.0001	1,248.62	0.00125	1.249

Table 4.2 Sample calculations related to mass causing force
and resulting in pressure. Note: Millinewton per square millimetre equals Pascal

The parameters of the substrate and the projected area of the contact lens to be tested need to be considered for calculating the forces and friction. For the example which follows, the diameter of the projected surface is 10mm and the radius of the shell is 12mm. The sample calculations below give an idea of the forces and partial forces applied.

A mass of one Kilogram represents a force of 9.81 Newton according to SI Standards (Taylor and Ambler, 2008). Distributed over an area of 1m² 9.81 N represent 9.81 Pascal or approximately 0.074mm Hg (or Torr). Since 1m² equals 1,000,000mm² the partial weight force over an area of 1mm² is 0.000010 N or 0.01 millinewton. 10 grams applied to an area of 78.54mm² causes a partial pressure of 1.25 pascal or millinewton per square millimetre at the projected area of a sphere segment of 10mm diameter (see Table 4.2 and Figure 4.8). To imagine the forces of the measurement results, the examples below should be kept in mind:

[1] The name SI unit comes from the International System of Units which is based on the metric system and adopted by most countries in the world.

- 0.1 N required 10.197 gram mass to be applied
- 1.0 N required 101.97 gram mass to be applied
- 10.0 N required 1019.72 gram mass to be applied
- 20.0 N required 2039.43 gram mass to be applied

The pressure of

- 1 Pascal requires a force of 1N per m^2
- 1 Pascal requires a force of 1 Millinewton per mm^2

4.9 *Review of soft contact lens tribometry*

Most of the published tribometric tests (Table 4.3) have been carried out with a small glass sphere loaded with a given force to the contact lens. It was assumed that the lubricant between glass sphere and lens surface always maintained a film between the surfaces so that lubrication was achieved. According to Stribeck's theory (Stribeck, 1902) different frictional forces apply. Applying more weight during the test changes the state of the tribological situation as well as the type of friction. Fluid friction between solids is caused by the viscosity of the lubricating liquid between the glass sphere and the lens. In other words, as long as liquid is between the glass sphere and the contact lens, the frictional properties of the liquid are always the same (Fowler, 2007). As soon the glass sphere squeezes the lubricant out, it has to be suggested that sliding friction without lubrication or mixed friction takes place (Higginson, 1962). A range of multipurpose, commercially available or custom made tribometers have been utilised and these have incorporated steel spheres or glass plates to test their frictional characteristics.

Senofilcon-A contact lenses (Johnson & Johnson) have been tested using a stainless steel sphere on a contact lens surface immersed in saline solution under a force of 0.5mN and 100 mN with sliding velocities of 0.01cm/s to 0.5cm/s (Zhou et al., 2011). In these conditions Amonton's law (*frictional force is linearly proportional to the load*) seemed to apply and it appears that viscosity plays little part in this arrangement.

A Biomechanical Universal Micro Tester (CETR UMT) has been used for contact lenses. Lenses have been tested using a pin on disc method using glass or steel discs.

The lenses tested have been immersed in their packaging solution (probably buffered saline). The graph presented showed a static friction coefficient of 1.1 while the dynamic, stick-slip friction varied between zero and 0.2 (Gitis, 2004). The TS-501 Triboster produced a friction coefficient with Acuvue Oasys lenses of μ=0.2 at a constant speed (EBATCO, 2012). Another test (Roba et al., 2011) used a commercial microtribometer (Basalt Must, Tetra, Germany) with a glass pad, instead of a spherical shaped pin, as substrate and this arrangement showed friction coefficients for 15 different types of contact lens between 0.018 and 0.542. The tests included simulation of mucin debris on the glass plate and blink cycles of 50 and 100 blinks using varying forces from 0.25 to 5 milliNewton (mN). Another pin on disc microtribometer (custom made) test investigated Vistakon lenses and used a 1mm diameter glass sphere with a normal force of 10-50 mN. The results showed friction coefficients between 0.01 and 0.1 depending on the position of the cantilever to the lens, (Rennie et al., 2005).

Bausch and Lomb SeeQuence and SeeQuence2 lenses have been tested with saline solution as lubricant utilising PMMA or PolyHema as substrate and the results showed friction coefficients between 0.045 und 0.308 (Niarn and Jiang, 1995).

Other techniques like atomic force microscopy have been used to measure friction of hydrogel contact lenses. The reported results showed an increasing roughness after wear of contact lenses (González-Méijome et al., 2009).

Kim et al. (2002) found that the presence of ionic functional groups at the surface lowered the friction and adhesion to a hydrophobic polystyrene tip. Tribological tests were carried out on contact lenses (Focus Dailies, CibaVision) containing polyvinylalcohol. These were immersed in an ionic environment and utilised a stainless steel arbour with the specimen immersed in an ionic solution kept in a steel container. Scanning probe microscopy was carried out at the same time. This showed that borate buffered saline induced more roughness on the lens surface but it seemed to be a reversible process when using pure water (Dong and Haugsted, 2011). The static COF of PHEMA 38% material was reported to be μ= 0.6 see Dunn et al. (2013a). They carried out friction measurements using atomic force microscopy on a silicone hydrogel daily disposable contact lens containing 33% water and an approximately 5μm thick copolymer surface layer with more than 80% water content. The substrate used was described as a *colloidal "silica particle"*

which indented between 40 and 200 nm into the copolymer surface layer. While the dynamic COF's reported to be μ=0.02 the numbers in Fig. 4b of the paper show a $F_{n=}$ 1000μN and a F_r= 700μN which resulted in a static friction of μ= $\frac{700}{1000} = 0.7$on the sponge-like polymer surface containing 80% water using a commercially available borate buffered saline solution. New but unpublished work was carried out by Thiele (2012) using a hydrogel as a substrate for friction measurement. In a telephone conference with the company advisor the following information was given: "*Comparison with literature findings is impossible. The substrate of the system is a hydrogel. Remember that speed and pressure give different measurement results. The coefficient of friction is judged as a systematic parameter and should not be used. The measurement results shown as curves allow better interpretation of the material properties".*

A general, not contact lens related, overview of the friction and lubrication of hydrogels was reported by Gong (2006). She described the differences between biological surfaces with an extraordinarily low friction coefficient in the range of 0.001 to 0.03 and the complexity of gel friction which hardly can be compared to rubber friction. The article concluded that gels do not obey Amonton's law, but hydrophilicity, electrical charge, crosslinking, water content, and elasticity play a role. In addition, Gong reported that substrate surfaces, their load, structure and hydrophobicity are further factors influencing the frictional behaviour of gels.

It seems to be necessary to differentiate fluid friction between solids from other types of friction. Various reasons could exist for the appearance of static friction in an *in vitro* testing environment that do not actually appear in soft contact lens wear. Gong (2006) described in her repulsion-absorption model of gel friction a gel containing non-adhesive tangeling (i.e brush-like) polymer chains which reduce friction on, for instance, glass dramatically while adhesive chains increase friction dramatically. The use of different substrates, different lubricating agents, i.e. Newtonian and non Newtonian fluids, different probes, different methods, the mix between static and dynamic friction resulted a variety of COF's some of which were lower than ice on ice (Mills, 2008), or synovial joints in humans (Serway and Jewett, 2013) as shown in Table 4.3

The substrate material e.g. steel or glass used as a probe together with saline solution could allow the probe to indent and have a direct, unlubricated contact with the lens surface. This could result in unlubricated friction. It is theoretically possible that a contact lens *in situ* could adhere to the corneal epithelium. Most possible substrates like polished glass or polished PMMA are suitable to hold the contact lens for testing but are unlikely to test the frictional properties of contact lens materials due to their deformation and/or destruction. The only way to overcome this problem was to use a more suitable substrate, for instance Teflon (Polytetrafluoroethylene) which is known to have extremely low frictional properties. When assessing friction, the measurement is a comparison between materials. This could be between two identical pieces of material or different materials. The frictional properties of fluids are a function of viscosity, as mentioned on page 42. The figure shows the friction between the material and the substrate. Using a different substrate would have produced different values. Materials with similar frictional and suitable chemical properties like fluorinated ethylene propylene (FEP) and Teflon-FEP needed to be evaluated.

When wearing soft contact lenses for a long time the nomal blinking rate of about 12 times per minute, normally triggered by evaporation of tear fluid, is reduced. The soft lens acts as a bandage with a tear layer between lens and eye. Tear evaporation occurs on the anterior lens surface and the blinking reflex was not triggered. Blinking is triggered as a habit and the rate decreases by the years of contact lens use. The author has observed blinking rates of one blink per minute and less with patients who have worn soft lenses for many years. As a result, the anterior lens surface becomes dry and various settling effects of the lens on the eye can be observed.

Researcher	Title	Tribometer type	Method	Specimen	Lubricant	Reported Friction Coefficients	Notes
Niarn, Tong-bi (1995)	Measurement of the Friction and Lubricity Properties of Contact Lenses	Custom built	Pad on disk	Seequence against PMMA or PHEMA	Saline	0.05 – 0.21	
Rennie et al. (2005)	Friction coefficient of soft contact lenses	Custom made	Glass Pin on Lens	Etafilcon A	Packing Solution (Saline)	0.025-0.075	
Roba et al. (2011)	Friction Measurements on Contact Lenses in Their Operating Environment	Basalt_x0003_ Must, Tetra_x0003_, Germany	Glass Pad on Lens	Various commercialy available products	5% Blood plasma with 5005ppm lysozyme	0.017- 0.34 Daily disposable 0.011-0.56 reusable	Results after 100 cycles
EBATCO (2012)	Friction of Contact Lenses in Saline Solution	TS 501 Triboster	Glass Pad on Lens	Acuvue Oasys	Saline	.25 (Static) 0.2 dynamic	10mm distance
Zhou et al. (2011)	A study of the frictional properties of senofilcon-A contact lenses	CSM Nano Tribometer	Steel ball on lens	Senofilcon A (Oasys)	Saline	0.001 (viscous flow) 0.1	Amontons Law applies
Steffen et al. (2004)	Finding the Comfort Zone	Not defined		Acuvue Adv., Focus Night & Day, Acuvue 2, Pure Vision		0.006, 0.049, 0.01, 0.02,	Data only
Gitis, N. (2004)	Tribometrological Studies In Bioengineering	UMT Microtester	Steel and glass disks	Focus and Pure vision	Saline	Static 1.1, dynamic 0.2	
Dong and Haugsted (2011)	Tribology study of PVA contact lens in ionic aqueous environments	Scanning Probe Microscopy		Focus Dailies	Saline	Arbitrary units reportet	Two saline types different results
Uruena et al. (2011)	Contact Lens Boundary Lubrication and Friction Reduction with Hyaluronic Acid	Microtribometer	Glass Pin on Lens	Acuvue Oasys Pure Vision	Various Hyaluronic acid conc. and Unisol Saline	<0.01 with Hyaluronic Acid @0.15mg/mL 0.6 with saline and lower concentration	
Thiele, E. (2012)		Custom built		not published	not published	not published	frictional forces pressure speed substrate depending
Ngai et al. (2005)	Friction of contact lenses: Silicone hydrogel versus conventional hydrogel	Not defined					
Kim et al (2002)	AFM and SFG studies of pHEMA-based hydrogel contact lens surfaces in saline	n/a	AFM and SFG microscopy	n/a	saline	not published	reduced friction with lubricant

Table 4.3 Reported friction coefficients

Chapter 5 - Rationale for in vitro experiments

5.1 *Introduction*

The aim of the experiments described in this chapter was to assess the frictional characteristics of contact lenses *in vitro* leading to the *in vivo* experiments in the chapter that follows. As there are no tribometers commercially available o specifically designed to test contact lens samples a custom made device was constructed and a selection of current contact lens materials chosen. The designs of all the soft lenses will be standardised.

It is necessary to clarify that the work presented in this chapter was not seeking to measure absolute frictional values related to the type of material used. Instead it was the authors's intension to simulate in vivo conditions and present results under these conditions. Absolute, material-related values collected by the same measurement equipment may differ because of different speeds of rotation, different normal forces, different duration of testing, or different resting times between measurements.

The frictional characteristics of contact lenses with a lubricant (physiological saline solution or a contact lens lubricating solution) was investigated. Contact lens lubricating drops are saline solutions containing viscosity enhancing substances to keep the eye moisturised (Dolder and Skinner, 1983). To avoid undesired adverse responses these solutions are marketed as artificial tears, tear substitutes, wetting or cushioning solutions and are packaged as monodose drops and should be free of preservatives. The European Pharmacopeia (European Directorate for the Quality of Medicines & Healthcare, 1986) and the Austrian Pharmacopeia (Arzneibuch, 1991) prescribe euhydric conditions[2] for eye drops. In contradiction to the legal requirement, lubricating solutions in question need to have a viscosity more than 25mPa but less than 55mPa (Dolder and Skinner, 1983). Viscosity agents that have often been used are: Dextrane 70, Hypromellose, Hydroxypropylcellulose, Polyvidone and Polyvinylalcohol; see Martindale, the extra Pharmacopoeia

[2] Euhydric conditions are described as isotonic, iso-osmotic and iso-oncotic. At least two of these conditions must be fulfilled to achieve comfort when instilling ophthalmic preparations onto the eye.

(Reynolds, 1989). Sodium Hyaluronate 0.1% administered to the eye resulted in tear stability of 10 dry eye patients for at least 40 minutes (Mengher et al., 1986). It is used in other moistening solutions such as Hylo-Comod eye drops by Croma-Pharma (Croma, 2012) and Blink eye drops by Abbot Medical Optics (Korb et al., 2005).

Ophthalmic preparations such as buffered physiological saline solution commonly used to store lenses prepared for sale in the original containers, most of them in sealed glass vials. Disposable contact lenses were stored in blister packs, containing one contact lens stored in a buffered saline solution. To enhance initial wearing comfort and wetting properties after lens insertion, so called wetting agents were added to saline solutions. Menzies and Jones (2011) investigated the properties of blister pack solutions and discussed the various properties of the solutions which were the result of non-specified ingredients to enhance wetting properties, resting time on the lens during wearing and reduction of surface tension. They concluded that these solutions containing these non-specified ingredients might have clinical implications for initial comfort after lens insertion. The question regarding adverse- or side effects was not raised. A work on the in vitro effect of surface active ingredients regarding contact lens wettability (Lin and Svitova, 2010) showed that the ingredients of the blister pack solutions tested contained surfactants to decrease the contact angle of the air-aqueous interface. The surface tension of all tested blister pack solutions was lower than water and indicated the presence of surfactants. The possibility of a relationship between in vitro lens surface wettability and clinical contact lens performance or in vivo tear film stability was not investigated. For users being sensitive to the "*soapy"* residues of the solution on the lenses they suggested that the lenses should be rinsed with surfactant-free rinsing solutions or should be disinfected with an overnight H2O2 disinfecting system prior to use. The possible types of surfactants and the consequences of instilling such substances systematically with the insertion of daily disposable lenses was not discussed. Polysorbate 20 and Polysorbate 80, are non ionic surfactants used in baby shampoos, various cosmetic products, drugs, food and in soft contact lens cleaners. The method of use was presented by Shinoda (1969) who presented the HLB system. Taniguchi et al. (1988) reported that with the use of Polysorbate 80 the corneal permeability was accelerated. It was reported (Salem and Katz, 2003) that surfactants caused cell

death as a result of injury. A friction study with pHEMA lenses on living epithelial cells (Dunn et al., 2008) caused significant cell death with sliding friction with a 500yN (0.0509g) load having a COF of 0.02 soaked in growth media bath between cell layer and contact lens substrate.

Celluvisc lubricant eye drops (Allergan, 2012) contain the active ingredient Carboxymethylcellulose sodium 1% in a phosphate buffered saline solution. It has been chosen as an extra-thick viscosity agent to demonstrate differences between iso-oncotic and hyperoncotic fluids in combination with soft contact lenses[3].

Tribometric testing of soft contact lenses needs to simulate reproducible environmental conditions that are comparable to a contact lens *in situ*. This includes the shape and the motion of the upper lid. A representative force can simulate lid tension. To ensure the measurements are as reliable and as consistent as possible, the radius of the substrate had the flattest possible radius, identical to the contact lens material (12mm) which helped to minimise errors.

The experiments described in this chapter attempted to show the frictional characteristics of the representative soft contact lens materials, as well as the characteristics of solid substances to reference materials without the use of a lubricant between the test material and the substrate. It is known that friction of elastomers and gels do not follow the laws of friction between solids. For example, adhesion, boundary layer effects, surface quality, resting time and force affect the frictional behaviour of the materials in question (Yurdumakan et al., 2007, Besdo et al., 2010, Gong, 2006). Gong (2006) concluded that a method of friction measurement to cover all different types of non-solid materials had not yet been found. To insure reproducibility of the findings, standardised commercially available substrates were chosen together with a reproducible method of manufacturing the contact lens surfaces. The same machinery, cutting tools, production methods and polishing slurries were used throughout. Further, the resting times between start, and subsequent restarts of the test, were controlled. The

[3] Oncotic pressure or colloidosmotic pressure is the pressure caused by colloids in addition to the osmotic pressure. Blood and cerebral fluid are judged as isooncotic, while the products in discussion are hyperoncotic (Schmidt & Florian 2007)

environmental relative humidity were kept between 40- 60% [4]. Force and speed parameters were standardised and attempted to simulate the forces and speed found in the natural blink. To this end, it was anticipated that the results found were more realistic and more capable of being averaged than those found with routine "industrial" tribometers. Charge, crosslinking, water content and elasticity of soft contact lens materials chosen were given factors for the materials chosen mentioned by Gong (2006). The setup of the contact lens tribometer was designed in an effort to avoid additional factors which could influence the results. Prior to measurement care was taken to position the specimen free of mechanical stress on top of the substrate so that the normal force was applied evenly and distributed over the tested material. Care was also taken not to bend the test samples or produce other than normal force.

5.2 *Experiment 1 - The construction and testing of a Contact Lens Tribometer*

Background

In general, there is no standard tribometer for all types of material, but there are commercially available multipurpose devices for testing friction. Friction appears commonly in daily life between solids, liquids and fluids. For the various types of friction, specific measurement methods and devices are used.

Friction coefficients of different soft contact lenses have been measured with sphere and plate type tribometers (Table 4.3). Atomic force microscopy has been used to visualise silicone hydrogel contact lens surfaces before and after use. Frictional properties of polyHEMA contact lenses immersed in physiological saline solution and also with dehydrated lens surfaces have been tested using atomic force microscopy with the obvious result that friction was significantly reduced when the lens was immersed in saline (Kim et al., 2002).

[4] Preliminary tests showed that a loss of weight, indicating loss of water content could not be observed. The maximal imaginable loss of water content was about 0.3% theoretically for a specimen with an average weight of 3grams.

5.3 *Physical principles*

Friction force, F_R = *Friction coefficient (*μ*) *Normal force (*F_n)

The friction coefficient is therefore calculated as

$$\mu = \frac{F_r}{F_n} \qquad \textit{Equation 8}$$

Brinckmann et al. (2000) noted that the pressure distribution in the hip joint can be calculated. He stated that *"the average pressure acting upon the surface of the joint can be taken as the quotient of the force and the projected area which can be determined. The projected area of the hip joint approximately is a circle having the radius of the hip head"*. The "average" force for a "projected" area of a sphere is calculated as:

$$P = \frac{H}{A} \qquad \textit{Equation 9}$$

where P is the "normal" force, "H" is the vector (direction) which, in these experiments, always will be the normal force ($F_{n)}$. The surface of the projected area is calculated as for any circular surface, i.e. $A= r^2\pi$ where r stands for the radius of the circular surface (note: this value of course differs from the radius of the sphere itself, see Figure 4.8) while the calculation for the curved surface area of such a spherical cap, if this were required for any reason, would be $A= 2rh\pi$ where A is the area, r is the radius of curvature and h is the sagittal height of the spherical segment.

Note: According to Amonton's law, friction is independent of the surface area. There is an exception concerning highly polished surfaces and specific materials like Teflon: *"First Law: The frictional properties of some very hard materials such as diamonds and certain very soft materials such as Du Pont's Teflon do not obey the first law. For these special materials, friction is not proportional to the load; instead it is proportional to some reduced value of the load"* (Guichelaar et al., 2008). In other words - in relation to the experiments, Amonton's first law only applies to small forces.

5.4 *The force to be applied to the substrate*

The force of the upper lid in the direction normal to the eye is reported to be 0.2 to 0.25 Newtons (Jin, 2002). In previous unpublished work, the thesis author has investigated the force required to release the contact between the back of the eyelid and the front surface of the eyeball, and this revealed that a 10g force would be sufficient in the vast majority of eyes. As a result, a minimum of 10g force was used for the in vitro experiments.

5.5 *Apparatus*

The tribometer developed by the author for this thesis was intended to be a standardised technique suitable for the contact lens industry and which mimicked the eye situation. However, the design would allow the tribometer to be used to test other non contact lens materials. Depending on the layout in terms of size and forces used, size of components might require adaptation

Tribometer Schema

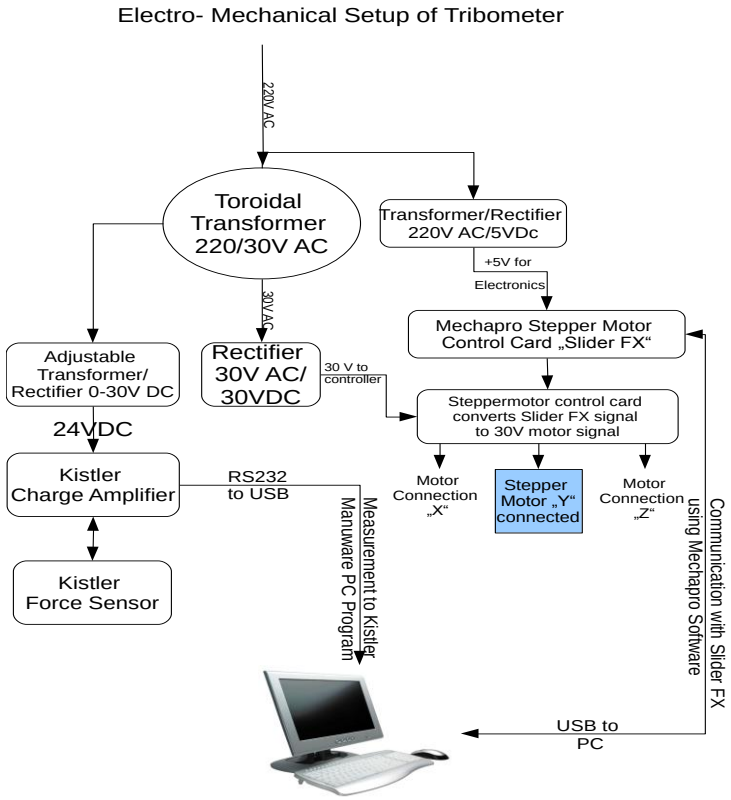

Figure 5.1 Tribometer Schema
to show how the different components of the tribometer apparatus
are connected to the Tribometer Base

Figure 5.1shows how all the components of the tribometer and recording apparatus are connected. The alloy tribometer base (see Figure 5.2 and Figure 5.3) supports a stepper motor which turns a spherical substrate made of a chosen material. The substrate has a circumference speed that approximates to the speed of a blink. An aluminium strip with a thickness of 1.5mm formed into an L shape is fixed to the force sensor and acts as the holder of the material specimen. The specimen exactly fits into a 10mm diameter hole in the strip without play or any binding to the aperture edge. The centre of the 10mm aperture is located 1mm above the apex of the substrate. The material sample disc has a diameter of 10mm and one surface has a concave radius of 12mm (12.1mm for the reference test with aluminium since the quantity of substance removed by polishing could not be foreseen and for the reference test, according to friction laws, the size is not important). The centre thickness of the material disc may be between 1.7mm and 2.5mm.

A Delrin tray holding the required additional weight is placed on the plano side of the material disc. The gross weight including the test material itself will be 10g. To measure friction without lubricious additives, the contact surfaces need to be free of any liquid substance. If necessary, a humidification housing for testing hydrophilic materials was used. A difference in weight of the test disc between the start and the end of the test indicates the need for such a housing.

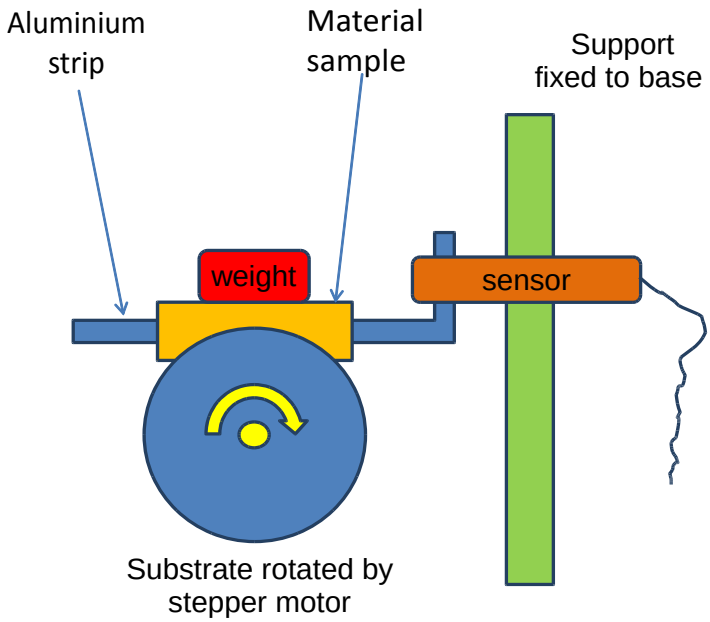

Figure 5.2 Tribometer set up.

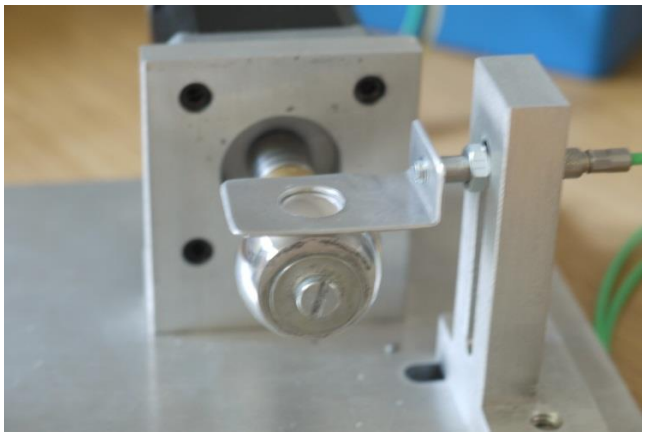

Figure 5.3 Tribometer base showing the substrate attached to the stepper motor and the disc holder located 1mm above the substrate. The sensor is attached to the aluminium strip.

.

Mechanical Scale

A mechanical balance (Figure 5.4) is mounted (Ohaus DIAL-O-GRAM® balance Model 310) on the tribometer base. This has a resolution of 0.01 grams and a maximum weighing capacity 310g. This is used to check reliability of the sensor and to add the necessary weight to the specimen in order to perform the measurements.

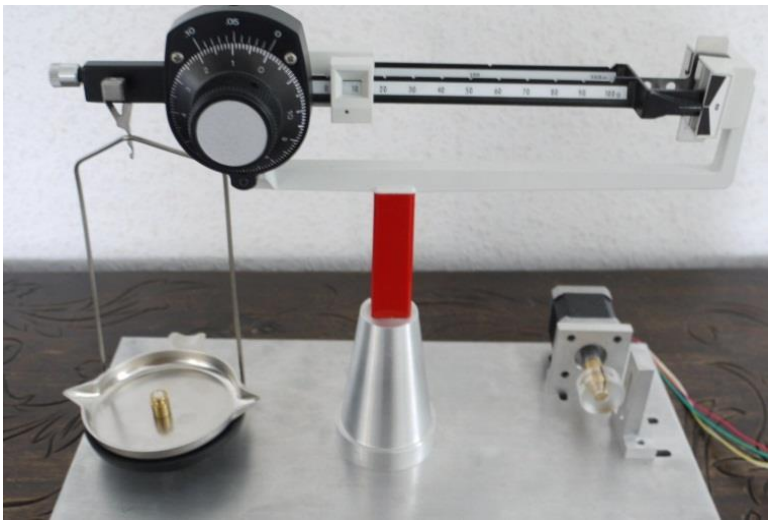

Figure 5.4 Tribometer balance attached to base.

The balance was necessary for calibration purposes and was intended to be used in conjunction with a container for tests in immersed conditions. Unfortunately the container mounted on the scale was not sufficiently stable to allow tests to be run

under immersed conditions. Although the stepper motor produced some high frequency noise when in use, vibration was not observed.

High resolution stepper motor

A stepper motor system is an electro-mechanical rotary actuator that converts electrical pulses into unique shaft rotations. This means that the speed is synchronous to the rate of pulsing. The result is precise speed and position. Stepper motors do not accelerate. The movement is performed with the "speed" the motor is built for. Stepper motors only have a "quasi" continuous movement. Sending signals to the stepper motor which allow movement of less than one complete step i.e. half steps or quarter steps per unit of time (termed microstepping) enhances accuracy of positioning. If too many steps per unit of time are sent to the motor, it starts stalling and will not move. Ramps to accelerate and decelerate for faster movement need to be programmed. Manufacturers of stepper motors release the necessary data to correct for these limitations. There was no particular advantage in using a servo rather than a stepper motor for the research carried out in this study. A servo motor necessarily requires a closed loop positioning control which would have presented challenges (National Instruments, 2014). Furthermore the author already had experience in setting up, managing and programming simple stepper motor applications. After preliminary testing the motion produced by microstepping at the speed suggested did not cause vibrations. Taking all this into consideration the stepper motor was chosen as the method of choice. Stepper motors have been in use in the contact lens field for many years. As long ago as the early 1980's polish-free lathe cutting was possible with machines such as Coburn lathes, which produced polish-free surfaces by smooth movement in any direction.

For the frictional tests of soft contact lenses the blinking velocity of the upper eyelid, which is approximately between 60mm/sec and 180 mm/sec (Nakamura et al., 2008), was simulated. The sliding properties and the coefficient of friction for PTFE is influenced by the sliding speed. For this reason an average substrate diameter had to be considered. This work does not relate to wear. Wear would cause damage to the anterior surface of the eye and of course is an unwanted phenomenon in contact lens use.

Considering the average substrate circumference of 73.13mm the required velocity of the substrate is 147.67 revolutions per minute at a speed of 180mm per second. The relationship between the circumference at the apex of a sphere and segments further from the geometrical centre are explained in Section 4.8, Contact lens friction and lubricity.

A high resolution stepper motor (Oriental PK245M-01BA) with a resolution of 400 steps per revolution i.e. 0.9 degrees per step was chosen. The torque characteristics are shown in Figure 5.5. In preliminary tests, using the anticipated settings, the motor did not stall and hence ramp calculations were not required.

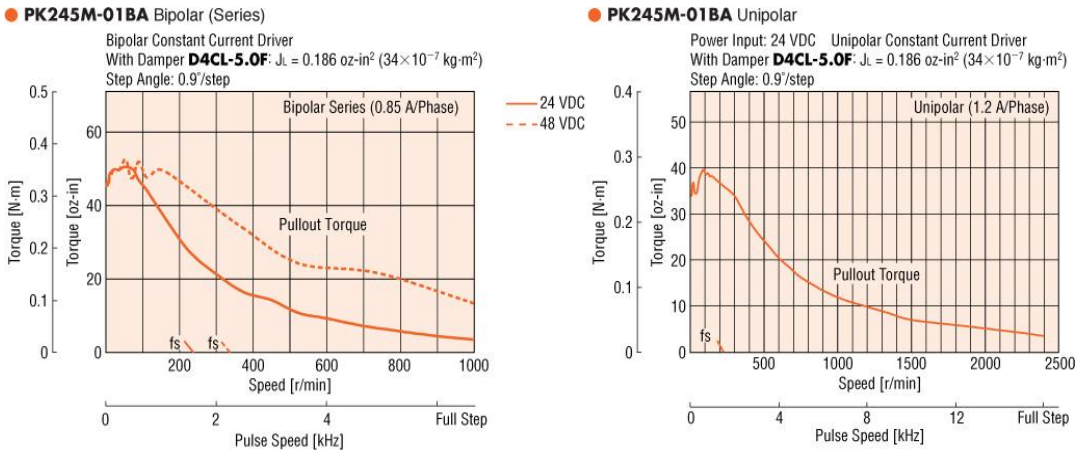

Figure 5.5 Torque graphs for stepper motor

Stepper motor control unit

A custom made stepper motor control unit was connected to a personal computer and provided current and motion control to the stepper motor. The control unit consists of an extra 5 Volt DC power supply, a toroidal transformer supplying 30 Volts for the stepper motor, a rectifier and DC voltage selector circuit to supply 24V DC to the Kistler Charge Amplifier (see **Error! Reference source not found.**) and supplying current to the two essential printed circuits for the stepper motor (Kistler Group, 2009).

Slider FX Stepper motor driver

The stepper motor driver sends the calculated current in a series of signals to the stepper motor which turns the axle of the stepper motor the required number of

increments at the given intervals. The driver card consists of three programmable output switches which are able to switch devices with up to 220Volts and 10amps. In order to control the stepper motor and to receive the data which are transposed to signals for the stepper motor, the driver card was connected to the motor controller.

NC-Pilot stepper motor controller

The stepper motor controller outputs step signals with pulse rates up to 50 kHz and is capable to control up to 4 axes with pulse and direction signals. The device is connected to the stepper motor driver and via its USB port to a personal computer. The computer runs a program that calculates the necessary data to move the stepper motor, starts and stops the motor, collects signals about operational status and controls the switches and relays of the Slider FX motor driver. With the software program provided, the following actions can occur:

the stepper motor can be switched on and off,

the number of steps and their direction can be determined,

stop and reference points can be set,

external devices can be switched on and off.

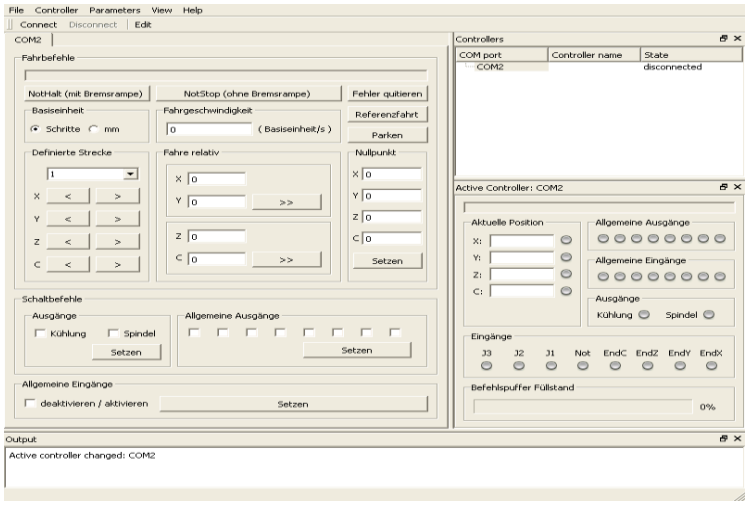

Figure 5.6 Mechapro motor control window

To set the necessary variables, the number of steps or microsteps per revolution, the number of steps per millimetre movement, the maximum range of travel, standard velocity, high velocity values and the home position have to be set in the stepper motor control window of the software (Figure 5.6). If required, ramp speeds for acceleration and deceleration require configuration.

To run the stepper motor in a way that mimics a blink, the average circumference of the substrate, the number of steps per mm and the speed of a blink were considered. Nakamura et al. (2008) measured blink speeds between 60mm/sec and 180 mm/sec. The controller software allows the motor speed and number of increments per test to be set (Table 5.1).

The settings were then entered into a calibration table and calculations using a small software program allowed the stepper motor to move with a defined speed (i.e. number or increments per time), with a defined number of steps (i.e.per mm of the circumference of the substrate) and with the required number of repetitions after triggering.

Stepper motor settings for 1600 steps/rev.						
Resolution in degrees	Substrate diameter at apex	Test sample diameter	Average substrate diameter	Average circum-ference	Movement in mm per step	Steps per mm
0.225	24	10	23.28	73.132	0.04626	21.87

Table 5.1 Stepper motor settings for a 24mm diameter disc.

Note: The effective mechanical settings of the apparatus had to be set by observation. One revolution equals 1600 steps. The steps per mm movement of the program supplied was compared to the spindle movement for lathes using a tapered spindle. Multiple trial and error tests gave a revolution of 50.9296[5] steps per mm for the machine setting.

Kistler high resolution force sensor 9215-1

Figure 5.7 Kistler low force sensor 9215-1

This is a piezo-electric force sensor (Figure 5.7) for measuring quasi-static, dynamic tensile and compression forces from -20N to 200N. It is mounted in a L shaped

[5] For calculating multiple steps with smallest positioning error possible 4 digits after the decimal point are necessary.

aluminium strip with a 10mm diameter aperture whose centre is located exactly at the apex of the substrate (Figure 5.3).

Charge Amplifier Kistler ICAM 5073

Figure 5.8 Kistler Charge Amplifier

The charge amplifier (Kistler, model ICAM 5073 see Figure 5.8) converts the piezo-electric charge signal from the sensor into an output voltage proportional to the mechanical input quantity. The ICAM control system operates via digital inputs and a serial interface. The amplifier is connected to the force sensor by a cable using BNC connectors. An extra power supply with 24Volt DC current has to be connected to the pins 11 and 9 of the 15 pin male connector. Pin #3 of the connector sends the amplified signal in 1Volt steps to the RS 232 interface. The RS 232C interface connects to the personal computer via an USB converter. With the software provided by Kistler the amplifier can be calibrated and set to the minimum and maximum voltage values.

Kistler Manuware Software

This is standard software to input the data produced from the charge amplifier. The Manuware software runs on personal computers using Windows operating systems and communicates with the Kistler Charge Amplifier over the serial port with null modem wiring to the USB port of a computer. The software acts as a multifunctional oscilloscope program which allows readings to be taken from the Kistler Charge Amplifier and to be displayed as a graphical representation in either volts or force (Newton) as shown in Figure 5.9.

The personal computer used was a standard device equipped with a 64bit Intel Core i3 CPU 540 @ 3.07 Ghz processor, 8 Gigabyte RAM, 500 Gigabyte disc storage, a built in Video Card, a second ATI Radeon Video Card, 8 USB connections, keyboard and mouse, a Samsung wide screen TFT monitor and a second Videoseven TFT monitor. The operating system was Windows 7, 64 bit version Service pack 1.

One monitor was used for watching the output of the tests and to control the stepper motor program in two separate windows. The second screen was used to run a small freeware program named Irfanview[6] to take hard copies of the collected data displayed on the screen and to save the screen images as pdf files on disc. Although various printers were available within the testing environment, printing was avoided in order to keep the electronically collected data available.

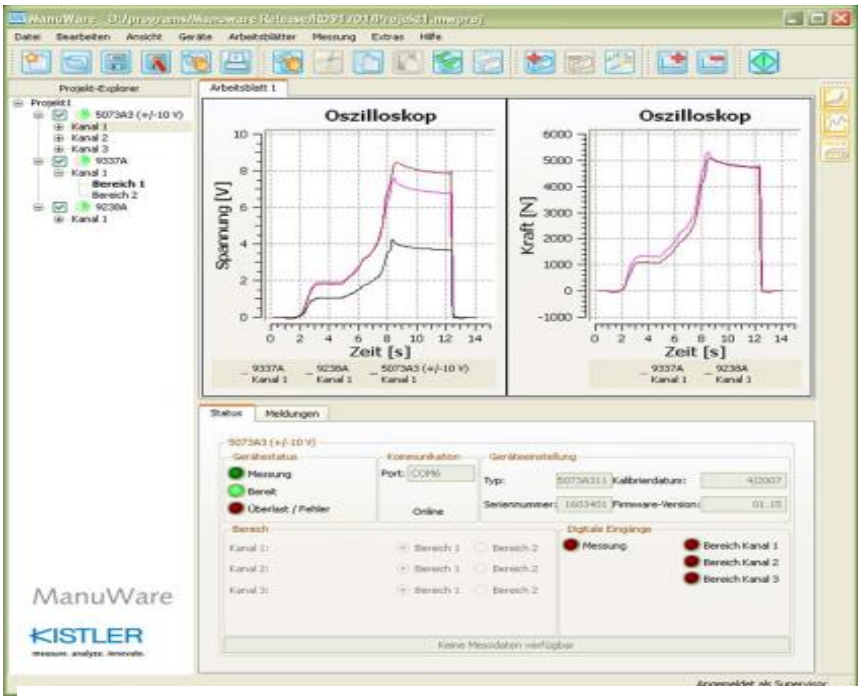

Figure 5.9 Sensor readings as shown on the computer screen.
The sotware simulates the appearance of a traditional oscilloscope screen.

Materials

Substrate used for testing

The chosen material must have moderate to low friction against the contact lens materials in order to avoid adhesion. In preliminary tests it was found that soft contact lenses placed on a congruent polished shape made of rigid materials such as PMMA, glass or polished metal, resulted in the lenses adhering to the substrate. The frictional properties of materials increase with the time the material is sitting on the substrate. This also applies to hydrogel materials. The phenomenon is known as

[6] By irfan skiljan, http://irfanview.tuwien.ac.at/

stiction. "*Stiction is a contact phenomenon whereby static friction increases relative to kinetic friction. As a rule, this effect increases dramatically with the static contact time. Thus, the time dependence of static friction is an important subject of tribological studies*" (Gitis and Volpe, 1992). Materials of known low friction, such as Teflon, are therefore the substrates of choice. The frictional properties of Teflon are low. The static coefficients of friction reported were μ= 0.04 – 0.15. For dynamic friction μ= 0.04 - 0.1 (Elert, 2004). Teflon is commercially available as a semi-finished product and is available in sheets, rods and other shapes. It is a plastic material that can be machined, ground and polished. It is inert against many materials. The Teflon material used was purchased from a Vienna based company (Wettlinger, 2012). They provide information about the material properties for all their products.

Hydrogel samples

Manufacturer	Material Name	Polymer	Water content	Dk	Class
Vista Optics	VSO 75	n-VP/MMA	75%	43*	Filcon II 2
Contamac	Contaflex GM3	Glycerol/MMA	58%	25.5*	Filcon II 1
Contamac	Definitive	Silicone Hydrogel	74%	60*	Filcon II 3
Vista Optics	LM55	HEMA/VP	55%	17*	Filcon II 1
Vista Optics	VSO 38	p HEMA	38%	7.68	Filcon I 1
* Data provided by Manufacturer					
Note: The materials chosen cover a representative range of monomer bases, which could show frictional and lubricating properties of the different materials.					

Table 5.2 Specification of tested materials.
Dk values are given for room temperature (20°C ± 5°C)

The soft contact lens materials chosen, (seeTable 5.2) cover a representative range of monomer bases which should have shown different frictional and lubricating properties. All materials are non-ionic. Hydrophilic contact lens materials with ionic load were omitted because it is well known that they attract adherent lipid deposits more than non-ionic materials. To test each material a semi finished lens, with a finished posterior surface, was manufactured out of standard contact lens blanks with a diameter of ½ inch and 5mm uncut thickness. As lathe cutting is a material removing technique the centre thickness of the semi finished lens is reduced by at least the amount of the sagittal height cut out.

Swell rates for hydrophilic contact lens materials are different for each type of material. Swell rates depend on water content, manufacturer of monomers, monomer composition and the polymerisation method. Swell rate data provided by contact lens raw material manufacturers may vary slightly from batch to batch and therefore need verification. The swell rate is the relation between a dimension measured in the dry state and a dimension measured in the fully hydrated state. The radial swell rate calculates the difference in radius between xerogel and hydrogel. For the required hydrogel diameter the linear swell rate is used.

5.6 *Experiment 1A - Verification of linear and radial swell rates*

Aim: to establish the linear and radial swell rates for the batches of contact lens materials received from manufacturers.

Apparatus: Micrometer callipers (Mitutoyo, resolution 0.1mm), Radiuscope (American Optical, measurement resolution 0.1mm, optical resolution 0.161 micron[7]), 3 sample blanks of each material with one surface cut to a radius of 7mm and a diameter of 10mm, Optimec soft lens analyser (linear and radial resolution 0.1mm, interpolation between tick marks enable 0.05mm resolution).

Method

Using the callipers, the diameter of each disc was measured three times across different diameters and the average value recorded. Using the radiuscope in a conventional way, the concave radius of each disc was similarly measured three times and the average value recorded.

The discs were then immersed in normal saline (at room temperature) for 24 hours so that each disc became fully hydrated.

The cells of the Optimec soft lens analyser were filled with fresh saline and this instrument was used to measure all the hydrated diameters and radii of each disc in

[7] Note: The measurement resolution is a function of a scale divided by tickmarks allowing a value to be read from the scale. The optical resolution is a function of the numerical aperture of the objective of an optical appliance. Related to a radiuscope it defines the ability to discriminate imperfections to the resolution mentioned.

turn. This cycle was repeated twice more so that three independent diameter and radii measurement were taken for each disc and the average values recorded.

Swell factor calculations can be performed from the dry xerogel[8] to the hydrogel state (or the reverse) using the following equation:

Xerogel to hydrogel (from dry to hydrated):

$$x = \frac{\text{hydrogel size}}{\text{Xerogel size}} \qquad \text{Equation 10}$$

For example:

Xerogel diameter 10mm = Hydrogel 10mm $x = \frac{10}{10}$ = 1.0 = no swell

Xerogel diameter 10mm = Hydrogel 12mm $x = \frac{12}{10}$ = 1.2 = larger than xerogel

Results

The swell rates then were used to calculate the manufacturing data for the material in xerogel state, linear swell rates for determination of the diameters, radial swell rates for the radii required in hydrogel state. See calculation examples in Method: (Page 76)

Material	Linear Swell (Diameter)			
	Sample 1	Sample 2	Sample 3	Average
Definitive	1.59	1.59	1.58	1.59
LM	1.43	1.44	1.44	1.44
GM	1.36	1.37	1.38	1.37
V38	1.30	1.29	1.29	1.29
V75	1.50	1.50	1.50	1.50

Table 5.3 Linear swell rates of the five chosen materials.

[8] *A xerogel is an organic polymer capable of swelling in suitable solvents to yield particles possessing a three-dimensional network of polymer chains* (McGraw-Hill Dictionary of Scientific & Technical Terms, 6E, Copyright © 2003 by The McGraw-Hill Companies, Inc.)

Material	Radial Swell (Radius)			
	Sample 1	Sample 2	Sample 3	Average
Definitive	1.58	1.57	1.59	1.58
LM	1.41	1.42	1.43	1.42
GM	1.37	1.36	1.37	1.37
V38	1.16	1.17	1.16	1.16
V75	1.50	1.52	1.50	1.51

Table 5.4 Radial swell rates of the five chosen materials

5.7 *Experiment 1B – Calibration of the sensor*

Aim – to evaluate the accuracy of the force sensor

Apparatus

The apparatus described above is connected correctly, switched on and allowed to stabilise.

Method

Figure 5.10 Calibration of the low force sensor.

A newly certified set of M1quality calibration weights was used to check the accuracy of the balance scale by comparing the calibration weights with the scale readings (Figure 5.10). There was no difference in readings compared to the given weight over the complete range. The Kistler sensor was then checked for accuracy by applying a given force (i.e. 10 grams) to the sensor using the balance scale (See Figure 5.10). At boot time the sensor, the amplifier and the software were set to zero. This made sure that force was measured only. The Kistler Manuware software showed the result in Newtons and this was then transposed to grams.

Results

The display (Figure 5.11) showed a reading of 0.002N at the outset and 0.1002N when 10 gram was applied to the sensor. The difference of 0.1N confirmed the correct calibration of the sensor. From time to time the reading in N initially was slightly greater than zero. This may have been due to electrical instability but it was not possible to provide a voltage offset to ensure that all the readings were takten from a starting point of zero volts. However, the correct result is given by the difference.

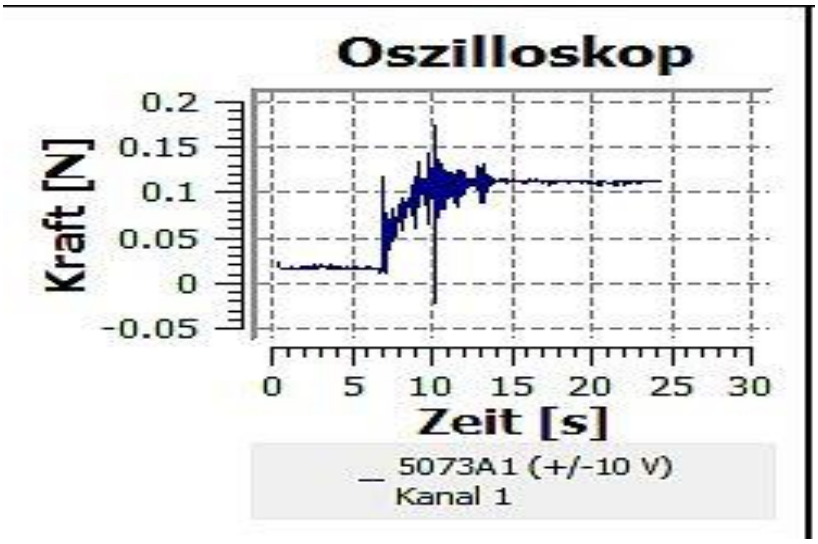

Figure 5.11 Oscilloscope display during sensor calibration between 'no force applied' and 'force applied'.

5.8 *Experiment 2 –Friction coefficients of the reference materials*

To ensure the functionality of the tribometer, comparison measurements of materials with known friction coefficients are required. The reference material of choice must have machining properties that enable contact lens lathes and polishers to produce reference material samples to a quality and accuracy needed for contact lenses. Metals of choice could be brass, aluminium or copper. Steel would be a good choice but the risk of machine damage is high. For the contact lens lathes available, aluminium against aluminium was chosen. Various sources report friction values (μ) under different conditions:

μ = 0.42 (Ahmad et al., 2011)

μ = 1.35 dry contact (Engineers Edge, 2010)

μ = 0.30 lubricated contact (Engineers Edge, 2010)

μ = 1.05-1.35 static (Beardmore, 2010)

μ = 1.4 sliding (Beardmore, 2010)

μ = 0.35 static lubricated (Beardmore, 2010)

μ = 0.32 at 0.6m/sec sliding speed and F_n=0.2N/mm² (Feyzullahoglu and Nehir, 2011)

μ = 0.36-0.43 at a constant sliding speed and F_n=0.1N and a surface rugosity of 0.05 (Garzino-Demo and Lama, 1995)

Besides aluminium coefficients, friction values for organic materials are also available from the same literature. PMMA has a reported friction coefficient of μ =0.8 and PTFE a friction coefficient of μ=0.04 (Beardmore, 2010) while Domininghaus (2007) expected μ between 0.1 and 0.25 for PTFE. It should be noted that friction coefficients found in such tables are average values found under unknown conditions. "*Extreme care is needed in using friction coefficients and additional independent references should be used. For any specific application the ideal method of determining the coefficient of friction is by trials"*.

Aim

To establish that the friction coefficients obtained with the experimental tribometer were comparable to the published values of rigid materials.

Apparatus and materials

Experimental tribometer, aluminium substrate and aluminium discs, PMMA substrate, PMMA discs, PTFE substrate and discs.

Method

The experiment was carried out at an ambient room temperature of 22°C (± 2°C) and the ambient humidity was 55% which is within the 20 ± 5° according to ISO 18369-3 (ISO, 2006) for measurements in air.

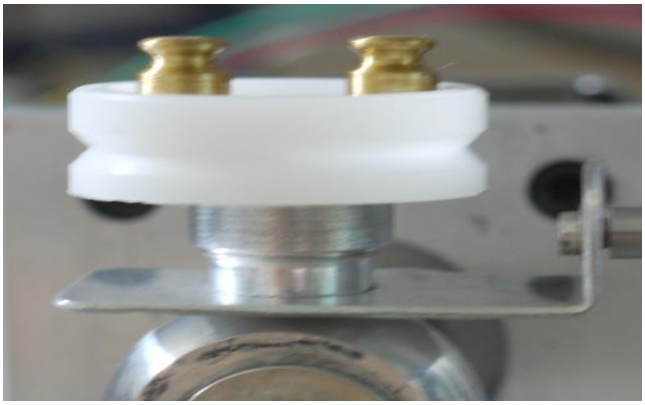

Figure 5.12 10g total force on top of the substrate aluminium substrate and aluminium sample.

For Aluminium, only one measurement of static friction can be taken since the test destroys the polished surface immediately, which is a common occurrence with sliding between two surfaces due to wear (Qu et al., 2005, Ahmad et al., 2011). As described in the technical informations for PTFE, wear does not occur at slow speeds and small forces applied (Polytetra, 2013). There was no destruction visible on the polished surfaces of the PMMA test materials. For PMMA and PTFE, three tests per substrate disc were carried out. The tested surfaces were free from scratches when observed in a radiuscope and the image of the filament (or measuring mark) at 12mm radius was crisp and sharp. Five consecutive movements of the substrate resulted in five peaks on the scale. The first peak on the scale is the relevant one for static friction. The rest of the graph is caused by dynamic friction, the destruction of the polished surface and finally the removal of the sample. To perform a new measurement the surface has to be refined again otherwise there are inherent errors.

The average of the five results was recorded. PTFE was also tested with saline as a lubricant. The reference rigid material disc and an additional weight of 10 grams were placed on top of the substrate (

Figure 5.13). At his point the stepper motor was started. To mimic lid motion, a saccadic movement of the stepper motor was necessary. Movement of the substrate was started with a set speed of 180mm per second. The force applied to the materials tested mimics the tension of the upper lid and the speed of a blink. The tested

material in the material holder moved towards the sensor. The measured value of the transferred force was shown on the oscilloscope.

The friction coefficient was obtained by dividing the force measured by the force applied. If, for example, the measured force was 1N (Figure 5.14) and the force applied was 1N then the friction coefficient (μ) would be 1. If, for example, the force measured was zero and the force applied was 1N then the friction coefficient (μ) would be zero. The first peak in Figure 5.13 would be judged as static friction. The vertical scribe lines between 5 and 7 seconds indicate stick-slip friction within a range between approximately 0.9 and 1.1 N.

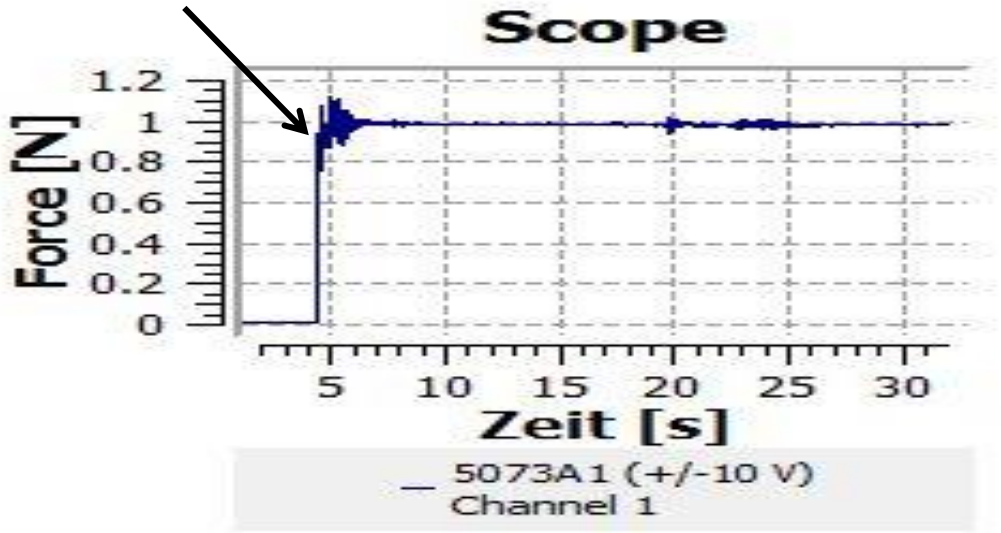

Figure 5.13 Example reading of static friction.

Zeit = time. Static friction is indicated at the first peak.

Results

The results for the reference materials PTFE, PMMA and Aluminium are shown inTable 5.5.

Specimen	Substrate dry	Weight in Grams	Weight in Newton	Average F_r (Newton)	Friction Coeff. μ	Std. Dev.	Average CoF
PTFE wet	PTFE	100.53	0.9862	0.240	**0.24**	0.022	
PTFE wet	PTFE	10.61	0.10408	0.018	**0.17**	0.003	
PTFEwet	PTFE	100.61	0.98698	0.161	**0.16**	0.010	**0.23**
PMMA dry	PMMA	10.5	0.10301	0.108	**1.05**	0.004	
PMMA dry	PMMA	100.5	0.98591	1.320	**1.34**	0.110	**1.19**
PMMA wet	PTFE	100.5	0.98591	0.240	**0.24**	0.022	
Alu dry	Alu	10.215	0.10021	0.031	**0.31**	0.007	
Alu dry	Alu	100.22	0.98311	0.244	**0.25**	0.009	
Alu dry	Alu	10.24	0.10045	0.029	**0.29**	0.015	
Alu dry	Alu	100.24	0.98335	0.240	**0.24**	0.012	**0.27**
Alu wet	PTFE	102.02	1.00082	0.153	**0.15**	0.158	
PTFE dry	PTFE	10.06	0.09869	0.021	**0.21**	0.004	
PTFE dry	PTFE	100.06	0.98159	0.345	**0.35**	0.049	**0.28**
PMMA dry	PTFE	10	0.0981	0.026	**0.27**	0.005	
Note: Substrate and specimen polished according to ISO 18369-3							

Table 5.5 Friction coefficients of rigid materials tested against each other.

Discussion

The forces applied were not exactly 10 or 100 grams since the specimens had slightly different weights. Adding one 10g or one 100g weight, instead of applying different weights up to 100g, achieved better mechanical stability of the apparatus. However, Coloumb's law states that such variations do not play a significant role. It was demonstrated that Coloumb's law applied to the forces and the materials tested. Some friction coefficients found differed from those in the literature. Some of the results for Aluminium found in the literature appear to be comparable to the experimental results in Table 5.5.

The friction coefficients for aluminium against aluminium found in the literature differ across a wide range as shown on page 79. A relationship between surface

quality and coefficient of firction was reported by several authors (Spijker et al., 2013, Feyzullahoglu and Nehir, 2011, Garzino-Demo and Lama, 1995).

The experimental results for polished aluminium against polished aluminium in the unlubricated state are shown in Table 5.5. The surfaces were free of imperfections at a 96x magnification and an optical resolution of 0.161 micron. Saline was used as lubricant. The CoF's for aluminium agree with the findings of Spijker et al. (2013), Feyzullahoglu and Nehir (2011) and Garzino-Demo and Lama (1995). Regarding the results published for lubricated friction, there is a lack of information about the lubricants. In the tests presented in this thesis water saline was used as lubricant.

The friction coefficient for Teflon (μ= 0.04) found in the literature (Beardmore, 2010, Engineers Edge, 2010) differs from the experimental results obtained (μ= 0.23). Other literature has stated a μ= 0.2 for PTFE (Elert, 2004). The specific PTFE material used for the tests was manufactured by the German Polytetra GmbH. According to the technical data provided, low load resulted in higher friction (i.e. μ=0.4) and decreased with increasing load to approximately μ=0.04 (Polytetra, 2013). Similar materials are manufactured by Du Pont under the trade name "Delrin", who reported a CoF between μ=0.1 and 0.4 (DuPont, 1996). Domininghaus (2007) also described the phenomenon of decreasing CoF with increasing load and reported that a CoF between 0.1 and 0.25 could be expected and DuPont (1996), Domininghaus (2007) and Polytetra (2013) described in detail the dependencies between load and coefficient of friction. They reported a CoF of 0.4 with extremely low loads, reducing to 0.05 with 345-517 kPa pressure applied. The results found from the author of the current thesis agree with these findings at low loads. The detailed figures 12 and 13 in DuPont's properties handbook for PTFE (DuPont, 1996) allowed a comparison with the current author's results. The equivalent coefficient of friction for a sliding speed of 180mm/sec, equivalent to about 35.43ft/min and a load between 345Pa and 3447Pa resulted in a CoF of about 0.22 in the handbook. Figure 13 in the handbook showed the dependency between normal force (load) applied and the coefficient of friction. The results for unlubricated PTFE against PTFE in Table 5.5(μ=0.21-0.35) agree with a CoF under similar conditions in Figure 13 of the Fluoropolymer Resin Properties Handbook (DuPont, 1996). Overlapping results found in the handbook allowed the assumption that a deviation between results can be possible. While surface quality and test

methods published in handbooks and general information, have not been detailed, the own experimental tests were carried out with materials having optical quality polished surfaces according to the ISO Standards for contact lenses (ISO, 2006). Bowden and Tabor (1950) investigated and demonstrated the influence of lubrication, and showed that lubrication and the use of lubricating agents alters frictional properties. The frictional properties of a lubricating layer between two surfaces solely act as long as other substances do not get into contact with each other. For example, if a contact lens is swimming in tears and does not touch the corneal epithelium, only the frictional forces of the tears are acting. If the tear layer gets thinner and thinner, then the friction produced is known as mixed friction. If there is only a very small amount of tears remaining, then the friction produced is known as borderline friction. In automotive techniques the properties of motor oils have this kind of borderline lubrication property to lubricate the crankshaft for a limited time even if the engine lubrication system does not work. Today it is known that multiple forces influence frictional behaviour and elastomers behave differently than solids. Since the loads for the experiments were very low, tests were carried out with a 10 fold load to esthablish if significant differences appeared (Table 5.6)

Material	Author's results	Other researchers results under similar conditions
Aluminium	0.27	0.32-0.43
PMMA	1.19	0.8
PTFE	0.28	0.1-0.4

Table 5.6 Coefficient of friction.
The author's results compared with other researchers

To estimate the relative differences in measurements obtained with approximately 10g and approximately 100g loads, the resulting force obtained with the 100g weight applied was divided by 10 (Table 5.7). The resultant standard deviations for the normalised 1g load are very low (see Table 5.7).

Material	Weight	F_r normalised to 10g F_n	SD for normalised F_n
PTFE	100.530	0.024	
PTFE	10.610	0.018	
PTFE	100.610	0.016	0.004
PMMA	10.500	0.108	
PMMA	100.500	0.132	0.017
PTFE	100.500	0.024	0.024
Alu	10.215	0.031	
Alu	100.215	0.024	
Alu	10.240	0.029	
Alu	100.240	0.024	0.003
PTFE	102.020	0.015	0.015
PTFE	10.060	0.021	
PTFE	100.060	0.035	0.010
PTFE	10.000	0.026	0.026

Table 5.7 Resulting (frictional) force for all tests normalised to a 10 g load.

The results for coefficient of friction for the non CL materials are shown in Table 5.8.

Material	Experimental CoF (dry)	Reference CoF (dry)	Experimental CoF (lubricated*)	Reference CoF (lubricated)
Aluminium	0.27	0.32-1.4	0.15	0.3
PMMA	1.19	0.8	0.24	0.8
PTFE	0.23	0.04-0.41	0.28	0.04**

* Lubrication agent: Saline solution

** Reported by Engineers Edge, LLC. with unknown lubricant

Table 5.8 Coefficient of friction for materials tested and compared with reference values

Compared to the loads and sliding speeds used by researchers in previous studies,the loads of both tests carried out by the author were low while the sliding speeds varied between much lower and much higher.

5.9 *Experiment 3 – Evaluation of soft lens materials*

Aim

To establish the coefficients of friction for five chosen materials (Table 5.2) under different conditions.

Apparatus

The experimental tribometer fitted with PTFE substrate.

Materials

Five test samples were made of each material chosen out of standard contact lens blanks with 12.5mm diameter and 5mm thickness in the dry state by lathe cutting and polishing.

BOZR 12mm

FOZR flat as supplied by blank manufacturer

Centre thickness 2.5mm

Standard polishing applied to BOZR only.

Lathe cutting is a material removing technique which naturally reduces the remaining amount of material. In order to produce a hollow shaped sphere out of the material specified, the thickness of the piece manufactured decreases. Using the experience gained in manufacturing contact lenses the author cut the BOZR to a centre thickness of 2.5mm which was preferred to assure accuracy regarding swell rates.

The material types have been chosen because all the materials can be lathe cut and polished. They represent typical materials used in normal contact lens practice. The material properties and manufacturers are listed in Table 5.2 Specification of tested materials.

.

Methods

Chapter 5 - described the aim to simulate in vitro conditions, mimicking the 'in eye' situation as closely as possible in vitro. It was also discussed that all measurements regarding frictional properties of contact lenses found in the literature failed to measure the materials themselves but instead measured the lenses under lubricated conditions, and failed to state whether these were boundary, mixed or fully lubricated conditions. In cases of full lubrication the measurement results were those obtained for the lubricant between specimen and substrate and not for the substrate (see Section 4.7 Tribology). Most of these friction measurements were dynamic friction measurements using Newtonian and non Newtonian lubricants. Unlike the methods used by the authors listed in Table 4.3 the tribometer described in Section 5.5 attempts to mimick the situation in the eye using a blinking speed as described by Nakamura et al. (2008). The tribometer used for the experiments enabled testing without causing indentations in the material, achieving parallel surface contact similar to the situation which occurs between eye and contact lens. The use of a type of semi-finished but hydrated contact lens with a centre thickness of 2.5mm made it possible to keep the lens as stress free as possible in a holder without deformation in the resting state. The viscosity, normal force and velocity were identical for all tests, so the lubrication modalities described were the only factor producing different readings. The only exception regarding viscosity was the use of a tear substitute for one test (see Table 5.12). The order of test samples was randomized and the experimenter was blind to which type of material was being tested. The hard copies of the results which appeared on the screen (see Figure 5.14 or Figure 5.16) were stored in a folder of the personal computer's operating system. After all tests were completed, the hard copies were sorted and placed in separate folders for each material. Then each hard copy of each reading was displayed on the screen, and the results were entered into spreadsheets and analysed.

Three different testing conditions were used:

a) *No lubricant between substrate and test sample.* The test sample stored in saline was removed from the storage container and the liquid removed by wiping the polished surface with a dry tissue as quickly as possible to avoid dehydration of the material itself. The test samples were weighed before and

after the friction test. A difference in weight was not observed and it can be assumed that no dehydration occurred and hence no humidification housing was necessary. The test sample was then placed into the aperture of the aluminium holder and the polished surface was in contact with the PTFE substrate to carry out the measurement under "unlubricated" conditions.

b) *A drop of saline on the polished surface of the test sample.* The test sample was removed from the storage container and shaken carefully to remove excessive saline. One drop of saline was placed on the polished surface of the test sample. The test sample was then placed into the aluminium holder on top of the PTFE substrate to carry out the measurement under "borderline" conditions.

c) *The test sample was removed from the storage container with the residual saline on the test sample.* A drop of saline was placed on the polished surface. The drop of saline produced a lubricant film between the areas of contact. By doing this, unlubricated friction was avoided at all times. A small container filled with saline was placed below the PTFE substrate so that part of the substrate was continuously immersed in saline. The saline container provided additional lubricant to maintain mixed friction. The PTFE substrate was splashed with saline. The test sample was placed into the aperture of the aluminium holder and placed on top of the PTFE substrate. The substrate/material interface was splashed again with saline to ensure excessive lubrication. This arrangement should mimic "mixed friction".

Soft contact lens surfaces were tested with a force of 10 grams in the vertical direction onto the substrate. The test samples had a hydrated radius of 12mm. A 12mm radius was the flattest possible radius that could be formed with the contact lens lathe available. The flattest radius was chosen to minimize tolerances in sagittal height between the substrate and the tested sample, both of which had the same radii. A saccadic motion of the stepper motor with a speed of 180mm per second was used in quarter step motion of the stepper motor to achieve the smoothest possible movement. This speed mimics the closure of the upper lid. With the equipment available, a slower speed of, for instance, 6mm per second would have caused undesirable vibrations from the torque of the stepper motor. The time

between the measurements was 6 seconds - approximately the time of a normal eye blink interval. For each of the five test samples five measurements per test sample were taken and the average values of the readings were calculated and recorded.

Results

a) Test samples in the hydrogel state with no lubricant. See sample print out of the oscilloscope output (Figure 5.14).[9]

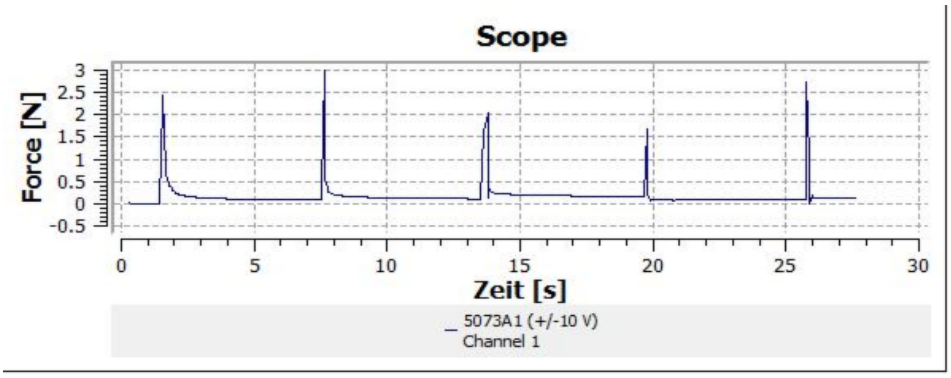

Figure 5.14 Oscilloscope reading for HEMA (V38) material - unlubricated friction.

b) Test samples in the hydrogel state with one drop of saline solution placed in between the interface of the test sample and the PTFE substrate to simulate borderline friction (Figure 5.15).

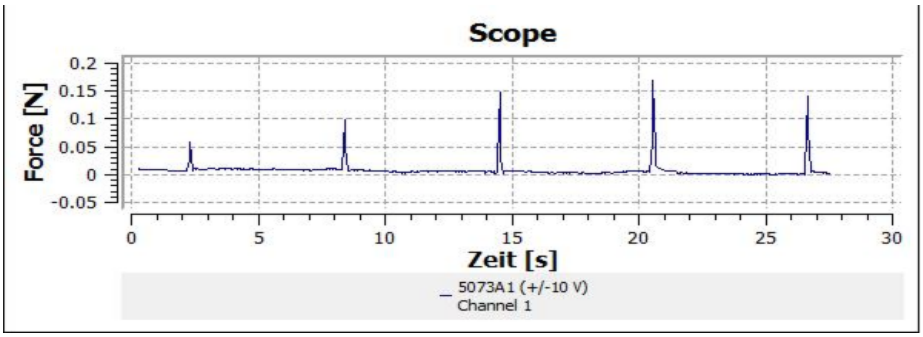

Figure 5.15 Oscilloscope reading for the LM material at borderline friction.

Note: The scaling in the graphs is generated automatically by the computer program.

[9] Hydrophilic contact lens materials contain water which is bound on the material matrix. There is no lubrication because water is bound to the material. Evaporation only reduces the water content.

It is necessary to remember, that besides the load attractive forces, i.e. van der Waals forces, charge and cohesion may result in different scaling. The reason for the low reading at the first peak in Figure 5.15 is unclear but may been caused by an unseen air bubble between the contact surfaces or too short a resting period after placing the test sample in the tribometer.

c) Test samples in the hydrogel state with one drop of saline solution placed between the interface of the test sample and the test substrate. A container with saline was placed under the PTFE substrate so that the substrate was continually wetted with saline solution. The substrate area surrounding the lens sample was kept wet with a few drops of extra saline during the test (see page 87 for detailed explanation) to simulate mixed friction. The ouput from the oscilloscope is shown in Figure 5.16.

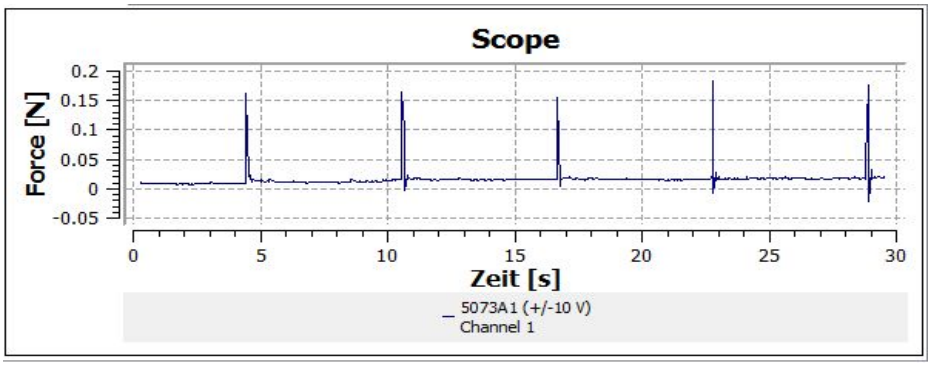

Figure 5.16 Oscilloscope reading for GM material

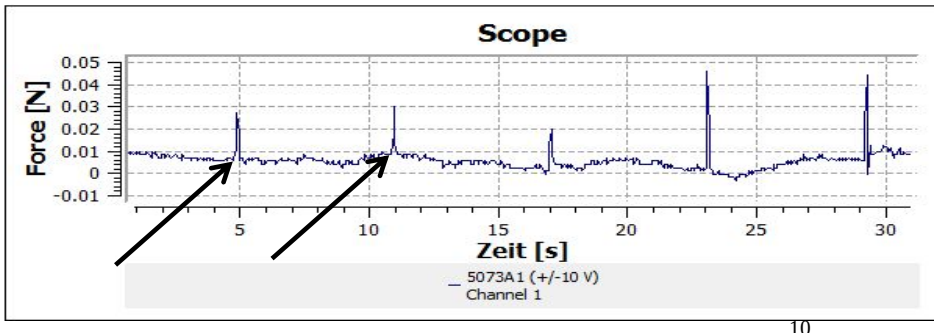

Figure 5.17 Oscilloscope reading of Definitive material at mixed friction[10].

[10] The 'basic noise' between the measurements shows a material relaxation between the measurements.

d) Test samples in the hydrogel state with one drop of Celluvisc (Allergan, 2012) placed on the contact area of the specimen and the substrate. Celluvisc is a normal ocular lubrication solution. The oscilloscope output is shown in Figure 5.17.

In Figure 5.17 the vertical scale reads in 0.002 N, unlike the previous three examples, which read to 0.2N or 3N, and therefore the baseline appears less flat. The height of the peaks appears to be quite different but, practically, the difference between the smallest and the largest is small (approx. 0.02N). The readings were taken from the base of the spike where the scribeline goes upwards, as indicated by arrows in Figure 5.17. The difference between the base and peak of the spike was taken as the measurement results, shown in Tables 5.9 to 5.12.

Substrate dry, surface free of liquid					
Material tested at 22°C and 55% relative humidity	HEMA vs PTFE dry	LM55 vs PTFE dry	VSO75 vs PTFE dry	GM 3 vs PTFE dry	Definitive vs PTFE dry
Av. measurement (N)	2.28	0.76	2.39	2.31	1.02
Applied Force (N)	0.098	0.098	0.098	0.098	0.098
Friction Coeff	23.24	7.79	24.37	23.58	10.44
Std. Dev. (N)	0.70	0.47	0.57	0.84	0.42

Table 5.9 Dry friction mesurements of 5 simulated blinks, with 6s between each measurement

Substrate dry, surface with a drop normal of saline (0.9% NaCl solution) (simulation of borderline friction)					
Material tested at 22°C and 55% relative humidity	HEMA vs PTFE	LM55 vs PTFE	VSO75 vs PTFE	GM 3 vs PTFE	Definitive vs PTFE
Av. measurement (N)	0.58	0.13	0.26	0.25	0.29
Applied Force (N)	0.098	0.098	0.098	0.098	0.098
Friction Coeff	5.89	1.32	2.68	2.59	2.93
Std. Dev. (N)	0.27	0.06	0.08	0.17	0.08

Table 5.10 Borderline friction measurement of 5 simulated blinks, with 6s between each measurement

Substrate in saline bath, surface completely wet (0.9% NaCl solution) (simulation of mixed friction)					
Material tested at 22°C and 55% relative humidity	HEMA vs PTFE	LM55 vs PTFE	VSO 75 vs PTFE	GM 3 vs PTFE	Definitive vs PTFE
Av. measurement (N)	0.08	0.17	0.27	0.14	0.38
Applied Force (N)	0.098	0.098	0.098	0.098	0.098
Friction Coeff	0.80	1.69	2.75	1.43	3.83
Std. Dev. (N)	0.07	0.14	0.07	0.04	0.11

Table 5.11 Mixed friction measurement of 5 simulated blinks,
with 6s between each measurement

Lens surface wetted with one drop of lubricating agent					
Material tested at 22°C and 55% relative humidity	HEMA vs PTFE with Celluvisc	LM55 vs PTFE Celluvisc	VSO 75 vs PTFE Celluvisc	GM 3 vs PTFE Celluvisc	Definitive vs PTFE Celluvisc
Av. measurement (N)	0.03	0.08	0.37	0.03	0.09
Applied Force (N)	0.098	0.098	0.098	0.098	0.098
Friction Coeff	0.35	0.80	3.73	0.27	0.89
Std. Dev. (N)	0.05	0.11	0.22	0.01	0.14

Table 5.12 Friction measurement of 5 simulated blinks, using the lubricating agent Celluvisc.
with 6s between each measurement

Discussion:

Materials having low friction coefficients showed smaller standard deviations. It is possible that the stick-slip phenomenon might be the reason for a higher standard deviation under unlubricated conditions. The results of the unlubricated tests have very little application to the conditions which apply during normal contact lens wear. The extraordinarily high friction coefficients recorded, exceeding for example rubber against glass (μ=2.0, Haney, 2004), might be related to the report that "*Contact lens adherence to the cornea is a particularly common problem in RGP extended wear."*(BCLA, 2011). Although the topic is not directly part of this study, the occurrence of such extraordinarily high friction coefficients might help to lead to a better understanding of the contact lens adherence phenomenon, which could be interpreted as a tribological sticking phenomenon. Various suggestions as to why contact lens adherence occurs have been made (Eiden and Schnider, 1996). Dry eye treatment with hydrophilic (bandage) lenses, as proposed in educational (Grehn,

2012) and other literature (Townsend, 2010), confirms the requirement of additional lubrication. In the current sudy, HEMA, the V38 material, the 75% MMA/VP material and one of the two materials which have, according to manufacturers' claims, "water loving" or "water binding" properties, have values of μ >20 (Table 5.9), while the other "water binding" material (LM55) showed the best, but still undesirable, frictional properties (μ= 7.79). It has to be kept in mind that measured forces resulting in a friction coefficient with μ >1 are higher than the force applied to the test material itself. The reliability of measurement results increases dramatically with the use of lubrication between the specimen and the substrate. The standard deviation of unlubricated HEMA material was 0.7N. The force transferred to the sensor was 2.28N while the force applied to the specimen was only 0.098N. Similar findings were reported with friction measurements of polyurethane layers with different ball shaped probes against different flat specimens, both unlubricated and lubricated (Caravia et al., 1993) showing CoF's up to 3.5. Jellinek (1960) investigated frictional properties of thin water films between glass plates. He found increased CoF's with a decrease of film thickness down to one micron or less and summarized that the phenomenon is a result of dry friction caused by asperities of the glass surfaces. A CoF of 0.45 for another hydrogel, polyacrylic acid, electrophoresis grade, using a glass lens as probe in an air environment was found, while in a water bath the CoF was approximately 0.12 using a normal force of 10 Millinewton. With increasing normal force to 50 Millinewton the CoF in air was reported to be about 0.12.

If a contact lens binds to the corneal epithelium some epithelial cells will adhere to the contact lens surface when the lens is removed from the eye. Considering that contact lenses are floating in a watery tear film, a friction coefficient close to that of ice (Mills, 2008) might be expected under lubricated conditions. The results of the *in vitro* experiments shown in Table 5.9 to Table 5.12 demonstrate that mixed or borderline friction occurs with different friction coefficients in different environmental conditions. The use of physiological saline which has similar oncotic properties as tears, causes different results depending on the type of material and the lubricating environment.

The results of the measurements under borderline conditions show that all materials develop a friction coefficient >1 (Table 5.10). The lowest friction coefficient was measured with the LM55 material (μ=1.32).

The test results presented in Table 5.11, in which mixed friction was simulated, showed small variance. The HEMA material (38% water content) showed a friction coefficient below 1 (μ=0.8). High water content materials, whether they contain silicone or not, still develop the highest friction coefficients (μ=2.75 and μ=3.83). As might be expected, the use of the tear lubricant helps to lower the friction coefficients dramatically. The only exception is the MMA/VP high water content material where the friction coefficient remained above 3. All other materials showed friction coefficients less than 1. These results showed, in most cases, different readings than those of other authors (see Chapter 5 -Rationale for in vitro experiments) with CoFs reported from 0.001 to 1.1 (Table 4.3). Although the test modality was dynamic friction under lubricated conditions, the lubricants used in other research varied and included packing solutions, saline (some with undefined content), Hyaluronic acid with a concentration up to 0.15mg/mL, 5% blood plasma containing lysozyme. Furthermore, while most of the measurement devices used in the literature were multipurpose tribometers, the experimental tribometer, as described in this thesis, simulated the *in vivo* situation as closely as possible. Notably, the area of contact used in these multipurpose tribometers was very small when compared with the ball shaped or a flat probe resting against a curved test sample with the large area of contact (78.54 mm^2) between specimen and PTFE probe of the author's testing set up. *"Kinetic friction and elastic contact behaviour of polymers"* were investigated by Tanaka (1984) who stated that an increasing area of contact was proportional to the frictional force but resulted in an increasing shearing strength with increasing load. As hypothesized by Jellinek (1960) the thickness of the lubricant layer played an important role regarding the CoF. The reliability of the tribometer used in the current study was demonstrated by careful comparison of the friction coefficients under similar conditions found (a) by the manufacturers of the PTFE materials under similar conditions, (b) in literature relating to PMMA and Aluminium.

It appears that the area of contact and the thickness of the lubricant layer were the explanation for the extraordinarily high friction coefficients found and these played an important role in contact lens friction simulating the ‘in eye’ situation. A difference in the lubricants used in the current tests and in the tests published by other authors was another factor which probably influenced the results. Saline solution, a Newtonian fluid, could play a role as a reference medium, and the use of tear substitutes or tear lubricants might enhance frictional properties. These products often have various rheological properties which may not be similar to those of tears, nor might they be Newtonian fluids.

Chapter 6 - Rationale for the in vivo experiments

6.1 *Introduction*

How does friction of a material affect soft lens performance in vivo and is there a relation to comfort and performance? In an attempt to answer this question, in this study identically shaped soft lenses made from the 5 selected soft lens materials were fitted to a sample of patients and the 'in-eye' performance of the lenses was evaluated. The lenses had a standardised design and did not aim to correct any ametropia present. Material properties, such as lubricity, frictional behaviour, and stiffness (i.e. tensile modulus), might require a different design of the posterior lens surface. The aim was to ensure that the fit of the soft lenses was also as standardised as possible. To this end, a series of PMMA trial lenses were manufactured to assess the ocular sagitta over a diameter of 14.5mm. Any soft lenses required would be custom made to the same sagitta. It is known (Bourassa and Benjamin, 1989) that the front surface of soft lenses acquire a biofilm very soon after lenses are placed in the eye and therefore the wetting angle is quite similar for many materials. One might therefore expect the friction characteristics to be similar for a diverse range of lenses when considering the effects of the eyelid on the front surface of the lens. The posterior surface is in a different position as there is no intermittent air interface. The experiments in this chapter aimed to establish if there is any statistical or clinical difference in lens performance which may be the result of differences in frictional characteristics. As the biofilms mentioned above differ with individual wearers, their individual tears, and the period of lens usage, it was decided to use unworn lenses only for the main tests.

The main measurements of contact lens performance are as follows:

Vertical lens movement after a blink

Lens tightness or looseness (Push-up-Test)

Vision (acuity, contrast, and stability)

Comfort

When the results of the clinical study are known, a comparison between the *in vitro* results and the *in vivo* results will be made.

6.2 *Corneal shape, bulbar shape and contact lens design*

The available corneal topographers (Oculus, Oculus Scheimpflug camera and Humphrey) all deliver measurements that relate to an area equivalent to that defined by a corneal diameter of about 10mm. However, soft contact lenses need to be larger than this in order to remain in place, as explained in Section 3.7 Contact lens movement on the eye. The Scheimpflug camera produces images of the cross sections of the anterior eye to a diameter of 14.2mm so the sagittal height of the eye can be measured. This allows the calculation of a radius of a sphere. This spherical radius is flatter than the radii calculated for rigid lenses using a topographer and is closer to reality as recommendations derived by experience used. Another method to find the required BOZR was evaluated by the use of specific manufactured PMMA lenses with a lens geometry which was used for the soft test lenses to find a parallel contact lens fit, with fluorescein dye used. The two methods were then compared to determine if there were differences in the BOZR's found and if any differences found were clinically significant and could affect the recommendations given by manufacturers or the values derived by experience in daily use.

A fundamental contact lens fitting criterion is the corneal shape. The average central radius according to Gullstrand's findings is 7.7mm but the corneal radius varies from person to person and may vary from 6.5mm to 8.5mm for normal eyes. The radius might vary at different axial directions on the same person, indicating corneal astigmatism[11]. The shape of a model cornea is considered to be a prolate ellipse i.e. the central radius is steeper than the periphery. In order to define the corneal shape, central and peripheral measurements with an ophthalmometer or a corneal topographer would be taken.

[11] To avoid confusion: Corneal astigmatism is not discussed further since it is not a fundamental topic of this research.

The shape of the ellipsoid cap is calculated by the formula used to calculate numerical eccentricity (ε) where ε=0 defines a circle; ε>0 and <1 defines an ellipse; ε=1 defines a parabola while ε >1 defines a hyperbola. Another way to describe the asphericity of the cornea is the 'shape factor', calculated as $1-\varepsilon^2$. The first attempts to calculate and measure corneal asphericity were carried out in the late 1960s (Wilms and Rabbetts, 1977). Today, computerised corneal image systems measure and map corneal shape to produce accurate results (Majorkovits et al., 2005) and claim to have the ability to provide contact lens fitting recommendations. The average numeric eccentricity of the human eye is approximately 0.39 or having a shape factor of 0.85 (Efron, 2002, Anderson and Kojima, 2007). An alternative way of defining the difference between the central corneal radius and the peripheral radius is the difference in sagittal height between a sphere and the estimated ellipsoid. This value is the "z" value and is measured in millimetres.

To predict how a contact lens matches to the corneal shape the corneal diameter plays an important role in conjunction with the corneal curvature. The depth of the anterior chamber, central corneal thickness and the horizontal corneal diameter allow the calculation of an equivalent spherical radius (Andre et al., 2001).

In the current study three methods were used to predict, evaluate and compare an equivalent spherical BOZR for a soft lens residing free from inner stress on an eye in primary gaze.

Note: If a soft contact lens is fitted "steep" i.e. the base curve radius of the contact lens is less than the (theoretical) radius of the area covered as described by Forst (1981) and by Leicht et al. (2005) the lens is stretched and/or bent to fit to the eye. As the lens material is not in the original shape there is inner (material) stress in the lens. This situation causes negative pressure between posterior lens surface and anterior surface of the eye covered by the lens (see detailed explanation in section 6.4).

a) Evaluating corneal and scleral geometry and calculating the equivalent radius.

b) Using PMMA trial contact lenses with soft lens design and using rigid contact lens fitting techniques, i.e. evaluating the fluorescein pattern.

c) Taking a Scheimpflug image of the anterior part of the eye and measuring the overall diameter and the sagittal height of the horizontal image to calculate the required BOZR.

6.3 *Predicting contact lens geometry by a mathematical approach*

According to Gullstrand's work the emmetropic eye has an overall length of 24 mm. Gullstrand's corneal radius is 7.7mm (Fink et al., 1996). Soft contact lenses differ in size and curvature from rigid contact lenses. Today, soft contact lenses may have a total diameter from 13.5 -15.0mm. Recommendations from the contact lens manufacturers and experience in soft contact lens fitting confirm the requirement of a back optic zone radius (BOZR) flatter than the measured corneal radii at the corneal apex. Recommendations (Baron and Ebel, 2008) for BOZR of soft lenses may range from 0.5 to 1.2mm flatter than the average apical corneal radius. The criteria for a well-fitted lens are - good visual acuity, good comfort and good physiological tolerance. Since there are no qualitative or quantitative methods known to control or confirm the fit of soft contact lenses, secondary criteria described in Section 3.6 (Soft contact lens fitting) are used. A geometrical and mathematical approach leads to better understanding of the required shape of the posterior side of the contact lens. The relation between sagittal height, corneal radii and BOZR is understood and has been discussed by various authors (Andre et al., 2001, Benz et al., 2008). Although scleral contact lenses have been made since 1888, there is variation in opinion regarding the scleral shape and scleral radii found in the eye (Drake et al., 2007). Gray's Anatomy, defines the globe as *"ball shaped"* while it has also been described as follows:*"As a three-dimensional object, the globe approximates an irregular oblong spheroid that can be divided topographically into segments of two modified spheres of different radii of curvature"* (Park and Karesh, 2006). Sagittal and axial MRI images of an eye show an upright ellipsoid shaped globe (Atchison et al., 2004). The researchers reported that *"myopic eyes tend to expand in all directions relative to*

emmetropic eyes, they are elongated more in the axial than in the vertical dimension and are elongated much less in the horizontal dimension". In other words, the ellipsoid shaped globes are orientated horizontally. Scleral radii of 45mm have been found (Hall et al., 2011) by using a Zeiss optical coherence tomographer (OCT) while measurements with an ocular Scheimpflug camera showed an average radius of 13.8mm (Tiffany et al., 2004). The geometry of the corneo-scleral profile (Stein et al., 2005) is further discussed in Annex A- The influence of scleral shape in relation to the Back Optic Zone Radius of a monocurve contact lens. To overcome the uncertainty of the shape of the scleral part of the eye a theoretical model related to the axial length of the eye was used with the following nomenclature:

a = sagittal height of the cornea at the limbus

b = sagittal height of the invisible scleral part covered by the cornea at the limbus

c = sagittal height of the sclera at the limbus.

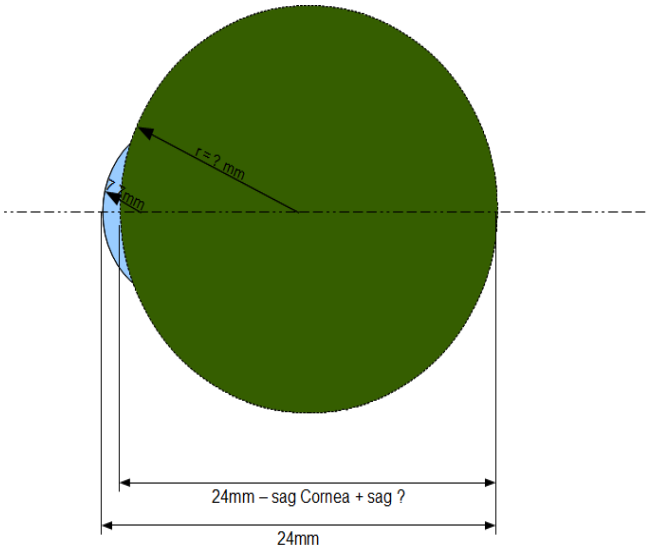

Figure 6.1 Explanation of the scleral model

The scleral diameter is 24mm – corneal sagitta + scleral sagitta where the sagittas are calculated in relation to the corneal diameter.

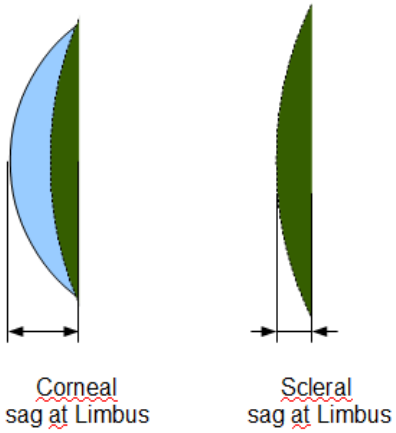

Figure 6.2 Separation of corneal and scleral sagittal heights

$$\text{The scleral radius} = \frac{24-a+b}{2} \qquad \text{Equation 11}$$

The sagittal height of a sphere is calculated as:

$$\boldsymbol{sag = r - \sqrt{r^2 - (\frac{h}{2})^2}} \qquad \text{Equation 12}$$

where r is the radius of curvature and h is the chord length. To calculate the sagittal height of an ellipse the following formulae are found in the literature (Sell, 1986) where ε stands for the numerical eccentricity, *a* is the long semi axis and X is the sagittal height of an ellipse cap:

$$a = \frac{r}{1-\varepsilon^2} \qquad \text{Equation 13}$$

$$\text{X} = a\left(1 - \sqrt{1 - \frac{h^2}{ra}}\right) \qquad \text{Equation14}$$

The scleral radii of 10.87mm and 10.73mm (Table 6.1) are based on bulbar lengths of 20 -25mm, a central corneal radius of 7.5mm and a numerical eccentricity of ε = 0.4. Due to the insignificant differences between the values calculated, the bulbar length used for further considerations and calculations is 24mm.

Bulbar length (mm)	K-reading (mm)	ε	Corneal Diam. (mm)	Sag height Cornea (mm)	Scleral dia. (mm)	Scleral radius (mm)	Scleral sag (mm)
20	7.5	0.4	10.5	2.08	19.41	9.70	1.54
21	7.5	0.4	10.5	2.08	20.33	10.16	1.46
22	7.5	0.4	10.5	2.08	21.25	10.63	1.39
23	7.5	0.4	10.5	2.08	22.19	11.09	1.32
24	**7.5**	**0.4**	**10.5**	2.08	**23.13**	**11.56**	**1.26**
25	7.5	0.4	10.5	2.08	24.08	12.04	1.21
Average					**21.73**	**10.87**	**1.36**
Std. Dev.					0.77	0.80	0.12
20	7.5	0.4	11.75	2.71	19.19	9.60	1.56
21	7.5	0.4	11.75	2.71	20.08	10.04	1.48
22	7.5	0.4	11.75	2.71	20.99	10.49	1.41
23	7.5	0.4	11.75	2.71	21.90	10.95	1.34
24	**7.5**	**0.4**	**11.75**	2.71	**22.82**	**11.41**	**1.28**
25	7.5	0.4	11.75	2.71	23.75	11.88	1.22
Average					**21.46**	**10.73**	**1.38**
Std. Dev.					0.76	0.78	0.12

Table 6.1 Calculation of the scleral diameter and radius
for bulbar lengths 20 - 25mm. The brown shaded cells refer to a typical bulbar length.

To evaluate the radius of a soft contact lens the following data are required

- Horizontal corneal diameter
- Central corneal radius
- Corneal eccentricity
- Contact lens diameter
- Theoretical scleral radius

Table 6.1 and Figure 6.3 explain how to calculate the required sagittal height. Once the sagittal height is known, the radius can be calculated.

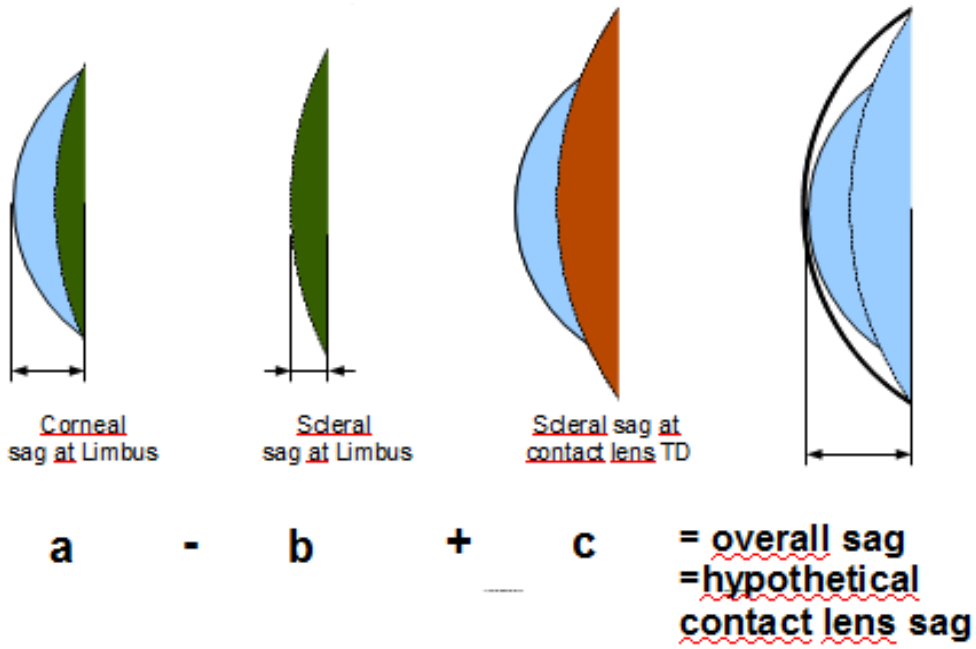

Figurto predict a BOZR of a soft contact lens with a known chord length

The variables in the formula are:

r = Radius of the circle

x = Sagittal height

d = Chord length (representing the diameter of the contact lens)

$$r = \frac{4x^2+d^2}{8x}$$ **Equation 15**[12]

Calculated BOZR values are found in Table 6.2 and Table 6.3

[12] The "sagitta" method is used to calculate the radius knowing the chord length and the sagittal height. This calculation is derived from the Pythagorean theorem.

Theoretical BOZR for contact lenses with TD 14.0mm								
K reading (mm)	CORNEAL DIAMETERS (mm)							
	10.00	10.30	10.60	10.90	11.20	11.50	11.80	12.10
7.5	9.2	9.1	9.0	8.9	8.8	8.7	8.6	8.7
7.6	9.3	9.2	9.1	9.0	8.9	8.8	8.7	8.7
7.7	9.3	9.2	9.2	9.1	9.0	8.9	8.8	8.8
7.8	9.4	9.3	9.2	9.1	9.0	8.9	8.9	8.9
7.9	9.4	9.4	9.3	9.2	9.1	9.0	8.9	9.0
8.0	9.5	9.4	9.3	9.3	9.2	9.1	9.0	9.0
8.1	9.6	9.5	9.4	9.3	9.2	9.2	9.1	9.1
8.2	9.6	9.5	9.5	9.4	9.3	9.2	9.1	9.2
8.3	9.7	9.6	9.5	9.5	9.4	9.3	9.2	9.3
8.4	9.7	9.7	9.6	9.5	9.4	9.4	9.3	9.3
8.5	9.8	9.7	9.6	9.6	9.5	9.4	9.4	9.4

Table 6.2 Calculated monocurve BOZRs for a 14.0mm diameter TD lens.

Theoretical BOZR for contact lenses with TD 14.5mm								
K reading (mm)	CORNEAL DIAMETERS (mm)							
	10.0	10.3	10.6	10.9	11.2	11.5	11.8	12.1
7.5	9.3	9.2	9.2	9.1	9.0	8.9	8.8	8.7
7.6	9.4	9.3	9.2	9.1	9.0	8.9	8.8	8.7
7.7	9.4	9.4	9.3	9.2	9.1	9.0	8.9	8.8
7.8	9.5	9.4	9.3	9.2	9.2	9.1	9.0	8.9
7.9	9.5	9.5	9.4	9.3	9.2	9.1	9.1	9.0
8	9.6	9.5	9.4	9.4	9.3	9.2	9.1	9.0
8.1	9.7	9.6	9.5	9.4	9.4	9.3	9.2	9.1
8.2	9.7	9.6	9.6	9.5	9.4	9.3	9.3	9.2
8.3	9.8	9.7	9.6	9.6	9.5	9.4	9.3	9.3
8.4	9.8	9.7	9.7	9.6	9.5	9.5	9.4	9.3
8.5	9.9	9.8	9.7	9.7	9.6	9.5	9.5	9.4

Table 6.3 Calculated monocurve lens
BOZRs with diameter TD=14.5mm and centre thickness tc=0.12mm.

Similar tables for contact lenses of different shapes could be calculated to estimate the required posterior curvature of soft contact lenses. Attention has to be drawn to the effective posterior diameter of the contact lens. To avoid undesired effects on the eye, the contact lens edges are rounded and polished or shaped in some way. Removing the sharp edge alters the diameter of the

contact lens on the posterior side. The result is a smaller contact zone in comparison to the lens TD, even at a lens thickness of 0.12mm. Figure 6.4 shows the difference in size between the lens TD (14.50mm) and the actual ocular contact zone (14.31mm).

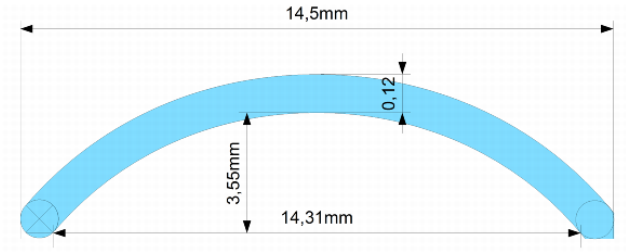

Figure 6.4 Section of a monocurve contact lens with effective inner lens diameter

To calculate the new diameter, the central angle has to be found using the following formulae where (not to scale).

α = central angle h = sagittal height r = radius of curvature s = chord length (or lens diameter)

Firstly, the sagittal height for the anterior radius has to be calculated from:

$$h = \sqrt{(r^2 - (\frac{s}{2})^2)} \qquad \text{Equation 16}$$

Then the central angle can be found from:

$$\alpha = 2 * \arccos(1 - \frac{h}{r}) \qquad \text{Equation 17}$$

Using the BOZR and the central angle α, the chord length (s) can be determined:

$$s = 2r * \sin(\frac{\alpha}{2}) \qquad \text{Equation 18}$$

The central angle α remains unchanged because the circles are concentric.

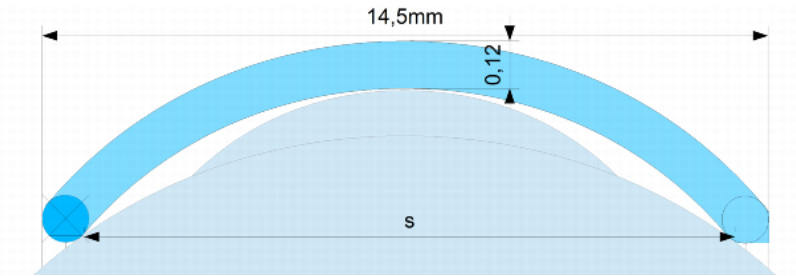

Figure 6.5 "Aligned" fit of a soft contact lens
(not to scale).

Figure 6.5 shows the area of contact for a soft contact lens with an ‘aligned’ contact lens fit.

There is a minimal apical touch not causing any corneal flattening.

Absolute correct values apply to a central angle of 90° only. Figure 6.6 explains the possible marginal deviation with a central angle of α ~ 105° and would apply for a contact lens diameter of 14.5mm and BZORs between 8.6mm and 9.4mm.

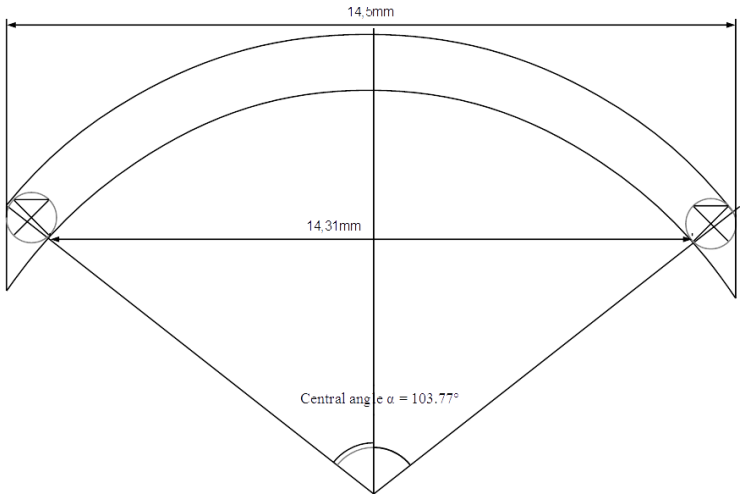

Figure 6.6 Approximation of contact area (not to scale). Central angle α defined

BOZR	tc	**FOZR**	TD	Sag (FOZR, TD)	α (radians)	α°	Effective inner diam. "s"
8.60	0.12	8.72	14.50	3.87	1.96	112.49	14.30
8.70	0.12	8.82	14.50	3.80	1.93	110.57	14.30
8.80	0.12	8.92	14.50	3.72	1.90	108.74	14.30
8.90	0.12	9.02	14.50	3.65	1.87	106.98	14.31
9.00	0.12	9.12	14.50	3.59	1.84	105.30	14.31
9.10	0.12	9.22	14.50	3.52	1.81	103.69	14.31
9.20	0.12	9.32	14.50	3.46	1.78	102.14	14.31
9.30	0.12	9.42	14.50	3.41	1.76	100.64	14.32
9.40	0.12	9.52	14.50	3.35	1.73	99.20	14.32

Table 6.4 Chord length "s" for contact lenand BOZRs 8.6 - 9.4mm

Table 6.4 contains the corrections according to Figure 6.4

6.4 *Design of the experimental soft lenses*

Standard soft contact lenses are often available in different radii and diameters. To determine the required base curve (BOZR) of a conventional contact lens, the central radii of the cornea are measured with an ophthalmometer (keratometer) or a computerised corneal mapping instrument. The BOZR is chosen by adding a value between 0.5mm and 1.2mm to the measured radii according to the personal experience and/or the manufacturer's recommendation. This results in a much flatter base curve in comparison to the measured radii of the apical corneal radii. Very few corneas are rotationally symmetrical and spherical. Soft lenses have to be larger than the corneal diameter in order to maintain stability. A proper fit of soft contact lenses may be judged by various parameters and tests such as lag, the result of the 'push-up-test' (Josephson, 1976), and movement after a blink in primary gaze or when looking upwards. To avoid unwanted peri-limbal depression of the contact lens edge, the properly fitted lens should rest free of internal stress on the eye in primary gaze. Internal stress of a soft contact lens *in situ* may reduce contact lens movement. To avoid erroneous findings when measuring frictional behaviour of contact lenses placed on an eye it is necessary to find the best lens curvature for the eye tested having no, or lowest possible, internal stress when placed on the eye in primary gaze.

In general, standard soft contact lenses consist of a spherical or aspheric base curve radius between 8.6 and 9.2 mm and a diameter between 14.0 and 14.5mm which, according to the manufacturers' recommendations, should fit in most cases. The three basic parameters of soft contact lenses are BOZR, power and total diameter.

The prerequisites for the calculations are: BOZR, lens thickness and total diameter. Lens power is not considered as the contact lenses will not correct any refractive errors. The FOZR is calculated by adding the central lens thickness to the BOZR.

Contact lens movement is influenced by the volume between the posterior contact lens surface and the anterior eye surface (Forst, 1981). Due to the lens movement a negative pressure results and this may differ from one lens

material to another. Tensile modulus, lens thickness, shape and water content of the material influence contact lens mobility on the eye (Leicht et al., 2005). For the measurement of frictional properties of a material the characteristics of the ocular tear film have to be considered. The pH, osmotic and oncotic pressure of tears, caused by environmental circumstances and nutrition influence the parameters of contact lenses (Holly, 1986, Holly, 2006). The experiments described in this thesis attempted to keep the variables as small as possible by using identical lens geometries and shapes for all lenses. As a result of these considerations some limitations of fit and behaviour can be expected. To this end, a set of PMMA contact lenses was produced having a single base curve, a front surface parallel to the base curve and with a centre thickness of 0.21 mm.

Design of the PMMA lenses

The BOZR of the lenses manufactured were similar to the radii of frequent replacement hydrophilic lenses marketed today.

The chord length for the posterior lens surface is 14.31mm for a lens having a TD of 14.5mm and a lens thickness of 0.12mm representing a standard sized hydrophilic lens. However, to avoid breakage of lenses a centre thickness of 0.21mm was substituted[13]. The usual way of finding the proper lens fit of rigid lenses is the use of fluorescein stain to visualise the tear layer between the posterior surface of the contact lens and the anterior surface of the eye. The eye is illuminated with blue light, e.g. a “Burton lamp” or a light beam of the biomicroscope with a cobalt blue filter in front of the illumination system. An aligned or parallel fit will not show fluorescence between the lens and the eye as the tear layer is too thin. A lens flatter than the eye will produce a black area in the centre and a green coloured tear reservoir in the periphery. A lens steeper than the corneal curvature will produce a green coloured tear reservoir in the centre.

[13] In order to get the proper chord length s= 14.31mm with a thickness of 0.21 instead of 0.12mm a lens diameter of 14.70 was necessary, but to avoid confusion the diameters are marked as 14.5mm.

6.5 *Experiment 4 – Use of a Scheimpflug image*

To find the overall radius of the area touching the corneal apex and the points of the largest visible area (i.e. 14.2mm) the Scheimpflug image allows these points to be found, and hence to quantify the sagittal height by using the formula shown in Equation 15 and explained in Section 6.4.

A cross sectional Scheimpflug image at approximately 180 degrees was taken with an Oculus HR 9000 camera to measure the horizontal section of the author's left eye.

The image was taken by a technician from the Oculus company in Austria.

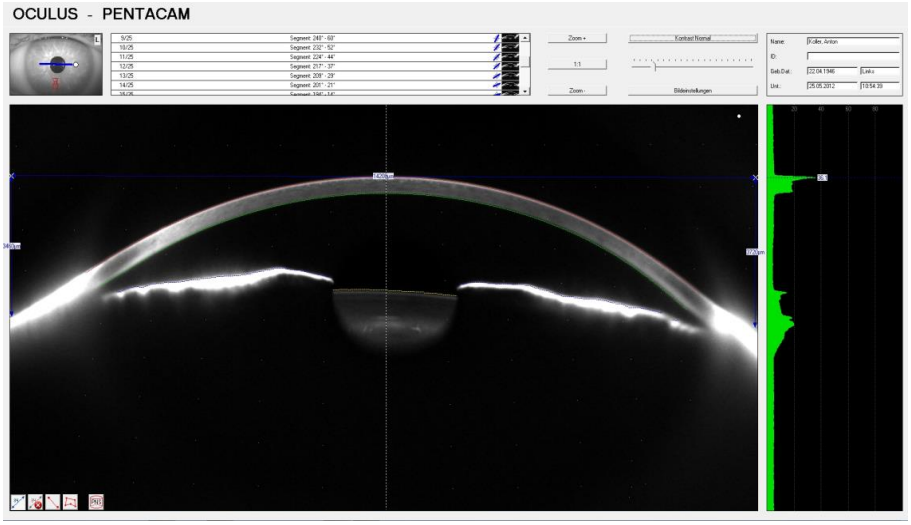

Figure 6.7 Scheimpflug image of the author's left eye.

The computer program associated with the Scheimpflug camera allowed measurements of the image shown in Figure 6.7.

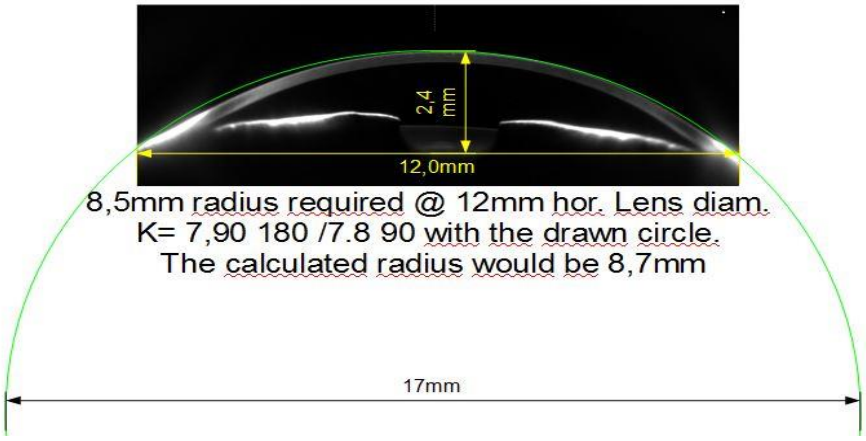

Figure 6.8 Explanatory drawing showing the resulting radius

These measurements were taken from the largest visible area (14.2mm). Because the image was slightly tilted, the average of the sagittal height on the left side (3.46mm) of the picture and the right side (3.72mm) of the picture was used to calculate a theoretical overall aligning sphere of 8.81mm. See drawn semi circle in Figure 6.8.

Discussion

The horizontal corneal diameter was 11.6mm. According to the results shown, the hypothetical BOZR for a lens having a TD of 14mm would be 9.0mm (See Figure 6.4 and Table 6.4). For the same eye the BOZR for a lens with a TD of 14.5 mm would be 9.1mm. The sagittal height found in the Scheimpflug image for a lens having a TD of 14.2 mm results in a radius of 8.82mm while the fluorescein pattern with the PMMA trial lens showed best alignment with a BOZR flatter than 8.7mm and steeper than 8.8mm. The comparison of the PMMA trial lens and the BOZR found with the Scheimpflug image showed quite good agreement with a difference in sagittal height of 0.08mm, while the mathematical approach results in a difference in sagittal height of 0.34mm. It is well understood that the bulbar shape is non-symmetrical and might have a conic, oblate, prolate, toric, spherical or a combination of these geometries. At the area of contact between the sclera and the contact lens, the differences in sagittal height based on the model described in Appendix A are limited. Neither the mathematical model presented nor the tests with the PMMA lenses were able to incorporate these uncertainties. All tests and measurements relate to the flatter corneal meridian. The mathematical model suggests a simplified model of the limbal zone. For the PMMA test lens, lid pressure might play a role and too steep a radius than necessary might be found resulting in a steeper BOZR than calculated.

A theoretical BOZR for a soft lens can be calculated using information from the Scheimpflug image or calculations based on keratometry and the horizontal corneal diameter (see Table 6.2 Calculated monocurve BOZRs for a 14.0mm diameter TD lens.

Other than manufacturers' recommendations or those found in the literature mentioned, which was probably based on clinical experience, the method

described above could be a valuable tool to obtain more accurate data for soft contact lens fitting. To measure the horizontal corneal diameter in vivo a suitable reticule mounted in the slit lamp's eyepiece together with some skill is required to achieve reproducible results. In the opinion of the author, this inexpensive method will lead to more accurate results than simply measuring the K values and adding some value recommended by contact lens manufacturers.

6.6 *Experiment 5 - Evaluation of the PMMA semi-scleral lenses on one eye.*

Introduction

During a scleral lens fitting course at the "Innovative Sclerals" company in Hertford, UK, it was mentioned that the sagittal depths of all normal corneas are approximately the same. This knowledge could lead to a fitting procedure for soft lenses utilising a rigid lens with exactly the same geometry as the proposed soft lens. The use of sodium fluorescein and assessment methods for rigid lenses will lead to the proper soft lens fit without material stress in primary gaze.

Aim: to conduct a pilot study on the author's own eye in order to assess the suitability and effectiveness of the semi-scleral lenses as a method to find the required base curve for soft contact lenses. The tests were also compared with the results found in 6.5 Experiment 4 – Use of a Scheimpflug image. Other than standard scleral lenses the geometry of the lenses necessary were identical to standard soft lens geometries used. The theoretical background was described in Annex 11.1, in Section 6.3 and, regarding material stress of soft contact lenses, in Section 6.2. Without knowing the outcome of the tests performed, a set of PMMA lenses with different BOZR's in 0.1mm steps between 8.6 and 9.3mm with a diameter of 14.5mm was manufactured.

Materials

An American Optical keratometer,

Sodium fluorescein solution 1%

An electric torch with UV LEDs

A Panasonic LUMIX or a Casio Exilim EXFH25 digital photo camera (Sodium fluorescein dye in conjunction with the UV lamp was used to visualise the tear layer between back surface of contact lens and anterior surface of the eye).

Subject: The author.

Observer: The camera was operated by the author's daughter who is a qualified optometrist. The contact lens fits were judged by the author and the author's daughter by evaluating the photographs.

Method

A radius 0.70mm flatter than the flattest keratometer reading (7.90mm for this subject) was chosen, i.e. 8.60mm. This would be approximately the recommendation for fitting a soft lens and was a reasonable starting point. A drop[14] (Zimmermann-Spinnler, 1983) of fluorescein was placed on the concave side of the lens and saline was added to half fill the lens with liquid.

The camera was mounted on a tripod and placed at a suitable distance and with a focal length setting to fill the frame. The UV torch was held by the subject. The aperture, time setting and film speed were set manually to achieve best quality. Each trial lens was fitted in turn and a fluorescein photograph taken after a period of 30 seconds to allow for any settling of the lens. There was no need to repeat the photo sessions once the method of applying the amount of fluorescein and the camera setting was found by experimentation.

The fluorescein pattern itself allowed the observer to judge if the lens was fitting steeply, aligned or flat on the eye.

RESULTS

The author's central corneal radii were 7.90 mm at 180 degrees and 7.80 at 90 degrees. The horizontal corneal diameter was 11.6mm.

[14] The volume of a drop in laboratory technique is usually calculated as 50µl. The size of a drop depends on the type of liquid and the size of the drop releasing area.

Figure 6.9 Semi-scleral PMMA lens 8.6/14.5mm.

Figure 6.9 shows an extremely steep contact lens fit. There is a huge air bubble and few tears under the lens. Figure 6.10 shows an air bubble smaller than the one shown in Figure 6.9.

Figure 6.10 Semi-scleral PMMA lens 8.7/14.5mm.

There is a central area at the corneal apex indicating minimal fluorescein between the posterior lens surface and the corneal apex.

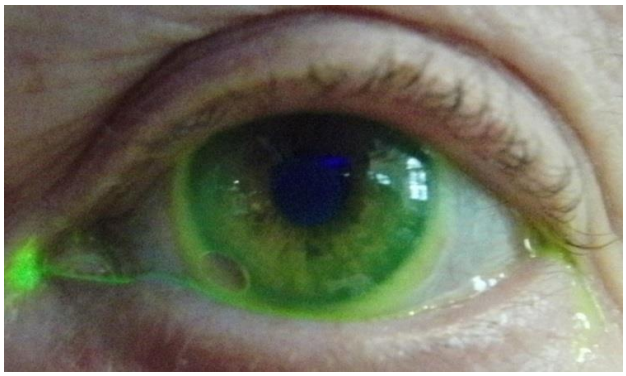

Figure 6.11 Semi-scleral PMMA Lens 8.80/14.5mm.

Figure 6.11 shows a decentred lens, riding “low” with a small air bubble at 8 o’clock indicating a fit flatter than an aligned fit.

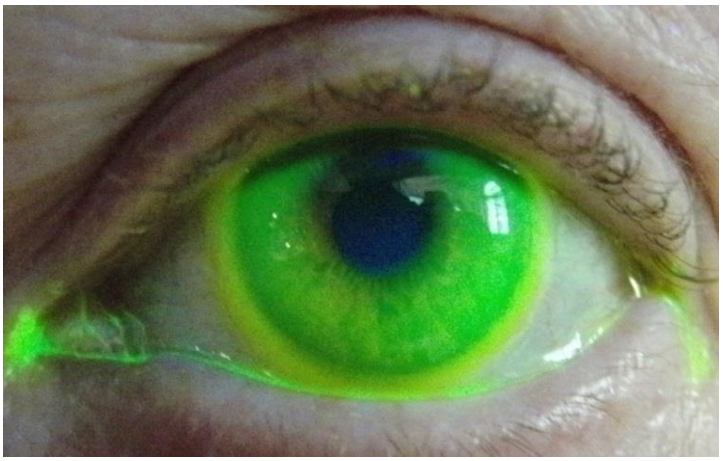

Figure 6.12 Semi-scleral PMMA lens 8.9/14.5mm

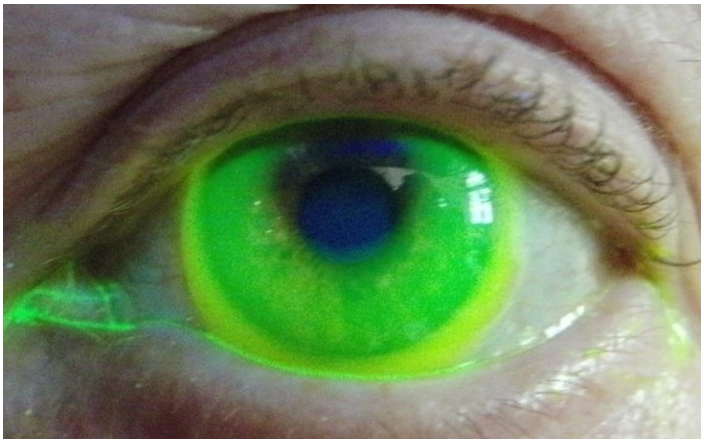

Figure 6.13 Semi-scleral PMMA lens 9.0/14.5mm

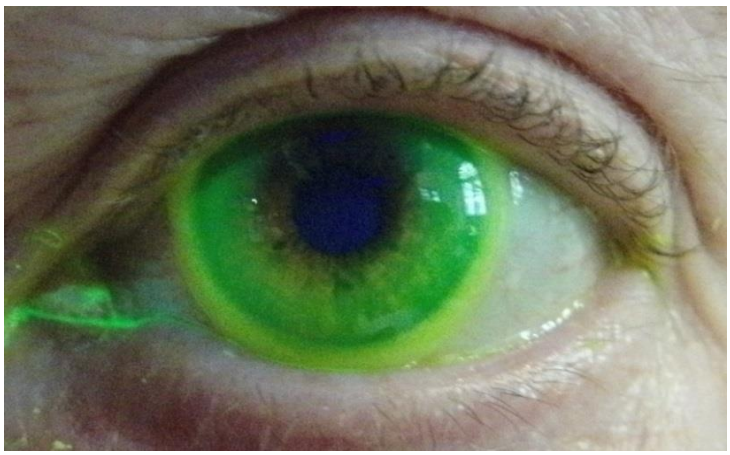

Figure 6.14 Semi-scleral PMMA lens 9.1/14.5mm.

The comparison between Figure 6.12 and Figure 6.14 shows little change in the fluorescein pattern. The contact area between corneal apex and lens may be

judged as becoming slightly larger and becoming oval shaped because of upper eyelid pressure.

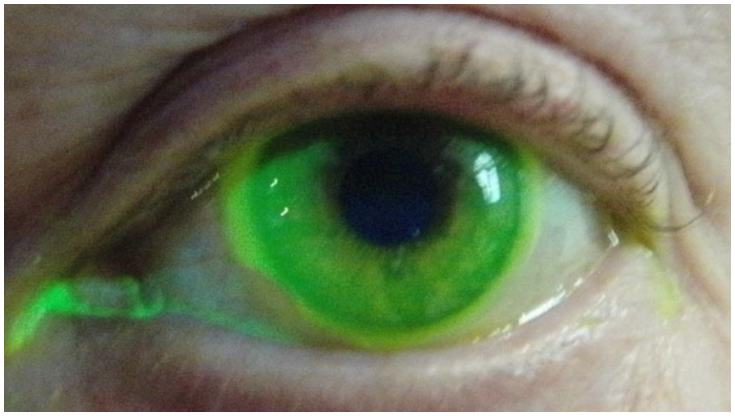

Figure 6.15 Semi-scleral PMMA lens 9.2/14.5mm.

Figure 6.15 shows an air bubble at 8 o'clock and a lifted off lens edge indicating a too flat contact lens. According to the figures shown above, the lens closest to alignment would be the 8.7mm radius with 14.5mm total diameter. Incidentally, best comfort was achieved with the 8.8/14.5mm lens.

Discussion

It is necessary to clarify that in contact lens production physical limits exist. Looking at sagittal heights for lathe turned lenses, the gauges used to calibrate the lathes have a resolution of 0.001mm or 1 micron. Gauges having a resolution of 1 micron have errors higher than the resolution shown. There are also tolerances within the threads, moving the spindle slides, material stress, heat build-up by cutting, cutting tool degradation, inaccuracy in tool positioning due to limitations of positioning mechanics, machine wear as well as shape alteration of the contact lens material by polishing the BOZR and the lens edge. Machining plastics differs from machining metals and is judged as an art by those involved in the industry. Different plastic materials behave differently when machined and require a lot of experience to ensure accuracy within the required tolerances. The true parameters of the test lenses, as shown in Table 6.5, meet the accuracy requirements according to ISO 13869-2.

Values produced				Internal Sag Height		Systematic Prod. Error	Step Sag height	Real Step Sag Height
BOZR	BVP	Centre thickness	Ext. Sag	Calculated (TD 14.5)	Measured (TD 14.5)			
8.60	-0.87	0.23	4.30	3.83	4.03	0.20	0.08	0.07
8.70	-0.87	0.19	4.15	3.75	3.96	0.21	0.08	0.07
8.80	-0.87	0.20	4.10	3.68	3.90	0.22	0.07	0.06
8.90	-0.87	0.22	4.06	3.61	3.84	0.23	0.07	0.06
9.00	-0.87	0.23	4.01	3.54	3.78	0.24	0.07	0.06
9.10	-0.75	0.24	3.94	3.48	3.70	0.22	0.06	0.08
9.20	-0.87	0.21	3.85	3.42	3.64	0.22	0.06	0.06
9.30	-0.87	0.24	3.82	3.36	3.58	0.22	0.06	0.06

Table 6.5 The production data and the measured values for the set of semi scleral PMMA lenses.

The step sag is defined as the difference between two adjacent values with the smaller being subtracted from the larger. The real step sag is between 0.06 and 0.08mm. As calculated in Table 6.4 the chord length for the posterior lens surface is 14.31mm for a lens having a TD of 14.5mm and a lens thickness of 0.12mm represents a standard sized hydrogel lens.

The comparison between Figure 6.14 and Figure 6.15 showed that a sagittal height difference of 70 microns caused a significant change in the appearance of the fluorescein pattern. The relationship between sagittal height and radius, in the relevant range, deviates from linearity by only up to 20 microns and can therefore be regarded as close to linear. The calculated difference in sagittal height between the test lenses was in a range of 20 microns. In soft contact lens fitting, contact lens shape is usually is defined by the BOZR and the TD. Because of the insignificant sagittal height variations between the test lenses, it was decided to describe the contact lenses using the commonly used parameters, BOZR and TD for clarity. The use of a local anaesthetic was not required. Without using an anaesthetic, the comfort of the PMMA test lenses would serve as a reference for the comfort of the soft lenses. Any contact lens larger than the lid aperture causes less sensation than a smaller contact lens.

It appeared that using a rigid lens as a template for custom-made soft lenses was a viable approach and enabled experimental soft lenses to fit individual eyes in a standardised manner and the lens choice agreed with the findings obtained with the Scheimpflug camera. Two methods for finding a BOZR of a soft contact lens causing least internal stress were demonstrated.

The use of a Scheimpflug camera to collect non-invasive data for evaluating contact lens designs is to be recommended. The software provided may meet the requirements for ophthalmologists and clinicians. Drawing and undoing lines and adding defined curves to evaluate back surfaces of contact lenses in a non-invasive way with the cross section images was not particularly difficult. The outcomes were used to find the best suitable BOZR for use in the in vivo experiments (Chapter 7 -).

6.7 *Experiment 6 - Measurement of soft lens parameters at elevated temperature*

Introduction

To measure frictional interactions between the soft contact lens in situ, the lid and the eye need to interact with the contact lens without undesired side effects that might influence results. Possible errors could arise from steepening caused by a temperature rise and changing tonicity conditions. The tolerances published by the International Standards Organisation could also influence the results. The ISO Standard 13869-2 (ISO, 2012) defines the tolerances for soft contact lenses.

The relevant ones are:

BOZR:	± 0.20mm
TD:	± 0.20mm

According to the tolerances accepted, a soft lens labelled:

BOZR 8.7mm TD: 14.5 (sag: 3.89mm)

might be anything between:

BOZR: 8.5mm TD: 14.7mm (sag: 4.23mm) and BOZR: 8.9mm TD: 14.3mm (sag: 3.6mm)

Lenses have to be measured in euhydric (isotonic, iso-osmotic and iso-oncotic) saline solution at room temperature. It is known that soft contact lenses might change their shape in environments other than saline solution at room temperature (Tranoudis and Efron, 2004). A pH other than neutral, tonicity, dehydration during wear and other conditions may alter the lens shape (Brujic and Miller, 2010, Nichols and Sinnott, 2006, Ramamoorthy, 2010).

The possible parameter variations of soft contact lenses between the in vivo situation and the in vitro environment were discussed in Section 5.8. Environmental conditions during lens production, such as temperature, humidity, wear of cutting tools, limits of measuring devices, varying swell rates of the same lens material and interpretation of measurements taken can all cause errors. Compensating for all these parameters to produce each of the five materials to an identical shape in situ for each individual subject in the study was not completely possible, despite all the precautions taken, because of the difficulty in maintaining an unchanged tear environment.

It was decided to produce soft lenses identical to the design of the PMMA test lenses as described in Section 6.6 to find the best suitable BOZR for the soft lenses. These PMMA lenses with the soft lens design had to have a minimum centre thickness of 0.9mm to avoid breakage in situ. Soft contact lenses generally are much thinner. The soft test lenses were manufactured with a centre thickness of 0.18mm. This thickness was chosen for stability reasons of the lens when measured. Thinner lenses, when immersed in a wet cell are even less stable which could have resulted in inaccurate measurement results. The thickness was chosen by experience and assured accurate measurement results within a thickness range used in normal contact lens wearing.

In contact lens practice it is well known that soft lenses produced by different manufacturers, but with identical parameters, behave differently in vivo. Contact lens practitioners address this fact by using different techniques to monitor the behaviour of the contact lenses in situ. The contact lenses in the current study were produced with extreme care and manufacturing tolerances were narrowed to less than 0.1mm for the radii, and less than 0.05mm for the diameter. It was necessary to produce up to three lenses to get at least one within these tolerances.

Aim:

To determine the difference in BOZR and TD values for a temperature change of 12°C

Materials

A reference set of soft contact lenses was manufactured from the five materials. The BOZR and TD were measured at ambient room temperature (22°C) and at the normal corneal temperature (34°C) (Klamann et al., 2012).

2 lenses from each of the 5 materials were made to a standardised design and produced to an accuracy of ± 0.05mm radius and ±0.05mm diameter in the hydrated state. The centre thickness was 0.18mm and the FOZR equalled the BOZR + tc.

Optimec soft lens measurement system.

Normal saline.

Laboratory thermometer.

Method

The unused hydrated lenses were measured with a calibrated Optimec soft lens measuring system. The temperature was measured with a standard laboratory mercury thermometer placed in the wet cell of the Optimec instrument. The saline solution was identical to that used in the in vitro experiments. Each lens was measured three times at room temperature and the average recorded.

To elevate the temperature in the wet cell a sufficient amount of hot saline was added to raise the temperature to 34°C. The temperature could easily be

maintained as soon as the housing of the wet cell reached 34°C (as soon the temperature dropped 0.5°C an adequate amount of hot saline was added in order to keep the temperature at 34°C). The temperature was checked before, during and after each measurement. The lens then was placed into the diameter gauge for 45 seconds to equilibrate. Three measurements were taken and the average TD recorded. The lens then was transferred to the radius gauge. The lens BOZR was also measured three times and the average value recorded.

Results

Material	BOZR 1 at 22°C (mm)	TD 1 at 22°C (mm)	BOZR 2 at 34°C (mm)	TD 2 at 34°C (mm)	Contraction factor		Internal Sag (mm)		
					BOZR	TD	22° BOZR1/TD1	34° BOZR2/TD2	Variation
V38	9.0	14.5	8.7	14.4	0.96	0.99	3.67	3.86	+0.19
V38	9.2	14.5	8.9	14.4	0.96	0.99	3.54	3.70	+0.17
LM	9.2	14.5	8.8	14.3	0.95	0.99	3.54	3.68	+0.15
LM	9.0	14.5	8.6	14.3	0.96	0.99	3.67	3.79	+0.12
Def.	9.0	14.5	8.5	14.1	0.95	0.97	3.67	3.75	+0.08
Def.	9.2	14.5	8.7	14.1	0.95	0.97	3.54	3.60	+0.07
V75	9.2	14.5	8.8	14.1	0.96	0.97	3.54	3.53	-0.01
V75	9.0	14.5	8.6	14.2	0.96	0.98	3.67	3.70	+0.04
GM	9.0	14.5	8.6	14.1	0.96	0.97	3.67	3.67	+0.00
GM	9.2	14.5	9.0	14.3	0.97	0.99	3.54	3.58	+0.05

Table 6.6 Comparison of radii, diameters and sags between ambient room temperature and 34°C for the five different soft lens materials.

Experiment 6 demonstrated that a small difference in the BOZR could change the contact lens fit from aligned to non-aligned. A lens with a diameter of 14.5mm and a radius of 8.7mm for the tested eye was found to give an aligned pattern. Pattern differences between the 0.1mm steeper and the 0.1mm flatter lens could easily be discriminated.

Discussion

All the soft lenses showed a decrease in BOZR and TD with increasing temperature. In virtually all cases this resulted in an increase in the sag value.

The maximum sag change occurred with the polyHEMA lenses with an average change of 0.18mm[15]. The results obtained from the polyHEMA and the V55 are in accord with the results obtained by other authors (Tranoudis and Efron, 2004).

For testing frictional behaviour in situ as a function of contact lens movement between blinks it could be reasonable to adapt geometric contact lens parameters, i.e. BOZR and TD to the temperature expected on the corneal surface (Kessel et al., 2010). A rise in temperature to 34°C showed that radii steepened and diameters reduced. It could be expected that for the lens fit a steeper radius would be compensated for by the smaller lens diameter within the range found. The results in Table 6.6 showed that there was no need for extra temperature compensation regarding the allowed tolerances for soft contact lenses. Labelling of relevant contact lens data is standardized by ISO and national standards. Soft contact lenses are measured at ambient room temperature. For the tests performed in the current author's research it was necessary to draw attention to the issue, since it could have been relevant regarding the relation between BOZR of the soft lens in situ at body temperature and the required shape of the lens.

[15] BOZR at 34°C are the averages of two different lenses measured per material.

Chapter 7 - In vivo experiments

7.1 *Ethical approval, inclusion and exclusion criteria*

Ethical approval

Ethical approval for the in-vivo experiments was obtained from Ethikkommission der Stadt Wien, Reference EK-13-150-0713.

Inclusion criteria

Suitable subjects must be of normal health

Age between 18 and 50 years

Male or female

Average K readings from 7.4mm to 8.2mm and

Horizontal corneal diameters from 10.2mm to 12mm.

Contact lens wearers must leave out their CLs for at least 24 h before any clinical tests

Exclusion criteria

Ocular tissue grades >1 (ISO/FDIS 11980, 2012)(pISO and Organisation, 2012)

Ptosis

Corneal astigmatism greater than 1.5 D

Any eye infection or inflammation, any diagnosed dry eye, a cold, or any other ocular or systemic condition or irregularity which could influence the normal physiological conditions of the eye and the nose.

HIV and AIDS

Blepharospasm (with or without contact lenses)

Severe discomfort with CL in place after the adaptation period.

Visual acuity (VA) with best spectacle correction less than 1.0 (6/6)

Contrast vision with Ginsburg distance charts less than within the normal range with best spectacle correction

Retinoscopic spot image presented with a chart projector having no sharp edges.

Non-invasive break-up-time (NIBUT) <10 secs.

Subjects

A significant change in mean comfort scores based on the VAS is in the region of 1-1.5cm a preclinical trial showed which would result in sample sizes of between 50-120 using a SD of 0.24cm a preclinical trial showed. Considering the inclusion and exclusion criteria it would be too difficult to recruit such a number of participants. Performing the complete test battery with five lenses for each of five lens types was extremely time consuming for subjects was another limiting factor and restricted the final sample size to five subjects. While a larger sample than five would have been ideal, the number of tests carried out would have to then be reduced due to time constraints. There were also limitations imposed by the large number of lenses to be manufactured to exceptionally tight tolerances.

Taking all these reasons into consideration, five suitable subjects were recruited. This required the fitting of five different lenses made of each of the five materials on each subject's eye, the manufacture of 250 lenses, and 25 test runs for each tested subject.

The use of five different lenses made of the same material helped to minimise the risk of possible errors caused by reasons not relevant for the comfort test, such as foreign body sensation, imperfect lens, bad optical performance, imperfect lens edges etc.

It was tried to find subjects suitable for soft lenses with identical parameters. Soft lenses with identical shape were believed to avoid effects that could influence the results caused by interactions of contact lenses in situ and

different limbal or corneal shapes with respect to contact lens movement triggered by blinking.

Subjects for the in vivo experiments were selected as described in Appendix C using the Clinical Record Forms 1-4.

A comprehensive optometric examination was carried out in order to rule out any non-suitable subjects. It was the aim of the study to have at least 5 subjects and to use both eyes of each subject. Those who were suitable would have the nature of the investigation carefully explained. Subjects would have the opportunity to ask questions from the trial supervisor.

The subjects who agreed to take part would read the consent and information form (see appendix B), had an opportunity to ask any questions, and signed this form.

7.2 *Equipment and materials*

Standard equipment for optometric examinations and contact lens fitting was used:

Inspection Lamp

American Optical Project O Chart to measure visual acuity using Snellen acuity.

Note: Lim et al. (2010) reported insignificant differences between Snellen and LogMar charts with healthy eyes, while the use of Snellen was less time consuming.

Phoroptor

Trial Frame and trial case lenses

American Optical Slit Lamp microscope with an eye piece containing a 0.1mm resolution reticule at 15x resolution.

Zeiss Slit Lamp microscope with an eye piece containing a 0.1mm resolution reticule at 15x resolution.

Haag-Streit 900 BQ LED slit lamp microscope containing the imaging module (Haag Streit, 2012)

American Optical Keratometer

Keeler TearScope. The evaluation of the tear film, its importance for contact lens wear and its influences was described by (Guillon et al., 1988)

Ginsburg Contrast Sensitivity distance charts

Pesola light scribe and hanging scale to measure lid tension (Manufacturer: Pesola AG, CH 6340 Baar, Switzerland)

Soft contact lenses matching the subjects' eyes made out of different contact lens materials.

Contact lens rinsing solution (i.e. saline solution for contact lenses)

Personal computer and software used:

64 bit Personal computer with 8 Gigabyte RAM fixed disk and Windows 7 as operating system

Haag-Streit "EyeSuite" program to store and manage the images obtained.

Open Source software "Image Grab" (Gagla, 2010) to extract single frames from the movie taken with the Haag-Streit slit lamp microscope.

Shareware software "PhotoFiltreX" (Da Cruz, 2012) to calibrate, size and overlay extracted images

Manufacture of soft contact lenses used in experiments

The lenses ordered initially from a local CE certified manufacturer fundamentally failed to meet quality requirements. The BOZR differed randomly up to – 0.8mm and the TD up to -0.5mm. It appeared impossible to obtain lenses of the necessary quality standards from conventional manufacturers. As a result it was necessary to manufacture all 250 soft test lenses to the following exceptionally tight tolerances (much stricter than those of ISO) at the author's own premises under his direction and supervision: BOZR having a tolerance +/- 0.05mm and a tolerance in diameter +/-0.05mm. The low tolerance for the BOZR was achieved by a lens design which allowed

accurate measurement of BOZR and TD. The measurement procedure, i.e. repeated measurement of the same lens, assured the accuracy described. The production of 250 of these very accurate custom-made lenses, only made possible through the avaialability of the author's own manufacturing facility, was costly and time-consuming, which made it impossible to manufacture greater numbers of lenses.

The production of 250 lenses was necessary because it was not possible to use of the same set of lenses for each subject, for safety, ethical and legal reasons. Furthermore, the lenses, when worn once on a patient's eye, even though they could be cleaned and refurbished, may have behaved differently on the subject's eye or on another subject's eye despite (nearly) identical lens parameters because the lens could carry a "biofilm" or be altered by a second autoclaving run.

Another notable feature of the materials used in this experiment was the lens shape. Standard contact lenses used for optical correction must contain a lenticular curve which reduces the useable optical part of the contact lens to an average pupil diameter. This lenticular curve controls the edge thickness which is defined, through clinical experience, by the contact lens manufacturer. The lens edge is a fundamental element regarding contact lens comfort. Its shape and thickness are determined by experience and there is little published literature on this topic (Bussacker, 1974). A ski-tip-like profile is the shape preferred. The illustration in Figure 4.5 shows the existence of a junction which could influence the mechanical stability of the contact lens and the movement in situ. Different optical powers change the thickness of the junction, especially for lenses to correct myopia. To overcome this uncertainty, in the current experiments the lenses were made with parallel curvature posterior and anterior, see sketch B in Figure 4.5. Such lenses are relatively unstable and "floppy" which required the centre thickness to be fixed at 0.15mm in a hydrogel state. The sharp lathe cut lens edges were ski-tip rounded by polishing. The edge thickness was reduced to the desired 0.12mm. The V75 material, as later mentioned, required a centre thickness of 0.18 mm for better stability. An adequate edge shape and thickness in each of the 250 test lenses could be assured.

7.3 *The clinical record forms.*

Clinical Record Form 1 (CRF1)[16]

The form contains the following data:

A code number to identify the subject

Exterior part of the eye, lids, lashes, conjunctiva, and cornea to be graded 0 to 4 using the slit lamp.

Any corneal staining, scars, opacities etc to be drawn.

Central keratometer readings (Ophthalmometer)

Best visual acuity with the actual prescription for both eyes (normal refraction method)

Check whether the retinoscopy spot presented with a chart projector is free of entoptic phenomena (Helmholtz, 1909, Tyler, 1978, Aulhorn, 1977, Hollwich and Kemmetmüller, 1975), (i.e. missing well defined sharp edge, halos or comet's tail as a result of steep or too flat lens fit or improper optical quality of the soft contact lens)

Contrast sensitivity for distance with the spectacle prescription using the Ginsburg Functional Acuity Contrast Test (FACT) Charts

Non-invasive tear break up time (NIBUT) (s)

Tear meniscus height at the lower lid area (mm)

Measurement of the upper lid tension using a "Pesola Lightline" hanging scale.[17]

---

[16] Clinical record form samples see appendix C

[17] The method was first used in an unpublished student project in April 2009 in the Vienna "Akademie für Optometrie, Augenoptik und Hörakustik". A small piece of adhesive was attached to the subject's relaxed upper lid while the head is bent. The clamp of the scale gripped the free edge of the adhesive and the scale carefully was pulled upwards to lift the lid to a tiny gap. The reading then was recorded. Although not extremely accurate, an estimation of the lid force was possible.

Clinical Record Form 2 (CRF2)

Trial lenses used on both eyes with the results (specifications)

Trial lenses chosen for the experiment (specifications)

For each soft CL material, the following are recorded:

Vertical movement (mm) of lenses with normal blinking 30 minutes after lens insertion

Movement of lenses using the "push up test" differentiated between "L" for loose, "N" for normal and "T" for tight.

Best visual acuity with complete over correction.

Check whether the retinoscopic spot presented with a chart projector is free of entoptic phenomena (missing sharp edge, halos, comet's tail).

Contrast sensitivity for distance with best over correction.

Visual check using a slit lamp, for conjunctival impression marks of the contact lens edge outside the limbal area to avoid steep fit and to compare the initial lens fit and the lens fit after 30 minutes of wear.

Subjective comfort using a Visual Analogue Scale 10cm in height

Subject and lenses suitable for video recording Yes [ ] No [ ]

Video reviewed briefly and found to be suitable for analysis

Yes [ ] No [ ]

Clinical Record Form 3 (CRF 3)

This is completed for each subject after the last lenses have been removed.

Slit lamp examination of the cornea and conjunctiva including staining with fluorescein

Best corrected visual acuity RE/ LE

Any reason for medical referral? Yes [ ] No [ ]

If, YES, give details of any adverse event and action taken for remedial treatment and management.

7.4 *Experiment 7 – In vivo experiments*

Introduction

There were two phases; the first used the PMMA trial lenses on the selected subjects in order to assess the BOZR and the TD necessary to obtain an aligned fit. The second phase will necessitated manufacturing soft lenses from the five materials to a design that replicated the PMMA design that gave an aligned fit. These soft lenses were fitted to the subjects in order to establish comfort and performance.

The results from the comfort and performance tests were compared to the friction characteristics of the five different materials.

Note: This work relates to contact lenses only. Tests for the right and left eyes were carried out sequentially even if the subject had lenses in both eyes.

Materials

- Contact lenses

The PMMA plano powered trial lenses were made and fitted in accordance with section 6.6.

The diameter of the soft lenses was set to 14.5mm which is typical of contemporary designs. The front curve was a single curve which avoided undesired dynamic side effects which could occur with multicurve or lenticular front curve designs.

Lenses were produced to an accuracy of ± 0.1mm in radius und ± 0.1mm in diameter. The centre thickness of all materials, except the VSO 75 material, was 0.15mm. The VSO 75 material had to have a centre thickness of 0.18 mm to avoid peripheral deformation.

- American Optical Radiuscope for rigid lenses
- Contact lens diameter gauge for rigid lenses
- Optimec soft lens analyser.

- Zeiss/Rodenstock focimeter equipped with contact lens support
- Haag-Streit 900 BQ LED slit lamp microscope containing the imaging module. This was connected via a USB cable to a personal computer.
- Haag-Streit "EyeSuite" program to store and manage the images obtained.
- Open Source software "Image Grab" (Gagla, 2010)
- Shareware software "PhotoFiltreX" (Da Cruz, 2012)
- Ginsburg contrast sensitivity charts.
- Visual acuity chart at 6m
- Refractor head.

Methods

Lens inspection, measurement and marking

Rigid lenses were checked in the normal way using a radiuscope and diameter gauge.

The BOZR and TD of each soft lens were measured in saline at ambient room temperature using the Optimec analyser. Each lens was measured independently five times.

The dioptric power was measured with the focimeter.

Each soft lens was ink-marked using an extra fine "Lumocolor" pigment marker with three small, non-elevated, equally distributed dots placed between the centre and the edge of each lens to video capture and measure contact lens movement in situ.

Soft lenses:

Five different soft lenses of each material chosen as selected in Table 5.2and were tested in both eyes of each subject using the pattern in Table 7.1. The subjects did not konow what lens type they were wearing. The lenses were inserted in the order shown, but the subjects were unaware if these were different lenses.

Subject 1		Subject 2		Subject 3		Subject 4		Subject 5	
RE	LE	RE	LE	RE	LE	RE	LE	RE	LE
m1,1	m1,2	m1,1	m1,2	m1,1	m1,2	m1,1	m1,2	m1,1	m1,2
m1,2	m1,1	m1,2	m1,1	m1,2	m1,1	m1,2	m1,1	m1,2	m1,1
m1,3	m1,4	m1,3	m1,4	m1,3	m1,4	m1,3	m1,4	m1,3	m1,4
m1,4	m1,3	m1,4	m1,3	m1,4	m1,3	m1,4	m1,3	m1,4	m1,3
m1,5	m2,1	m1,5	m2,1	m1,5	m2,1	m1,5	m2,1	m1,5	m2,1
m2,1	m1,5	m2,1	m1,5	m2,1	m1,5	m2,1	m1,5	m2,1	m1,5
m2,2	m2,3	m2,2	m2,3	m2,2	m2,3	m2,2	m2,3	m2,2	m2,3
m2,3	m2,2	m2,3	m2,2	m2,3	m2,2	m2,3	m2,2	m2,3	m2,2
m2,4	m2,5	m2,4	m2,5	m2,4	m2,5	m2,4	m2,5	m2,4	m2,5
m2,5	m2,4	m2,5	m2,4	m2,5	m2,4	m2,5	m2,4	m2,5	m2,4
m3,1	m3,2	m3,1	m3,2	m3,1	m3,2	m3,1	m3,2	m3,1	m3,2
m3,2	m3,1	m3,2	m3,1	m3,2	m3,1	m3,2	m3,1	m3,2	m3,1
m3,3	m3,4	m3,3	m3,4	m3,3	m3,4	m3,3	m3,4	m3,3	m3,4
m3,4	m3,3	m3,4	m3,3	m3,4	m3,3	m3,4	m3,3	m3,4	m3,3
m3,5	m4,1	m3,5	m4,1	m3,5	m4,1	m3,5	m4,1	m3,5	m4,1
m4,1	m3,5	m4,1	m3,5	m4,1	m3,5	m4,1	m3,5	m4,1	m3,5
m4,2	m4,3	m4,2	m4,3	m4,2	m4,3	m4,2	m4,3	m4,2	m4,3
m4,3	m4,2	m4,3	m4,2	m4,3	m4,2	m4,3	m4,2	m4,3	m4,2
m4,4	m4,5	m4,4	m4,5	m4,4	m4,5	m4,4	m4,5	m4,4	m4,5
m4,5	m4,4	m4,5	m4,4	m4,5	m4,4	m4,5	m4,4	m4,5	m4,4
m5,1	m5,2	m5,1	m5,2	m5,1	m5,2	m5,1	m5,2	m5,1	m5,2
m5,2	m5,1	m5,2	m5,1	m5,2	m5,1	m5,2	m5,1	m5,2	m5,1
m5,3	m5,4	m5,3	m5,4	m5,3	m5,4	m5,3	m5,4	m5,3	m5,4
m5,4	m5,5	m5,4	m5,5	m5,4	m5,5	m5,4	m5,5	m5,4	m5,5
m5,5	No lens	m5,5	No lens	m5,5	No lens	m5,5	No lens	m5,5	No lens

Table 7.1 Sequence of lenses tested in subjects eyes

The procedure was performed consecutively and interrupted by the necessary breakes only according to the ethical approval (see Section 7.1). The subjects wore lenses in each eye. This gave 25 runs for each test person and the left eye without lens for the 25th test run.

Subjects were allowed regular breaks, and after testing two materials (m1,1 to m2,5 shown in Table 7.1) the subjects had finished testing for that session and returned the following day for a second session. This approach was adopted to avoid overtesting the subjects.

The sequence was repeated for the other 4 subjects (Subject 2, Subject3, Subject 4 and Subject 5).

For each lens tested the following procedure took place:

Lens insertion and a check for any foreign body present under the lens.

20 minutes waiting time to allow the lens to settle.

Unaided visual inspection of the lens.

Over refraction to achieve the best visual acuity.

Assessing the appearance of the retinoscopic spot.

Assessing contrast sensitivity function.

Making the mark for comfort on the VAS.

Slit lamp examination followed by taking the video sequence with the Haag-Streit Video Slit lamp and storing the recorded video into the subjects file.

The above was repeated for the fellow eye.

Pilot studies revealed that the whole procedure would take 40 to 50 minutes per person with one lens in the right and another lens in the left eye.

Comfort

In pain research, visual analogue scales (VAS) are commonly used (Gould et al., 2001) with a grading of pain from “no pain” to “just bearable pain”. While in pain research “just bearable pain” would indicate the maximum value this is

unlikely to occur with contact lenses hence the term “not acceptable” was chosen. The orientation of the scale, if numbering is used, plays a role regarding the outcome (Paul-Dauphin et al., 1999). In this work, a vertical line 10cm long was used and only the terms “comfortable” at the bottom of the line and “not acceptable” at the top of the line were used.

When a comfort assessment has to be made, the subject has to place a horizontal mark on the “scale” for each separate observation consistent with their subjective assessment of comfort. The distance in cm, from the bottom of the scale to the mark made by the subject, was recorded.

In an unpublished study carried out by the author, an attempt to find the accuracy of marks placed on an upright VAS scale was made with 35 participants. Each participant then was asked to put a mark in the middle of the 10cm scale and then put the sheet to one side. This was repeated with another 9 prepared sheets. The marks on all 350 test sheets were measured. The average value found for the middle of the line (5.0 cm) was 5.13cm (maximum value 5.9cm and minimum value 4.3cm). The standard deviation was 0.24. In light of these findings, a significant difference in contact lens comfort was noted if marks differed by at least twice the SD, i.e. ± 5mm.

Visual acuity

Refractive error was measured in the conventional way with spheres and cylinders for correction using a phoroptor and a distance chart, after retinoscopy, and visual acuity recorded. With contact lenses being worn, the over-refraction using spheres and cylinders giving optimum acuity was obtained some 20-30 minutes later and this visual acuity recorded

Contrast sensitivity

The testing methods and theoretical background is described in the manual provided with the Functional Activity distance Contrast Test (Ginsburg, 1988). The five test plates were equally and correctly illuminated and were not

relocated during the test period. The test distance was 3.5m. This test is based on the ability to differentiate between sine wave gratings with different frequencies and different contrast. The test chart consists of circular shaped fields containing sine wave gratings.

Line	Cycles /deg.(cpd)	Contrast sensitivity value key							
		1	2	3	4	5	6	7	8
A	1.5	3	7	12	20	35	70	120	170
B	3.0	4	9	15	24	44	85	170	220
C	6.0	5	11	21	45	70	125	185	260
D	12.0	5	8	15	32	55	88	125	170
E	18.0	4	7	10	15	26	40	65	90

Table 7.2 Contrast sensitivity values. Rowslines A – E define frequency.

Where the cells containing "3" representing the frequency patterns with the highest and those containing "260" representing frequency patterns with the lowest contrast[18]. Each frequency pattern contains 8 gratings with changing contrast starting from field no. 1 (highest contrast) to field no. 8 (lowest contrast). Each line starts with high contrast in column 1 and ends with the lowest contrast in column 8. The gratings are aligned either upright, orientated 15° left or 15° right from the vertical. The lowest contrast grating just detected of the nine indicates the contrast threshold. This was recorded.

Contrast sensitivity was tested without contact lenses and with the best spectacle correction according to CRF1. Three different plates randomly were used for each test with the right eye tested first.

[18] The contrast level values are not defined in the user manual, while the term contrast is defined as *"the difference in brightness levels from one part of a visual image to another."*

A contact lens was inserted into the right eye, and a visual and a slit lamp check was carried out to ensure the lens was fitting adequately and was comfortable. The CS was measured with the over-correction in place.

This procedure was repeated for the other eye and with all the alternative lenses.

The Ginsburg Charts were used because of their ready availability and the author's judgment that they were quick and accurate.

Retinoscopic spot phenomena

According to the author's 35 years of contact lens experience the use of a projected retinoscopic spot is a simple diagnostic tool to anticipate if haze or blurred vision might occur whilst wearing the contact lenses[19]. In addition, a crisp and sharp projected spot through the subject's eyes indicates a soft lens is neither too steep nor too flat. Undesired entoptic phenomena start to occur approximately within a second if a lens is too steep. If the phenomenon occurs immediately the lens might be inserted inside out, or, in rare cases too flat.

The image of a projected retinoscopic spot is projected onto a screen. In a healthy eye with clear media the image should be crisp and sharp without an "aura", a halo or a comet's tail. The crisp, sharp image also indicates a proper optical correction and the desired contact lens fit. Comets' tails between 10 o'clock and 2 o'clock are described as vertical tails and comets' tails between 3 o'clock and 9 o'clock are described as horizontal tails.

Lens movement

Most literature about contact lens rotation relates to toric soft lenses (Young, 2003, Edrington, 2011, Tomlinson and Bibby, 1980, Tomlinson et al., 1994, Tomlinson et al., 1980). In addition to the toroidal shape on either the posterior or anterior surface, these lenses need a design feature in order to stabilise the

[19]Note: This technique has been used by the author successfully for many years but has not yet been published.

lenses. Results from research investigating such non-rotational contact lenses cannot be used as comparison data with the results of the current work.

In order to measure lens movement with a contact lens in place, a video analysis was carried out in several steps. To facilitate observation of lens movement, each lens had three equally spaced coloured dots in the mid periphery of the lens. Each dot was equidistant from the centre of the lens.

The procedure began with a video film of a normal complete blink was taken using the slit lamp. A single frame was extracted with the eye in primary gaze, just before a blink started. A second frame was extracted and stored when the lid opened and the contact lens reached its uppermost position. More than one complete blink was recorded, as well as one or more push-up-tests. Because of the influence of tear production dynamics, the first sequence was for analysis.

With the software “PhotoFiltreX”, the frames were resized to scale using a frame of a filmed reticule as shown in Figure 7.1 Reticule photograph for calibration. The video procedures was repeated for the left eye.

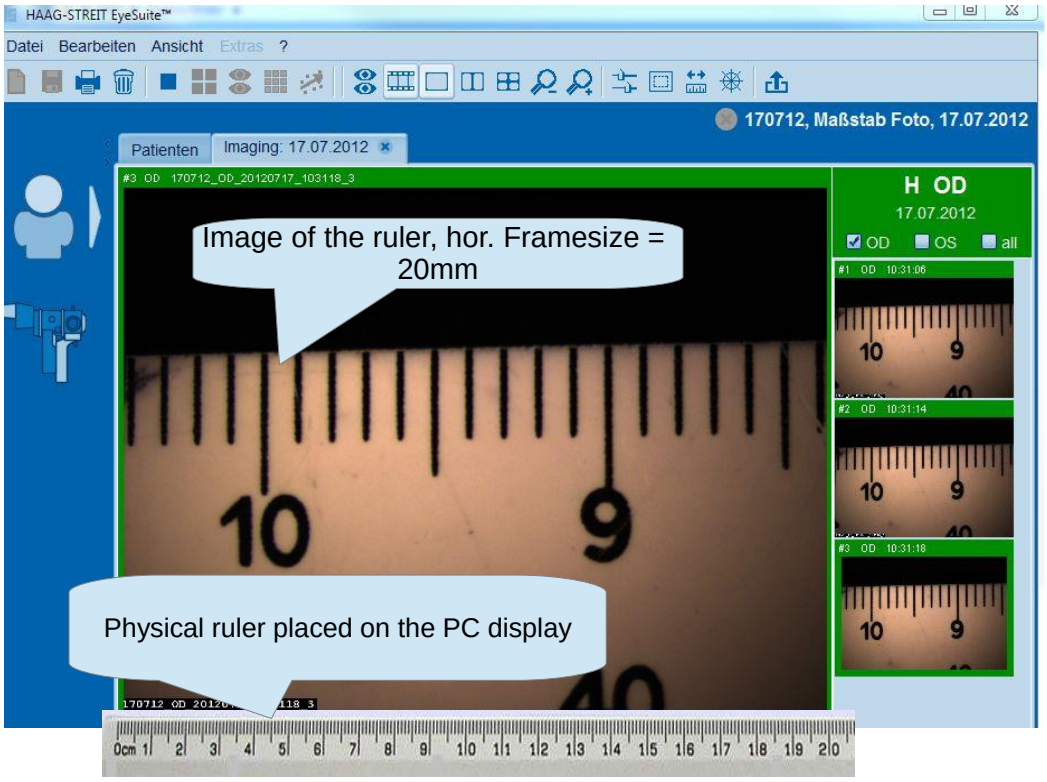

Figure 7.1 Reticule photograph for calibration

To measure the vertical movement of the lens, the first of the two extracted frames was loaded into the FotoFiltre program. At least one image of the visible ink dots was located and marked with the relevant drawing tool. The colours of the marked dots then were inverted and made 40% to 50% transparent. The second marked area was then was cut and copied on top of the first loaded frame with the pupil acting as the reference shape. Since the dot of the overlaid part had changed the colour from orange to blue, for example, the starting and the end position of the lens could be found. The final picture then was resized to a 10:1 scale and the distance between the two dots measured on a screen using a physical ruler to the nearest 0.01mm.

demonstrates the overlay technique

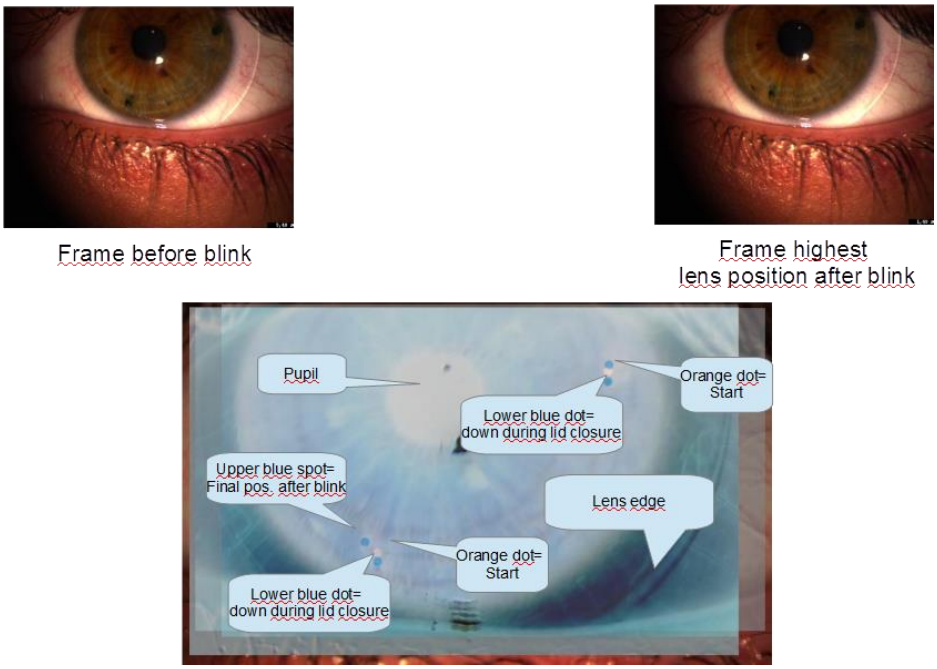

Figure 7.2 Overlay demonstration with 3 visible out of 4 overlaid frames.

In the pictures without the overlays the physical marks at 2 o' clock and 7 o' clock are visible. The blue and orange marking dots in the overlay picture have a size of 0.2mm in diameter. The lens then moved 0.2mm down as soon the pupil was visible after lid closure and travelled from there 0.4 mm upwards at the 2 o' clock position. Pilot studies indicated that the lenses appeared to rotate clockwise[20], which is in contradiction to the published research (Hanks and

[20] From the examiner's view

Weisbarth, 1983, Abel and Thiele, 1968). 88% of rotationally symmetrical spherical lathe cut lenses did rotate (Harris et al., 1976) while less rotational movement was observed with spun cast lenses (Harris et al., 1975). Since a number of tested lenses did not seem to rotate at all in the pilot studies, only vertical lens movement would be measured in the current study. Lens movement was also assessed using the push up test (PUT) and the result recorded on the CRF2.

Results

CRF1 Results

A total of 16 potential subjects between the ages of 25 and 50 years, who were willing to participate in the tests described in 7.1. were evaluated. There were 15 Caucasians and one African, and 9 subjects were female and 7 were male.

The CRF1 tests were carried out at least two days before the CRF2 tests took place. During the CRF1 evaluation all paperwork including the explanation, agreement and signature of the informed consent leaflet was completed for the subjects selected.

Table 7.3- Table 7.5 show the subjects ID, race, age, gender, keratometer readings, prescriptions, visual acuity with best correction, slit lamp gradings, tear meniscus height, corneal diameters, whether the subjects used contact lenses and all other findings according to the CRF1 form.

Contrast threshold with best prescription (cycles per degree)										
	RE Field					LE field				
Subject	1.5	3.0	6.0	12	18.0	1.5	3.0	6.0	12	18.0
1	5	6	3	3	1	5	5	5	3	1
2	4	8	3	2	0	5	6	4	2	0
3	5	6	4	4	2	4	5	4	4	4
4	4	6	6	4	2	4	6	6	5	3
5	4	6	6	3	2	5	5	6	3	2
mean	**4.4**	**6.4**	**4.4**	**3.2**	**1.4**	**4.6**	**5.4**	**5.0**	**3.4**	**2.0**
SD	0.5	0.8	1.4	0.7	0.8	0.5	0.5	0.9	1.0	1.4

Table 7.3 Contrast sensitivity for participating subjects with spectacle prescription.

Subject	Age	Sex	Exterior Part of the Eye: Slit Lamp grading 0-4								Corn. Diameter (mm)	
			Lids		Lashes		Conjunctiva		Cornea			
			RE	LE	RE	LE	RE	LE	RE	LE	RE	LE
1	28	f	0	0	0	0	0	0	0	0	11.0	11.0
2	29	f	0	0	0	0	0	0	0	0	11.4	11.3
3	28	f	0	0	0	0	0	0	0	0	11.5	11.5
4	30	m	0	0	0	0	0	0	0	0	11.2	11.2
5	29	f	0	0	0	0	0	0	0	0	11.5	11.5
6	46	m	0	0	0	0	0	0	2	2	12.0	12.0
7	31	f	0	0	0	0	0	0	0	0	9.5	9.8
8	27	f	0	0	0	0	0	0	0	0	10.5	10.5
9	52	m	2	2	0	0	0	0	0	0	12.0	11.0
10	32	f	0	0	0	0	0	0	0	0	12.0	12.0
11	28	f	0	0	0	0	0	0	0	0	11.5	11.5
12	27	m	0	0	0	0	0	0	0	0	11.8	11.8
13	40	m	0	0	0	0	0	0	0	0	11.0	11.5
14	34	m	0	0	0	0	0	0	0	0	11.5	11.5
15	35	m	0	0	0	0	0	0	0	0	12.2	12.2
16	30	f	0	0	0	0	0	0	0	0	12.0	12.0
									Average		11.4	11.4
									Std. Dev.		0.7	0.6

Caukasian	15
African	1
Female	9
Male	7
Lid findings	1
Corneal findings	1

Table 7.4 CRF1 results: Ocular tissue grades and corneal diameters for all 16 subjects.

Subject	Tear meniscus lower lid (mm)		Keratometer readings (mm)					
			Right eye			Left eye		
	RE	LE	Flattest	Axis	Steepest	Flattest	Axis	Steepest
1	0.2	0.2	7.98	5	7.84	7.95	170	7.90
2	0.2	0.2	7.80	5	7.60	7.80	2	7.60
3	0.2	0.2	7.90	5	7.75	7.84	0	7.62
4	0.2	0.2	7.62	10	7.58	7.68	0	7.65
5	0.2	0.2	7.65	5	7.54	7.65	0	7.54
6	0.3	0.3	8.09	0	7.91	8.15	0	7.82
7	0.3	0.3	7.43	3	7.29	7.46	14	7.38
8	0.3	0.3	7.72	87	7.84	7.7	91	7.84
9	0.2	0.2	7.37	0	7.38	7.31	0	7.41
10	0.1	0.1	8.19	30	8.15	8.2	135	8.05
11	0.2	0.2	7.51	0	7.49	7.5	0	7.51
12	0.1	0.1	7.6	0	7.5	7.65	175	7.55
13	0.1	0.1	7.6	0	7.62	7.4	0	7.5
14	0.1	0.1	7.71	0	7.54	7.5	0	7.43
15	0.3	0.2	7.7	0	7.68	7.75	0	7.5
16	0.3	0.3	7.98	0	7.85	7.97	0	7.78
Average	**0.2**	**0.2**	**7.7**	**0**	**7.7**	**7.7**	**0**	**7.6**
SD	0.1	0.1	0.2	0	0.2	0.2	0	0.2

Table 7.5 CRF1 results: Tear meniscus height at lower lid and keratometer readings.

Subject	Best spectacle correction							
	Right eye				Left eye			
	Sph.	Cyl.	Axis	VA	Sph.	Cyl.	Axis	VA
1	+0.25			1.0	+0.25			1.0
2	-6.25	-0.50	30	1.0	-6.25	-0.50	173	1.0
3		-0.50	165	1.2		-0.50	180	1.2
4				1.2				1.2
5	-0.50	-0.50	20	1.0		-1.25	10	1.0
6	-0.75			1.0	-0.75			1.0
7	-0.25	-0.25	70	1.6	-0.25			1.6
8	-1.25	-0.50	165	1.2	-1.20	-0.50	170	1.2
9	+0.50			1.0	+0.50			1.0
10	-2.50	-0.50	35	1.0	-2.25	-1.00	130	0.0
11	-1.00			1.0	-0.50	-0.25	30	1.0
12	+0.75			1.0	+0.50			1.0
13	+0.50			1.2	+0.50			1.2
14	-3.00			1.2	-3.00			1.2
15	-3.75	-0.50	5	1.0	-1.25	-2.50	170	0.8
16	+0.50			0.8	+0.50			0.8
Average				**1.1**				**1.1**
SD				0.2				0.2

Table 7.6 Best spectacle correction.
There were 25 eyes with with-the-rule astigmatism, seven eyes with oblique or against-the-rule astigmatism and five subjects were contact lens wearers.

Eleven subjects were excluded (see Table 7.7)

Number of Exclusions	Reason for exclusion
1	Epithelial Corneal Dystrophy
1	VSO38 9.2/14.5 too steep, NIBUT <10 @ L.E.
1	Test lens diam. 14.5mm too large for subject
1	Blepharitis, NIBUT <10 sec.
2	NIBUT <10 secs.
1	Upper lid tension far beyond 10g (squeezer)
1	Unable to participate / time consuming
1	Unable to participate / time consuming
1	VA on left eye < 1.0; too large corn. Diam.
1	VA <1.0, NIBUT < 10 secs.

Table 7.7 Excluded subjects and reason for exclusion.

Five subjects participated in the in vivo test. Four were female and one was male. The females were Caucasian and the male was African.

The exterior parts of all subjects' eyes were free from any abnormalities. The grading for lids, lashes, conjunctiva and cornea was zero throughout for all subjects.

One female and one male subject did not require any spectacle correction, and one female subject required correction for myopia of approximately -6.00 D.

Within the participants the astigmatism was between 0.00 D and -1.25 D.

Subject	Projected retinoscopic spot						Keeler NIBUT (seconds)		Lid Tension (grams)		Contact lenses (y/n)
	Right eye			Left eye							
	Sharp edge y/n	Halos y/n	Comet's tail clock dir 0=none	Sharp edge y/n	Halos y/n	Comet's tail clock dir 0=none	RE	LE	RE	LE	
1	y	n	0	y	n	0	16.4	20.6	5	4	n
2	y	n	0	y	n	0	23.5	16.1	7.5	9	y
3	y	n	0	y	n	0	15.7	13.5	8.6	6	n
4	n	n	1	n	n	12	18.9	15.3	6.5	6	n
5	n	n	0	n	n	0	20.8	22	3	3	y
6	y	n	0	y	n	0	16	14			n
7	y	n	0	y	n	0	10	14			n
8	y	n	0	y	n	0	12	9			n
9	y	n	0	y	n	0	4	5			y
10	y	n	0	y	n	0	9	8			n
11	y	n	0	y	n	0	9	9			y
12	y	n	0	y	n	0	20	20	15	15	n
12	y	n	0	y	n	0	18	17			n
14	y	n	0	y	n	0	14	18			n
15	y	n	0	y	n	0					n
16	y	n	0	y	n	0	9.9	8.9			y

Table 7.8 The retinoscopy spot findings and tear break-up times.

CRF2 Results

PMMA test lenses

PMMA Lens TD 14,5mm		BOZR		VAS (cm)		Average VAS (cm)
ID	subject	R	L	R	L	
1	S.V	9.2	9.2	4.2	4.5	4.4
2	K.M.	9.2	9.2	0.3	0.3	0.3
3	S.E.	9.2	9.2	3.3	3.2	3.3
4	A.S.	9.2	9.2	4.4	4.6	4.5
5	K.V.	9.2	9.2	4.8	4.7	4.8
Average		**9.2**	**9.2**	**3.4**	**3.5**	
SD		**0**	**0**	**1.6**	**1.7**	

Table 7.9 Best aligned PMMA trial lenses as described in 6.6

The results presented in Table 7.9, when compared with with the results in section 6.3, section 6.5 and section 6.6 demonstrated that the results obtained with the mathematical model and the results obtained with the PMMA test lenses showed excellent agreement. The results of 6.7 were compared with the BOZR radii in Table 7.9. As explained on page 121 the steeper radii at elevated temperature were within the allowed tolerance according to ISO tolerances for the BOZR. For subject SV the BOZR chosen was slightly flat.

Comfort

		VSO38		LM55		GM3		VSO75		Definitve	
subject	Test run	R	L	R	L	R	L	R	L	R	L
SV	1	4.9	4.7	1.1	1.1	2.4	2.6	0.7	0.8	0	0
SV	2	4.1	4.3	0.5	0.5	1.6	1.7	1.3	1.0	0.2	0.2
SV	3	2.9	3.0	0.5	1.2	1	1.2	0.5	1.2	1.1	0
SV	4	2.5	1.7	0.7	1.0	0.4	0.4	2.6	1.6	0.5	0.6
SV	5	0.6	1.1	0.9	0.7	0.4	0.4	0.5	0.8	0.5	0.5
KM	1	2.6	3.6	0.9	0.5	0.2	0.2	0.0	0.0	0.9	0.5
KM	2	1.2	1.2	0.2	0.5	0.3	0.3	0.0	0.0	0.2	0.5
KM	3	1.2	1.4	0.4	0.5	0	0	0.0	0.0	0.4	0.5
KM	4	4.8	4.8	0.0	0.5	0	0	0.0	0.0	0	0.5
KM	5	1.1	0.2	0.1	0.5	0	1	0.0	0.0	0.1	0.5
SE	1	6.5	6.5	1.0	1.0	4.1	3.5	3.2	3.6	1	1
SE	2	6.0	6.2	3.3	3.2	2	2.1	4.7	4.7	2.5	2.7
SE	3	5.6	6.0	3.9	4.0	6.3	6.6	3.7	4.7	1.8	2
SE	4	6.2	6.2	3.2	3.2	5.2	4.8	3.5	3.3	2.8	3.8
SE	5	3.5	4.8	4.7	5.6	3.8	4	2.6	2.9	4.7	3.3
AS	1	3.3	4.0	0.9	0.9	2.1	2.8	3.5	3.4	2.3	3.2
AS	2	3.5	2.5	1.0	1.0	1.8	2.1	2.8	2.8	0.5	2.4
AS	3	3.2	3.1	1.0	1.0	2	3.4	1.0	1.1	1	1.7
AS	4	2.6	3.2	1.0	1.0	2.5	2.9	4.3	2.8	1.3	2.5
AS	5	3.3	3.3	1.0	1.0	2.2	3.3	2.3	1.7	0.7	1.8
KV	1	3.8	4.5	3.6	3.5	3.6	1.1	2.0	2.8	0.2	0.1
KV	2	4.9	4.5	2.6	2.3	1.7	3.6	3.5	4.2	0	0
KV	3	3.5	3.0	1.3	1.5	2.5	2.5	3.2	4.0	0	0
KV	4	3.7	4.2	3.5	3.3	2.2	3.4	3.5	3.7	0.3	0.1
KV	5	3.5	3.4	3.4	3.5	1.9	2	2.9	2.3	2	3
Median		3.5	3.6	1.0	1.6	2.1	2.4	2.5	1.1	0.5	0.8
MAD		1.1		1.2		1.1		1.3		0.8	
Mean		**3.47**	**3.65**	**1.59**	**1.71**	**1.98**	**2.24**	**2.08**	**2.09**	**0.97**	**1.24**
SD		**1.54**		**1.31**		**1.52**		**1.44**		**1.06**	

Table 7.10 Comfort values as recorded using the VAS.

Table 7.10 shows the recorded marks on the upright unmarked VAS scale (length 10 cm). Each mark for each lens was placed on a separate sheet of an A5 size, upright-oriented sheet of white paper on which the VAS scale was printed. Subject KM was the routine contact lens wearer, and seemed to tolerate the test lenses better than the rest of the cohort. Subject SV showed

increased comfort with the VSO38 lenses which may reflect a learning effect. The table allows differences within the five test samples of each material to be revealed. KM's test run number 4 showed a decrease of comfort for both eyes. A foreign body sensation, lens damage or imperfect edges were ruled out, however the reason for the decrease in comfort was unknown.

		VSO38		LM55		GM3		VSO75		Definitive	
Initials	Test run	R	L	R	L	R	L	R	L	R	L
SV	1	-0.6	-0.4	3.3	3.3	2.0	1.8	3.7	3.6	4.4	4.4
SV	2	0.3	0.0	3.9	3.9	2.8	2.7	3.1	3.4	4.2	4.2
SV	3	1.5	1.4	3.9	3.2	3.4	3.2	3.9	3.2	3.3	4.4
SV	4	1.9	2.7	3.7	3.4	4.0	4.0	1.8	2.8	3.9	3.8
SV	5	3.8	3.3	3.5	3.7	4.0	4.0	3.9	3.6	3.9	3.9
KM	1	-2.3	-3.3	-0.6	-0.2	0.1	0.1	0.3	0.3	-0.6	-0.2
KM	2	-0.9	-0.9	0.1	-0.2	0.0	0.0	0.3	0.3	0.1	-0.2
KM	3	-0.9	-1.1	-0.1	-0.2	0.3	0.3	0.3	0.3	-0.1	-0.2
KM	4	-4.5	-4.5	0.3	-0.2	0.3	0.3	0.3	0.3	0.3	-0.2
KM	5	-0.8	0.1	0.2	-0.2	0.3	-0.7	0.3	0.3	0.2	-0.2
SE	1	-3.3	-3.3	2.3	2.3	-0.9	-0.3	0.0	-0.4	2.3	2.3
SE	2	-2.8	-3.0	0.0	0.0	1.3	1.2	-1.5	-1.5	0.8	0.6
SE	3	-2.4	-2.8	-0.7	-0.8	-3.1	-3.4	-0.5	-1.5	1.5	1.3
SE	4	-3.0	-3.0	0.0	0.0	-2.0	-1.6	-0.3	0.0	0.5	-0.6
SE	5	-0.3	-1.6	-1.5	-2.4	-0.6	-0.8	0.7	0.4	-1.5	0.0
AS	1	1.2	0.5	3.6	3.6	2.4	1.7	1.0	1.1	2.2	1.3
AS	2	1.0	2.0	3.5	3.5	2.7	2.4	1.7	1.7	4.0	2.1
AS	3	1.3	1.4	3.5	3.5	2.5	1.1	3.5	3.4	3.5	2.8
AS	4	1.9	1.3	3.5	3.5	2.0	1.6	0.2	1.7	3.2	2.0
AS	5	1.2	1.2	3.5	3.5	2.3	1.2	2.2	2.8	3.8	2.7
KV	1	1.0	0.3	1.2	1.3	1.2	3.7	2.8	2.0	4.6	4.7
KV	2	-0.2	0.3	2.2	2.5	3.1	1.2	1.3	0.6	4.8	4.8
KV	3	1.3	1.8	3.5	3.3	2.3	2.3	1.6	0.8	4.8	4.8
KV	4	1.1	0.6	1.3	1.5	2.6	1.4	1.3	1.1	4.5	4.7
KV	5	1.3	1.4	1.4	1.3	2.9	2.8	1.9	2.5	2.8	1.8
Median		0.3	0.9	2.2	2.1	1.5	1.2	1.1	1.8	2.5	2.1
MAD		1.6		1.6		1.4		1.2		1.6	
Mean		**-0.05**	**-0.18**	**1.81**	**1.73**	**1.42**	**1.20**	**1.32**	**1.31**	**2.40**	**2.17**
SD		**1.86**		**1.64**		**1.67**		**1.36**		**1.80**	

Table 7.11 VAS results in Table 7.9 minus the VAS results using PMMin Table 7.10

Table 7.11 demonstrates the difference in comfort between the PMMA test lenses mentioned in Table 7.9 and the tested soft lenses. Positive values define better comfort, negative values define worse comfort compared with the PMMA test lenses which were used as the comfort reference.

The significance of these results in relation to the accuracy of marks placed on an unmarked VAS scale as described on page 133 required consideration and differences of less than 0.5cm were regarded as not significantly different.

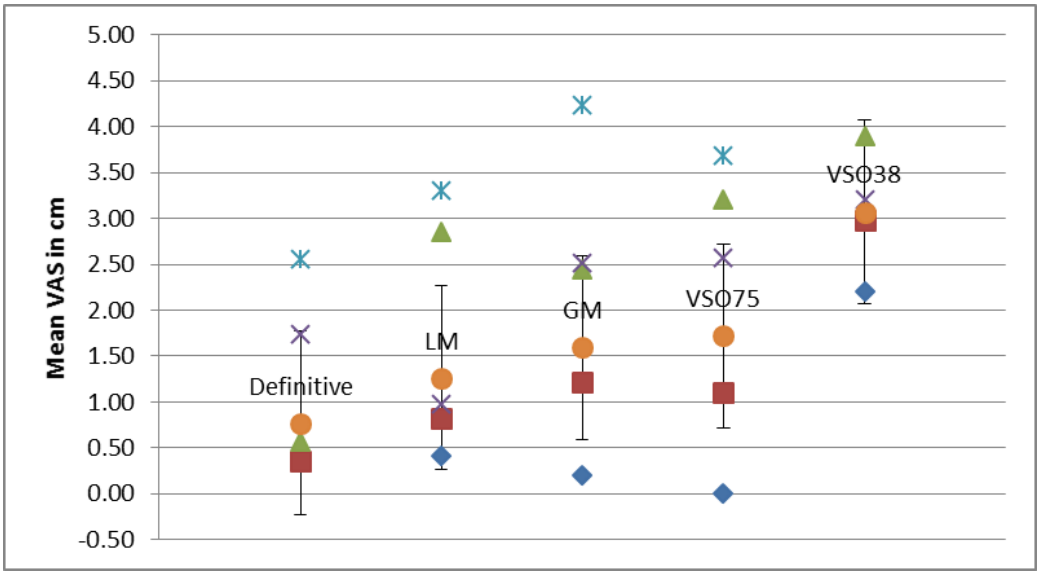

Figure 7.3 Comfort separated by material types in ascending order.
Low values indicate good comfort. The error bars show one standard deviation from the average of each material

Subject	Definitive	LM	GM	VSO75	VSO38	PMMA
KM	0.41	0.41	0.20	0.00	2.21	0.30
SV	0.36	0.82	1.21	1.10	2.98	4.35
KV	0.57	2.85	2.45	3.21	3.90	4.75
AS	1.74	0.98	2.51	2.57	3.20	4.50
SE	2.56	3.31	4.24	3.69	5.75	3.25
Median	0.49	0.90	1.83	1.84	3.09	4.43
SD	0.83	1.11	1.25	1.26	1.11	1.55

Table 7.12 Average VAS results in cm for each material and each subject.

Comparing the results in Table 7.12 with the results obtained with the PMMA semi-scleral test lenses, better comfort was reported with the soft lenses in most cases (Table 7.9).

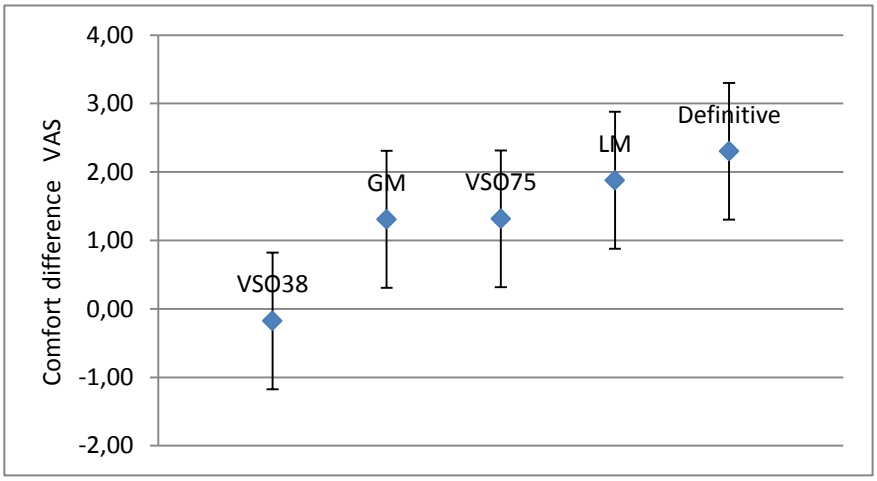

Figure 7.4 Comfort difference between the PMMA semi scleral lenses and the tested soft lenses.

Note: Plus values indicate better comfort than PMMA. The error bars show one standard deviation from the average.

Figure 7.4 shows better comfort with most materials compared to the PMMA trial lenses. However, subject KM wore frequent replacement lenses while subject SE did not require any optical correction and had no contact lens experience. Subjects KM and SE reported reduced comfort with the VSO 38 material than with the PMMA scleral lenses while SV reported an improvement in comfort with soft lenses in general.

Table 7.13 shows the difference in comfort between the PMMA test lenses (Table 7.9) deducted by the values in Table 7.12. The values containing a minus sign show less comfort with the soft lenses compared with the PMMA test lenses.

Subject	Definitive	LM	GM	VSO75	VSO38
SV	3.99	3.53	3.14	3.25	1.38
AS	2.76	3.52	1.99	1.93	1.30
KV	4.18	1.90	2.30	1.54	0.85
KM	-0.11	0.50	0.10	0.30	-1.91
SE	0.69	-0.06	-0.99	-0.44	-2.50
Mean	2.30	1.88	1.31	1.32	-0.18
SD	1.73	1.49	1.52	1.29	1.68

Table 7.13 Comfort difference in VAS between PMMA semi scleral test lenses and the tested materials for the five subjects.

SUMMARY	*Count*	*Sum*	*Average*	*Variance*
Definitive	5	5.64	1.128	0.96047
LM	5	8.37	1.674	1.71703
GM	5	10.61	2.122	2.31747
VSO75	5	10.57	2.114	2.34753
VSO38	5	18.035	3.607	1.798745
PMMA	5	17.15	3.43	3.39075
KM	6	3.53	0.588333	0.654697
SV	6	10.815	1.8025	2.351038
KV	6	17.73	2.955	2.02687
AS	6	15.5	2.583333	1.468267
SE	6	22.8	3.8	1.21768

ANOVA

Source of Variation	*SS*	*df*	*MS*	*F*	*P-value*	*F crit*
Rows	24.02142	5	4.804285	6.594161	0.00089	2.71089
Columns	35.55665	4	8.889163	12.20089	3.49E-05	2.866081
Error	14.57133	20	0.728567			
Total	74.1494	29				

Table 7.14 Results of a two way analysis of variance in comfort between materials and subjects tested.

The two way ANOVA shown in Table 7.14 showed no significant comfort difference among the materials tested (including the semi scleral lenses made of PMMA), while there was a significant difference between subjects.

Performance

Friction tests:

Note: Detailed tables of the results are located in Chapter 10 -

Lens movement in situ

All the test lenses fitted were rotationally symmetrical lenses with a BOZR of 9.2mm ± 0.1mm and a TD of 14.5mm ±0.1mm as described in Section 7.2. Due to lens breakage during handling, the results for the lenses GM#5 for subjects 1 and 3 and the VSO75 #5 for subject 3 could not be evaluated for lens movement[21]. The GM#5 right lens for subject #4 was squeezed out of the right eye by blinking just before recording started. Even after several attempts the lens continued to be squeezed out and could not be part of the friction test. The relevant cells in Table have been marked with a "n" to represent missing data and a "l" for the lost lens. These cells were excluded from the statistical analysis.

subject	VSO38 per subject				LM per subject				GM per subject			
	Av.	SD	Med	MAD	Av.	SD	Med	MAD	Av.	SD	Med	MAD
SV	0.94	0.47	0.90	0.38	0.27	0.18	0.25	0.15	0.20	0.20	0.15	0.18
KM	0.23	0.19	0.18	0.16	0.33	0.24	0.20	0.21	0.40	0.50	0.15	0.40
SE	0.26	0.14	0.20	0.13	0.17	0.18	0.10	0.13	0.19	0.17	0.15	0.11
AS	0.85	0.63	0.80	0.51	0.30	0.26	0.25	0.20	1.47	1.54	1.10	1.17
KV	0.35	0.33	0.20	0.26	0.54	0.50	0.40	0.40	0.24	0.12	0.20	0.10

Table 7.15 Average, SD, median and absolute median (MAD) of lens movement for VSO 38, LM55 and GM3 materials.

[21] These subjects were unable to return for any further testing.

subject	VSO75 per subject				Definitive per subject			
	Av.	SD	Med.	MAD	Av.	SD	Med.	MAD
SV	1.08	0.68	1.00	0.54	0.31	0.20	0.35	0.19
KM	0.26	0.16	0.20	0.13	0.95	1.00	0.20	0.98
SE	0.45	0.39	0.30	0.31	0.19	0.17	0.15	0.13
AS	1.07	0.92	0.80	0.76	0.39	0.28	0.45	0.23
KV	0.24	0.18	0.20	0.16	0.20	0.20	0.10	0.17

Table 7.16 Average, SD, median and absolute median (MAD) of lens movement for VSO75 and Definitive materials.

The analysis was based on data from Figure 7.5 for both eyes of all participants. Figure 7.5 shows the large range of movement for each lens material. Only the upwards movement after the blink was measured.

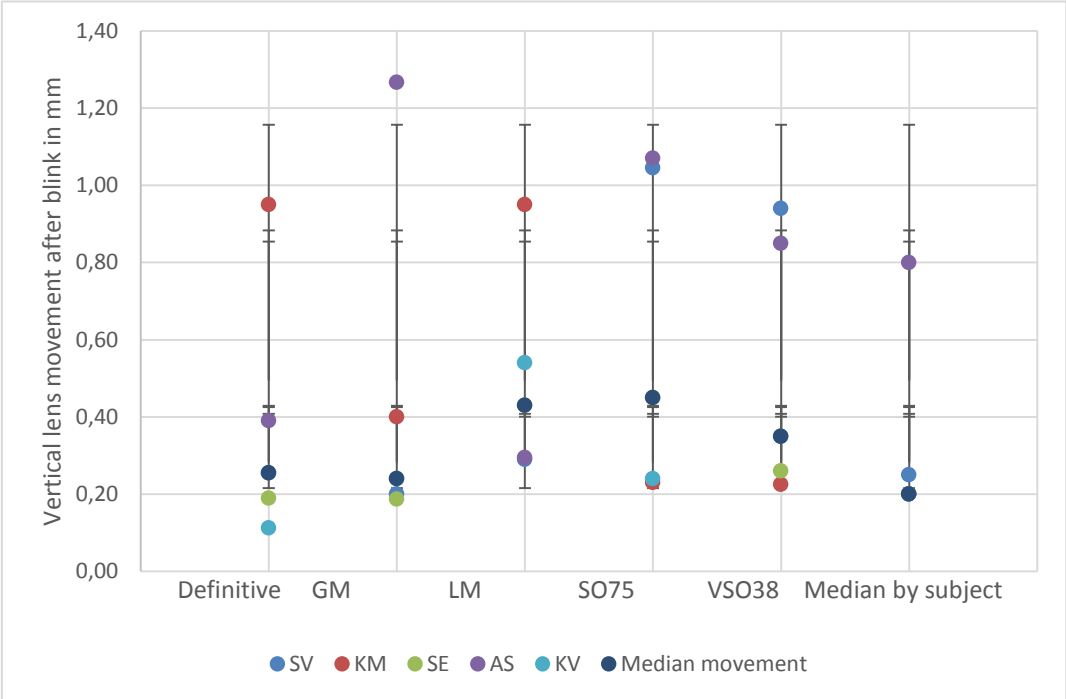

Figure 7.5 Median lens movement in mm.

The vertical bars representing one SD of the Average per material tested in the positive direction..

Init	Average of vertical movements				
	VSO38	LM	GM	VSO75	Def.
SV	0.94	0.27	0.20	1.08	0.31
KM	0.23	0.33	0.40	0.26	0.95
SE	0.26	0.17	0.19	0.45	0.19
AS	0.85	0.30	1.47	1.07	0.39
KV	0.35	0.54	0.24	0.24	0.20

Table 7.17 Average and standard deviation of vertical lens movement for all materials and all subjects.

	Definitive	GM	LM	VSO75	VSO38	Median by Subject
Mean movement	0.38	0.46	0.50	0.61	0.53	0.33
Median movement	0.26	0.24	0.43	0.45	0.35	0.20
Mean CoF	2.93	2.59	1.32	2.68	5.89	

Table 7.18 Mean and average lens movements after a blink.
Mean borderline CoF for comparison is given in the last row.

Table 7.18 gives a brief overview between average values of lens movement after a blink and median values of lens movement after a blink. The mean borderline CoF in the last line shows that the material having the lowest borderline CoF did not result in the smallest movement after blinking while the HEMA material with the highest CoF produced more movement with blinking.

Lens movement and Friction

Visual inspection (Figure 7.6) shows no obvious correlation between lens movement and the friction coefficient of each material. This was tested by calculation of Spearman's r_s which was 0.1 and which confirmed the absence of any rank correlation between lens movement and coefficient of friction.

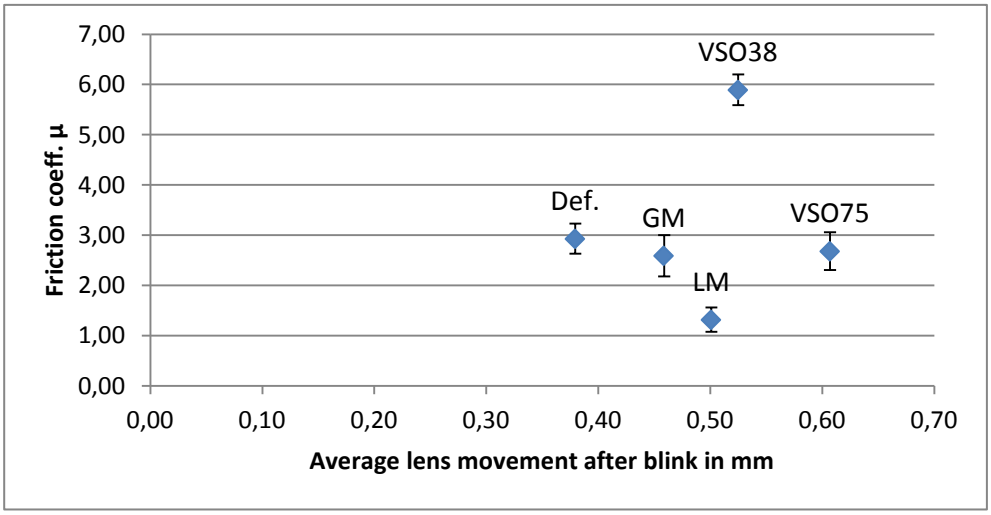

Figure 7.6 The association between lens movement and friction coefficient.

Because it is impossible to measure the resulting force on the soft contact lens produced by the upper lid force, the friction coefficient cannot be accurately calculated. The measured upper lid force moves the lens in some instances. Sometimes the lens does not move and sometimes it does. In view of this, the following statements can be made:

- If the lens does not move with a blink, the friction coefficient of the material is larger than the lid force.
- If the lens moves with a blink, a connex between force and friction coefficient of the material might exist.
- It may be further stated that if the lens moves with a blink, the frictional properties of the conjunctival tissue in the upper lid are greater than the one of the eye.

However, it is known that the lid force acts against the lens and causes a lens movement with a blink. This allows a comparison of lens movement against lid force (see Figure 7.7)

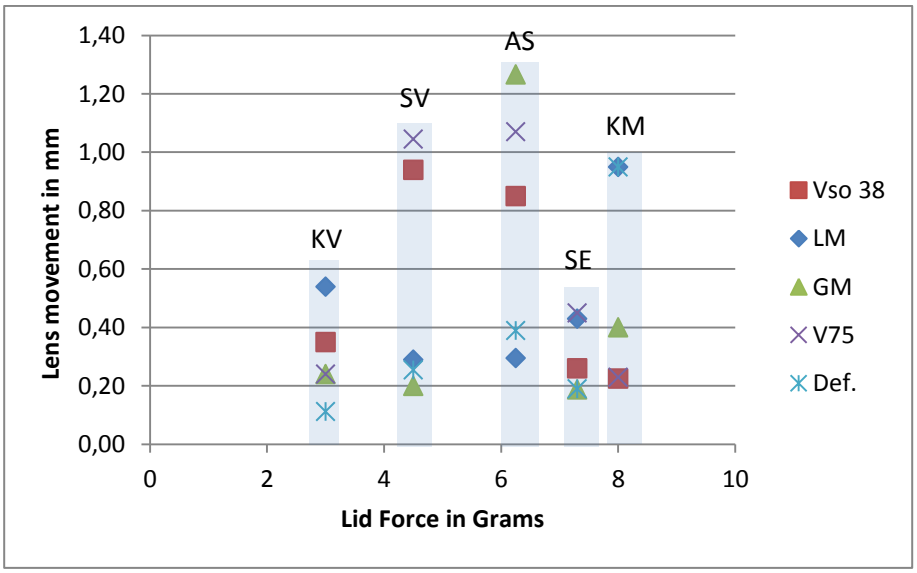

Figure 7.7 Contact lens movement versus lid force for the five subjects
Each semi-transparent bar represents one subject.

Figure 7.8 shows the frequency of lens movements after a blink, measured in 0.1mm steps, for all lenses tested with all five subjects. The displacement of the lenses after a blink was between zero and 0.5mm in 76% of cases, no matter which material was used. In 24% of cases the lenses moved between 0.6 and 2.4mm.

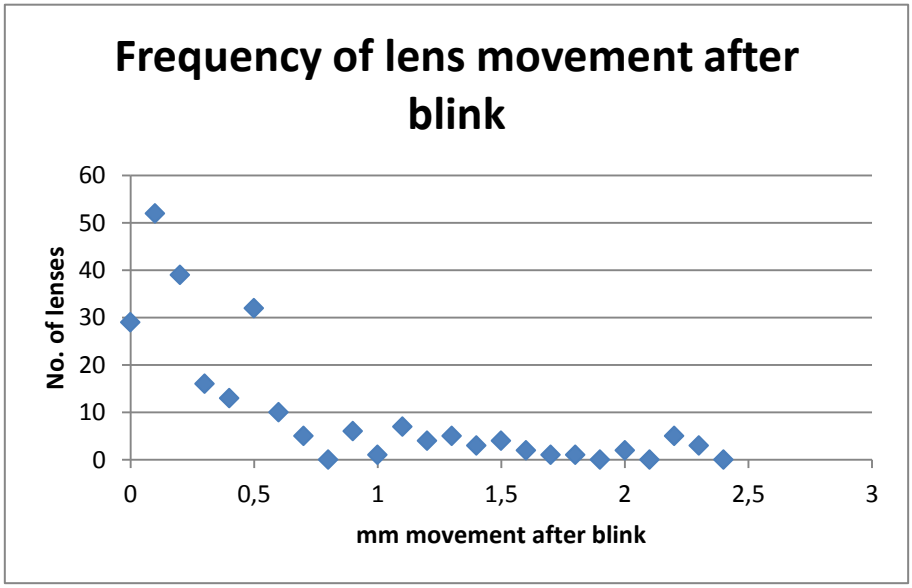

Figure 7.8 Scattergram of lens movement, measured in 0.1mmsteps, after a blink
for all lenses tested with all five materials

Push up tests (PUT)

There were 212 lens tests that were judged as 'normal' and 32 lens tests judged as 'loose' for the PUT result (Table 7.19)

Total per material	VSO38		LM		GM		VSO75		Def.	
Normal	42	0	44	0	40	0	38	0	47	0
Loose	8	0	6	0	6	0	10	0	3	0
n/a	0	0	0	0	4	0	2	0	0	0

Table 7.19 Results of PUT test

All lenses judged to be loose moved => 1mm between blinks as judged from the video recordings. Table 7.19 shows the materials listed with a PUT judged as normal only. Compared to PUT judged as normal, the highest number of loose lenses occurred with the VSO 75 and the smallest number of loose lenses was found with the Definitive material. This shows a trend towards decreasing lens movement with increasing water content.

	Lens movement in mm			
PUT Normal	0-0.2	0.3-0.6	0.7-0.9	>=1.0
VSO38	19	14	4	6
LM55	23	16	3	2
GM3	26	12	0	2
VSO75	20	14	3	1
Definitive	30	15	1	1

Table 7.20 Frequency of lens movements for lenses judged as normal using the PUT

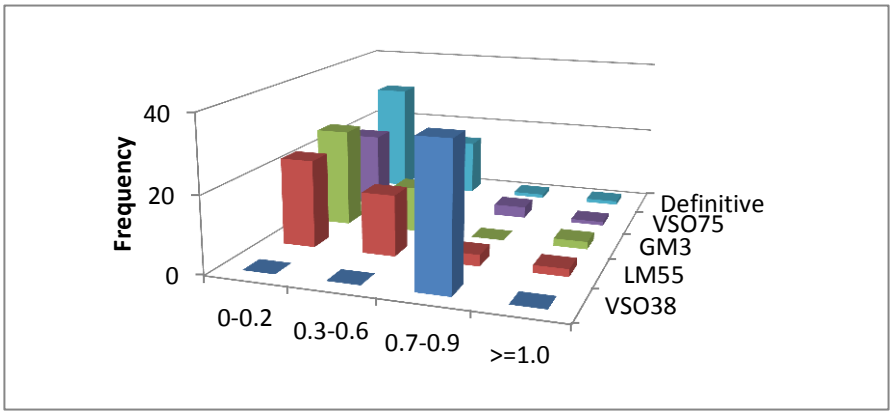

Figure 7.9 Lens movement for lenses judged as normal using the PUT, see Table 7.20

PUT Loose	Lens movement in mm			
	0-1.5	1.6-3.0	3.1-4.5	4.6-6.0
VSO38	6	1	0	0
LM55	3	3	0	0
GM3	3	2	0	1
VSO75	7	3	0	0
Definitive	0	3	0	0

Table 7.21 The number of lenses judged as loose using the PUT.

The findings with lenses judged as loose (see Table 7.21) and the accompanying histogram.

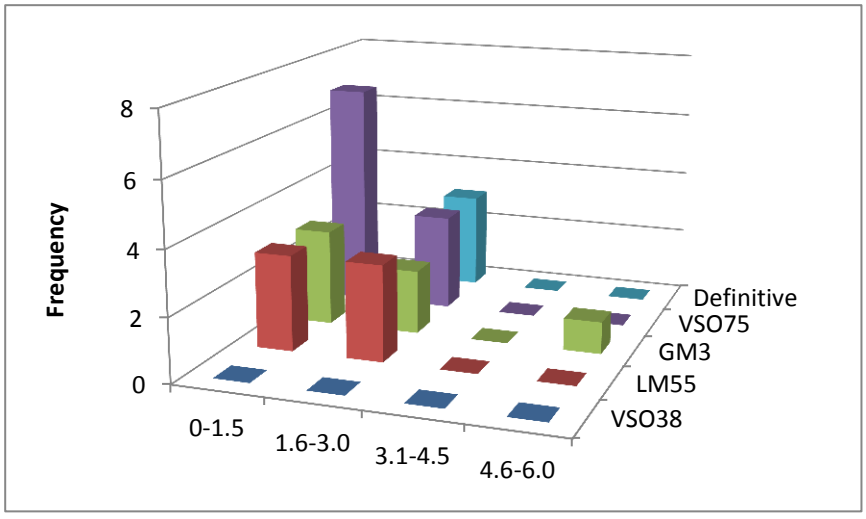

Figure 7.10 Lens movement for the lenses judged as loose (using the PUT)

The x axis shows lens movement in mm

Visual acuity:

Visual acuity (VA) with soft lenses and best overcorrection was measured 25 minutes after the lens was inserted and the results are shown in Table 7.22.

VA	V38	LM	GM	V75	Def.	Mean	SD
SV	1.0	1.0	1.0	1.0	1.0	1.0	0.0
KM	0.8	0.9	0.9	0.8	1.0	0.9	0.1
SE	1.0	1.0	1.0	1.0	1.0	1.0	0.0
AS	1.0	1.0	1.0	1.0	1.0	1.0	0.0
KV	1.0	1.0	1.0	0.9	1.0	1.0	0.0
Average	0.97	0.98	0.99	0.95	0.98	**0.98**	0.03
SD	0.09	0.02	0.03	0.07	0.02	**0.05**	**0.04**

Table 7.22 Visual acuitiy with soft lenses and best overcorrection

The VA results were also deducted from the VA values with best spectacle correction and the results are shown in Table 7.23.

Difference in VA	V38	LM	GM	V75	Def.
SV	-0.2	0.0	0.0	0.0	0.0
KM	-0.2	-0.1	-0.1	-0.2	-0.1
SE	-0.2	-0.2	-0.2	-0.2	-0.2
AS	-0.2	-0.2	-0.2	-0.2	-0.2
KV	0.0	0.0	0.0	-0.1	-0.1
Average	-0.16	-0.10	-0.09	-0.13	-0.10
SD	0.07	0.08	0.08	0.08	0.08

Table 7.23 Difference in VA between spectacle correction and VA obtained with contact lens plus over-correction

The results, in general, showed a slight drop in VA compared to the best spectacle VA for the lenses tested. For subjects SV and KV there was little difference between average VA with spectacle correction and contact lens overcorrection. The myopic subject KM just reached a VA of 1.0 with spectacle correction, while the VA with lenses fell on average to 0.9. For those two subjects (SE and AS) who did not need any distance correction the overall drop in VA with contact lenses was consistently 0.2 for all lens types.

Contrast sensitivity

Contrast vision comparison	Pattern (right eye)					Pattern (left eye)				
	1.5	3	6	12	18	1.5	3	6	12	18
Average	**0.95**	**-0.34**	**0.55**	**0.31**	**0.51**	**0.83**	**0.65**	**-0.22**	**-0.09**	**-0.15**
Overall SD	**0.60**	**1.07**	**1.37**	**0.81**	**1.05**	**0.61**	**0.61**	**1.10**	**1.01**	**1.28**

Table 7.24 Summarised difference between contrast sensitivity with spectacle correction and CS with contact lenses and overcorrection.

The frequencies and contrast values used in the test were performed according to Table 7.2. The average values of the five lenses per material on each eye and for each specific frequency and contrast tested are shown in Table 7.24

The black printed values indicate improved contrast sensitivity with contact lenses compared to the spectacle correction, while the red printed minus values indicate a decrease in contrast sensitivity compared to the spectacle correction.

	Pattern (right eye)					Pattern (left eye)				
	1.5	3	6	12	18	1.5	3	3	12	18
VSO38	**5**	**6**	**5**	**3**	**2**	**5**	**6**	**5**	**3**	**2**
LM	**5**	**6**	**5**	**3**	**2**	**5**	**6**	**5**	**3**	**2**
GM	**5**	**6**	**5**	**4**	**2**	**6**	**6**	**5**	**4**	**2**
VSO75	**5**	**6**	**5**	**4**	**2**	**5**	**6**	**5**	**3**	**2**
Def.	**5**	**6**	**5**	**3**	**2**	**5**	**6**	**5**	**3**	**2**
Unaided	4	6	4	3	1	5	5	5	3	2

Table 7.25 Average contrast sensitivity results for all subjects using best correction

Average change	Pattern (right eye)					Pattern (left eye)				
	1.5	3	6	12	18	1.5	3	3	12	18
VSO38	**1.0**	**-0.4**	**0.6**	**0.1**	**0.2**	**0.8**	**0.6**	**-0.2**	**-0.1**	**-0.4**
LM	**0.8**	**-0.4**	**0.5**	**0.0**	**0.6**	**0.8**	**0.7**	**-0.4**	**-0.3**	**-0.2**
GM	**1.1**	**-0.2**	**0.7**	**0.8**	**0.7**	**1.0**	**0.7**	**-0.0**	**0.5**	**0.1**
VSO75	**1.0**	**-0.2**	**0.6**	**0.8**	**0.7**	**0.8**	**0.7**	**-0.1**	**-0.1**	**0.1**
Def.	**0.9**	**-0.4**	**0.3**	**-0.1**	**0.3**	**0.7**	**0.6**	**-0.4**	**-0.5**	**-0.3**

Table 7.26 Average difference between CS results with contact lenses using best overcorrection and best spectacle correction

Note: Detailed results are located in Section 10 (Tables, Contrast sensitivity).

Retinoscopic spot occurrences

With the soft lenses in situ after a wearing time of approximately 30 minutes, 63 abnormal occurrences were seen from a total of 750 observations i.e. 8.4%. A summary of these occurrences is give in Table 7.27.

Total		Sharp		Halos		Comets tail	Comets tail direction	
OK	687	OK	230	**NO**	233	224	10-2	3-9
Not OK	58	Not OK	20	**Yes**	17	21	99	127
VSO38		Sharp		Halos		Comets tail	Comets tail direction	
OK	126	OK	39	**NO**	42	45	10-2	3-9
Not OK	19	Not OK	11	**Yes**	8	0	4	1
LM		Sharp		Halos		Comets tail	Comets tail direction	
OK	139	OK	47	**NO**	47	45	10-2	3-9
Not OK	11	Not OK	3	**Yes**	3	5	1	4
GM		Sharp		Halos		Comets tail	Comets tail direction	
OK	142	OK	50	**NO**	50	42	10-2	3-9
Not OK	8	Not OK	0	**Yes**	0	8	8	0
VSO75		Sharp		Halos		Comets tail	Comets tail direction	
OK	148	OK	49	**NO**	50	49	10-2	3-9
Not OK	2	Not OK	1	**Yes**	0	1	1	0
Def.		Sharp		Halos		Comets tail	Comets tail direction	
OK	132	OK	45	**NO**	44	43	10-2	3-9
Not OK	18	Not OK	5	**Yes**	6	7	5	2

Table 7.27 Summarised retinoscopic spot occurrences for all five materials.

CRF 3 Post-trial examination

There were no impression marks, abnormal slit lamp findings, decrease in visual acuity or contrast sensitivity, neither were there any incidents requiring medical treatment (Table 7.28).

CRF3	Abnormal slit lamp inspection y/n		Fluorescein staining		Visual acuity with best correction		Medical referral y/n	Details of adverse event	Action provided
Initials	Cornea right	Cornea left	R	L	R	L			
SV	n	n	0	0	1	1	n	n/a	n/a
KM	n	n	0	0	1	1	n	n/a	n/a
SE	n	n	0	0	1.2	1.2	n	n/a	n/a
SA	n	n	0	0	1.2	1.2	n	n/a	n/a
KV	n	n	0	0	1	1	n	n/a	n/a

Table 7.28 CRF 3 results

7.5 *Discussion of the in-vivo results*

Comfort

Comfort is a subjective judgement and many factors will influence the grading of this sensation. In this trial, the inclusion of subjects who were currently contact lens wearers or who had previous experience of wearing contact lenses undoubtedly had an effect on the results. These subjects will generally be more tolerant of contact lenses than non-wearers. Fatigue during the test sessions may also have played a role. Hollwich and Kemmetmüller (1975) noted that contact lens wearers adapted to their PMMA lenses. A decrease in corneal sensivity with the long term use of contact lenses was reported by Tanelian and Beuerman (1980). They suggested that *"the sensory decrement induced by contact lens wear cannot be attributed to simple adaptation."* A sensivity loss with the use of both, soft and rigid gas permeable (RGP) lenses was reported by Millodot (1978). A decrease of corneal sensitivity was observed with overnight wear of OrthoK contact lenses, but no decrease was detected with one single overnight wear of conventional RGP lenses or silicone hydrogel lenses (Lum et al., 2013). Although most literature regarding the use of VAS

related to pain research and empiric social research in which the participant places a mark for a subjective perception, the use of VAS seemed appropriate for the current research (see Section 7.4). VAS and category scales were compared by (Funke, 2004) who recommended the use of a VAS in general. The intensity of a sensation differs from one subject to the other. The use of a reference material, the PMMA contact lens with soft lens design, facilitated the detection of any difference in perception when subjects were wearing an identical contact lens. This experimental design allowed the investigation of any relationship between contact lens materials and comfort.

When comparing the absolute comfort levels between the subjects, the overall VAS value for the subject with frequent and long-term contact lens experience (subject KM) showed an average for all the lenses tested of 0.3 cm. In contrast, subject SV with absolutely no contact lens experience had an average value of 1.0cm. Subject SE experienced more discomfort with all the lenses than all other participants, with an average value of 3.8cm. Subject KV, having sporadic contact lens experience, had an average of 3.0cm for all tested soft lenses. Subject AS, the only male, showed an overall average of 2.3cm. These results are similar to those found in other studies, for examples see Table 7.29

Study	Material	Average (cm)	
Jones, 2007	Comfilcon	1.1	SD ± 0.9
	Balafilcon	1.7	SD ± 1.2
Epstein and Friedman, 2003		3.8 pm value	5.3 cm end of day value

Table 7.29 Comfort results from research literature. pm = afternoon

It is likely that in the last 10 years developments in soft lens materials have improved upon the ‘end-of-day’ value of 5.3cm found by Epstein and Freedman (2003) (Table 7.29).

Normally, when a comparison is made between rigid lenses and soft lenses, it is between a rigid corneal lens diameter of about 9.5mm and a soft lens diameter of about 14mm. With a corneal lens, the eyelid moves across the lens edge during a blink and causes a distinct sensation. With the soft lens, the edge of the lens is under the top lid and there is less sensation during the blink. With

semi-scleral rigid lenses the TD of the lens is comparable to that of a soft lens and therefore with this type of rigid lens the eyelid does not have to pass over the lens edge, hence there is less sensation than with a corneal lens (Pullum, 2012).

Four of the five subjects in the trial felt there was a subjective improvement in comfort with the soft lenses compared to the PMMA lenses. This would be due to the material characteristics and lens design rather than the edge effect.

In this trial the highest difference was between PMMA and soft lenses was shown by subject SV with a 3.4cm improvement, a result that might be expected as this subject was a non-wearer of contact lenses. Subject KM reported that there was very little to choose between either lens type and the poor comfort results perhaps indicated that, because this subject had sensitive eyes, she would not be a good contact lens candidate at all.

By measuring the wearing comfort of the rigid, large diameter lenses as a baseline for each individual it was possible to compare these findings with the comfort levels of the soft lenses. These results, (Table 7.30) showed better comfort with most soft lenses compared with the PMMA test lenses. Subject KM was wearing frequent replacement lenses while subject SE did not need any optical correction and has never had any contact lens wearing experience. Both noted little or no difference between PMMA and soft lenses. KM and SE both reported reduced comfort with the VSO 38 material than with the PMMA scleral lenses, though preferred the other soft lens materials to PMMA, while SV felt an improvement with soft lenses in general.

subject	Average VAS (PMMA -Soft CL)
SV	3.4
KM	0.0
SE	-0.5
AS	2.2
KV	1.8

Table 7.30 Comfort difference on the VAS between PMMA semi scleral trial lenses and the 5 soft lens materials.

The compensated results showed that the overall comfort (using the 10cm VAS scale) was as follows:

The best -	Definitive	(2.4 cm more comfortable than PMMA)
	LM55	(1.8 cm more comfortable than PMMA).
	GM3	(1.4 cm more comfortable than PMMA)
	VSO 75	(1.3 cm more comfortable than PMMA)
	VSO 38	(0.05 cm less comfortable than PMMA)

However, the ANOVA revealed that with such large variances and small sample sizes there was no significant difference between the materials as regards comfort.

The subjects were not aware of which material they had been wearing but the various soft lens materials were not randomised for each subject[22]. PMMA evaluation was the first lens wear experience and a few days after this the soft lenses were evaluated in the following order:

VSO 38,

LM55;

GM3,

VSO75 and

Definitive.

This may well have resulted in a preference for the later lenses compared to the earlier lenses used. One would not be surprised to find a comfort preference in roughly the same order. A randomised order would not have given different results.

[22] Note: In order to ensure that 250 different lenses drifting around were not confused and to keep records in proper order it was necessary to follow a strict routine which carefully was evaluated.

Performance

Visual acuity

The was a slight decrease in visual acuity with all soft lenses and for all subjects compared with VA with best spectacle correction. The decreases ranged from an average of -0.08 for the LM material to -0.13 for the VSO 75 material when compared to spectacle correction.

Subject #1 showed an increase in acuity with the VSO 38 material on two occasions while there were no differences observed with all other tested lenses.

Subject #5 showed an increase in acuity of 0.2 with one GM lens, a decrease of -0.2 with another GM lens and decreases of -0.2 and -0.3 with two Definitive lenses.

The literature confirms that a decrease of visual acuity occurs with soft lenses (Bailey et al., 2001, Wechsler, 1978, Kirkpatrick and Roggenkamp, 1985). Other authors have claimed, that visual acuity does not change with soft contact lenses compared to spectacle correction and that *"spherical aberration control contact lenses have little effect on visual quality"* (Lindskoog-Pettersson et al., 2011). While the results show a slight drop in visual acuity for all lenses tested, the averaged results for subject 1 and subject 5 showed no difference between spectacle correction and contact lens overcorrection.

Contrast sensitivity

Performance of soft contact lenses as regards contrast sensitivity has produced conflicting views in the research literature. Kirkpatrick (1983) did not find significant differences between spectacle values and contact lens values. Guillon et al. (1988) found an improvement in contact lens contrast sensitivity compared to spectacles but conversely Grey (1986) found a gradual reduction in contrast sensitivity with soft lenses at the first hour of contact lens wear with a worsening tendency with increasing lens thickness.

In the current study the largest improvement in monocular contrast sensitivity was seen for 1.5cpd for both the right and the left eyes. For the right eyes an

overall improvement was observed for the frequencies 6, 12 and 18cpd. For 3cpd, an improvement was shown for the left eyes (see section 7 Tables).

There was no evidence that contrast sensitivity was significantly different for any of the five soft materials but it was slightly lower compared to the values found with spectacle corrections. For some frequencies it was better and for some it was worse.

Retinoscopic spot appearances

The few contact lens related optical phenomena reported were with subject SE for one of the VSO 38 lenses in both eyes and two of the GM3 lenses in both eyes. The lenses in question were checked for optical quality after all the tests had been completed using a manual projection focimeter. The images were crisp and the phenomena could not be attributed to poor lens quality. Since the optic phenomena reported by other subjects occurred on one eye only, it might be possible that tear- related problems might have been the reason for the phenomena.

Testing the appearance of the retinoscopic spot on the projection screen ensured, that the lenses were fitted in a uniform way with an aligned fit. There were no steep fitting lenses which would have caused abnormal appearances. By performing the test with subjects wearing their best spectacle correction optic phenomena related to media and tear related problems were ruled out. This quick and simple test further ensured, that optical problems caused by either lenses that were too steep lenses or poor optical performance of the lenses themselves did not exist.

Lens movement

Lens movement was investigated in two ways. The first recorded full blinks using video and these were later analysed. These videos showed the effect of the lid force on the lens itself but the make-up of the subject's tears, lid tension, lid flexibility, etc. would all have had some effect on the outcome. This video technique demonstrated in Figure 7.2 using a 10x magnification worked very well and allowed an observer to resolve a lens movement to 0.1mm. However, it has to be considered that this technique had its limits in terms of accuracy,

for example a lens movement of less than 0.1mm might be judged as no movement or 0.1mm.

The second method (PUT) relied on the observer physically moving the lens by pushing up the lower lid against the lens. This subjective assessment was trying to assess the force to overcome the adhesive forces between the lens and eye and the friction existing between the two surfaces under lubricated conditions. Although there would be some friction between the front surface of the lens and the lid, this test was more concerned with the back surface of the lens and the eye. The nature of the bulbar conjunctiva will also affect the movement of the lens using the PUT. An example is shown in Figure 7.11., Figure 1 in the cited article of Cui et al. (2012) which is an ultra-high resolution OCT image of a contact lens covering the limbus with the lens edge depressing the bulbar conjunctiva just outside the limbus. The perilimbal impression can be verified at the point marked “t”.

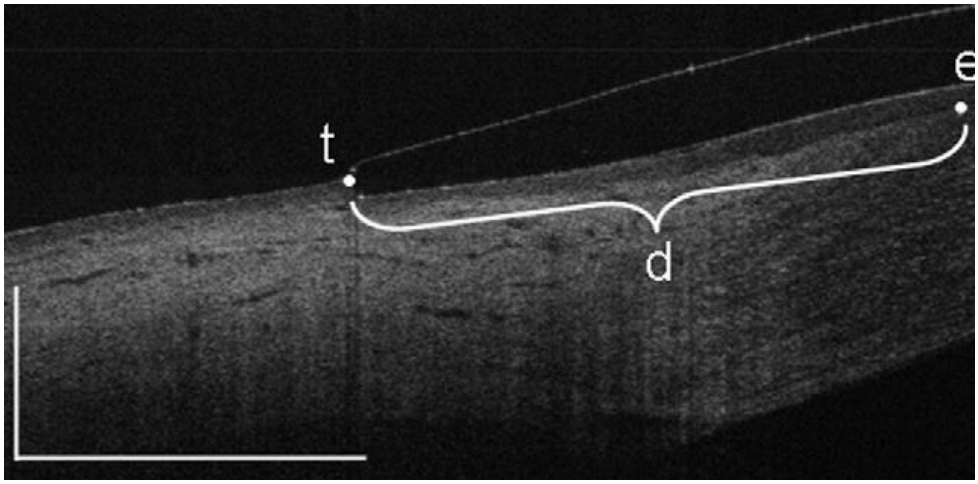

Figure 7.11 Ultrahigh resolution OCT of the limbal area of an eye and a conjunctival impression caused by a soft lens

From the video results, that the averages and standard deviations for lens movement showed insignificant differences between materials, while the median values ranged from 0.4 mm for the VSO38 and the VSO75 material down to 0.1mm for the Definitive material. The minimum movement was zero mm and the maximum movement was 4.6mm.

It was demonstrated that the lenses manufactured for the specific tests in these experiments had an unusually flat (9.2mm) Back Optic Zone compared to the more normal BOZR value (8.6mm) found in conventional hydrogel lenses. The

experimental lenses had an unexpectedly small dynamic range. The possible presence of adhesive forces due to the close proximity between the tissue (i.e. cornea or lid) and the lens could be another explanation for the small lens movements seen. The lenses did not have an anterior second curve (lenticular curve) whereas most contemporary lenses do have peripheral curves on either the front or back surface of the lens (see 4.8 Contact lens friction and lubricity). It is reasonable to assume that these elements affect the lens movement.

Results of soft contact lens movement using optical coherence tomography (OCT) with normal Acuvue Advance, Acuvue 2, Pure Vision and O2 Optix lenses showed an average vertical movement of 0.366mm ± 0.155mm (Cui et al., 2012). Neither keratometer readings nor sagittal heights were not mentioned in Cui et al's paper. In addition the deformation of the normally dish-shaped soft contact lens just between the limbus (above the "d") and the point marked with "t" in showed that the area was altered to a straight line which might indicate a steep lens causing stress within the contact lens material.

Another study (Golding et al., 1995b, Golding et al., 1995a) reported that soft lens movement was related to blink rate. They found lens movements from 0.07mm at 10 blinks per minute to 0.19mm at 30 blinks per minute and it was suggested: *"that the extent of lens settling and the degree of post-insertion lens movement are determined by the time-average pressure for post-lens tear film expulsion exerted on the lens by the eyelids."* In the experiments on lens movement, the author of the current thesis was not aware of any subject blinking at an abnormally high or low rate.

The PUT results showed no tight lenses or lenses adhering to the eye. As might be expected, nearly all lenses with excessive movement, judged by the video, were also seen as 'loose' with the PUT. There were a few lenses that had a 'normal' PUT but the lenses moved excessively when analysed using the video.

Except for the VSO 75 material there was an increase in the number of lenses judged as normal with the PUT and showing a movement after a blink between 0 and 0.2mm ascending from VSO 38 with 19 lenses to Definitive with 30

lenses. However the difference from one material to another is very small and there is little evidence to support the view that water content or friction are major factors in lens movement or friction.

Chapter 8 - General discussion and conclusions

Friction

Static friction

Static frictional force is the force required to get a stationary body moving and requires more force than dynamic friction.

Dynamic friction

Dynamic friction is present between the contact surfaces of bodies moving linearly to each other and requires less force than static friction to maintain linear motion.

To measure frictional properties two surfaces are required, for example, a contact lens and the eye. Normally, frictional tests would be carried out without lubrication. As soon as a lubrication layer is introduced between the two surfaces, the substance tested is the lubricant and not the material in question.

The physical and chemical properties of the lubricant will determine whether fluid friction, mixed friction, or boundary friction takes place. Along with static friction, any of these three types of friction can occur with a contact lens surrounded by tears, in conjunction with a blink.

The in vitro tests carried out were designed with the above in mind. The materials themselves were tested without lubricant as well as with saline and a lens wetting agent as a lubricant.

It is essential to understand that there is no friction coefficient for a contact lens material unless it is tested against a substrate. The friction coefficients obtained experimentally were the result of force applied to a specimen placed upon a substrate and the force required to move the specimen was measured. The variables that can influence the results were the force applied, potential errors associated with the methods of measurement, the presence or absence of lubricant, lubricant properties, the relationship between adhesive forces and forces applied, the material properties of both the substrate and specimen, such as roughness, hardness, speed, and the area of surface contact. All these can act to influence the force required to slide one object upon another.

The knowledge of static and dynamic friction with respect to the contact lens and eye considered separately is not necessarily identical to what occurs regarding friction of contact lenses in the eye. If the lens sticks, the force triggered by closing the eyelid is too weak to move the lens. If the lens moves with blinking, the force might just be enough to move the lens or it may be higher. When all this is considered, it may appear impossible to obtain a static friction value. The following conclusions have been drawn from the current research:

- the physical property of the pairing: the cornea and conjunctiva should be regarded as elastomers,
- the action triggered by the lid does not necessarily lead to a lens movement,
- because of the very short time span during which the blink occurs, dynamic friction plays little to no role.

The friction characteristics of soft lenses is a topic which has received relatively little attention in the literature. Contact lenses are spherical or aspherical in nature and therefore do not readily lend themselves to mechanical testing. It is easier to carry out laboratory investigations on flat slabs or sheets of material. The instrument used to assess friction is the tribometer and various devices have been used. Niarn and Jiang (1995) used a pad on disk arrangement; Rennie et al. (2005) and Urueña et al. (2011) both used a glass pin on the lens. A glass pad on the lens were used by Roba et al. (2011) and EBATCO (2012). Zhou et al. (2011) used a steel ball on the lens surface and Gitis (2004) used steel and glass disks. Some of the devices were custom made and some were commercially available devices. All tribometers used a method where the area of contact theoretically is infinitely small. One difficulty associated with the use of pins of different radii is that they indent into the soft material to some extent. Even the use of a flat glass pad would cause some indentation. A tribometer system which produces small amounts of punctal pressure might fulfil testing requirements for some solids but it is not optimal for contact lenses.

In the absence of a tribometer design which is custom made for testing contact lenses, one major objective of the author's research was to design, build and test a tribometer specifically for measurement friction characteristics in contact lenses. One feature of this tribometer design, which makes it more applicable to contact lenses, is the ability to test a larger surface substrate in contact with the specimen. A further feature was to mimic the ocular situation with a spherical shaped substrate. From contact lens material blanks, test pieces were accurately lathe cut to form integral parts of the apparatus.

It was also the aim of the work to 'calibrate' the equipment by taking commercially available solids and assessing if the coefficients of friction were comparable to published data. The materials chosen were aluminium, PMMA, and PTFE[23].

Unlike, the research in other publications (Urueña et al., 2011, Opdahl et al., 2003, Kim et al., 2001, Dunn et al., 2013b, Niarn and Jiang, 1995, Rennie et al., 2005, Roba et al., 2011, EBATCO, 2012, Zhou et al., 2011, Steffen and McCabe, 2004, Gitis, 2004, Dong and Haugsted, 2011, Thiele, 2012, Ngai et al., 2005), the experimental in vitro friction measurements tried to mimic as far as possible the contact lens/eye interface. Notably, the resting time between measurements was similar to the minimum interval between blinks. Properties of elastomers, such as hardness, flexibility and modulus do have a wide range. For materials such as rubber, soft contact lenses, soft plastic material or agar which are judged as elastomers or gels, frictional properties differ from those of solids. These materials adhere more tight to a substrate because they are soft. The toothing and the adhesive forces between two elastomers are stronger than between solids.

As a contact lens is in a lubricated state when in the normal eye it was decided in the work described in this thesis to assess the friction in three modes i.e. unlubricated, borderline (minimal) lubrication and mixed friction (significant lubrication). A selection of five CL materials were evaluated, ranging from a

[23] PMMA= Polymethylmatacrylate (Plexi glass), PTFE = Polytetrafluoroethylene (Teflon)

38% water content material to a 75% water content material and including a silicone hydrogel material.

The contact lens tribometer was designed to measure friction with spherical or cylindrical shaped components. Either substrate or specimen could be shaped as a sphere while the counterpart had to have a hollow spherical or cylindrical shape not larger than a hemi-sphere or a semi-hollow cylinder. The sphere, driven by a motor tends to move the hollow counterpart sitting upright on top of the sphere and fixed on an immobile force sensor measuring the resulting force. This logical and simple design allows one to measure all types of machineable substances which can be of any size. To mimic what is happening with a contact lens, a stepper motor starting with its absolute speed can mimic the speed of the eyelid. This setup makes it possible to measure the frictional forces of a contact lens material in vitro. It was possible to design the apparatus to measure static and dynamic friction in both a 'pushing' direction and in a 'pulling' direction. The decision, only to measure only the pushing friction instead of measuring both the friction with the pushing motion (mimicking lid closure) and the pulling motion (mimicking lid opening) was taken for the following good reasons.

Starting with the open eye lid and the lens in the resting position, the upper lid sweeps over the contact lens within a fraction of a second; within microseconds, static friction takes place. The lens moves, dynamic friction takes place but cannot be measured because of the short time span; the eye is closed and the lens is possibly displaced. As described by Forst (1981) and Leicht et al. (2005) displaced soft lenses tend to find their own way to their resting position. Due to the extremely short resting time, the inner force of the deformed and displaced lens manifests forces which would influence the result and cause less measurable friction, despite the fact that momentum might play a role by reversing the direction of movement.

The design of the tribometer was successful with all components working as expected. In its current state the tribometer can be used for any substance, either solid or elastomer. Related to contact lenses the tribometer is limited to be used with spherical or other rotational symmetric shaped substrates and to specimens which are congruent with the substrate. To test a commercially

available contact lens with the tribometer, a holder congruently shaped to the anterior contact lens surface would be required. 3D image scanning and modelling for each lens could perhaps be a possibility to measure the frictional properties of the posterior and anterior surface.

The relationship between adhesive forces and the normal force, i.e. the weight of the specimen itself play an important role if long low weights are used. While the tests were carried out using 98 milliNewton normal force for experimental purposes, 980 milliNewton were used to evaluate any possible differences of results. The CoF of the PTFE material used in the current study is almost identical to that reported by Polytetra (2013) for similar normal forces applied. For aluminium, Garzino-Demo and Lama (1995) reports a dependency surface quality, i.e. lathe turned or polished starting with a load of 0.1N/mm² and a CoF of 0.9 with a rugosity of 1.3. With the same load (0.1N/mm²) but with a rugosity of 0.5 they found a CoF of μ= 0.5. Feyzullahoglu and Nehir (2011) found a decreasing CoF with increasing load for aluminium With a F_n= 0.2 N they measured a CoF of 0.35 and with a F_n = 1.0N the CoF was 0.25. In general it seems that for published coefficients of friction higher loads (F_n) were used and detailed literature investigations show a rather wide range of measured CoF's using different measurement methods.

The data from other workers on the CoF of CL materials are shown in Table 8.1.

Study	Material	WC %	Cof	Comments
Niarn, Tong-bi (1995)	B&L Seequence	38.6	0.05 - 0.21	Substrate PMMA, Phema
Rennie et al. (2005)	Etafilcon A	58.0	0.025-0.075	
Roba et al. (2011)	Daily disposal	58.0	0.017-0.34	100 cycles
Roba et al. (2011)	Reuseable	24.0	0.011-0.56	100 cycles
EBATCO (2012)	Acuvue Oasys	38.0	0.25 static	10mm distance
EBATCO (2012)	Acuvue Oasys	38.0	0.2 dynamic	10mm distance
Zhou et al. (2011)	Senofilcon A (Oasys)	38.0	0.10	Amontons Law applies
Steffen et al. (2004)	Acuvue2	58.0	0.006-0.049	Data only
Gitis, N. (2004)	Ciba vision Focus	24.0	1.1 static 0.2 dynamic	
Dong and Haugsted (2011)	Focus Dailies	69.0	Arbritary units only	Two saline types different results
Uruena et al. (2011)	Acuvue Oasys Pure Vision	38;36	0.01-0.6	Different lubricants
Thiele, E. (2012)	Not published		not published	Pressue, speed and substrate depending
Ngai et al. (2005)	Silicone Hydrogel vers. Hydrogel	Not defined		Pressure speed and lubrication depending

Table 8.1 Published coefficients of friction for a range of contact lenses.
WC = water content

Note: All the tests listed in Table 4.3 and in Table 8.1 used a ball shaped substrate, apart from Niarn and Jiang (1995), Rennie et al. (2005) and (EBATCO, 2012) which used a flat pad. If the tests had been undertaken under fully lubricated conditions then fluid friction took place and the frictional properties of the fluid were measured.

Using the author's experimental tribometer, the results shown in Table 8.2 Coefficients of friction measured under unlubricated conditions and different lubricated states with the experimental contact lens tribometer.

were obtained:

Type of friction and load	CoF				
	VSO 38	GM3	LM 55	VSO 75	Definitive
Dry	23.24	23.58	7.79	24.37	10.44
Lubricated saline, 100 g	1.38	1.63	0.58	1.63	1.73
Borderline saline, 10g	5.89	2.59	1.32	2.68	2.93
Lubricated saline, 10 g	0.80	1.43	1.69	2.75	3.83
Celluvisc 10g	0.35	0.27	0.80	3.73	0.89

Table 8.2 Coefficients of friction measured under unlubricated conditions and different lubricated states with the experimental contact lens tribometer.

The exceptionallly high coefficients of friction for the completely unlubricated materials reflect the comments in literature regarding rubber friction and friction of elastomers (Deladi, 2006, Deutsches Institut für Kautschuktechnologie, 2004, Besdo et al., 2010). A paper by van der Steen (2007) described the reason for a decreasing CoF with increasing load.

Keeping in mind that the CoF for ice on water, known to be remarkably low, is around 0.05 for static and 0.04-0.02 for dynamic friction, the low values reported for low water content contact lenses (Niarn and Jiang, 1995) probably indicate the presence of fluid friction. On the other hand, the higher values for CoF of 0.21 (Niarn and Jiang, 1995) and 0.56 (Roba et al., 2011) probably indicate the presence of fluid friction while the higher values reported as CoF 0.21 (Niarn and Jiang, 1995) are quite similar to the author's own measurement result with Celluvisc and saline as a lubricant with the similar VSO 38 material. Furthermore, Gitis (2004) reported a static CoF of 1.1 for the Focus lens compared to a CoF of 0.8 for the VSO 38 (with mixed friction and saline as lubricant) found by the author.

The current study finding for CoF with the GM3 material with Celluvisc as lubricant (CoF 0.27), being a mid-water content material, is similar to the findings of Roba et al. (2011) for the Etafilcon A lenses (58% water content) and is assumed to be mixed friction.

CoF's of high water content materials were be found in literature. However the author's experimental findings show higher coefficients of friction than for other contact lens materials.

While the author's results for the use of a lubricant and a few results with saline agree quite closely with those found in literature (Table 8.1 and Table 8.2), marked differences appear with the results regarding borderline lubrication with saline, with CoFs of up to 5.89 (for VSO 38) with a load of 10 gram, and up to 1.73 (for the Definitive material) with a 10 fold greater load (100gram).

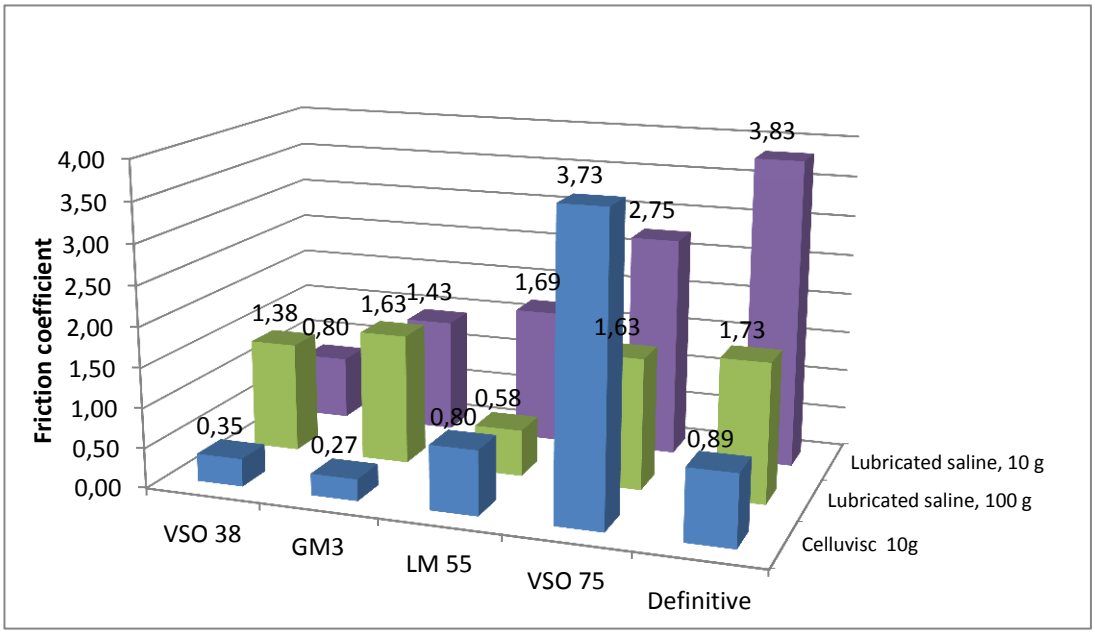

Figure 8.1 Average coefficients of friction in ascending order

Figure 8.1 shows the quasi-linear increase in static friction from low to high water content under mixed friction conditions and with a 10 gram load. While the coefficient of friction increases with the 100 gram load for the VSO38 material, there was little difference for the GM3. With the LM55, VSO75 and Definitive materials the CoF dropped with the increasing load (Table 5.5 Friction coefficients of rigid materials tested against each other.). The test results with the VSO75 material and the Celluvisc as a lubricant were reviewed for typing errors or confused material codes. Since five different specimens of the material were used an error seems to be unlikely and the measured CoF of 3.73 for the VSO75 material was confirmed. The LM55 CoF with the Celluvisc as lubricant was slightly higher than that measured with the elevated 100 gram

load (0.58) but still only 50% lower than that measured with the standard load of 10 grams.

Comfort

An in vivo study was designed to investigate if any of the material(s) showed comfort or performance values were related to the CoF. If this was the case then knowing this property of the lens material could influence clinicians when a CL material was chosen for a particular patient. It is been well known (Bourassa and Benjamin, 1989) that all contact lenses acquire a biofilm in vivo and in terms of the wetting angle on the surface of the lens, no significant difference in wetting is seen with a range of materials. Whether the CoF would change with the CL materials in vivo was the question addressed to the current research.

Comfort was assessed on a VAS as this method had been used successfully in many clinical trials (e.g Paul-Dauphin et al. (1999). Performance was monitored by visual acuity, contrast sensitivity using five frequencies, and the retinoscopic image produced through the lens. When a soft lens moves on the eye it is affected by a number of different forces. But the fact that there is movement between two different surfaces must imply that friction is one of these forces. Two aspects of lens movement were investigated - one being a measurement of natural lens movement with blinking and the other an average of the push-up-test (PUT) results following the application of pressure to move the lens from the primary gaze position.

The measurement of vision and contrast sensitivity was carried out using quite conventional methods. Evaluation of the retinoscopic image has not been used in clinical trials but the author had found it valuable in clinical practice for assessing vision quality. Lens movement was captured on video from a slit lamp microscope. The lens had previously been marked with dots and an analysis of the video images enabled an observer to calculate rotation as horizontal and vertical vectors.

16 subjects were recruited for the trial and it was hoped that the majority would be suitable. Unfortunately, only a small number managed to pass the acceptance criteria. With hindsight, this final number of five subjects was too

small to pick up the small differences expected but further recruitment was not possible.

A novel approach was taken regarding the fitting of the soft lenses. Rather than using 'conventionally' designed lenses made from the five materials, i.e. with conventional radius and diameter values, the author designed the lenses so that minimal stress was induced by the lens fit. To this end, a series of PMMA lenses was made with various BOZR values and one TD (14.5mm). These semi-scleral lenses were fitted in turn to the subjects until central alignment was obtained. Interestingly, the same lens achieved the desired fit with all 5 subjects, namely the 9.2mm BOZR and the 14.5mm TD. This was in accordance with the observation reported by Pullum (2003). Soft lenses were manufactured under the author's supervision from the five materials to this design for each of the subjects. All lenses had the same thickness profile as there was no optical correction incorporated. The front surface was parallel to the back surface.

As comfort is a subjective variable, comfort levels werw first measured with the semi-scleral PMMA lenses in situ, which gave a baseline measurement against which the other materials could be assessed. As these lenses are large, there was no lens edge for the lid to blink over. The comfort values measured with the various soft lenses were compensated by taking the baseline PMMA value into account.

The comfort results are shown in Table 8.3 and Table 7.11:

VAS v/s PMMA	Material				
	VSO38	LM55	GM3	VSO75	Definitive
Average	-0.05	1.81	1.42	1.32	2.40
SD	1.86	1.64	1.67	1.36	1.80
Median	0.3	2.2	1.5	1.1	2.5

Table 8.3 Average VAS differences in comfort between the tested material and PMMA test lens. Positive values indicate better comfort.

For the VSO 38 material, a slight decrease in average comfort was found largely due to the result obtained from one subject. The median statistic, however, showed a general increase in comfort for all soft materials compared with PMMA.

Visual acuity

In terms of visual acuity, the results are shown in Table 8.4:

VA	Average	SD
Spectacles	1.1	0.2
V38	**0.97**	0.11
LM	**0.98**	0.07
GM	**0.99**	0.07
V75	**0.95**	0.10
Def.	**0.98**	0.08

Table 8.4 Average visual acuity with best spectacle correction and with contact lenses[24]

There was no significant difference in visual acuity among the test lenses and between test lenses and best spectacle lens correction.

Contrast sensitivity

Contrast sensitivity was measured at distance using Ginsburg Contrast Sensitivity distance charts with best spectacle correction and with best overcorrection over the contact lenses in situ

Cycles /deg.	Contrast vision with:					
	Spectacles	VSO38	LM	GM	VSO75	Definitive
1.5	4.5	5.4	5.3	5.6	5.4	5.3
3	5.9	6.0	6.1	6.1	6.1	6.0
6	4.7	4.9	4.8	5.0	5.0	4.7
12	3.3	3.3	3.2	3.9	3.6	3.0
18	1.7	1.6	1.9	2.1	2.1	1.7

Table 8.5 Average contrast sensitivity of all eyes tested[25].
The numbers printed in red show the results with only the best spectacle correction in place.

The average of all eyes tested showed slightly better contrast sensitivity with contact lenses than with spectacles.

[24] Taken with the soft lens in situ and a sphere-cylinder over-correction

[25] Spectacle correction using spheres and cylinders, contact lens in situ + sphere-cylinder over-correction

Retinoscopic spot images

The retinoscopic images were evaluated by the appearance of comets' tails or other optical phenomena from the spot image projected onto a screen. Comets' tails were also recorded by the direction of the tail. Those images reported to have a sharp edge were taken as normal.

Asking the subject to describe the appearance of the projected retinoscopic spot is a simple, quick, qualitative check. The subjects were asked if the spot appeared to have a sharp edge and, if not, to describe how the spot appeared. If the subject reported a sharp edged spot it was assumed that:

- The best correction had been found
- There were no undesired entities regarding the optical media such as
    - poor quality optics of the optical appliance
    - inadequate optical correction caused by
        - incorrect determination of refraction
        - incorrect contact lens geometry
    - inadequate tear composition or quantity
    - irregularities of the ocular optical media.

The results of the retinoscopic spot appearance are presented in Table 8.6.

Appearance	Retinoscopic spot appearance					
	Spectacles	VSO38	LM	GM	V75	Definitive
Normal	49	39	39	42	48	32
Halos	1	3	3	0	0	6
Comets tail	0	5	5	8	1	7
Not sharp	0	3	3	0	1	5

Table 8.6 Overall retinoscopic spot appearances with the best overcorrection.

Lens movement in vivo compared to in vitro friction

The findings from the video analysis of lens movement were as follows:

In vivo movement and in vitro CoF	Material				
	VSO 38	GM3	LM 55	VSO 75	Definitive
Average movement	**0.53 mm**	**0.50 mm**	**0.32 mm**	**0.62 mm**	**0.41 mm**
SD movement	0.34 mm	0.55 mm	0.14 mm	0.42 mm	0.31 mm
Borderline CoF	5.89	2.59	1.32	2.68	2.93
Mixed friction CoF	0.80	1.43	1.69	2.75	3.83
Celluvisc CoF	0.35	0.27	0.80	3.73	0.89

Table 8.7 Average lens movement with video analysis compared with CoF at borderline and mixed lubrication with saline and mixed lubrication with a lubricating agent.[26]

It is difficult to compare a measurement expressed as a distance in mm with the dimensionless coefficient of friction. The aligned fit with the contact lenses ensured that reasons for lens movement, other than friction, were minimised. The average values for lens movement with each lens material were not significantly different, provided the surfaces are lubricated. The in vitro results showed significant CoF differences among the five materials as long as saline solution is used.

Rank movement	Rank Borderline CoF	Rank Mixed CoF	Rank Celluvisc CoF
2	1	5	4
3	4	4	5
5	5	3	3
1	3	2	1
4	2	1	2
rho	**0.5**	**-0.2**	**0.2**

Table 8.8 Spearmans rho rank correlation for CL movement after a blink and CoF

[26] The lens movement is expressed in mm after a blink. The dimensionless coefficient of friction (CoF) is expressed with the Greek μ.

The extraordinary increase with the CoF of the Vistagel 75 material with the Celluvisc lubricating agent was re-evaluated and is in contradiction to the other results. Since the in vitro results vary considerably, the material properties appear to play an important role in the frictional behaviour of soft lens materials. Movement against borderline CoF showed a correlation factor of 0.5 showing the best value compared to mixed friction CoF and Celluvisc CoF. However, the factor shows that there is a moderate correlation between lens movement after the blink and the CoF with borderline friction. A correlation between rank movement and either mixed or celluvisc CoF was not found (Table 8.8).

Push-up-test (PUT)
Using the PUT there were no lenses which were deemed to be 'tight'. The remainder were either 'normal' or 'loose' (Table 8.9)

PUT vs. CoF	Material				
	VSO 38	GM3	LM 55	VSO 75	Definitive
Number of normal values	42	40	44	38	47
Number of loose values	8	6	6	10	3
Borderline CoF	µ 5.89	µ 2.59	µ 1.32	µ 2.68	µ 2.93
Mixed friction CoF	µ 0.80	µ 1.43	µ 1.69	µ 2.75	µ 3.83

Table 8.9 Push-up test results compared with borderline and mixed friction CoF's

In this small sample there was no association found between frictional behaviour and PUT for all the contact lens materials used (Table 8.9).

Chapter 9 - CONCLUSIONS

Soft contact lenses are hydrogels and behave as elastomers regarding friction. Friction coefficients as low as ice on melting water were reported in literature (Niarn and Jiang, 1995, Roba et al., 2011, Rennie et al., 2005, Steffen and McCabe, 2004) but have little to do with daily contact lens wear. Adhesion between soft contact lenses and the eye or other substrates being in contact with require more force to move the specimen than probably expected. There was no difference in frictional behaviour with saline as lubricant between the different contact lens materials. With the use of lubricant drops, the coefficient of friction was higher for the high water content MMA VP material. For the other materials tested the use of a lubricating solution resulted in a lower coefficient of friction which then were similar to the results found in literature provided mixed friction was measured. The in vivo friction testing confirmed that a relationship between material type and frictional properties was not present. These experiments have led to a better understanding of the nature of what is happening with the lens in the eye regarding lens adhesion and lens movement.

The specially designed tribometer built for this study allowed the measurement of friction in contact lens materials in a simple way, in conditions that approximated to those which are encountered in contact lens wear. Since friction took place between two surfaces the disadvantage of not using finished lenses was not apparent. It would be possible to use finished lenses but the exact shape of the anterior lens surface needs to be known to produce a negative shaped lens holder. 3D scanning, modelling and copying would be required. Whilst this is not impossible, it would be expensive.

The results regarding comfort once more proved that there is little difference in feeling between a rigid scleral lens and a soft lens. The participating subject who used contact lenses for many years was more tolerant regarding comfort

than those who never used contact lenses. So contact lens comfort differences seem to be more related to the subject's history rather than to different contact lens materials.

The slit lamp examinations and the videos taken showed that in many instances the lid closure went together with the eye turning upwards. This phenomenon causes the impression that contact lenses move more than they do in reality.

A major part of the in vivo experiments was required to ensure that the lenses were optimally aligned in the subject's eye. This included the use of the PMMA trial lenses, the manufacture of 250 soft contact lenses to exceptionally tight tolerances the contrast vision tests, the visual acuity tests and the tests using the projected retinoscopic spot.

The work presented in this thesis brought new understanding of the required contact lens shape, frictional behaviour of soft lenses in reality, the influence of body temperature and contact lens shape, the understanding of elastomer friction between the contact lens and the eye. In terms of borderline friction, the friction coefficients of the five materials did not produce changes in performance. Other materials may produce different results. More investigation is necessary to fully understand the interactions between contact lens, the eye, tears and lubricants in various physiological and environmental conditions. A more concise clinical protocol and the use of more subjects should make experiments more productive.

Chapter 10 - Appendices

10.1 *Results of CRF1 tests*

Initials	Contrast test sensitivity with best prescription right eye					Contrast test sensitivity with best prescription left eye				
	Pattern					Pattern				
	A	B	C	D	E	A	B	C	D	E
SV	5	6	3	3	1	5	5	5	3	1
KM	4	8	3	2	0	5	6	4	2	0
SE	5	6	4	4	2	4	5	4	4	4
AS	4	6	6	4	2	4	6	6	5	3
KV	4	6	6	3	2	5	5	6	3	2
Average	4	6	4	3	1	5	5	5	3	2
SD	0	1	1	1	1	0	0	1	1	1

Table 10.1 Contrast sensitivity with best correction CRF 1 for selected individuals

ID No	Race	Age	Sex	Corneal diameter (mm)		Keratometer right (mm)			Keratometer left (mm)			Prescription RE				Prescription LE				Contact lenses ?
				RE	LE	1. Mer.	Axis	2. Mer.	1. Mer.	Axis	2. Mer.	Sph.	Cyl	Axis	VA	Sph.	Cyl	Axis	VA	
1	K	26	f	10.3	10.3	7.98	5	7.84	7.95	170	7.90	+0.25			1.0	+0.25			1.0	n
2	K	27	f	11.4	11.3	7.80	5	7.60	7.80	2	7.60	-6.25	-0.50	30	1.0	-6.25	-0.50	173	1.0	y
3	K	27	f	11.5	11.5	7.90	5	7.75	7.84	0	7.62		-0.50	165	1.2		-0.50	180	1.2	n
4	A	29	m	11.2	11.2	7.62	10	7.58	7.68	0	7.65				1.2				1.2	n
5	K	28	f	11.7	11.7	7.65	5	7.54	7.65	0	7.54	-0.50	-0.50	20	1.0		-1.25	10	1.0	y
6	K	45	m	12.0	12.0	8.09	0	7.91	8.15	0	7.82	-0.75			1.0	-0.75			1.0	n
7	K	30	f	9.5	9.8	7.43	3	7.29	7.46	14	7.38	-0.25	-0.25	70	1.6	-0.25			1.6	n
8	K	26	f	10.5	10.5	7.72	87	7.84	7.7	91	7.84	-1.25	-0.50	165	1.2	-1.25	-0.50	170	1.2	n
9	K	51	m	12.0	11.0	7.37	0	7.38	7.31	0	7.41	+0.50			1.0	+0.50			1.0	y
10	K	31	f	12.0	12.0	8.15	120	8.19	8.2	135	8.05	-2.50	-0.50	35	1.0	-2.25	-1.00	130		n
11	K	27	f	11.5	11.5	7.51	0	7.49	7.5	0	7.51	-1.00			1.0	-0.50	-0.25	30	1.0	y
12	K	26	m	11.8	11.8	7.6	0	7.5	7.65	175	7.55	+0.75			1.0	+0.50			1.0	n
13	K	38	m	11.0	11.5	7.6	0	7.62	7.4	0	7.5	+0.50			1.2	+0.50			1.2	n
14	K	33	m	11.5	11.5	7.71	0	7.54	7.5	0	7.43	-3.00			1.2	-3.00			1.2	n
15	K	34	m	12.2	12.2	7.7	0	7.68	7.75	0	7.5	-3.75	-0.50	5	1.0	-1.25	-2.50	170	0.8	n
16	K	28	f	12.0	12.0	7.98	0	7.85	7.97	180	7.78	+0.50			0.8	+0.50			0.8	y
Average		**32**		**11.4**	**11.4**	**7.74**		**7.66**	**7.72**		**7.63**	**-1.12**	**-0.41**		**1.1**	**-0.95**	**-0.93**		**1.1**	
Std. Dev.		**7**		**0.72**	**0.66**	**0.22**		**0.22**	**0.25**		**0.19**	**1.91**	**0.17**		**0.17**	**1.81**	**0.72**		**0.19**	

Table 10.2 Results of CRF 1: Fundamental data, K-readings, spectacle correction and if CL wearer. K = Kaukasian, A = African

ID No	Ext. Eye: Slit Lamp grade 0-4								Tear Men.mm		Ret. spot RE			Ret.spot LE			Keeler NIBUT		Lid tension		Reason for exclusion
	Lids		Lashes		Conj.		Corn.				Y/N		Com. Tail	Y/N		Com.tail	Secs.		Grams		
	R	L	R	L	R	L	R	L	R	L	Sharp	Halo		Sharp	Halo		R	L	R	L	
1	0	0	0	0	0	0	0	0	0.2	0.2	y	n	0	y	n	0	16.4	20.6	5	4	
2	0	0	0	0	0	0	0	0	0.2	0.2	y	n	0	y	n	0	23.5	16.1	7.5	8.5	
3	0	0	0	0	0	0	0	0	0.2	0.2	y	n	0	y	n	0	15.7	13.5	8.6	6	
4	0	0	0	0	0	0	0	0	0.2	0.2	n	n	1	n	n	12	18.9	15.3	6.5	6	
5	0	0	0	0	0	0	0	0	0.2	0.2	n	n	0	n	n	0	20.8	22	3	3	
6	0	0	0	0	0	0	2	2	0.3	0.3	y	n	0	y	n	0	16	14			Epithelial Corneal Dystrophy
7	0	0	0	0	0	0	0	0	0.3	0.3	y	n	0	y	n	0	10	14			VSO38 9,2/14,5 too steep, NIBUT <10 @ L.E.
8	0	0	0	0	0	0	0	0	0.3	0.3	y	n	0	y	n	0	12	9			Test lens diam. 14,5mm too large for subject
9	2	2	0	0	0	0	0	0	0.2	0.2	y	n	0	y	n	0	4	5			Blepharitis, NIBUT <10 sec.
10	0	0	0	0	0	0	0	0	0.1	0.1	y	n	0	y	n	0	9	8			NIBUT <10 secs.
11	0	0	0	0	0	0	0	0	0.2	0.2	y	n	0	y	n	0	9	9			NIBUT <10 secs.
12	0	0	0	0	0	0	0	0	0.1	0.1	y	n	0	y	n	0	20	20	15	15	Upper lid tension far beyond 10g (squeezer)
13	0	0	0	0	0	0	0	0	0.1	0.1	y	n	0	y	n	0	18	17			Unable to participate / time consuming
14	0	0	0	0	0	0	0	0	0.1	0.1	y	n	0	y	n	0	14	18			Unable to participate / time consuming
15	0	0	0	0	0	0	0	0	0.3	0.2	y	n	0	y	n	0					VA on left eye < 1,0; too large corn. Diam.
16	0	0	0	0	0	0	0	0	0.3	0.3	y	n	0	y	n	0	9.9	8.9			VA <1,0, NIBUT < 10 secs.
						Average			**0.2**	**0.2**							**14.5**	**14.0**			
						Std. Dev.			**0.1**	**0.1**							**5.2**	**5.0**			

Table 10.3 Results of CRF1: Exterior part of the eye, Tear meniscus Retinoscopic spot, NIBUT, lid tension, exclusion reasons

10.2 *Results of CRF 2 tests*

Performance

Visual acuity

subject	Lens ID R	Lens ID L	VA with CL and overcorrection											
			VSO38		LM		GM		VSO75		Def.		Average	
			R	L	R	L	R	L	R	L	R	L	R	L
SV	1	2	1.0	1.0	1.0	1.0	1.0	0.8	1.0	1.0	1.0	1.0	1.0	1.0
SV	2	1	1.2	1.0	1.0	1.0	1.0	1.0	1.0	1.0	1.0	1.0	1.0	1.0
SV	3	4	1.0	1.2	1.0	1.0	1.0	1.0	1.0	1.0	1.0	1.0	1.0	1.0
SV	4	3	1.0	1.0	1.0	1.0	1.0	1.0	1.0	1.0	1.0	1.0	1.0	1.0
SV	5	5	1.0	1.0	1.0	1.0	1.0	1.0	1.0	1.0	1.0	1.0	1.0	1.0
KM	1	2	0.8	0.7	1.0	1.0	0.8	1.0	0.8	0.8	1.0	1.0	0.9	0.9
KM	2	1	0.8	0.8	1.0	0.8	1.0	1.0	0.8	0.8	1.0	0.8	0.9	0.8
KM	3	4	0.8	0.8	1.0	0.8	1.0	0.8	0.8	0.8	1.0	0.8	0.9	0.8
KM	4	3	0.8	0.8	1.0	1.0	1.0	1.0	0.8	0.8	1.0	1.0	0.9	0.9
KM	5	5	0.8	0.8	1.0	0.8	0.8	1.0	0.8	0.8	1.0	0.8	0.9	0.8
SE	1	2	1.0	1.0	1.0	1.0	1.0	1.0	1.0	0.8	1.0	1.0	1.0	1.0
SE	2	1	1.0	1.0	1.0	1.2	1.2	1.0	1.0	1.0	1.0	1.2	1.0	1.1
SE	3	4	1.0	1.0	1.0	1.0	1.0	1.0	1.0	1.0	1.0	1.0	1.0	1.0
SE	4	3	1.2	1.2	1.0	1.0	1.0	1.0	1.0	1.0	1.0	1.0	1.0	1.0
SE	5	5	1.0	1.0	1.0	0.8	1.0	1.0	1.0	1.2	0.8	1.0	1.0	1.0
AS	1	2	1.0	1.0	1.0	1.0	1.0	1.0	1.0	1.0	1.0	1.0	1.0	1.0
AS	2	1	1.0	1.0	1.0	1.0	1.0	1.0	1.0	1.0	1.0	1.0	1.0	1.0
AS	3	4	1.0	1.0	1.0	1.0	1.0	1.0	1.0	1.0	1.0	1.0	1.0	1.0
AS	4	3	1.0	1.0	1.0	1.0	1.0	1.0	1.0	1.0	1.0	1.0	1.0	1.0
AS	5	5	1.0	1.0	1.0	1.0	1.0	1.0	1.0	1.0	1.0	1.0	1.0	1.0
KV	1	2	1.0	1.0	1.0	1.0	1.0	1.0	0.8	0.8	1.0	0.8	1.0	0.9
KV	2	1	1.0	1.0	1.0	1.0	1.0	1.2	1.0	1.0	1.0	1.0	1.0	1.0
KV	3	4	1.0	1.0	1.0	1.0	1.0	1.0	1.0	1.0	1.0	1.0	1.0	1.0
KV	4	3	1.0	1.0	1.0	1.0	1.0	1.0	1.0	1.0	1.0	1.0	1.0	1.0
KV	5	5	1.0	1.0	1.0	0.8	1.0	1.0	1.0	0.8	0.7	1.0	0.9	0.9
Average			**0.97**		**0.98**		**0.99**		**0.95**		**0.98**			
SD			**0.11**		**0.07**		**0.07**		**0.10**		**0.08**			

Table 10.4 Visual acuity with soft CL and best overcorrection

Initials	Lens ID R	Lens ID L	VA with CL and overcorrection minus spectacle VA											
			VSO38		LM		GM		VSO75		Def.		Average	
			R	L	R	L	R	L	R	L	R	L	R	L
SV	1	2	0	0	0	0	0	-0.2	0.0	0.0	0.0	0.0	0.0	0.0
SV	2	1	0.2	0	0	0	0	0	0.0	0.0	0.0	0.0	0.0	0.0
SV	3	4	0	0.2	0	0	0	0	0.0	0.0	0.0	0.0	0.0	0.0
SV	4	3	0	0	0	0	0	0	0.0	0.0	0.0	0.0	0.0	0.0
SV	5	5	0	0	0	0	0	0	0.0	0.0	0.0	0.0	0.0	0.0
KM	1	2	-0.2	-0.3	0	0	-0.2	0	-0.2	-0.2	0.0	0.0	-0.1	-0.1
KM	2	1	-0.2	-0.2	0	-0.2	0	0	-0.2	-0.2	0.0	-0.2	-0.1	-0.2
KM	3	4	-0.2	-0.2	0	-0.2	0	-0.2	-0.2	-0.2	0.0	-0.2	-0.1	-0.2
KM	4	3	-0.2	-0.2	0	0	0	0	-0.2	-0.2	0.0	0.0	-0.1	-0.1
KM	5	5	-0.2	-0.2	0	-0.2	-0.2	0	-0.2	-0.2	0.0	-0.2	-0.1	-0.2
SE	1	2	-0.2	-0.2	-0.2	-0.2	-0.2	-0.2	-0.2	-0.4	-0.2	-0.2	-0.2	-0.2
SE	2	1	-0.2	-0.2	-0.2	0	0	-0.2	-0.2	-0.2	-0.2	0.0	-0.2	-0.1
SE	3	4	-0.2	-0.2	-0.2	-0.2	-0.2	-0.2	-0.2	-0.2	-0.2	-0.2	-0.2	-0.2
SE	4	3	0	0	-0.2	-0.2	-0.2	-0.2	-0.2	-0.2	-0.2	-0.2	-0.2	-0.2
SE	5	5	-0.2	-0.2	-0.2	-0.4	-0.2	-0.2	-0.2	0.0	-0.4	-0.2	-0.2	-0.2
AS	1	2	-0.2	-0.2	-0.2	-0.2	-0.2	-0.2	-0.2	-0.2	-0.2	-0.2	-0.2	-0.2
AS	2	1	-0.2	-0.2	-0.2	-0.2	-0.2	-0.2	-0.2	-0.2	-0.2	-0.2	-0.2	-0.2
AS	3	4	-0.2	-0.2	-0.2	-0.2	-0.2	-0.2	-0.2	-0.2	-0.2	-0.2	-0.2	-0.2
AS	4	3	-0.2	-0.2	-0.2	-0.2	-0.2	-0.2	-0.2	-0.2	-0.2	-0.2	-0.2	-0.2
AS	5	5	-0.2	-0.2	-0.2	-0.2	-0.2	-0.2	-0.2	-0.2	-0.2	-0.2	-0.2	-0.2
KV	1	2	0	0	0	0	0	0	-0.2	-0.2	0.0	-0.2	0.0	-0.1
KV	2	1	0	0	0	0	0	0.2	0.0	0.0	0.0	0.0	0.0	0.0
KV	3	4	0	0	0	0	0	0	0.0	0.0	0.0	0.0	0.0	0.0
KV	4	3	0	0	0	0	0	0	0.0	0.0	0.0	0.0	0.0	0.0
KV	5	5	0	0	0	-0.2	0	0	0.0	-0.2	-0.3	0.0	-0.1	-0.1
Average			**-0.10**		**-0.08**		**-0.09**		**-0.13**		**-0.10**			
SD			**0.12**		**0.11**		**0.11**		**0.10**		**0.11**			

Table 10.5 Visual acuity with soft CL and best overcorrection minus best visual acuity with spectacle correction.

Retinoscopic spot appearances

			VSO 38 material RE			VSO 38 material LE		
	Lens ID							
subject	R	L	sharp y/n	Halos y/n	Comet's tail o'clock	sharp y/n	Halos y/n	Comet's tail o'clock
SV	1	2	y	n	0	y	n	0
SV	2	1	y	n	0	y	n	0
SV	3	4	y	n	0	y	n	0
SV	4	3	y	n	0	y	n	0
SV	5	5	y	n	0	y	n	12
KM	1	2	y	n	0	y	n	0
KM	2	1	y	n	0	y	n	0
KM	3	4	y	n	0	y	n	0
KM	4	3	y	n	0	y	n	0
KM	5	5	y	n	0	y	n	0
SE	1	2	y	y	0	y	y	0
SE	2	1	y	n	12	y	n	12
SE	3	4	y	n	5	y	n	0
SE	4	3	y	n	0	y	n	0
SE	5	5	n	n	0	n	y	0
AS	1	2	y	n	0	n	y	0
AS	2	1	n	n	0	n	y	0
AS	3	4	n	n	0	n	y	0
AS	4	3	n	n	0	n	y	0
AS	5	5	n	n	0	n	y	12
KV	1	2	y	n	0	y	n	0
KV	2	1	y	n	0	y	n	0
KV	3	4	y	n	0	y	n	0
KV	4	3	y	n	0	y	n	0
KV	5	5	y	n	0	y	n	0
OK per Material R+L			39	42	45			
Not OK per Material			11	8	0			

Table 10.6 Retinoscopic spot occurrences VSO 38 material

			LM 55 material RE			LM 55 material LE		
	Lens ID							
subject	R	L	sharp y/n	Halos y/n	Comet's tail o'clock	sharp y/n	Halos y/n	Comet's tail o'clock
SV	1	2	y	n	0	y	n	0
SV	2	1	y	n	0	y	n	0
SV	3	4	y	n	0	y	n	0
SV	4	3	y	n	0	y	n	0
SV	5	5	y	n	0	y	n	0
KM	1	2	y	n	0	y	n	0
KM	2	1	y	n	0	y	n	0
KM	3	4	y	n	0	y	n	0
KM	4	3	y	n	0	y	n	0
KM	5	5	y	n	0	y	y	5
SE	1	2	n	y	5	y	y	0
SE	2	1	y	n	0	y	n	0
SE	3	4	y	n	0	y	n	0
SE	4	3	y	n	0	n	n	11
SE	5	5	y	n	0	y	n	4
AS	1	2	y	n	0	y	n	0
AS	2	1	y	n	0	y	n	0
AS	3	4	y	n	0	y	n	0
AS	4	3	y	n	0	y	n	0
AS	5	5	y	n	0	y	n	0
KV	1	2	y	n	0	y	n	0
KV	2	1	y	n	0	y	n	0
KV	3	4	y	n	0	y	n	0
KV	4	3	y	n	0	y	n	0
KV	5	5	n	n	3	y	n	0
OK per Material R+L			47	47	45			
Not OK per Material			3	3	5			

Table 10.7 Retinoscopic spot occurrences LM 55 material

Material			GM3 material RE			GM3 material LE		
	Lens ID							
subject	R	L	sharp y/n	Halos y/n	Comet's tail o'clock	sharp y/n	Halos y/n	Comet's tail o'clock
SV	1	2	y	n	0	y	n	12
SV	2	1	y	n	0	y	n	12
SV	3	4	y	n	0	y	n	0
SV	4	3	y	n	12	y	n	0
SV	5	5	y	n	0	y	n	0
KM	1	2	y	n	0	y	n	0
KM	2	1	y	n	0	y	n	0
KM	3	4	y	n	0	y	n	0
KM	4	3	y	n	0	y	n	0
KM	5	5	y	n	0	y	n	0
SE	1	2	y	n	0	y	n	0
SE	2	1	y	n	0	y	n	0
SE	3	4	y	n	12	y	n	12
SE	4	3	y	n	12	y	n	12
SE	5	5	y	n	11	y	n	0
AS	1	2	y	n	0	y	n	0
AS	2	1	y	n	0	y	n	0
AS	3	4	y	n	0	y	n	0
AS	4	3	y	n	0	y	n	0
AS	5	5	y	n	0	y	n	0
KV	1	2	y	n	0	y	n	0
KV	2	1	y	n	0	y	n	0
KV	3	4	y	n	0	y	n	0
KV	4	3	y	n	0	y	n	0
KV	5	5	y	n	0	y	n	0
OK per Material R+L			50	50	42			
Not OK per Material			0	0	8			

Table 10.8 Retinoscopic spot occurrences GM3 material

Material			VSO 75 material RE			VSO 75 material LE		
	Lens ID							
subject	R	L	sharp y/n	Halos y/n	Comet's tail o'clock	sharp y/n	Halos y/n	Comet's tail o'clock
SV	1	2	y	n	0	y	n	0
SV	2	1	y	n	0	y	n	0
SV	3	4	y	n	0	y	n	0
SV	4	3	y	n	0	y	n	0
SV	5	5	y	n	0	y	n	0
KM	1	2	y	n	0	y	n	0
KM	2	1	y	n	0	y	n	0
KM	3	4	y	n	0	y	n	0
KM	4	3	y	n	0	y	n	0
KM	5	5	y	n	0	y	n	0
SE	1	2	y	n	0	y	n	0
SE	2	1	y	n	0	y	n	0
SE	3	4	y	n	0	y	n	0
SE	4	3	y	n	0	y	n	0
SE	5	5	y	n	0	y	n	0
AS	1	2	y	n	0	y	n	0
AS	2	1	y	n	0	y	n	0
AS	3	4	y	n	0	y	n	0
AS	4	3	y	n	0	y	n	0
AS	5	5	y	n	0	y	n	0
KV	1	2	n	n	2	y	n	0
KV	2	1	y	n	0	y	n	0
KV	3	4	y	n	0	y	n	0
KV	4	3	y	n	0	y	n	0
KV	5	5	y	n	0	y	n	0
OK per Material R+L			49	50	49			
Not OK per Material			1	0	1			

Table 10.9 Retinoscopic spot occurrences VSO 75 material

Material			Definitive material RE			Definitive material LE		
	Lens ID							
subject	R	L	sharp y/n	Halos y/n	Comet's tail o'clock	sharp y/n	Halos y/n	Comet's tail o'clock
SV	1	2	y	n	0	y	n	0
SV	2	1	y	n	0	y	n	0
SV	3	4	y	n	0	y	n	0
SV	4	3	y	n	0	y	n	0
SV	5	5	y	n	0	y	n	0
KM	1	2	y	n	0	y	n	0
KM	2	1	y	n	0	y	n	0
KM	3	4	y	n	0	y	n	0
KM	4	3	y	n	0	y	n	0
KM	5	5	y	n	0	y	y	5
SE	1	2	n	y	5	y	y	0
SE	2	1	y	y	0	n	y	11
SE	3	4	y	n	0	y	n	0
SE	4	3	y	n	0	y	n	0
SE	5	5	y	y	0	y	n	0
AS	1	2	y	n	0	y	n	12
AS	2	1	y	n	0	y	n	0
AS	3	4	y	n	0	y	n	0
AS	4	3	y	n	0	y	n	0
AS	5	5	y	n	0	y	n	0
KV	1	2	y	n	0	y	n	0
KV	2	1	n	n	1	y	n	0
KV	3	4	y	n	0	n	n	2
KV	4	3	n	n	11	y	n	0
KV	5	5	y	n	0	y	n	0
OK per Material R+L			45	44	43			
Not OK per Material			5	6	7			

Table 10.10 Retinoscopic spot occurrences Definitive material

Contrast sensitivity tables

Change to 'Contrast sensitivity with CLs and overcorrection												
	ID	subject	Right eye, field number in line					Left eye field number in line				
			A	B	C	D	E	A	B	C	D	E
VSO38	1	SV	6	6	5	4	3	5	6	5	4	3
	2	KM	5	5	4	2	0	5	6	4	3	1
	3	SV	5	6	5	4	3	5	6	6	4	2
	4	AS	6	6	6	3	2	5	6	5	3	1
	5	KV	6	6	5	3	1	6	6	4	3	1
Average			**5**	**6**	**5**	**3**	**2**	**5**	**6**	**5**	**3**	**2**
SD			**0**	**0**	**1**	**1**	**1**	**0**	**0**	**1**	**1**	**1**
LM	1	SV	5	6	6	4	2	5	7	5	3	3
	2	KM	5	6	4	2	0	5	6	4	2	1
	3	SV	5	6	5	4	4	5	6	5	5	3
	4	AS	5	6	5	3	2	6	6	5	3	2
	5	KV	6	6	5	3	2	6	6	4	2	1
Average			**5**	**6**	**5**	**3**	**2**	**5**	**6**	**5**	**3**	**2**
SD			**0**	**0**	**1**	**1**	**1**	**0**	**0**	**1**	**1**	**1**
GM	1	SV	6	7	6	5	3	6	7	6	4	3
	2	KM	5	6	4	3	0	5	6	4	3	1
	3	SV	5	6	5	5	4	6	6	6	5	4
	4	AS	5	6	6	5	2	6	6	5	5	2
	5	KV	6	6	5	2	1	6	6	4	2	1
Average			**5**	**6**	**5**	**4**	**2**	**6**	**6**	**5**	**4**	**2**
SD			**0**	**0**	**1**	**1**	**1**	**0**	**0**	**1**	**1**	**1**
VSO75	1	SV	6	7	5	5	3	6	6	6	4	2
	2	KM	5	5	4	3	0	5	6	4	3	1
	3	SV	5	6	5	5	4	5	6	5	4	4
	4	AS	5	6	5	5	2	6	6	5	3	2
	5	KV	6	6	5	3	2	6	6	5	3	1
Average			**5**	**6**	**5**	**4**	**2**	**5**	**6**	**5**	**3**	**2**
SD			**0**	**1**	**0**	**1**	**1**	**0**	**0**	**1**	**1**	**1**
Definitive	1	SV	5	6	5	4	3	5	6	5	4	3
	2	KM	5	6	4	2	0	5	6	4	2	1
	3	SV	5	6	5	5	3	5	6	5	3	2
	4	AS	6	6	5	3	2	6	6	5	3	2
	5	KV	5	6	4	2	0	5	5	4	2	0
Average			**5**	**6**	**5**	**3**	**2**	**5**	**6**	**5**	**3**	**2**
SD			**0**	**0**	**1**	**1**	**1**	**0**	**0**	**1**	**1**	**1**

Table 10.11 Contrast sensitivity 30 min. after lens insertion

Contrast sensitivity with and without overcorrection												
			Right eye, field number In line					Left eye field number In line				
	ID	subject	A	B	C	D	E	A	B	C	D	E
VSO38	1	SV	1	0	2	1	2	0	1	0	1	2
	2	KM	1	-3	1	0	0	0	0	0	1	1
	3	SV	0	0	1	0	1	1	1	2	0	-2
	4	AS	2	0	0	-1	0	1	0	-1	-2	-2
	5	KV	2	0	-1	0	-1	1	1	-2	0	-1
Average			**1.0**	**-0.4**	**0.6**	**0.1**	**0.2**	**0.8**	**0.6**	**-0.2**	**-0.1**	**-0.4**
SD			**0.6**	**1.1**	**1.3**	**0.6**	**1.0**	**0.5**	**0.5**	**1.1**	**1.1**	**1.3**
LM	1	SV	0	0	3	1	1	0	2	0	0	2
	2	KM	1	-2	1	0	0	0	0	0	0	1
	3	SV	0	0	1	0	2	1	1	1	1	-1
	4	AS	1	0	-1	-1	0	2	0	-1	-2	-1
	5	KV	2	0	-1	0	0	1	1	-2	-1	-1
Average			**0.8**	**-0.4**	**0.5**	**0.0**	**0.6**	**0.8**	**0.7**	**-0.4**	**-0.3**	**-0.2**
SD			**0.6**	**1.0**	**1.4**	**0.7**	**0.8**	**0.6**	**0.7**	**1.1**	**0.9**	**1.2**
GM	1	SV	1	1	3	2	2	1	2	1	1	2
	2	KM	1	-2	1	1	0	0	0	0	1	1
	3	SV	0	0	1	1	2	2	1	2	1	0
	4	AS	1	0	0	1	0	2	0	-1	0	-1
	5	KV	2	0	-1	-1	-1	1	1	-2	-1	-1
Average			**1.1**	**-0.2**	**0.7**	**0.8**	**0.7**	**1.0**	**0.7**	**0.0**	**0.5**	**0.1**
SD			**0.5**	**0.9**	**1.4**	**1.0**	**1.2**	**0.6**	**0.8**	**1.4**	**0.9**	**1.3**
VSO75	1	SV	1	1	2	2	2	1	1	1	1	1
	2	KM	1	-3	1	1	0	0	0	0	1	1
	3	SV	0	0	1	1	2	1	1	1	0	0
	4	AS	1	0	-1	1	0	2	0	-1	-2	-1
	5	KV	2	0	-1	0	0	1	1	-1	0	-1
Average			**1.0**	**-0.2**	**0.6**	**0.8**	**0.7**	**0.8**	**0.7**	**-0.1**	**-0.1**	**0.1**
SD			**0.6**	**1.2**	**1.2**	**0.6**	**0.9**	**0.5**	**0.5**	**0.9**	**1.1**	**1.1**
Definitive	1	SV	0	0	2	1	2	0	1	0	1	2
	2	KM	1	-2	1	0	0	0	0	0	0	1
	3	SV	0	0	1	1	1	1	1	1	-1	-2
	4	AS	2	0	-1	-1	0	2	0	-1	-2	-1
	5	KV	1	0	-2	-1	-2	0	0	-2	-1	-2
Average			**0.9**	**-0.4**	**0.3**	**-0.1**	**0.3**	**0.7**	**0.6**	**-0.4**	**-0.5**	**-0.3**
SD			**0.6**	**1.0**	**1.5**	**0.6**	**1.2**	**0.7**	**0.5**	**1.0**	**0.9**	**1.3**

Table 10.12 Comparison of contrast sensitivity with CL + overcorrection and spectacle contrast sensitivity

Lens movement in situ results

Vertical movement (mm)				VSO38		LM		GM		VSO75		Definitive	
ID	subject	R	L	R	L	R	L	R	L	R	L	R	L
1	SV	1	2	0.5	0.8	0.4	0.3	0.1	0.0	0.6	1.0	0.0	0.2
1	SV	2	1	1.8	1.3	0.0	0.1	0.0	0.5	2.5	0.5	0.5	0.5
1	SV	3	4	0.7	1.5	0.2	0.5	0.0	0.5	1.5	1.0	0.5	0.1
1	SV	4	3	0.7	1.0	0.2	0.5	0.3	0.2	1.4	0.2	0.0	0.5
1	SV	5	5	0.1	1.0	0.1	0.6	n	n	0.5	1.3	0.2	0.1
2	KM	1	2	0.0	0.4	2.3	2.2	1.5	0.3	0.3	0.2	2.3	2.2
2	KM	2	1	0.2	0.6	0.3	0.1	0.0	0.1	0.0	0.2	0.3	0.1
2	KM	3	4	0.2	0.4	0.1	0.1	1.2	0.2	0.2	0.1	0.1	0.1
2	KM	4	3	0.0	0.1	0.1	2.0	0.0	0.1	0.6	0.4	0.1	2.0
2	KM	5	5	0.3	0.1	0.1	2.2	0.5	0.1	0.3	0.0	0.1	2.2
3	SE	1	2	0.1	0.4	0.1	0.0	0.2	0.1	0.2	0.0	0.1	0.0
3	SE	2	1	0.1	0.2	0.0	1.0	0.1	0.2	0.2	1.3	0.0	0.2
3	SE	3	4	0.4	0.5	0.1	0.5	0.2	0.1	0.2	0.4	0.2	0.5
3	SE	4	3	0.1	0.2	1.1	0.5	0.0	0.6	0.5	0.8	0.1	0.1
3	SE	5	5	0.2	0.4	0.5	0.5	n	n	n	n	0.2	0.5
4	AS	1	2	0.0	0.3	0.2	0.7	0.0	0.6	0.5	1.6	0.4	0.5
4	AS	2	1	0.7	2.2	0.8	0.3	1.7	0.3	0.1	0.4	0.6	0.6
4	AS	3	4	0.9	0.5	0.0	0.4	0.3	1.6	0.8	0.0	0.8	0.4
4	AS	4	3	0.2	1.0	0.1	0.0	1.3	4.6	0.8	3.0	0.0	0.0
4	AS	5	5	1.3	1.4	0.3	0.2	l	1.0	1.2	2.3	0.0	0.6
5	KV	1	2	0.1	0.2	1.5	0.5	0.4	0.1	0.2	0.5	0.6	0.1
5	KV	2	1	1.2	0.2	0.1	0.3	0.3	0.2	0.1	0.1	0.0	0.3
5	KV	3	4	0.5	0.1	0.7	0.2	0.2	0.1	0.5	0.2	0.1	0.1
5	KV	4	3	0.5	0.5	1.4	0.5	0.2	0.2	0.5	0.2	0.1	0.1
5	KV	5	5	0.1	0.1	0.0	0.2	0.5	0.2	0.0	0.1	0.1	0.1
		Average		0.5		0.5		0.5		0.6		0.4	
		SD		0.5		0.6		0.8		0.7		0.6	
		Median		**0.4**		**0.3**		**0.2**		**0.4**		**0.1**	
		MAD		**0.4**		**0.4**		**0.4**		**0.5**		**0.4**	

Table 10.13 Soft lens friction by measuring lens movement between blinks

subject	VSO38 per subject				LM per subject				GM per subject			
	Av.	SD	Med.	MAD	Av.	SD	Med.	MAD	Av.	SD	Med.	MAD
SV	0.94	0.47	0.90	0.38	0.27	0.18	0.25	0.15	0.20	0.20	0.15	0.18
KM	0.23	0.19	0.18	0.16	0.33	0.24	0.20	0.21	0.40	0.50	0.15	0.40
SE	0.26	0.14	0.20	0.13	0.17	0.18	0.10	0.13	0.19	0.17	0.15	0.11
AS	0.85	0.63	0.80	0.51	0.30	0.26	0.25	0.20	1.47	1.54	1.10	1.17
KV	0.35	0.33	0.20	0.26	0.54	0.50	0.40	0.40	0.24	0.12	0.20	0.10

Table 10.14 Average, SD, median and MAD for VSO 38, LM55 and GM3 materials.

subject	VSO75 per subject				Definitive per subject			
	Av.	SD	Med.	MAD	Av.	SD	Med.	MAD
SV	1.08	0.68	1.00	0.54	0.31	0.20	0.35	0.19
KM	0.26	0.16	0.20	0.13	0.95	1.00	0.20	0.98
SE	0.45	0.39	0.30	0.31	0.19	0.17	0.15	0.13
AS	1.07	0.92	0.80	0.76	0.39	0.28	0.45	0.23
KV	0.24	0.18	0.20	0.16	0.20	0.20	0.10	0.17

Table 10.15 Average, SD, median and median absolute deviation for VSO75 and Definitive materials.

Movement/Lid force (N)							
subject	Def.	GM	LM	V38	V75	Average	SD
SV	5.78	4.53	6.57	21.30	23.68	12.37	8.32
KM	12.11	5.10	12.11	2.87	2.93	7.02	4.23
SE	2.65	2.62	6.01	3.63	6.29	4.24	1.60
AS	6.36	20.67	4.81	13.87	17.46	12.63	6.16
KV	3.82	8.16	18.35	11.90	8.16	10.08	4.86
Average	6.15	8.21	9.57	10.71	11.70		
SD	3.27	6.47	5.06	6.86	7.69		

Table 10.16 Ratio between lid force and lens movement after blink

Vertical travel (mm)	Frequency count					N
	V38	LM	GM	V75	Def.	
0	3	6	7	5	8	29
0.1	10	11	9	5	17	52
0.2	8	6	10	10	5	39
0.3	2	5	5	2	2	16
0.4	5	2	1	3	2	13
0.5	6	8	4	7	7	32
0.6	1	1	2	2	4	10
0.7	3	2	0	0	0	5
0.8	0	0	0	0	0	0
0.9	1	1	0	3	1	6
1	1	0	0	0	0	1
1.1	3	1	1	2	0	7
1.2	1	1	1	1	0	4
1.3	2	0	1	2	0	5
1.4	1	1	0	1	0	3
1.5	1	1	1	1	0	4
1.6	0	0	1	1	0	2
1.7	0	0	1	0	0	1
1.8	1	0	0	0	0	1
1.9	0	0	0	0	0	0
2	0	1	0	0	1	2
2.1	0	0	0	0	0	0
2.2	1	2	0	0	2	5
2.3	0	1	0	1	1	3
2.4	0	0	0	0	0	0

Table 10.17 Prevalence of vertical travel in 0.1mm increments after blink

Push up test(PUT)

Push up test results											
		VSO38		LM		GM		VSO75		Def.	
ID	subject	R	L	R	L	R	L	R	L	R	L
1	SV	n	n	n	n	n	n	n	l	n	n
1	SV	l	l	n	n	n	n	l	n	n	n
1	SV	n	l	n	n	n	n	l	l	n	n
1	SV	n	l	n	n	n	n	l	n	n	n
1	SV	n	l	n	n	-	-	n	l	n	n
2	KM	n	n	l	l	n	n	n	n	l	l
2	KM	n	n	n	n	n	n	n	n	n	n
2	KM	n	n	n	n	l	n	n	n	n	n
2	KM	n	n	n	n	n	n	n	n	n	n
2	KM	n	n	n	l	n	n	n	n	n	l
3	SE	n	n	n	n	n	n	n	n	n	n
3	SE	n	n	n	l	n	n	n	l	n	n
3	SE	n	n	n	n	n	n	n	n	n	n
3	SE	n	n	l	n	n	n	n	n	n	n
3	SE	n	n	n	n	-	-	-	-	n	n
4	AS	n	n	n	n	n	n	n	l	n	n
4	AS	n	n	n	n	l	n	n	n	n	n
4	AS	n	n	n	n	n	l	n	n	n	n
4	AS	n	n	n	n	l	l	n	n	n	n
4	AS	l	l	n	n	l	n	l	l	n	n
5	KV	n	n	n	n	n	n	n	n	n	n
5	KV	l	n	n	n	n	n	n	n	n	n
5	KV	n	n	n	n	n	n	n	n	n	n
5	KV	n	n	l	n	n	n	n	n	n	n
5	KV	n	n	n	n	n	n	n	n	n	n
Total per material		VSO38		LM		GM		VSO75		Def.	
Normal		42	0	44	0	40	0	38	0	47	0
Loose		8	0	6	0	6	0	10	0	3	0
n/a		0	0	0	0	4	0	2	0	0	0

Table 10.18 Results of push up tests where n = normal and l = loose.

Chapter 11 - Annexes

11.1 *Annex A- The influence of scleral shape in relation to the Back Optic Zone Radius of a monocurve contact lens*

In recent literature different scleral radii were reported. Scleral radii ranged from 7.5 to 312.5 mm (Hall et al., 2011) and 13.3 to 14.3 mm (Tiffany et al., 2004). It is known, that the shape of the junction between cornea and sclera, the limbus differs from eye to eye.

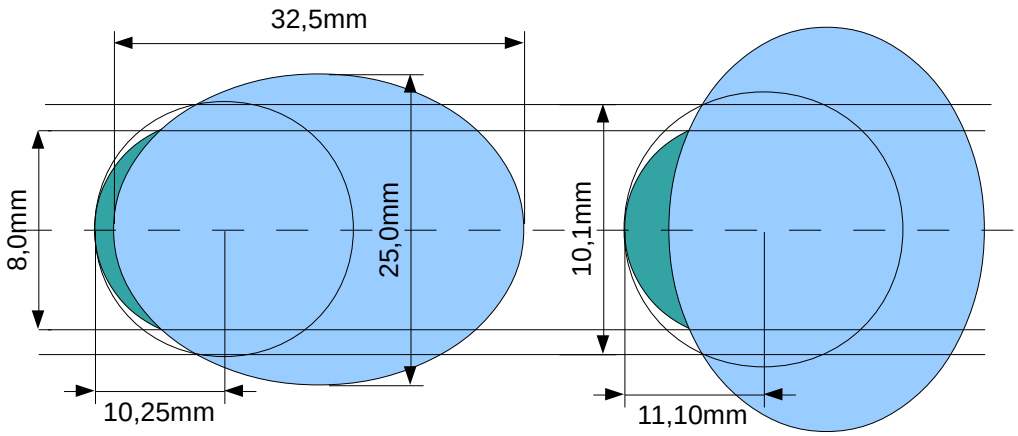

Figure 11.1 The influence of scleral shape in relation to the BOZR of a monocurve contact lens

The sketches attempt to demonstrate that the shape of the scleral part of the eye has limited influence to the theoretical shape of a contact lens as long the corneal parameters, i.e. keratometer readings and corneal diameter do not change even when the scleral part of the area involved differs dramatically. The blue coloured ellipses represent the scleral part of the eye, the smaller light green partial visible circles represent the corneas and the transparent circles simulate the overall radius touching the apex of the corneas and simulate the BOZR of a monocurve contact lens. The apical radius related to the prolate area of the ellipse would be 19.2mm while the apical radius related to the oblate part of the ellipse would be 42.2mm[27]. Geometric

[27] Note: Relates to different shapes only and does not represent an eye or contact lens in reality. The sketches have been drawn to scale but not calculated and try to demonstrate the relationships only.

fundamentals alter the sagittal depth in the presented model. It is well known and described in section 1.2 Cornea and Sclera that a corneal diameter might vary from 10 to 13mm. It also is obvious that the two extreme ovals cause extreme different sagittal heights for the corneal segment. However, in nature, neither such differences in scleral shape probably will appear. The drawn sketches show a difference from 10.25mm to 11.1 mm in theoretical BOZR. For calculations the overall axial length of an eye is determined with 24mm. A numerical eccentricity of $\varepsilon = 0.4$ is can be used to calculate the radius of the scleral part of the eye.

11.2 *Annex B- Patient information and consent form*

This study is designed to assess how contact lenses made from different materials rotate when in normal use. The lenses are designed to fit your individual eye and be comfortable. To this end it will be necessary to try various trial lenses in your eye in order to arrive at the correct end point. Some will be made from a rigid material and some from a soft material. The investigator may choose to use a local anaesthetic; the effect of this only lasts 20 mins. Some coloured dyes are used to assess the fit of the lenses – these are not permanent.

The lens materials used are in everyday use for contact lenses and are NOT 'experimental' in any way. Lenses will have been sterilised before being inserted.

The movement of the lenses is recorded with a camera and the pictures taken only record the area of your eye and the contact lens. You cannot be identified from the film.

If any of the data collected is used in any publication, you will only be identified by a code number. No names will be used.

The risks to your eyes are very minimal. They are the same, or less, than those found with the normal daily wear of contact lenses due to the short time they are in the eye. In the unlikely event of any serious event affecting your eyes you will be referred immediately to an ophthalmologist at no cost to yourself.

You now have the opportunity to ask the investigator any questions about the study or have any aspects explained in more detail. If you are agreeable to taking part, please sign the form below.

I,……(PRINT NAME)

have read the above and have had the opportunity to ask questions about the study. I understand that I can withdraw from the study at any time.

Signed……..Date……

Witness

(investigator)……..(signed)……(date)

1. **Safeguard or precautions**

   - Equipment and material will be used according to medical device regulations.
   - Subjects will be under permanent control and supervision during the test by the investigator.

2. **Statement of the findings of any risk analysis undertaken with regard to the subject's safety and well-being.**

   The contact lenses used in this study are standard contact lenses classified as Class 2a Medical devices. Risk assessment for medical devices, i.e. for contact lenses in for the use by the public have to be judged as follows:

   a. **Hazards in conjunction with Energy**, such as electrical energy, radiation,
   b. **Biological hazards and contributory factors,** such as Bio(in)compatibility, faulty dispensing, faulty formulation, toxicity, allergenicity re/cross infection, impossibility to maintain hygiene,
   c. **Environmental hazards** such as incompatibility with other products possibly used in conjunction with the tested product
   d. **Hazards related to the use of the medical device and accompanying factors,** such as insufficient specification of medical device accessories, insufficient specification for testing prior to use, insufficient warning against possible hazards, incorrect measurements or other metrological aspects, misinterpretation of results, incompatibility of consumables, accessories or other medical devices, insufficient packing, faulty reuse, **Have to be judged as unimaginable**.
   e. **Environmental hazards** such as possible use outside the prescribed environmental conditions, accidental mechanical damage, insufficient labelling insufficient user manual or warnings, insufficient warning of side effects, hazards caused by functional failure, service, insufficient performance for the proposed use, missing or insufficient specifications for service insufficient service, loss of mechanical integrity, loss of functionality as result of reuse

      Have to be judged as a "so insignificant as reasonably practicably minor, unlikely occurring" hazard.

With regard to the proposed research the possible hazards mentioned under "e." do have to be judged as unimaginable, because the subjects are under constant control of the investigator who is not only a registered optometrist but has over 30 years of experience in the contact lens field. The contact lenses used for the tests only will be used once at a single eye and not be inserted into other subjects' eyes.

It has to be assumed that there is less risk for the persons participating at the research compared to a normal contact lens user.

3. Analysis of results

Parametric and non-parametric methods will be applied where necessary.

11.3 *Annex C- Clinical record forms 1-3*[28]

Clinical Record Form 1

Code	Name

xterior Part of the eye Slit Lamp grading (0-4

	Lids	Lashes	Conjunctiva
R:			
L:			

Tear meniscus lower lid (mm)	
R:	
L:	

Keratometer

	1. Meridian	Axis	2. Meridian	Axis
R:				
L:				

Prescription

	Sph.	cyl.	Axis	VA
R:				
L:				

Entoptic phenomena of retinoscopic spot from Chart Projector

	Ret. Spot w. corr.	Sharp edge (y/n)	Halos (y/n)	Comets tail (clock direction) 0=none
R:				
L:				

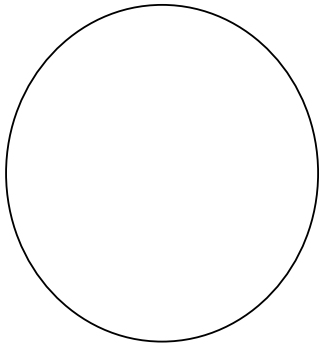

Corn. staining, scars, opacities etc.Right

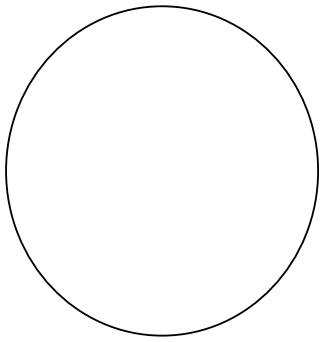

Corn. staining, scars, opacities etc.Left

Contrast test sensivity with Ginsburg Functional Acuity Contrast Test Charts

Line	Number of field in line read				
	A	B	C	D	E
R:					
L:					

Tear breakup time with Keeler TearScope non		Tear meniscus (mm) lower lid		Upper lid tension 0-10g or 11 is >10g	
R:		R:		R:	
L:		L:		L:	

Table 11.1Clinical Record Form 1 (CRF 1)

Clinical record form 2 page 1

[28] Note: The copies of the record forms are reduced size hardcopies from the original leaflets. The originals do not consist of the required spacing and binding edges.

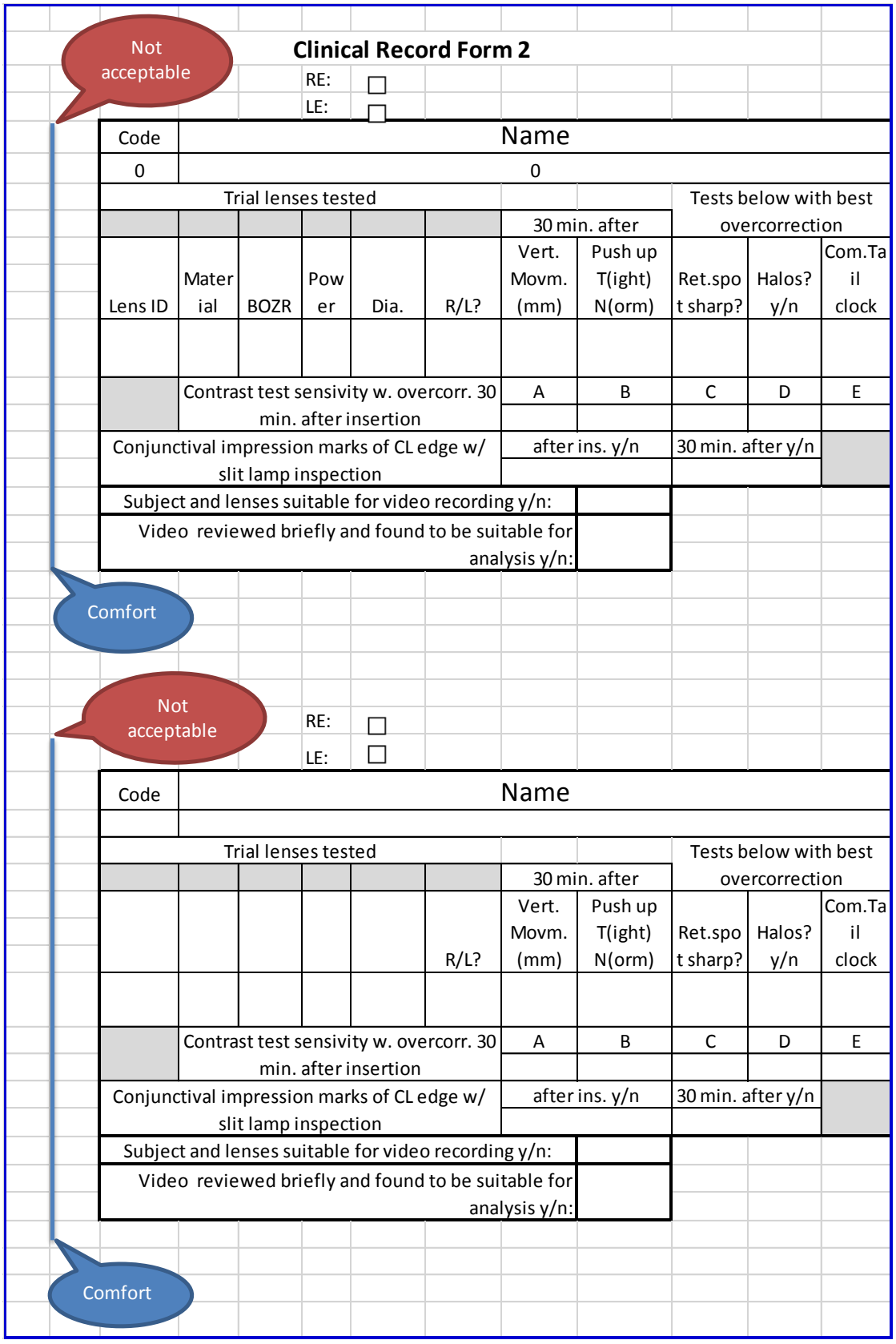

Table 11.2 Clinical record Form 2 page 1 (CRF2)

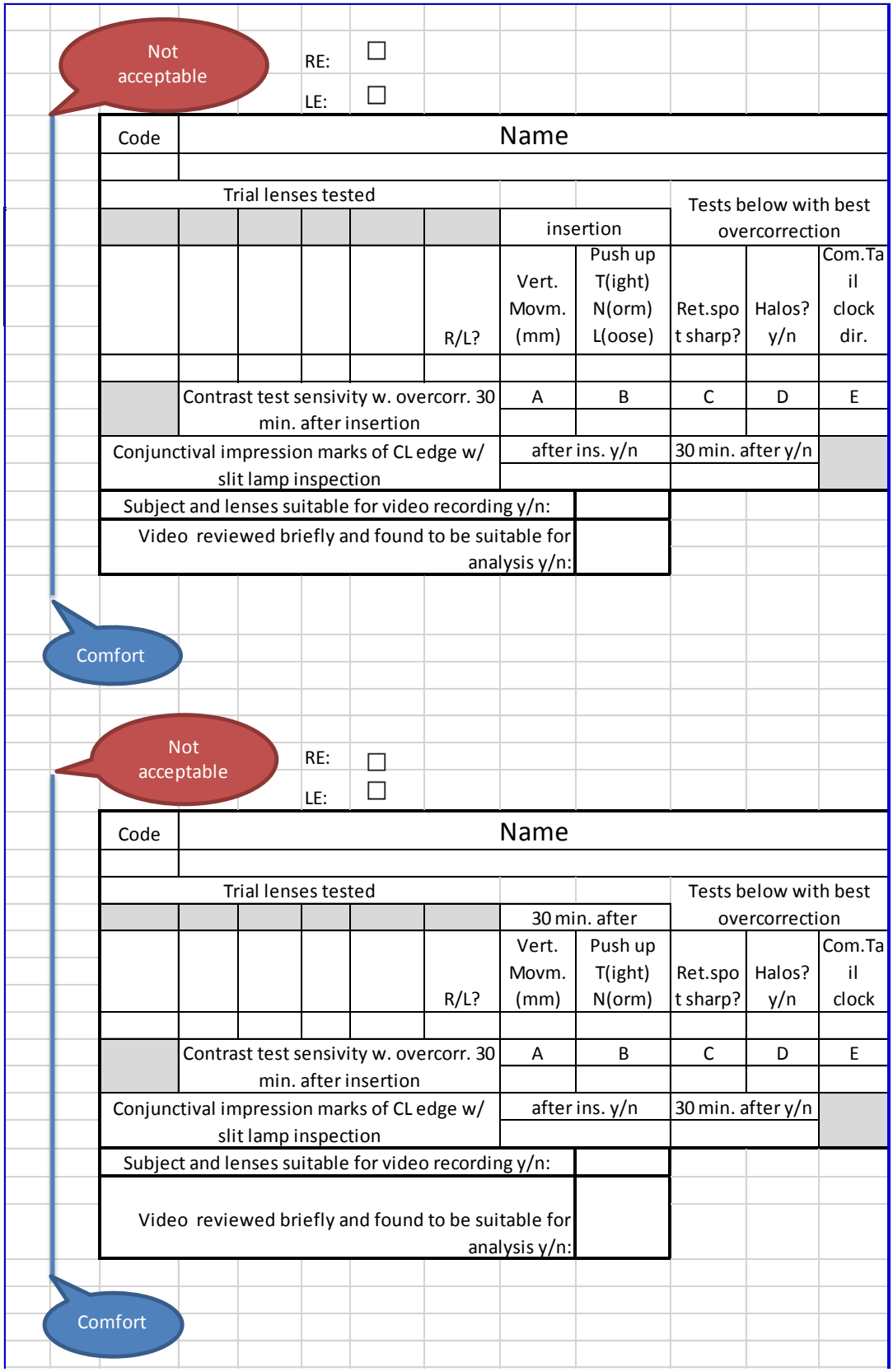

Table 11.3Clinical record form Page 2

Clinical record form 2

Clinical Record Form 3			
Code	Name		
1			
After lenses have been removed			
Slit lamp examination			
	Cornea	Conjunctiva	Fluorescein staining
R:			
L:			
Best corrected visual acuity			
R:			
L:			
Medical referral required (y/n			
If, YES, give details of adverse event and action provided for remedial treatment and management			

Table 11.4 Clinical record Form 3 (CRF3)

Chapter 12 - References

Abel, P. & Thiele, W. (eds.) 1968. *Handbuch der Optometrie Band VI, Kontaktlinsen, III Praktische Grundlagen, Die Anpassung bifokaler Kontaktlinsen,* Heidelberg: Median Verlag Heidelberg.

Ahmad, F., Raza, M. R., Rani, A. M. A. & Lo, S. H. J. 2011. Wear Properties of Alumina Particles Reinforced Aluminium Alloy Matrix Composite. *Journal of Applied Sciences,* 11**,** 1673-1677.

Allergan. 2012. *Refresh Celluvisc* [Online]. Irvine. Available: http://www.refreshbrand.com/html/practitioner/products.asp.

Amonton, G. 1699. De la Resistance Caussée Dans les machines. *Proc. French R. Acad. Sci. A* [Online], 12. Available: http://gallica.bnf.fr/ark:/12148/bpt6k35013/f1.image.langEN.

Anderson, D. & Kojima, R. 2007. Understanding and Applying Corneal Topography. (cover story). *Review of Cornea & Contact Lenses***,** 22-27.

Andre, M., Davies, J. & Caroline, P. J. 2001. A New Approach to Fitting Soft Contact Lenses. *Eyewitness,* 4th Quater**,** 1-4.

Arzneibuch, Ö. 1991. Wien: Verlag der Österreichischen Staatsdruckerei.

Atchison, D. A., Jones, C. E., Schmid, K. L., Pritchard, N., Pope, J. M., Strugnell, W. E. & Riley, R. A. 2004. Eye Shape in Emmetropia and Myopia. *Investigative Ophthalmology & Visual Science,* 45**,** 3380-3386.

Augustin, A. J. (ed.) 2007. *Augenheilkunde,* Berlin: Springer.

Aulhorn, E. 1977. Entoptische Erscheinungen, Fotopsien und „Augenflimmern". *In:* PAU, H. (ed.) *Therapie in der Augenheilkunde.* Springer Berlin Heidelberg.

Axel, P. T. S. 2009. *Measuring Rubber and Plastic Friction for Analysis* [Online]. Available: www.axelproducts.com. [Accessed 20.11.2010 2010].

Bailey, M. D., Walline, J. J., Mitchell, G. L. & Zadnik, K. 2001. Visual acuity in contact lens wearers. *Optometry and vision science,* 78**,** 726-731.

Baron, H. & Ebel, J. (eds.) 2008. *Kontaktlinsen,* Heidelberg: DOZ Verlag.

Bartz, W. J. (ed.) 1988. *Handbuch der Tribologie und der Schmierungstechnik,* D-71272 Renningen: Expert Verlag.

Bausch & Lomb. 2015. *SilSoft and Silsoft Super Plus Contact Lenses* [Online]. Internet: Bausch and Lomb. Available: http://www.bausch.com/our-products/contact-lenses/lenses-for-cataract-patients/silsoft-and-silsoft-super-contact-lenses#.VLVC-yuG98F [Accessed 01/15 2015].

Bcla. 2011. *Contact Lens Adherence* [Online]. Available: http://www.bcla.org.uk/en/post-conference-section/photographic-competition/2011-photographic-entries.cfm/contact-lens-adherence 2012].

Beardmore, R. 2010. *Roymech* [Online]. Available: http://roymech.co.uk/Useful_Tables/Tribology/co_of_frict.htm [Accessed 08.12.2010 2010].

Benz, B., Lesjak, G. & Seira, P. 2008. Messung der Gesamtscheiteltiefe von Austausch-Kontaktlinsen. *Deutsche Optikerzeitung,* 5**,** 92-95.

Besdo, D., Heimann, B., Klüppel, D. M., Kröger, M., Wriggers, P. & Nackenhorst, U. (eds.) 2010. *Elastomere Friction,* Berlin: Springer.

Blausen.Com, S. 2014. *Blausen gallery 2014* [Online]. Available: https://en.wikiversity.org/wiki/Wikiversity_Journal_of_Medicine/Blausen_gallery_2014 [Accessed 15.03.2015 2015].

Bourassa, S. & Benjamin, W. J. 1989. Clinical findings correlated with contact angles on rigid gas permeable contact lens surfaces in vivo. *Optometry-Journal of the American Optometric Association,* 60**,** 584-590.
Bowden, F., P., & Tabor, D. (eds.) 1950. *The Friction and Lubrication of Solids*: Oxford University Press.
Bowden, T. J. (ed.) 2009. *Contact Lenses The Story*: Bower House Publications.
Boxer Wachler, B. S., Phillips, C. L., Schanzlin, D. J. & Krueger, R. R. 1999. Comparison of Contrast Sensitivity in Different Soft Contact Lenses and Spectacles. *Eye & Contact Lens,* 25**,** 48-51.
Brinckmann, P., Frobin, W. & Leivseth, G. (eds.) 2000. *Orthopädische Biomechanik,* Stuttgart: Georg Thieme Verlag.
Brujic, M. & Miller, J. 2010. Confront contact lens discomfort. *Review of Cornea & Contact Lenses,* - 147**,** 10 - 11.
Bürki, E. (ed.) 1991. *Augenaerztliche Kontaktlinsenanpassung,* Stuttgart: Ferdinand Enke Verlag.
Bürki, E. 2008. *USAN-Klassierung der Kontaktlinsenmaterialien (ISO 18369-1)* [Online]. Thun. Available: www.augenaerzte-thun.ch/pdf/aerzteinfo/softlens1.pdf [Accessed 2.2.2010.
Bussacker, H. 1974. Einfluss der Randgestaltung auf die Verträglichkeit von Corneallinsen. *Die Kontaktlinse,* 8**,** 4-13.
Caravia, L., Dowson, D. & Fisher, J. 1993. Start up and steady state friction of thin polyurethane layers. *Wear,* 160**,** 191-197.
Cimbala, J. M. 2012. *Fluid Mechanics Electronic Learning Supplement* [Online]. Available: http://www.mne.psu.edu/cimbala/Learning/Fluid/Fluid_Prop/fluid_property.htm [Accessed 12.3.2013 2013].
Contamac, L. 2008. *Introducing Definitive - The Latheable Lilicone Hydrogel* [Online]. Germany. Available: http://www.gclabsite.com/index.php/hotnews/item/introducing-efinitivem-the-lathable-silicone-hydrogel/ [Accessed 13/01/2015 2015].
Cox, I. 1995. Effect of base curve, power, and center thickness on visual acuity with thin, low-water hydrogel lenses. *International Contact Lens Clinic,* 22**,** 124-130.
Croma, P. 2012. *Hylo Commod Augentropfen* [Online]. Available: http://www.croma.at/en/cromaproducts/ophthalmology/products/dry-eye-range/hylo-comod-eye-drops.
Cui, L., Shen, M., Wang, M. R. & Wang, J. 2012. Micrometer-Scale Contact Lens Movements Imaged by Ultrahigh-resolution Optical Coherence Tomography. *American Journal of Ophthalmology,* 153**,** 275-283.e1.
Da Cruz, A. 2012. *Photo Filtre* [Online]. Available: http://www.photofiltre.com/.
Damms, T. & Guzek, B. 2014. Kurzlehrbuch der Augenheilkunde. 1 ed.: Elsevier GmbH., Urban & Fischer Verlag, München.
Deladi, E. 2006. *STATIC FRICTION IN RUBBER-METAL CONTACTS WITH APPLICATION TO RUBBER PAD FORMING PROCESSES.* PhD Dissertation, University of Twente.
Deutsches Institut Für Kautschuktechnologie, E. V. 2004. Einfluss von Grenzflächentopographie und -chemie

auf die Reibeigenschaften elastomerer Werkstoffe. *In:* KLÜPPEL, D. M. (ed.). Deutsches Institut für Kautschuktechnologie e. V.: Deutsches Institut für Kautschuktechnologie e. V.
Dolder, R. & Skinner, F., S. (eds.) 1983. *Ophthalmika,* Stuttgart: Wissenschaftliche Verlagsgesellschaft m.b.H.
Domininghaus, H. 2007. *Kunststoffe: Eigenschaften und Anwendungen*, Springer-Verlag.
Dong, J. & Haugsted, G. D. 2011. Tribology study of PVA contact lens in ionic aqueous environments Available: http://www.charfac.umn.edu/polymerspm/PubImages/Poly05/Poly05.pdf [Accessed 4.12.2011].
Drake, R. L., Vogl, W. & Mitchell, A. W. M. (eds.) 2007. *Gray's Anatomie für Studenten,* München & Jena: Urban & Fischer.
Du Pont, D. N. 2013. *Delrin Acetal resin* [Online]. Available: http://plastics.dupont.com/plastics/pdflit/europe/delrin/DELLWLFe.pdf.
Dua, H. S., Faraj, L. A., Said, D. G., Gray, T. & Lowe, J. 2013. Human Corneal Anatomy Redefined: A Novel Pre-Descemet's Layer (Dua's Layer). *Ophthalmology,* 120**,** 1778-1785.
Dunn, A., Cobb, J., Kantzios, A., Lee, S., Sarntinoranont, M., Tran-Son-Tay, R. & Sawyer, W. G. 2008. Friction Coefficient Measurement of Hydrogel Materials on Living Epithelial Cells. *Tribology Letters,* 30**,** 13-19.
Dunn, A., Urueña, J., Huo, Y., Perry, S., Angelini, T. & Sawyer, W. G. 2013a. Lubricity of Surface Hydrogel Layers. *Tribology Letters,* 49**,** 371-378.
Dunn, A. C., Tichy, J. A., Urueña, J. M. & Sawyer, W. G. 2013b. Lubrication regimes in contact lens wear during a blink. *Tribology International,* 63**,** 45-50.
Dupont 1996. Fluoropolymer Resin Properties Handbook. DuPont, Fayetteville, NC.
Ebatco 2012. Friction Measurements. 7127 Shady Oak Road, Eden Prairie, MN 55344, U.S.A.: Exponential_Business_and_Technologies_Company.
Edrington, T. B. 2011. A literature review: The impact of rotational stabilization methods on toric soft contact lens performance. *Contact Lens and Anterior Eye,* 34**,** 104-110.
Efron, N. 2002. Contact Lens Practice. Butterworth Heinemann.
Efron, N., Brennan, N. A., Currie, J. M., Fitzgerald, J. P. & Hughes, M. T. 1986. Determinants of the initial comfort of hydrogel contact lenses. *American journal of optometry and physiological optics,* 63**,** 819-823.
Ehrmann, K., Francis, I. & Stapleton, F. 2001. A novel instrument to quantify the tension of upper and lower eyelids. *Contact Lens and Anterior Eye,* 24**,** 65-72.
Eiden, B. & Schnider, C. 1996. Adherence of Daily Wear RGP Contact Lenses. *Contact Lens Spectrum***,** 1-5.
Elert, G. 2004. *Coefficients of Friction for Teflon* [Online]. Available: http://hypertextbook.com/facts/2004/GarvinTam.shtml [Accessed 20.11.2010 2010].
Engineers Edge, L. 2010. *Coefficients of Friction* [Online]. Available: http://www.engineersedge.com/coeffients_of_friction.htm [Accessed 16.11.2011 2011].
Epstein, A. & Stone, R. 2010. Surface and polymer chemistry: the quest for comfort. *Review of Cornea and Contact Lenses,* 147**,** 15-19.

Epstein, A. B. & Freedman, J. M. 2003. The Four Cs for Preventing Contact Lens Dropout. *Review of Optometry,* 1401:03**,** 1-4.
European Directorate for the Quality of Medicines & Healthcare 1986. European Pharmacopoeia. Strassbourg: EDQM Council of Europe.
Feyzullahoglu, E. & Nehir, S. 2011. The tribological behaviours of aluminium-based materials under dry sliding. *Industrial Lubrication and Tribology,* 63**,** 350-358.
Fick, E. A. 1888. Eine Contactbrille. *Archiv fuer Augenheilkunde,* 18.
Fink, W., Frohn, A., Schiefer, U., Schmid, E., W., Wendelstein, N. & Zrenner, E. 1996. Visuelle Abbildung bei hohen Ametropien. *Klinische Monatsblätter für Augenheilkunde***,** 472-475.
Fonn, D., Situ, P. & Simpson, T. 1999. Hydrogel Lens Dehydration and Subjective Comfort and Dryness Ratings in Symptomatic and Asymptomatic Contact Lens Wearers. *Optometry & Vision Science,* 76.
Forst, G. 1981. Wie hängt die Beweglichkeit einer Kontaktlinse von der Form ihrer Rückfläche ab. *Deutsche Optikerzeitung,* 1**,** 6.
Fowler, M. 2007. *Lectures on Fluids* [Online]. Available: http://galileo.phys.virginia.edu/classes/152.mf1i.spring02/Viscosity.htm [Accessed 12.12.2009 2009].
Funke, F. 2004. *Vergleich Visueller Analogskalen mit Kategorialskalen in Offline- und Onlinedesign.* Magisterarbeit. Kassel: Justus-Liebig-Universität Gießen 2004.(http://bit. ly/Y4OekR [Stand: 21.06. 2013, 21: 35 Uhr]).
Gagla, P. 2010. *Image Grab* [Online]. Available: http://www.chip.de/downloads/ImageGrab_32892154.html [Accessed 14.08.2012 2012].
Galifa, C. A. 2006. Ablagerungen an Contactlinsen – Erkennen und vermeiden. *Galifa News* 1-4.
Garzino-Demo, G. A. & Lama, F. L. 1995. Friction and wear of metallic and non-metallic surfaces. *Surface and Coatings Technology,* 76–77, Part 2**,** 487-493.
Gasson, A. 2008. *Contact Lens History* [Online]. London. Available: http://www.andrewgasson.co.uk/opioneers_wichterle.htm [Accessed 6.4.2009 2009].
Gasson, A. & Morris, J. 1992. *The contact lens manual : a practical fitting guide*, Butterworth-Heinemann (1992).
Gaylord, N. G. 1977. *Method for correcting Visual Defects, Co9positions and articles of Manufacture useful therein*. USA patent application.
Ginsburg, A. 1988. *Introduction to Contrast Sensivity* [Online]. Dayton. Available: http://www.agingeye.net/cataract/Vistech2.pdf 1988].
Ginsburg, A. P. 1984. A new contrast sensitivity vision test chart. *Am J Optom Physiol Opt,* 61**,** 403-7.
Gitis, N. 2004. Tribometrological Studies In Bioengineering. Proceedings of the 2004 SEM X International Congress and Exposition on Experimental and Applied Mechanics, 2004 Costa Mesa California, USA. 1-11.
Gitis, N. V. & Volpe, L. 1992. Nature of static friction time dependence. *Journal of Physics and Applied Physics,* 25**,** 605-612.
Golding, T. R., Bruce, A. S., Gaterell, L. L., Little, S. A. & Macnamara, J. 1995a. Soft lens movement: effect of blink rate on lens settling. *Acta ophthalmologica Scandinavica,* 73**,** 506-511.

Golding, T. R., Harris, M. G., Smith, R. C. & Brennan, N. A. 1995b. Soft lens movement: effects of humidity and hypertonic saline on lens settling. *Acta Ophthalmol Scand,* 73**,** 139-44.
Gong, J., Iwasaki, G. K. & Osada, Y. 2000. Surface dynamic friction of polymer gels. *高分子科学,* 18**,** 271-275.
Gong, J., Ping 2006. Friction and lubrication of hydrogels-its richness and complexity. *Soft Matter,* 2**,** 544-552.
Gong, J. P., Kagata, G., Iwasaki, Y. & Osada, Y. 2001. Surface friction of polymer gels: 1. Effect of interfacial interaction. *Wear,* 251**,** 1183-1187.
Gong, J. P. & Osada, Y. 1998. Gel friction: a model based on surface repulsion and adsorption. *The Journal of chemical physics,* 109**,** 8062-8068.
González-Méijome, J. M., López-Alemany, A., Almeida, J. B. & Parafita, M. A. 2009. Surface AFM microscopy of unworn and worn samples of silicone hydrogel contact lenses. *Journal of Biomedical Materials Research Part B: Applied Biomaterials,* 88B**,** 75-82.
Gould, D., Kelly, D., Goldstone, L. & Gammon, J. 2001. Examining the validity of pressure ulcer risk assessment scales: developing and using illustrated patient simulations to collect the data INFORMATION POINT: Visual Analogue Scale. *Journal of Clinical Nursing,* 10**,** 697-706.
Gouveia, S. M. & Tiffany, J. M. 2005. Human tear viscosity: An interactive role for proteins and lipids. *Biochimica et Biophysica Acta (BBA) - Proteins & Proteomics,* 1753**,** 155-163.
Grehn, F. 2012. *Augenheilkunde,* Springer.
Greivenkamp, J. E., Schwiegerling, J. I. M., Miller, J. M. & Mellinger, M. D. 1995. Visual Acuity Modeling Using Optical Raytracing of Schematic Eyes. *American Journal of Ophthalmology,* 120**,** 227-240.
Grey, C. P. 1986. Changes in contrast sensitivity during the first hour of soft lens wear. *Am J Optom Physiol Opt,* 63**,** 702-707.
Guichelaar, P. D., Bruce, R., W., Godfrey, D., Ryason, R., Booser, E. R. & Flaherty, A. 2008. *Basics of Friction* [Online]. Available: http://www.stle.org/resources/lubelearn/friction/default.aspx#second [Accessed 08.04.2012 2012].
Guillon, M. 2009. Fitting contact lenses has changed... but still requires practitioner expertise. *Cont Lens Anterior Eye,* 32**,** 259.
Guillon, M., Lydon, D. P. M. & Solman, R. T. 1988. Effect of target contrast and luminance on soft contact lens and spectacle visual performance. *Current Eye Research,* 7**,** 635 - 648.
Guillon, M. & Maissa, C. 1999. Tear exchange – Does it matter. *Optician,* 218**,** 28-30.
Guryca, V., Hobzová, R., Prádný, M., Sirc, J. & Michálek, J. 2007. Surface morphology of contact lenses probed with microscopy techniques. *Contact Lens and Anterior Eye,* 30**,** 215-222.
Györffy, I. 1990. *Contact lens molding* [Online]. Budapest. Available: http://www.makot.hu/rolunk.htm.
Haag Streit 2012. Leaflet Haag Streit Slit Lamp BQ 900 LED with imaging module.
Hall, L. A., Young, G., Wolffsohn, J. S. & Riley, C. 2011. The influence of corneoscleral topography on soft contact lens fit. *Investigative Ophthalmolology and Visual Science,* 52**,** 6801-6806.
Hanks, A. & Weisbarth, R. 1983. Troubleshooting soft toric contact lenses. *International Contact Lens Clinic,* 1983**,** 3015-3017.

Harris, M. G., Harris, K. L. & Ruddell, D. 1976. Rotation of lathe-cut hydrogel lenses on the eye. *Am Journal of Optomometry and Physiological Optics,* 53**,** 20-26.
Harris, M. G., Rich, J. & Tandrow, T. 1975. Rotation of spin-cast hydrogel lenses. *Am Journal of Optomometry and Physiological Optics,* 52**,** 22-30.
Helmholtz, H. V. E. A. (ed.) 1909. *Einführung in die Methoden der Dioptrik der Augen des Menschen (Introduction to the methods of the dioptrics of the human eyes),* Hamburg: Leopold Voss.
Heunen, M. M. T. H. 2012. *What are the implications for the tear film with modern silicone hydrogel contact lenses?* MSc in Clinical Optometry, City University London.
Higginson, G. R. 1962. A model experiment in elasto-hydrodynamic lubrication. *International Journal of Mechanical Sciences,* 4**,** 205-210.
Hollwich, F. & Kemmetmüller, H. (eds.) 1975. *Die Kontaktlinse als Refraktionshilfe und Therapeutikum,* Stuttgart: Ferdinand Enke.
Holly, F. J. 1986. *The Preocular Tear Film In Health, Disease, and Contact Lens Wear,* Lubbock, TX. .
Holly, F. J. 2006. *COLLOIDAL OSMOSIS - ONCOTIC PRESSURE* [Online]. Available: http://www.freshkote.com/news/Oncotic%20Pressure%20Rev%2010_07.pdf .
Hom, M., M. & Bruce, A., S. 2006. Manual of Contact Lens Prescribing and Fittin. Elsevier Health Sciences.
Honegger, H., Dausch, D. & Maris, P. 1980. Verweildauer und Wirkung von Medikamenten im Bindehautsack. *In:* JAEGER, W. (ed.) *Plastische Chirurgie der Lider und Chirurgie der Tränenwege.* J.F. Bergmann-Verlag.
Iso 2012. ISO 18369-2. *In:* ORGANISATION, I. S. (ed.) *Tolerances.*
Iso, I., Standards, Organisation 2006. ISO 18369-3 Ophthalmic Optics-Contact lenses Part 3 Measurement Methods. *In:* ORGANISATION, I. S. (ed.).
Jacobson, B. 2003. The Stribeck memorial lecture. *Tribology International,* 36**,** 781-789.
Jellinek, H. H. G. 1960. SOME FRICTIONAL PROPERTIES OF THIN WATER FILMS. DTIC Document.
Jin, Z. M. 2002. Biotribology. Bradford.
Jones, L. 2013. *Hydrogel contact lens materials: Dead and buried or about to rise again?* [Online]. Internet. [Accessed 15.01.2015 2015].
Josephson, J. 1976. Edge-push effect. *International Contact Lens Clinic,* nov/dec 1976.
Kanski, J. J. & Bowling, B. (eds.) 2012. *Klinische Ophthalmologie,* München: Elsevier, Urban und Fischer.
Kaufmann, H. & De Decker, W. (eds.) 2003. *Strabismus,* Stuttgart: Georg Thieme Verlag.
Keir, N. & Jones, L. 2013. Wettability and silicone hydrogel lenses: a review. *Eye Contact Lens,* 39**,** 100-8.
Kern, J., Rappon, J., Bauman, E. & Vaughn, B. 2013. Assessment of the relationship between contact lens coefficient of friction and subject lens comfort. *Invest. Ophthalmol. Vis. Sci.,* 54**,** 494-.
Kessel, L., Johnson, L., Arvidsson, H. & Larsen, M. 2010. The relationship between body and ambient temperature and corneal temperature. *Investigative Ophthalmolology and Visual Science,* 51**,** 6593-6597.

Kim, S. H., Marmo, C. & Somorjai, G. A. 2001. Friction studies of hydrogel contact lenses using AFM: non-crosslinked polymers of low friction at the surface. *Biomaterials,* 22**,** 3285-3294.

Kim, S. H., Opdahl, A., Marmo, C. & Somorjai, G. A. 2002. AFM and SFG studies of pHEMA-based hydrogel contact lens surfaces in saline solution: adhesion, friction, and the presence of non-crosslinked polymer chains at the surface. *Biomaterials,* 23**,** 1657-1666.

Kim, S. H. M., C. Somorjai, G. A., 2001. Friction studies of hydrogel contact lenses using AFM: non-crosslinked polymers of low friction at the surface. *Biomaterials,* 22**,** 3285-3294.

Kirkpatrick, D. L. 1983. *Effects of Soft Contact Lenses on Contrast Sensivity.* MS, Pacific University.

Kirkpatrick, D. L. & Roggenkamp, J. R. 1985. Effects of soft contact lenses on contrast sensitivity. *Am J Optom Physiol Opt,* 62**,** 407-12.

Kistler Group, E., 8408 Winterthur, Switzerland 2009. Industrial Charge Amplifier for Applications in Manufacturing.

Korb, D. R., Scaffidi, R. C., Greiner, J. V., Kenyon, K. R., Herman, J. P., Blackie, C. A., Glonek, T., Case, C. L., Finnemore, V. M. & Douglass, T. 2005. The Effect of Two Novel Lubricant Eye Drops on Tear Film Lipid Layer Thickness in Subjects With Dry Eye Symptoms. *Optometry & Vision Science,* 82**,** 594-601.

Leicht, G. V., Wimmer, M., Weder, P., Federico, D. & Cieslik, C. 2005. Funktionieren Einheitsparameter? Wann funktionieren sie nicht? *Deutsches Optikerjournal,* 1**,** 76-82.

Lemp, M. A. & Bielory, L. 2008. Contact Lenses and Associated Anterior Segment Disorders: Dry Eye Disease, Blepharitis, and Allergy. *Immunology and Allergy Clinics of North America,* 28**,** 105-117.

Lemp, M. A. & Nichols, K. K. 2009. Blepharitis in the United States 2009: A Survey-based Perspective on Prevalence and Treatment. *The Ocular Surface,* 7**,** S1-S14.

Lim, L. A., Frost, N. A., Powell, R. J. & Hewson, P. 2010. Comparison of the ETDRS logMAR, /`compact reduced logMar/' and Snellen charts in routine clinical practice. *Eye,* 24**,** 673-677.

Lin, M. C., Graham, A. D., Polse, K. A., Mandell, R. B. & Mcnamara, N. A. 1999. Measurement of Post Lens Tear Thickness. *Investigative Ophthalmology & Visual Science,* 40**,** 2833-2839.

Lin, M. C. & Svitova, T. F. 2010. Contact lenses wettability in vitro: effect of surface-active ingredients. *Optom Vis Sci,* 87**,** 440-7.

Lindskoog-Pettersson, A., Martensson, L., Salkic, J., Unsbo, P. & Brautaset, R. 2011. Spherical aberration in relation to visual performance in contact lens wear. *Cont Lens and Anterior Eye,* 34**,** 12-16; quiz 50-51.

Lum, E., Golebiowski, B., Gunn, R., Babhoota, M. & Swarbrick, H. 2013. Corneal Sensitivity with Contact Lenses of Different Mechanical Properties. *Optometry & Vision Science,* 90**,** 954-960.

Majorkovits, H., Rier, A. & Zsidek, C. 2005. *Topographenvergleich* [Online]. Hall in Tirol: Private HTL Hall/Tirol. Available: http://phtl-hall.tsn.at/sites/phtl-hall.tsn.at/files/upload/Topograph.pdf [Accessed 03.04.2012 2012].

Mann, A. & Tighe, B. 2013. Contact lens interactions with the tear film. *Experimental Eye Research,* 117**,** 88-98.

Mc Monnies, C. W. 2007. Incomplete blinking: Exposure keratopathy, lid wiper epitheliopathy, dry eye, refractive surgery, and dry contact lenses. *Contact Lens and Anterior Eye,* 30**,** 37-51.
Mengher, L. S., Pandher, K. S., Bron, A. J., And & Davey, C. C. 1986. Effect of sodium hyaluronate (0.1%) on break-up time (NIBUT) in patients with dry eyes. *Britisch Journal of Ophthalmology,* 70**,** 442-447.
Menzies, K. L. & Jones, L. 2011. In vitro analysis of the physical properties of contact lens blister pack solutions. *Optom Vis Sci,* 88**,** 493-501.
Millar, T. 2006. Elucidate the Contribution of Proteins to Tears. A Challenge for Researchers. *Archivos de la Sociedad Espanola de Oftalmologia,* 81**,** 187-190.
Miller, D. 1967. Pressure of the Lid on the Eye. *Archive of Ophthalmology,* 78**,** 328-330.
Millodot, M. 1978. Effect of long-term wear of hard contact lenses on corneal sensitivity. *Archives of ophthalmology,* 96**,** 1225-1227.
Mills, A. 2008. The coefficient of friction, particularly of ice. *Physics Education,* 43**,** 392.
Mueller, A. 1889. *Brillenglaeser und Hornhautlinsen: Inaugural-Dissertation.* University of Kiel.
Nagyová, B. a. T., J. M. 1999. Components responsible for the surface tension of human tears. *Current Eye Research,* 19**,** 7.
Nakamura, Y., Matsuda, J., Suzuki, K., Toyoda, H., Hakamata, N., Shimamoto, T. & Kinoshita, S. 2008. [Measurement of spontaneous blinks with a high-speed blink analyzing system]. *Nippon Ganka Gakkai Zasshi,* 112**,** 1059-1067.
National Instruments, C. 2014. *Motor Fundamentals* [Online]. Available: http://www.ni.com/white-paper/3656/en/ [Accessed 24.12.2014 2014].
Nelson, J. D. 1995. Simultaneous evaluation of tear turnover and corneal epithelial permeability by fluorophotometry in normal subjects and patients with keratoconjunctivitis sicca (KCS). *Transactions of the American Ophthalmological Society,* 93**,** 709-753.
Ngai, V., Medley, J. B., Jones, L., Forrest, J. & Teiehroeb, J. 2005. Friction of Contact Lenses: Silicone Hydrogel versus Conventional Hydrogel. *In:* D. DOWSON, M. P. G. D. & LUBRECHT, A. A. (eds.) *Tribology and Interface Engineering Series.* Elsevier.
Niarn, J. A. & Jiang, T.-B. 1995. Measurement of the Friction and Lubricity Properties of Contact Lenses. *Proceedings of ANTEC 1995.* Boston, MA, May 7-11, 1995.: Society of Plastics Engineers.
Nichols, J. J. & King-Smith, P. E. 2003. Thickness of the Pre- and Post-Contact Lens Tear Film Measured In Vivo by Interferometry.
Nichols, J. J. & Sinnott, L. T. 2006. Tear Film, Contact Lens, and Patient-Related Factors Associated with Contact Lens-Related Dry Eye. *Investigative Ophthalmolology and Visual Science,* 47**,** 1319-1328.
Obrig, T. E. 1942. *Contact lenses,* New York, Chilton Co., Printing Division.
Opdahl, A., Kim, S. H., Koffas, T. S., Marmo, C. & Somorjai, G. A. 2003. Surface mechanical properties of pHEMA contact lenses: Viscoelastic and adhesive property changes on exposure to controlled humidity. *Journal of Biomedical Materials Research Part A,* 67A**,** 350-356.

Park, J. D. J. & Karesh, J. 2006. Duane's ophthalmology on CD-ROM, Chapter1. *In:* DUANE, T. D., TASMAN, W. & JAEGER, E. A. (eds.) 2006 ed. ed. Philadelphia :: Lippincott Williams & Wilkins.

Paul-Dauphin, A., Guillemin, F., Virion, J. M. & Briancon, S. 1999. Bias and precision in visual analogue scales: a randomized controlled trial. *American Journal of epidemiology,* 150**,** 1117-1127.

Pearce, J. 2001. Norman Gaylord, a Chemist, Is Dead at 84. *The New York Times,* Sept. 21. 2007.

Pesola, A. 2011. *Pesola Produkte* [Online]. Available: http://www.pesola.com/ 2011].

Piso & Organisation, I. S. 2012. ISO/FDIS 11980:2012 Ophthalmic optics — Contact lenses and contact lens care products — Guidance for clinical investigations *In:* ISO (ed.).

Polytetra, G. 2013. Technical data PTFE. *Polytetra GmbH.* Mönchengladbach.

Popov, V. (ed.) 2009. *Kontaktmechanik Und Reibung,* Berlin Heidelberg: Springer.

Pruitt, J., Qiu, Y., Thekveli, S. & Hart, R. 2012. Surface characterization of a water gradient silicone hydrogel contact lens (delefilcon A). *Investigative Ophtalmology and Visual Science,* 53**,** 6107.

Pullum, K. 2003. A keratoconus fitting system using the axial profile to establish optimum lens parameters. *Cont Lens and Anterior Eye,* 26**,** 77-84.

Pullum, K. 2012. *Scleral Lenses* [Online]. Internet. Available: http://www.kenpullum.co.uk/scleral [Accessed 25.11.2012 2012].

Qu, J., Blau, P. J., Watkins, T. R., Cavin, O. B. & Kulkarni, N. S. 2005. Friction and wear of titanium alloys sliding against metal, polymer, and ceramic counterfaces. *Wear,* 258**,** 1348-1356.

Ramamoorthy, P. L. T. N. J. J. 2010. Contact lens material characteristics associated with hydrogel lens dehydration. *Ophthalmic & Physiological Optics,* - 30**,** 160 - 166.

Rennie, A. C., Dickrell, P. L. & Sawyer, W. G. 2005. Friction coefficient of soft contact lenses: measurements and modeling. *Tribology Letters,* 18**,** 499-504.

Reynolds, J. E. F. 1989. Martindale The Extra Pharmacopoeia. *In:* J.E.F. REYNOLDS, K. P. (ed.) *Martindale The Extra Pharmacopoeia.* 29 ed. London: The Pharmaceutical Press.

Roba, M., Duncan, E., Hill, G., Spencer, N. & Tosatti, S. 2011. Friction Measurements on Contact Lenses in Their Operating Environment. *Tribology Letters,* 44**,** 387-397.

Salem, H. & Katz, S. A. 2003. *Alternative toxicological methods,* CRC Press.

Schmidt, R. F. & Florian, L. (eds.) 2007. *Physiologie des Menschen,* Heidelberg: Springer Medizin Verlag Heidelberg.

Sell, H. J. 1986. Formelsammlung und Formelableitung zur Hornhaut-Topometrie (Schluß). *Die Kontaktlinse***,** 34-35.

Serway, R. & Jewett, J. 2013. *Physics for scientists and engineers with modern physics,* Cengage learning.

Shaw, A. J., Davis, B. A., Collins, M. J. & Carney, L. G. 2009. A Technique to Measure Eyelid Pressure Using Piezoresistive Sensors. *IEEE Transactions on Biomedical Engineering,* 56**,** 2512-2517.

Shinoda, K. The comparison between the PIT system and the HLB-value system to emulsifier selection. Proceedings of the 5th International Congress of Surface Activity, 1969. 275-283.

Sivamani, R. K., Goodman, J., Gitis, N. V. & Maibach, H. I. 2003. Coefficient of friction: tribological studies in man - an overview. *Skin Research and Technololgy,* 9**,** 227-234.

Snyder, C. 2004. A Primer on Contact Lens Materials. *Contact Lerns Spectrum***,** 33-38.

Spijker, P., Anciaux, G. & Molinari, J.-F. 2013. Relations between roughness, temperature and dry sliding friction at the atomic scale. *Tribology International,* 59**,** 222-229.

Stapleton, F., Marfurt, C., Golebiowski, B., Rosenblatt, M., Bereiter, D., Begley, C., Dartt, D., Gallar, J., Belmonte, C., Hamrah, P. & Willcox, M. 2013. The TFOS International Workshop on Contact Lens Discomfort: report of the subcommittee on neurobiology. *Invest Ophthalmol Vis Sci,* 54**,** TFOS71-97.

Steffen, R. B. & Mccabe, K. 2004. Finding the Comfort Zone with the newest Silicone Hydrogel Technology. *Contact Lens Spectrum*.

Stein, H., A., Stein, R., M., Freeman, M. & Lynn, M. (eds.) 2005. *Duane's Ophthalomology, Chap. 55: Basics of soft contact lens fitting*: Lippincott Williams & Wilkins Publishers.

Stoll, A. & Strangfeld, M. 2012. Chapter 10 - Experimental Friction Behavior of Elastomers on Glass. *Automotive Buzz, Squeak and Rattle.* Oxford: Butterworth-Heinemann.

Stribeck, R. 1902. Die Wesentlichen Eigenschaften der Gleit-und Rollenlager, Z. . *Verein. Deut. Ing.,* 46.

Sturzu, A. & Luca-Motoc, D. 2011. Theoretical eye models comparison based on MTF evolution. *Bulletin of the Transilvania university of Brasß ov, Ser. I. Eng. Sci,* 4**,** 33-38.

Tanaka, K. 1984. Kinetic friction and dynamic elastic contact behaviour of polymers. *Wear,* 100**,** 243-262.

Tanelian, D. & Beuerman, R. 1980. Recovery of corneal sensation following hard contact lens wear and the implication for adaptation. *Investigative ophthalmology & visual science,* 19**,** 1391-1394.

Taniguchi, K., Itakura, K., Morisaki, K. & Hayashi, S. 1988. Effects of Tween 80 and liposomes on the corneal permeability of anti-inflammatory steroids. *J Pharmacobiodyn,* 11**,** 685-93.

Taylor, B. N. & Ambler, T. 2008. THE INTERNATIONAL SYSTEM OF UNITS (SI). *In:* (NIST), N. I. O. S. A. T. (ed.) *Special Publication 330.* 2008 ed. Washington: National Institute of Standards and Technology.

Thai, L. C., Tomlinson, A. & Ridder Iii, W. H. 2002. Contact lens drying and visual performance: the vision cycle with contact lenses. *Optometry & Vision Science,* 79**,** 381-388.

Thiele, E. 2012. *Entwicklung und Konstruktion eines Prüfstandes zur Charakterisierung der Reibungseigenschaften an Kontaktlinsen.* Graduate study Graduation, Fachhochschule Lübeck.

Tiffany, J. M., Grande, E. F. & Todd, B. S. 2004. Measurement Of Scleral Curvature By Scheimpflug Photography. *Investigative Ophthalmolology and Visual Science,* 45**,** 2389-B24.

Tomlinson, A. & Bibby, M. M. 1980. Movement and rotation of soft contact lenses. Effect of fit and lens design. *Am J Optom Physiol Opt,* 57**,** 275-279.

Tomlinson, A. & Khanal, S. 2005. Assessment of Tear Film Dynamics: Quantification Approach. *The Ocular Surface,* 3**,** 81-95.

Tomlinson, A., Ridder, W. H., 3rd & Watanabe, R. 1994. Blink-induced variations in visual performance with toric soft contact lenses. *Optometry and vision science,* 71**,** 545-549.
Tomlinson, A., Schoessler, J. & Andrasko, G. 1980. The effect of varying prism and truncation on the performance of soft contact lenses. *Am Journal of Optomometry and Physiological Optics,* 57**,** 714-720.
Townsend, W., F. 2010. *Beyond the Basics: Treating Severe Dry Eye* [Online]. Newtown Square PA 19073: Review of OPtometry. Available: http://www.reviewofcontactlenses.com/content/d/dry_eye/c/19881/ [Accessed 16.03.2012 2012].
Tranoudis, I. & Efron, N. 2004. In-eye performance of soft contact lenses made from different materials. *Cont Lens Anterior Eye,* 27**,** 133-48.
Tucker, R. C., Quinter, B., Patel, D., Pruitt, J. & Nelson, J. 2012. Qualitative and Quantitative Lubricity of Experimental Contact Lenses. *Invest. Ophthalmol. Vis. Sci.,* 53**,** 6093-.
Tuohy, K. 1948. *Contact Lens*. USA patent application. 6.6.1950.
Tyler, C. W. 1978. Some new entoptic phenomena. *Vision Research,* 18**,** 1633-1639.
Urueña, J. M., Dunn, A. C. & Sawyer, W. G. 2011. Contact Lens Boundary Lubrication and Friction Reduction with Hyaluronic Acid. *Tribology Lubrification Technology,* 67**,** 2.
Van Der Steen, R. 2007. Tyre/road friction modeling Literature survey. May 2007 ed. Eindhoven, the Netherlands: Eindhoven University of Technology.
Veys, J., Meyler, J. & Davies, I. (eds.) 2003. *Essential Contact Lens Practice Page 34,* London: Butterworth-Heinemann.
Walcott, B. 1998. The Lacrimal Gland and Its Veil of Tears. *News Physiol Sci,* 13**,** 97-103.
Walker, J., Hay, M., Blalock, J., Mack, C., Knezich, G. & Henderson, T. L. 2003. Evaluating Steeper Base Curve Lens Movement. *Contact Lens Spectrum***,** 1-2.
Wang, J., Fonn, D., Simpson, T. L. & Jones, L. 2003. Precorneal and Pre- and Postlens Tear Film Thickness Measured Indirectly with Optical Coherence Tomography. *Investigative Ophthalmolology and Visual Science,* 44**,** 2524-2528.
Wechsler, S. 1978. Visual acuity in hard and soft contact lens wearers: a comparison. *Jounal of the American Optometric Association,* 49**,** 251-256.
Wettlinger, K. 2012. *PTFE ... Polytetrafluorethylen* [Online]. Vienna: Wettlinger Available: http://wettlinger.at/wpress/wp-content/uploads/2009/06/ptfe.pdf.
Wichterle, O. 1990. History and development of hydrophilic contact lenses. *International Society of Contact Lens Specialists.* Oslo.
Wichterle, O. & Lim, D. 1956. *Process for producing shaped articles from three dimensional hydrpphilic high polymers*. USA patent application. 28. 3. 1^961.
Wichterle, O. & Lim, D. 1960. Hydrophilic Gels for Biological Use. *Nature,* 185**,** 117-118.
Wichterle, O., Lim, D. & Dreifus, M. 1961. On the problem of contact lenses. *Ceskoslovenska oftalmologie,* 17**,** 70-74.
Wilms, K. H. & Rabbetts, R. B. 1977. Practical concepts of corneal topometry. *Optician,* 174**,** 7-13.
Wolff, E. (ed.) 1954. *Anatomy of Eye and Orbit,* New York: Plakiston Co.

Wolffsohn, J. S., Hunt, O. A. & Basra, A. K. 2009. Simplified recording of soft contact lens fit. *Cont Lens and Anterior Eye,* 32**,** 37-42.
Wolkoff, P., Nøjgaard, J. K., Troiano, P. & Piccoli, B. 2005. Eye complaints in the office environment: precorneal tear film integrity influenced by eye blinking efficiency. *Occupational and environmental medicine,* 62**,** 4-12.
Yao, H., Della Rocca, G., Guduru, P. R. & Gao, H. 2008. Adhesion and sliding response of a biologically inspired fibrillar surface: experimental observations. *Journal of the Royal Society Interface,* 5**,** 723-733.
Young, G. 2003. Toric contact lens designs in hyper-oxygen materials. *Eye and Contact Lens,* 29**,** S171-173; discussion S190-1, S192-4.
Young, G., Chalmers, R. L., Napier, L., Hunt, C. & Kern, J. 2011. Characterizing contact lens-related dryness symptoms in a cross-section of UK soft lens wearers. *Contact Lens and Anterior Eye,* 34**,** 64-70.
Young, R. & Tapper, T. 2008. A New Silicone Hydrogel for Custom Lens Manufactura. *Global Contact,* 49**,** 30-33.
Yurdumakan, B., Nanjundiah, K. & Dhinojwala, A. 2007. Origin of higher friction for elastomers sliding on glassy polymers. *Journal of Physical Chemistry C,* 111**,** 960-965.
Zeng, H. 2013. *Polymer Adhesion, Friction, and Lubrication*, John Wiley & Sons.
Zhou, B., Li, Y., Randall, N. & Li, L. 2011. A study of the frictional properties of senofilcon-A contact lenses. *Journal of the Mechanical Behaviour of Biomedical Materials,* 4**,** 1336-1342.
Zimmermann-Spinnler, M. 1983. *Labortechnik,* Basel, Rocom, Editiones Roche

Chapter 13 - Abbreviations

Abbreviation	Meaning
μ	friction coefficient
μm	micrometre (micron)
ACLM	Association of Contact Lens Manufacturers
Alu	Aluminium
astig	astigmatism
av	average
BOZR	Back Optic Zone Radius
BVP	Back Vertex Power
CAB	Cellulose Acetate Butyrate
circumf	circumference
CL	Contact lens
Coeff	Coefficient
CoF	Coefficient of friction
Com. Tail	Comets tail
Conj	conjunctiva
Corr	correction
cpd	cycle per degree
CRF	clinical record form
CS	Contrast sensitivity
cyl	cylinder
Diam	diameter
Dk	Oxygen permeability
D	dioptres
ε	eccentricity

Abbreviation	Meaning
EGDMA	ethylglycoldimethacrylate
ext	external
NaCl0.9	Saline solution
NIBUT	Non invasive break up time
nm	nanometre
no.	number
num Ex	numerical eccentricity
NVP	n vinylpyrrolydone
OCT	optical coherence tomography
PMMA	Polymethylmethacrylate
proj	projected
psi	pounds per square inch
PTFE	Polytetrafluoroethylene or TEFLON
PVA	Polyvinylalcohol
PVP	Polyvinylpyrrolidone
r	Radius of curvature
RE	Right eye
RGP	Rigid gas permeable
RX 56	Trade mark of a CAB contact lens
s	seconds
Σ	sum
sag	sagitta
SD	Standard deviation
secs	seconds
Si	Silicone

Abbreviation	Meaning
sph	sphere
Std Dev	Standard deviation
Sys.prod	Systematic production (error)
t	fluid friction or for pushing tension
tc	Centre thickness
TD	Total diameter
Torr	Pressure in mm mercury
V 38	VSO 38 soft lens material
V 75	VSO 75 soft lens material
VA	Visual acuity
VAS	Visual analogue scale
vs	versus
w	with
w/o	without
WTR	with-the-rule (astigmatism)
Zeit	time (German)